Fixed millimetric and microwave network planning

in a cellular environment and the introduction of

the 38GHz band into the Brisbane area.

A thesis for examination for the degree of M.Phil.

at the University of London

Neil Peter Forknall

Department of Electronic and

Electrical Engineering
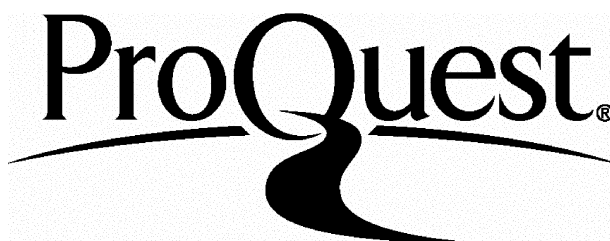
University College London

December 1999

ProQuest Number: U642913

ProQuest.®

ProQuest U642913

Abstract

Cable and Wireless Optus is an operator in Australia which provides a GSM service. The availability of its transmission network is controlled by establishing a minimum standard between the mobile switching centre and any base station in the network. Maximum frequency reuse has been achieved by limiting the transmission power of the fixed radios to a level where the quality objectives of the hop are met but the interference is kept to a minimum. Optus use propagation models provided by the International Telecommunications Union to predict availability on fixed radio hops.

In 1996 Optus made the decision to use the 38GHz band in the Brisbane area in 1998. However, the 38GHz band had not been used previously in this area, by Optus or any other operator, and no data was available on 38GHz propagation in the region. To evaluate the accuracy of the availability predictions, based on the data and models provided by the International Telecommunications Union, a 38GHz field trial was established. Over a 12 month period the received power level was recorded on a 2.1km vertically polarised path operating at 38GHz. The rainfall, wind speed and wind direction were also recorded. Based on a rainfall intensity estimate provided in ITU–R PN.837–1, and the rainfall attenuation model outlined in ITU–R P.530–7, the link was predicted to experience fading of 25dB for approximately 52.6 minutes. However, fading of 37 dB was recorded for 53.48 minutes and fading of 25 dB was exceeded for 97.6 minutes during the measurement period.

Although a one year observation period is not a long period of time, suggestions for planning 38GHz links in this area have been made which should help to ensure the availability figures demanded by Cable and Wireless Optus are satisfied.

Acknowledgment

The author wishes to than thank the following people for their indispensable contribution to this thesis.

Mr S. Dimitrios from Cable and Wireless Optus for his diligent collection of the raw data between 1 February 1997 and 31 January 1998 and for his help in commissioning and decommissioning the research hop in December 1996 and February 1998.

Prof R.S. Cole from University College London and Dr J. Henriksson from Nokia for their supervision and guidance during this project.

Mr H. Glud, Mr T. Villberg, Mr K. Martikainen and Mr M. Jarventausta from Nokia and Mr P. Babai and Mr A. Bancroft from Cable and Wireless Optus who collectively covered all the costs associated with this research.

Finally, the author would like to thank his wife Kati, his children Emma and Joel and his parents Margaret and Peter for their support.

	Contents	Page

Contents   **Page**

Contents   **Page**

Contents | Page

•

	Diagrams	Page

	Tables		**Page**

16

17

Glossary

BSC	Base station controller
BTS	Base station
CPM	Continuous phase modulation
DMR38	Nokia 38GHz digital radio
GSM	Global system for mobile communication
ITU–R	International Telecommunication Union (Radio Section)
MSC	Mobile switching centre
MTBF	Mean time between failure
MTTR	Mean time to restoration
NokiaQ1	Nokia specific element manager protocol
PSK	Phase shift keying
QAM	Quadrature amplitude modulation
V.11	Electrically balanced serial interface
V.28	Electrically unbalanced serial interface

1 Introduction

1.1 Introduction

The thesis has been written in six chapters, starting with an introduction which provides the reasons for the research and describes how it was carried out. The second chapter reviews the literature which considers the physics that affects millimetric and microwave radio signals. In the third chapter planning issues related to the use of millimetric and microwave radios in a cellular network are considered. The fourth section discusses how the measurements were made and how the data was compiled. The fifth chapter presents the finding from the analysis of a one–year collection of data. The results are summarised in the sixth chapter together with conclusions concerning these results.

1.2 Background

Cable and Wireless Optus is an operator in Australia which provides a public digital cellular network that complies with the international standards for GSM. Mobile base stations, BTS's, broadcast traffic channels at 900MHz which may be used by mobile phone subscribers in the vicinity. The area covered by a BTS, and the number of traffic channels broadcast within that area depend on the number of mobile calls generated by the subscribers in the busiest hour of the week and how many of those calls the operator intends to carry, which in turn depends on the limitation of the cellular equipment and on how mature the network is.

Initially BTS's provided coverage for the city centres with enough capacity to carry 98% of the estimated traffic generated by subscribers in the busiest hour of the week. Wherever possible the BTS's were connected to a base station controller, BSC, with point–to–point transmission radio systems. These radios are quick to install and provided Optus

with ownership of the transmission network between the BSC and BTS's, and therefore control of roll–out, performance and availability. The BSC's are connected to a mobile switching centre, MSC, with optical fibres in a protected configuration.

The difference between the normal received power level on a point–to–point radio and the power level which would cause a bit error rate of one error in a thousand is termed the fade margin. In order to meet the performance and availability requirements set by Optus between the BTS's and the MSC it is necessary for the engineers with responsibility for planning the network to maintain a large enough fade margin to allow satisfactory performance in adverse weather conditions. It is therefore the responsibility of the planning engineer to select frequencies for the radio hops which will not cause interference with other radios. If a new hop is allocated a frequency which interferes with an existing radio in the network, the existing radio may experience a reduction in its fade margin and therefore a reduction in the availability and performance targets which were set for it.

Transmission radio systems which operate above 10GHz suffer from attenuation caused by rainfall. To aid with the planning of transmission radio networks the International Telecommunications Union (Radio Section), ITU–R, publish world–wide rainfall region charts and a corresponding table which estimates the rainfall exceeded, with rainfall intensity integrated over one minute, for a given percentage of the year in the various regions. The ITU–R also provide mathematical formulae which enable the planning engineer to predict over what percentage of time a given fade margin operating at a stated frequency will be completely attenuated by the rainfall in that rainfall region. The method used by the ITU–R calculates the attenuation exceeded for 0.01% of an average year based on the rainfall intensity exceeded for 0.01% of an average year, the operating

frequency, polarisation, path length and fade margin.

In order to meet the availability requirements set by Optus between the MSC and any BTS in the network it is essential to be able to predict the unavailability caused by rainfall on any radio which will connect a BTS to the network.

1.3   Reason for the field trial

Optus began operations as a GSM operator in 1992. Originally it used 15GHz for its point–to–point fixed links in the Brisbane area but with the rapid expansion of the network it became necessary to use 18GHz in 1995. By 1996 crowding of the frequency bands used by Optus for its fixed microwave network was making frequency selection difficult. The limited number of channels available made it a complex task to ensure that newly installed links would not interfere with existing links. If the new microwave link did not have a carefully selected carrier frequency it could reduce the carrier to interference threshold of existing radios, reducing the flat fade margin and thereby adversely affecting the availability figure which the network had originally been designed to meet. To avoid reducing the existing availability of their network Optus started to use the 23 GHz microwave band in 1996 and intended to use the 38 GHz millimetric band for new radio links in crowded urban areas from 1998. However as Optus increased the frequency of its microwave links it became noticeable that the availability model which was being used, based on ITU–R P.530, was unreliable and that rain was causing unacceptably high unavailability on some links. Since the 38GHz band had not been used in the Brisbane area previously it was considered to be essential to test its performance before any commercial traffic was carried.

To reduce interference in their network Optus were interested in reducing the flat fade

margin on radio links in chain networks by attenuating the transmit power with a wave-guide attenuator which was built into the Nokia 18, 23 and 38 GHz radios. However experience had revealed that the fade margin required, according to the ITU model, to meet an availability target was incorrect, and rather than improving the network the attenuator was only reducing availability. Since the error seemed to increase with increasing frequency a key objective from the 38GHz field trial was to be able to use the ITU model at 38GHz and obtain accurate results, which would allow the use of the attenuator in a chain or star topology in order to reduce interference in the network.

In October 1996 Optus and its supplier Nokia agreed to conduct research into millimetric propagation at 38 GHz in Brisbane. It was decided to commission a 38 GHz link and monitor its performance over a twelve month period between 1 February 1997 and 31 January 1998. The project was to be jointly funded with the results form the project, which are regarded as commercially valuable, remaining company confidential until January 2000. University College London was invited to take a consultative role in the research providing it did not reveal any work relating to the project until January 2000.

1.4   The test hop

Since fixed 38GHz transmission radio links had not been used in the Brisbane area by Optus, or any other operator, a 2.1km, 38GHz test hop with vertical electrical polarisation was commissioned in December 1996, and decommissioned in February 1998. During this period the receive power was measured along with the rainfall, wind speed and wind direction. The 38GHz radios used were the DMR38 C Model supplies by Nokia. This radio consisted of an indoor baseband unit and an outdoor radio unit. The radio used continuous phase modulation to transmit four 2Mbit/s signals within a 7MHz

bandwidth. One end of the hop was located on top of the Optus office complex. The other end of the hop was located on top of the Royal Brisbane Hospital. Rain gauges with battery powered internal data loggers were located at each end of the hop. The monitoring of wind speed and direction was performed at the Optus end using a dedicated data logger. The received power level of the radio at the Optus end was logged using a personal computer. The results were recorded for a calendar year between the 1 February 1997 and the 31 January 1998.

2 Review of literature

2.1 Introduction

The aim of this literature review is to inform the reader about the various mechanisms which can affect the performance of a millimetric or microwave signal. Refractivity is the first topic to be covered. Radio refractivity is introduced, and the effect of humidity, temperature and pressure on its value is discussed. The concept of an exponential atmosphere is presented, and the graphical representation of the trajectory of a radio path is described using k values. Variations in the refractivity gradient, and standard, subrefractive and superrefractive conditions are examined, along with the corresponding conditions for diffraction fading, scintillation, atmospheric multipath and ducting. Surface reflections are also considered. Different forms of diversity are reviewed, the isotropic model is introduced and interference is considered. Rain attenuation and the variability of rainfall statistics from year to year and location to location are discussed. Rain types, the horizontal structure of rainfall, and effective path lengths are introduced. Attenuation by snow and hail is also mentioned. Sand and dust storms are reviewed, the effects of atmospheric gases are considered, and cross polar discrimination is introduced. The effect of interference on performance and availability objectives is examined, and the role of millimetric and microwave radios in a cellular network is discussed

2.2 Refractivity

The refractivity of the troposphere varies with humidity, temperature, and air pressure [3]. Refractivity varies with the height above the Earth's surface which causes the microwave signal to bend as it is continually refracted [3]. At sea level the refractive index, n, of a standard atmosphere is approximately 1.000300 [4]. Since this is an awkward

number to deal with a different unit, radio refractivity, N, is normally used to study

microwave propagation [4]. Radio refractivity, N, is defined in terms of refractive index

, n, [5] as

$$N = (n-1) \times 10^6 \text{ Nunits}$$

Formula A-1   **Radio refractivity in terms of refractive index**

or alternatively [6] as

$$n = 1 + N \times 10^{-6}$$

Formula A-2   **Refractive index in terms of radio refractivity**

In terms of humidity, temperature and pressure, radio refractivity, N, can be expressed

[5] as

$$N = 77.6 \frac{P}{T} + 3.73 \times 10^5 \frac{e}{T^2}$$

Formula A-3   **Radio refractivity and humidity, temperature and pressure**

where, e is water vapour pressure (hPa), T is temperature (K), and P is atmospheric pres-

sure (hPa). This formula consists of two components [6], the dry term

$$N_{dry} = 77.6 \frac{P}{T}$$

Formula A-4   **The dry component of radio refractivity**

and the wet term

$$N_{wet} = 3.73 \times 10^5 \frac{e}{T^2}$$

Formula A-5   The wet component of radio refractivity

The dry term is fairly constant with a value around 265N units, but the wet term provides most of the variability [7]. Microwave signals are refracted the most in the lower, denser part of the atmosphere [8]. Up to the late 1940's it was believed that refractivity decreased linearly with height, but while refractivity appears linear in the lower atmosphere a more accurate model shows an exponential variation with height [9]. The exponential variation of radio refractivity, N, with height can be expressed as [5]

$$N(h) = N_A e^{-b_A h}$$

Formula A-6   Variation of radio refractivity with height

where N_A, the average radio refractivity at the surface, is equal to 315N units, and b_A is equal to 0.136, h is the height in kilometres, and N(h) is radio refractivity at height h, in kilometres.

2.2.1   The k value

The path taken by a microwave signal as it is bent by refraction when it propagates through the atmosphere can be related to the arc of a circle by the following approximation [10]

$$\frac{1}{R} \approx \frac{dn}{dh}$$

Formula A-7   The relationship between refractive index and the signal path

where R is the radius of the path, and dn/dh represents the vertical gradient of the refractive index. This approximation is valid when the launch angle is nearly horizontal and refractivity, n, is close to unity [11]. The variation of radio refractivity with height in a standard atmosphere is approximately −44N/km when averaged over the first 200 metres above sea level, and −39N/km when averaged over the first 2 kilometres [12]. However, a common reference value for terrestrial microwave radio systems operating in a standard well mixed atmosphere is −40N/km [13]. Taking this gradient of refractivity as a reference for a well mixed atmosphere, the radius of curvature of the microwave signal of radius, R, has a value of

$$R \approx \frac{dh}{dn} \approx \frac{1000m}{\left(\frac{40}{1000000}\right)} \approx 2.5 \times 10^7 \, m$$

Formula A-8   Curvature of the microwave signal in standard atmosphere

which is approximately four times greater than the radius of the Earth,[14]

$$\frac{25000 \text{ km}}{6400 \text{ km}} \approx 3.9a$$

Formula A-9   Ratio between the signals radius and the radius of the Earth

assuming that the average radius of the Earth is approximately 6400km. Using this relationship a radio system can be represented as a curved radio path over a curved Earth.

However, the curvature of both the Earth and the radio signal arc can be decreased, while maintaining the same relative curvature, until the radio signal path becomes a straight line. This corresponds with an increase in the radius of the Earth by a value, k ,[15]

$$ka \triangleq \dfrac{1}{\left(\dfrac{1}{a} + \dfrac{dn}{dh}\right)} \triangleq \dfrac{1}{\left(\dfrac{1}{a} - \dfrac{1}{4a}\right)}$$

Formula A-10   **The relationship between the radius of the microwave signal, the radius of the Earth and the gradient of refractive index**

therefore

$$k \triangleq \dfrac{1}{a\left(\dfrac{1}{a} - \dfrac{1}{4a}\right)} \triangleq \dfrac{1}{\left(\dfrac{1}{1} - \dfrac{1}{4}\right)} \triangleq \left(\dfrac{4}{3}\right)$$

Formula A-11   **The value of k in a well mixed atmosphere**

This means that in a well mixed atmosphere, when the variation of radio refractivity is approximately equal to −40N/km, the exponential model of refractive index can be represented by a linear model in the lowest kilometre of the atmosphere, and the radio path can be represented as a straight line when the radius of the Earth is multiplied by 4/3, the k value of a standard atmosphere [11].

Standard

Real Situation
Curved Earth Curved Path

Graphical Representation
Curved Earth (x4/3) Staight Path
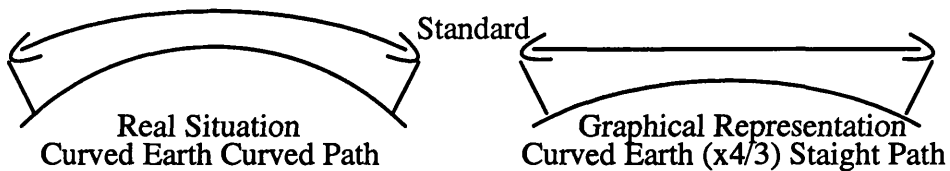
Diagram 1-1   **The path profile in standard atmospheric conditions**

2.2.2   Antenna heights

Propagation can be modelled by The Huygens Principle, where every point on the wavefront can be considered as a radiating source, with the resulting field intensity being the

superimposition of fields from all the radiating sources [16]. However, obstacles on the Earth's surface can cause a plane wave to be diffracted, affecting the received field strength relative to that of free space conditions.
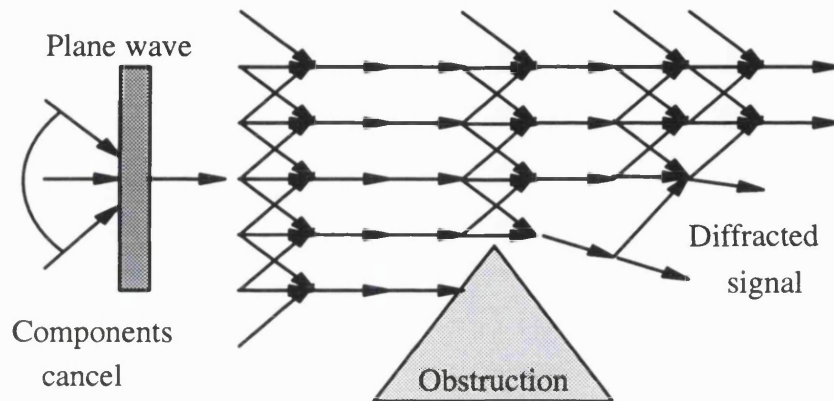
Diagram 1-2   Diffraction of a plane wave

Since most engineering models calculate the received power of a radio system assuming free space conditions, the antennas should be placed at a height which allows this. The clearance required from obstacles on the path will depend on the wavelength of the propagating signal and the distance involved. It can be defined in terms of the first Fresnel zone. The first Fresnel zone can be described as the volume contained within a three dimensional ellipsoid defined between the transmitting and receiving antennas. At any point on the ellipsoid two lines can be drawn, one to the transmitting antenna and one to the receiving antenna, such that the combined length of the two lines will be half a wavelength longer than a direct line drawn between the transmitting and receiving antennas [16].

First Fresnel Zone

d

F_1

d_1

d_2

$d_1 + d_2 = d + \lambda/2$
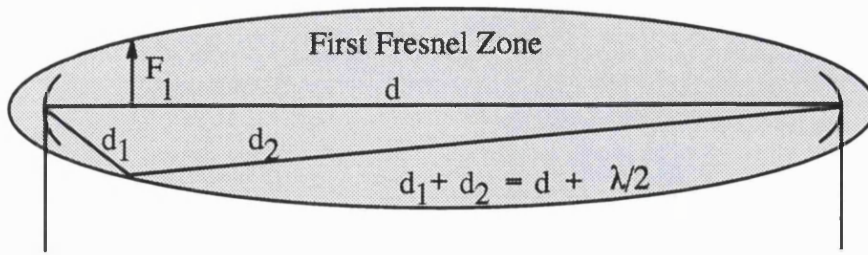
Diagram 1-3   **The first Fresnel zone**

The radius of the first Fresnel zone, F1, is given by

$$F_1 = 17.3 \sqrt{\frac{d_1 d_2}{f\ d}}$$

Formula A-12   **The radius of the first Fresnel zone**

where d1 and d2 are the distances in km of the two lines from the transmitting and receiving antennas to the edge of the first Fresnel zone, d is the distance in km of the direct line between the transmitting and receiving antennas, and f is the frequency in GHz. If two lines originating from a point on the boundary of the second Fresnel zone are drawn to the the centre of the transmitting and receiving antennas the combined length of these lines will be one wavelength longer than the direct ray. For the third and forth Fresnel zones the combined length of the lines would be one and a half, and two wavelengths longer than the direct ray, and so on [16]. In the middle of the hop the radius of the second Fresnel zone F2 is the radius of the first Fresnel zone multiplied by the square root of two, and the radius of the third Fresnel zone F3 is the radius of the first Fresnel zone multiplied by the square root of three etc [16].

31

$$F_2 = \sqrt{2}\ F_1$$

$$F_3 = \sqrt{3}\ F_1$$

$$F_4 = \sqrt{4}\ F_1$$
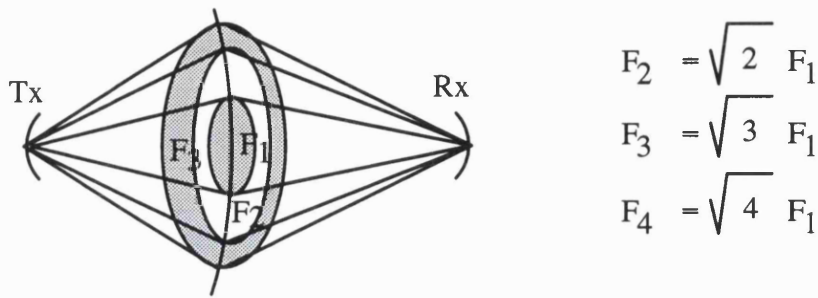
Diagram 1-4   The Fresnel zones

To approximate free space propagation conditions the clearance between any obstacle

on the radio path, and the direct ray, between the antennas, needs to be at least 60% of

the first Fresnel zone [17]. For economical reasons within Nokia it has been decided that

for a k value of 4/3 an initial plan would require 50% of the first Fresnel zone to be clear

for frequencies below 3GHz, but 100% should be clear for frequencies above 7GHz,

when hop availability around 99.99% or better is required [1]. As frequencies increase

the size of the first Fresnel zone is reduced and the change in path trajectory under subre-

fractive conditions will have a much greater impact on the percentage of the first Fresnel

zone which is obstructed by an obstacle [1].

First Fresnel Zone 38 GHz

First Fresnel Zone 2 GHz
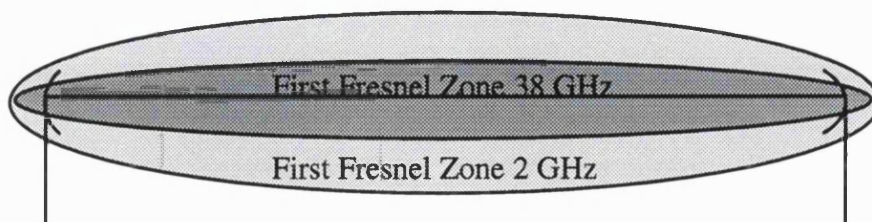
Diagram 1-5   The frequency dependency of the first Fresnel zone radius

Some research scientists believe that for microwave frequencies below 6GHz, 30% of

the first Fresnel zone should be clear for k values of 3/2, while for frequencies above

7GHz, 58% of the first Fresnel zone should be clear for a k value of 0.7 [19]. However,

the clearance required is determined by the average annual percentage of time that the radio system can be allowed to fade to the threshold value. ITU–R P.530–7 [17] suggests that in the absence of detailed local refractivity data, the antennas on a hop, which does not employ diversity, should be selected to allow the first Fresnel zone to be free from obstruction for a k value of 4/3. The Report also states that the effective k value, ke, exceeded for 99.9% of the time in a temperate climate should also be estimated from 'ITU–R P.530–7 Figure 2'. Using this value, in temperate climates, the direct path should be allowed to pass unobstructed over a single isolated obstruction. For a path with an obstruction which extends along a portion of the path, or for multiple obstructions, 30% of the first Fresnel zone should be clear when the profile is drawn using an effective k value, ke from 'figure 2'. For tropical paths with hop lengths longer than about 30km, 60% of the first Fresnel zone should be clear when using a ke value exceeded for 99.9% of the time, since ITU–R P.530–7 provides data which is valid for a temperate climate.
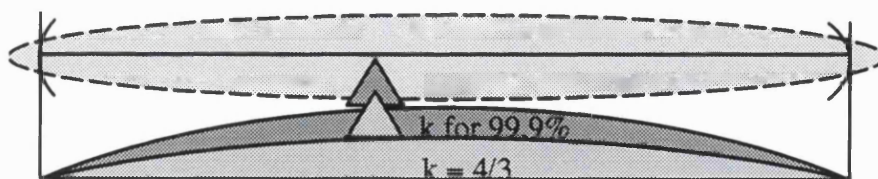
Diagram 1-6   Antenna heights, diffraction fading and the atmosphere

Over a twelve month period between February 1974 and January 1975 Vigants monitored a 4.13GHz, 38.9km path in Florida, USA. He identified diffraction fading, caused by obstructions of the path, greater than 35dB on four nights during the year [124]. The characteristic fading slope observed, for clearances less than half of the first Fresnel zone, was approximately 20dB for a reduction in clearance equivalent to the height of

the first Fresnel radius. Fading for obstructions in the range +0.5 to –1.5, relative to the direct ray, can be estimated from the expression [35][124].

$$L(a) = 10 - 20 (h / F1)$$
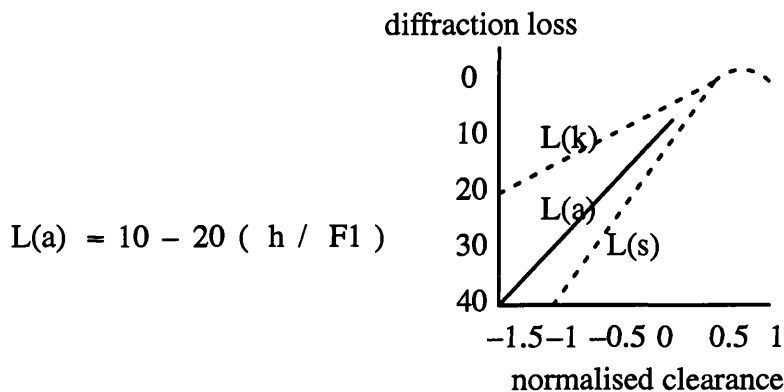
Formula A-13   Diffraction loss

Where L(a) is the loss in decibels, relative to free space loss, for average terrain, F1 is the radius of the first Fresnel zone in metres, and h is the clearance in metres, which is negative when the direct ray is obstructed. The values L(k) and L(s) represent the theoretical losses for knife edged and smooth obstructions respectively. This expression predicts that when antenna heights on a hop in average terrain, which have been selected using a ke value which allow the direct ray to pass for 99% of the time, the receive level should be greater than the normal fade margin less 10 dB for 99% of the time.

It has been suggested by Martin [2] that ITU–R P.530–7 greatly overestimates the period of time that the effective k value, ke, is less than 4/3, resulting in antenna locations which are too high. Vigants identified diffraction fading based on three criteria Firstly, depressed signal levels over a period of ten minutes, secondly, increased fading with decreased antenna height, and thirdly, a high degree of simultaneous fading on the upper receiving antennas [124]. However, Martin [2] has shown that not all fading attributed to obstructions is caused by diffraction fading. A stable reflective or refractive layer

could redirect two second signal towards the receiving antennas, and if both receiving antennas received secondary signals which were in antiphase to to direct signal the effect could appear like diffraction fading caused by obstructions on the path[2].

2.2.3   Statistical variation of k

The bending of microwave signals in the atmosphere is nearly independent of frequency [20]. For practical purposes bending can be considered as virtually independent of frequency when the gradient of refractivity does not vary significantly over a distance of one wavelength [15]. Ten years of data from Poland show that the value of k, in the lowest one hundred metres of the atmosphere, exceeded 0.55 for 99% of the time, was greater than 10 for 1% of the time [21]. The median value of k was shown to be 1.3 for the year, 1.41 for August, and 1.29 for February. The variability was found to be greatest in the summer, with k exceeding 0.36 for 99% of the time, while the least variability was seen in the winter time, with k exceeding 1.1 for 99% of the time in the winter months [21]. However, large local variations in the value of k over a height of a few tens of metres can distort the gross k value when it is averaged over the lower atmosphere at one location [2]. Therefore, this average value of k ,which varies at every point along a path, should itself be averaged over the path length, and this effective k value used in the design of radio links [35]. It has been reported that on a 55km path in the United Kingdom the effective k value was greater than 0.9 for 99% of the time, and that in Japan on a 112.7 km path the effective k value was greater than 0.99 for 99.9% of the time [35]. However, the report [35] does not state over what period of time the k value was measured in either case. ITU–R P.530–7 [17] presents a graph which shows the effective k value exceeded for 99.9% of the time in a continental temperate climate. The graph

shows that at 20km, 30km, 40km and 50km the effective k values are approximately 0.57, 0.67, 0.75, and 0.8 respectively. At 100km the effective k value is 0.93, and at 200km it is 1. Gradients of refractivity all over India have been found to be minimum during the monsoon period, and maximum in the pre–monsoon period, with variability greatest in the coastal regions [22].

2.2.4   Subrefraction

A standard well mixed atmosphere has an average refractivity gradient, or lapse rate, of −40N/km, which corresponds to a k value of 4/3 [13]. If the gradient is considerably greater than −40N/km the radio path will experience subrefractive conditions. [7]. Under subrefractive conditions the radio path becomes straighter, compared to its path in a well mixed atmosphere, and travels closer to the Earth. This increase in gradient is described by a corresponding reduction in the value of k. If the radio refractivity gradient was increased from its normal well mixed value of −40N/km to 0N/km there would no longer be a gradient to refract the microwave signal, the k value would be reduced to unity, and the signal would propagates in a straight line in the lower atmosphere. Continued increases in the gradient would cause positive values of radio refractivity per kilometre, represented as reductions in the value of k, to values less than one. A positive gradient, corresponding to k values less than unity produces a concave propagation pathway from the surface of the Earth [7].
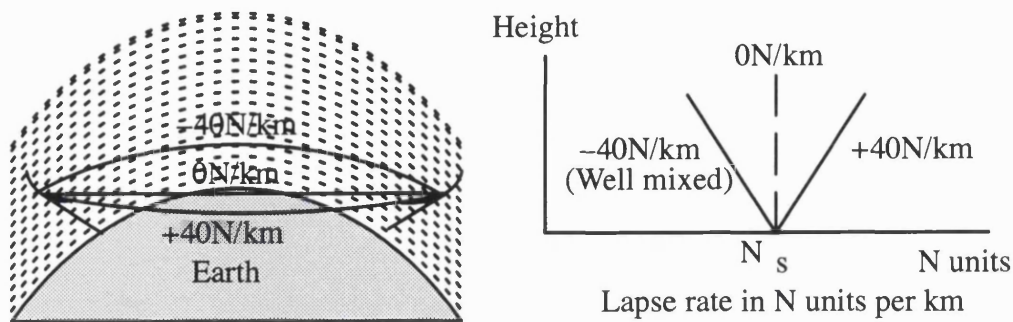
Diagram 1-7   **Propagation in standard and subrefractive conditions**

When the gradient becomes greater than –40N/km, with the associated straightening of

the radio path, the launch and reception angles at the antennas will change. This will

cause a reduction in the transmitted and received signal strength if the antennas are

aligned for maximum power under standard atmospheric conditions, although this

reduction in power is usually very small [1]. Also, the straightening of the radio path

under subrefractive conditions takes the signal closer to the Earth's surface, and can

cause diffraction fading. This is shown graphically by a reducing the k value, and caus-

ing the surface of the Earth to 'bulge' closer to the radio path, affecting free space propa-

gation, and eventually obstructing the path.
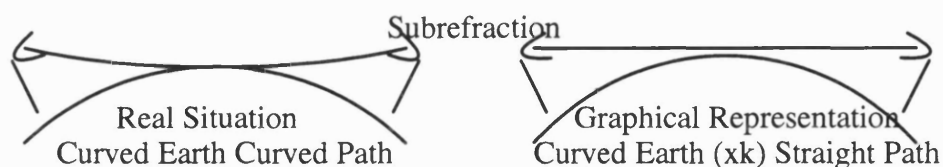
Diagram 1-8   **The path profile in subrefractive atmospheric conditions**

Frequently radio paths which have been designed to operate under subrefractive fading

conditions experience deep fades which last for hours [2]. On many occasions the fading

has not been caused by subrefractive conditions, but is due to a stable ground based layer

of air which is capable of causing a strong reflected or refracted signal to destructively interfere with the main signal [2]. Analysis has shown that when an atmosphere with a standard radio refractivity profile of k close to 4/3 rests on a stable ground based layer of air with a large gradient of refractivity, destructive interference at the receiver has the appearance of diffraction fading [2]. Therefore, it has been suggested that subrefractive conditions are not as common as is currently believed [2].

2.2.5   Superrefraction

When the gradient of radio refractivity is reduced substantially so that it is much less than –40N/km superrefractive conditions will exist [7]. The arc followed by the radio signal reduces in radius, and the k value increases [13]. This increases the clearance between the radio path and surface of a spherical Earth.
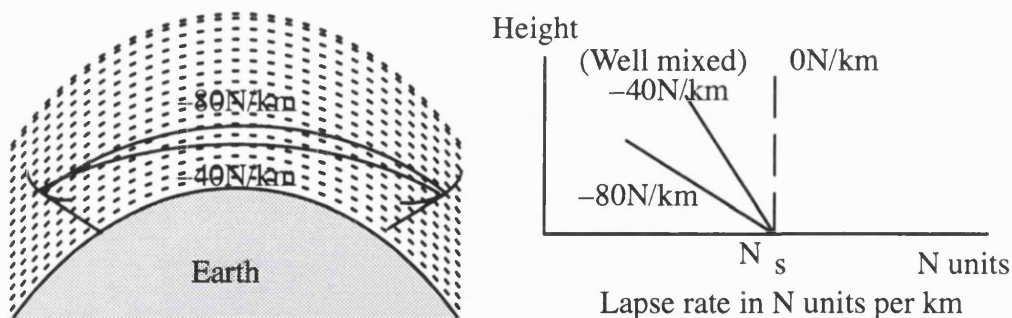
Diagram 1-9   Propagation in standard and superrefractive conditions

The increased curvature of the radio path causes the launch angle and the angle of arrival to change. If the antennas are aligned for maximum power during standard atmospheric conditions, there will also be a slight reduction in the effective transmitted and received power if the signal passes though a region with a strong negative gradient[1]. When the lapse rate is reduced to –157N/km, the arc of the radio path will have the same radius as the Earth, and the k value would have a value of infinity. This corresponds to a straight

radio path over a flat earth. Further reductions in the gradient of radio refractivity would cause the arc taken by the radio wave to have a radius less than that of the Earth, with a corresponding negative k value. Under these conditions ducting may occur. This is typically shown graphically as a straight line radio path, and the Earth's surface as being concave.

Superrefraction

Real Situation
Curved Earth Curved Path

Graphical Representation
Curved Earth (x4/3) Staight Path
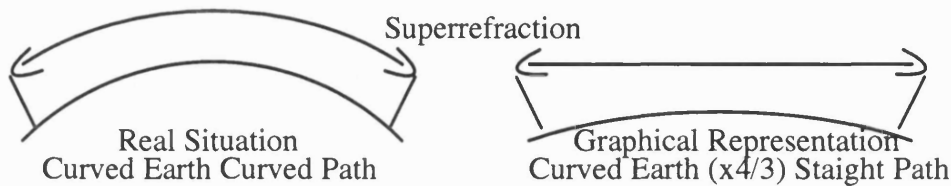
Diagram 1-10   The path profile in superrefractive atmospheric conditions

However, a strong superrefractive region is not likely to be present over the whole of the lower troposphere, and will be limited in length, width and height with the vertical dimensions of these layers usually confined to a few tens of metres[2]. Within a superrefractive region the arc followed by the radio signal will be reduced in radius, with a corresponding increase in the k value, but it is misleading to represent the whole of the lower troposphere as being very superrefractive by graphically representing the Earth as being nearly flat or even concave[2].

Superrefractive Layer

Earth

Misleading

Display

k = infinity
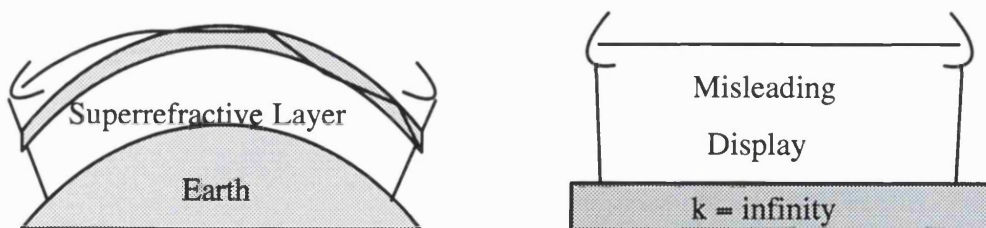
Diagram 1-11   A path profile in strong superrefractive conditions

2.2.6   Atmospheric layers

A well mixed atmosphere is created by convection, eddy turbulence, and molecular diffusion [23]. However, a stable atmosphere can suppress vertical motion of air [24], and subsidence can intensify the refractivity gradients near the surface [20]. Atmospheric layers affect the refractivity lapse rate, and inversions can form as a result of radiation nights, advection, subsidence, and frontal systems [7]. Radiation nights occur over land when a cold night follows a warm day, resulting in the surface of the Earth cooling and the air at the surface cooling down faster than the air higher up in the atmosphere, causing a temperature inversion. Advection is caused by high pressure systems moving land based warm dry air over cooler moist air above the sea, causing a temperature inversion. Subsidence is the descent of dry air in a high pressure system, that becomes heated by compression, and spreads out over cooler moist air causing a temperature inversion. Localised temperature inversions can also be caused by frontal systems driving cold air beneath warmer air. In valley regions the drainage of cold air from higher slopes can create multiple layers, and in coastal areas, land–sea breezes and trade winds can cause layers [22].
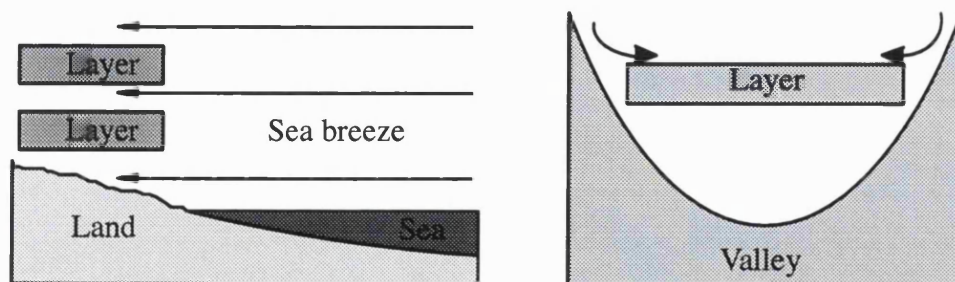
Diagram 1-12   **The formation of atmospheric layers**

Large daytime temperature inversions can also exist over a locally cool grey soil, when it is surrounded by a black surface which has been warmed by the sun [25]. In desert

areas, surface layers of air with large temperature gradients can form close to the ground [2]. Over large bodies of water the temperature may increase with height. The effects of temperature inversions are intensified by increased humidity near the surface [25]. The extent of these strong temperature inversions over the sea may be influenced by ocean currents, and/or ocean depth [5]. During the day solar radiation heats the land causing convection currents to mix the atmosphere, but after sunset convection stops and inversion layers are able to form [26]. Radiative cooling allows fog to form on still nights. A ground based inversion layer may followed the profile of the land and have a strong refractivity gradient which it was capable of reflecting the microwave signal [27]. Fog may also be associated with enhancements of over 20dB, which last for periods of 1 to 3 hours [28]. With subsidence, advection and radiative cooling there is a tendency for stratification of the lower atmosphere, and ducting layers with a refractivity gradient of −157N/km, or less, may be immersed in a broader region [5]. A sea breeze is capable of creating superrefractive elevated layers[29], and such layers are capable of defocusing the direct microwave signal if the layers were to cross the path at the antenna height[30]. Defocusing and fading can also be caused when convection currents force ground based inversion layers through the line of sight after sunrise [24].
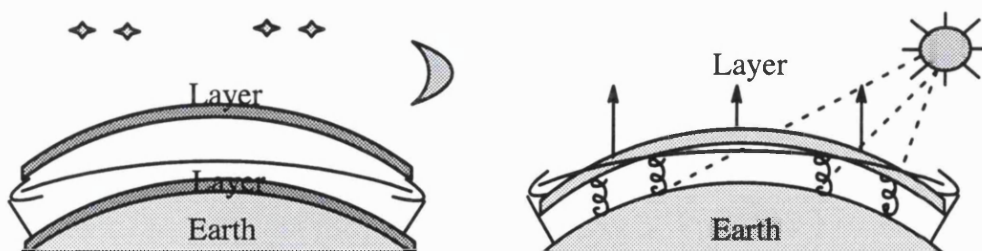
Diagram 1-13   **Convection forcing the ascent mixing of atmospheric layers**

When humid air settles above drier surface immediately above the Earth's surface re-

fractivity increases with height causing a positive refractivity gradient and subrefractive

conditions [124].

2.2.7   Fronts

Jones [31] refers to Kuhn and Ogulwicz [S1] who reported a rise in signal levels with

the passage of some warm fronts, and a drop in signal level with the passage of some

cold fronts. Jones analyzed the fronts using the two models, shown below, to predict

regions of superrefractivity at the base of a front, caused by subsidence. He observed

two three–hour periods of enhancement on a 66km coastal link in southern England

which he attributed to a kata type front. The first period was ascribed to subsidence

ahead of the warm front, and the second period was believed to be caused by the dry zone

behind the front. However, because of the great variety of frontal systems, it is not poss-

ible, at present, to predict their short–term effect on signals.
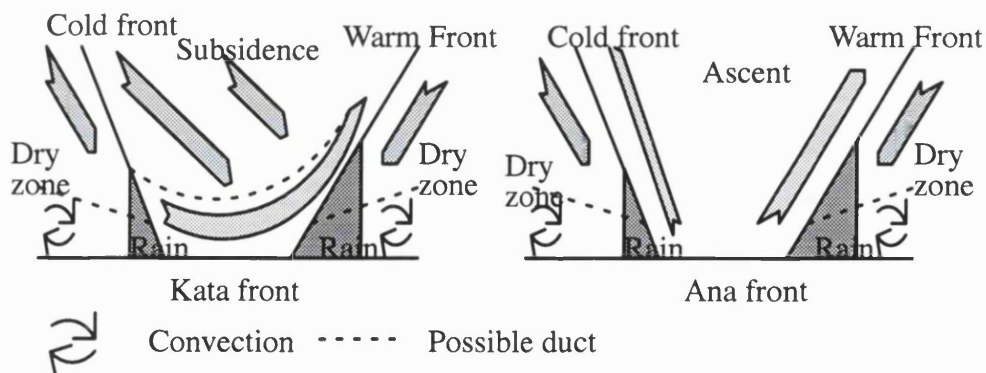
Diagram 1-14   Weather fronts

2.3   Atmospheric multipath

It is possible for several rays launched from a transmitting antenna to arrive at the receiv-

ing antenna after taking different routes though layers with different refractivity gradi-

ents [10][27].
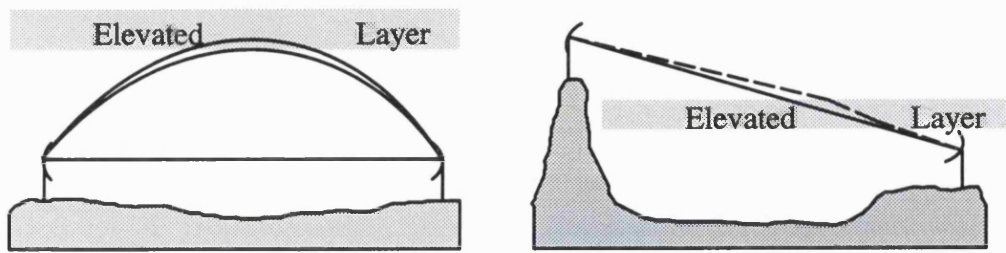
Diagram 1-15   Atmospheric multipath

When two signals arrive at the receiving antenna with half a wavelength phase differ-

ence fading will result [13]. If there are several independent secondary signals, the

resultant phase will be uniformly distributed between plus and minus 180 degrees [2].

The severity of the fading will depend on the amplitude of the resultant secondary signal

relative to the main signal [2]. If the resultant secondary signal has an amplitude 2dB

less than the main signal level the probability of fading will have a slope of 10dB a dec-

ade during the fading activity [2]. The probability of fading exceeding a given fade

depth depends on the percentage of time that fading is present in an area and the ampli-

tude of the resultant secondary signal during fading activity[2].

If a frequency range is swept, with a constant delay, the superimposition of two interfer-

ing signals will create a series of constructive peaks and destructive troughs as the delay

corresponds to inphase or antiphase conditions for the frequency used. Taking the ampli-

tude of the direct signal to be unity, and the second signal to have an amplitude, b, the

notch depth, B, relative to the flat fade level, will have an amplitude [13]

$$B \quad = \quad -20 \log_{10} (1 - b)$$

Formula A-14   Depth of a notch caused by a secondary signal at the receiver

which is termed minimum phase fading, as shown.

Longer delay   Shorter delay
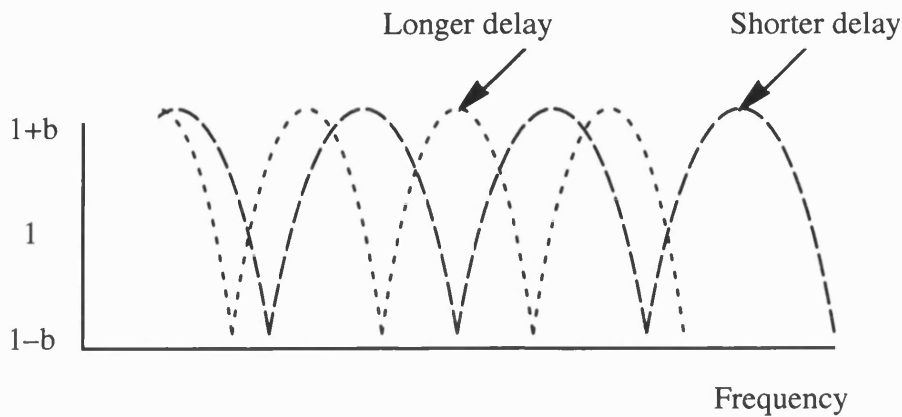
Diagram 1-16   Frequency, delay, notch separation and the two ray model

When the delayed signal, b, is larger than the direct signal, taken as unity, it is termed nonminimum phase fading, and the peaks have an amplitude b+1, and the troughs have an amplitude b–1.

When considering the superposition of the main signal and a single secondary signal the frequency separation between notches, in Hertz, is the reciprocal of the delay, in seconds, since the notch position is a function of wavelength and delay [2], An additional third signal, with an amplitude much weaker than the main signals, will not significantly effect the notch depth but may add ripples [32]. However, when several secondary signals arrive at the receiver the notch depth and position will depend on the amplitude and phase shift of the resultant secondary signal after superposition [2]. Ignatius Lam, and Webster [30] found that for stable multipath conditions in a swept frequency environment between 9.5GHz and 10.5 GHz two rays with comparable amplitude and a relative delay of 9ns caused nine deep notches over the 1GHz band.

The power received on a wideband system can be calculated by integrating over the whole bandwidth over a period of time [2]. Although fades caused by notches are limited

to part of the bandwidth, the signal can be seriously affected by the distortion caused by notches [7] . Continuous wave signals are only affected by the notch depth [2]. Narrowband digital systems have bandwidths that are small compared to the notches, and their performance can be approximated by flat fading [7]. Therefore, in the absence of interference the fade margin of a narrow band digital systems can be approximated from the thermal noise present, without considering the distortion caused by a notch [19]. For a given notch depth, and a given frequency distance from the notch, there is a critical flat fade level which if exceeded would result in a bit error rate greater than a specified error threshold [19][113]. A signature is the locus of the notch depths required to produce a specified bit error rate, when the relative delay, and flat fade margin have been fixed [7]. The area contained by the locus is the ability of the radio to withstand a notch, or its slope, within its bandwidth. Signatures are defined for minimum and nonminimum phases fades. Early demodulators behaved very differently to the two types of fading [7].
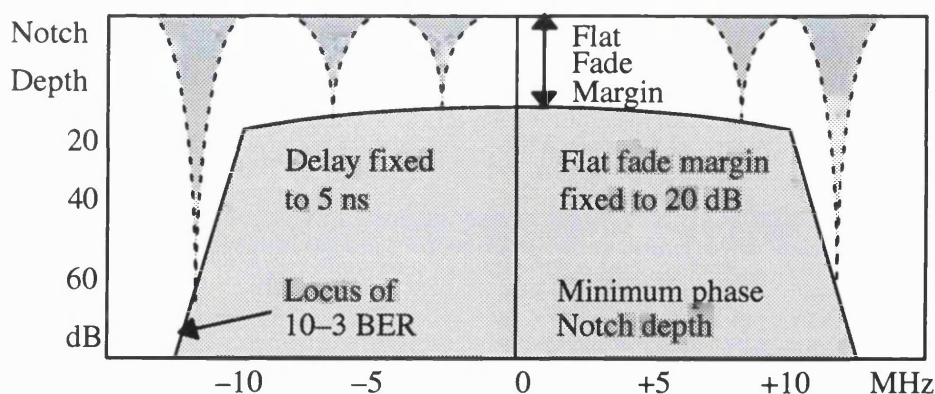
Diagram 1-17   The signature of a radio system

The notch moves when the medium changes the delay of the second signal, since this effects the difference in path length between the main and secondary signal [32]. On

a 35km, 11GHz overland coastal hop in Melbourne, Australia, notch speeds caused by atmospheric layers and surface reflections for 1% of the time reached 35MHz/s and 200MHz/s respectively [32]. An adaptive equalizer can reduce the effects of multipath if the response speed of the equalizer is suitable [32]. In a separate experiment two adjacent 6GHz, 40MHz wide channels on a 42km path were used to measure the notch speed [33]. It was found that notch speeds reached 60MHz/s indicating that the medium changed over a period of a few tens of milliseconds, which was slow compared to both propagation time and symbol rate [33], providing the opportunity to employ electronic countermeasures to compensate for distortions introduced by the notch into the received spectrum [130].
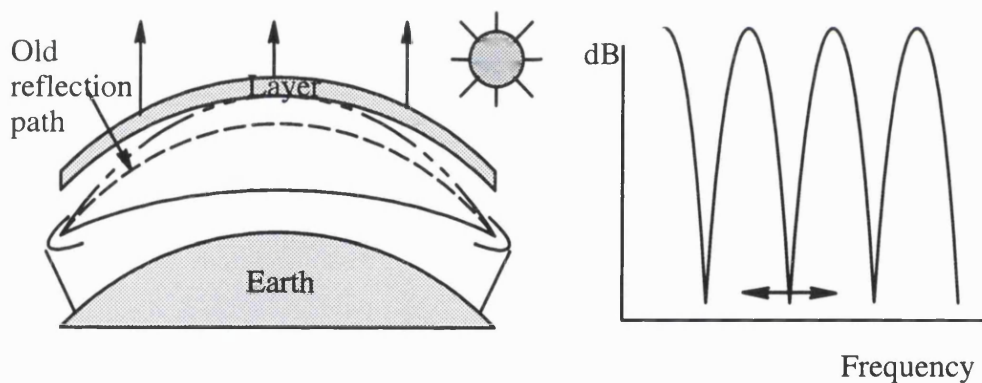
Diagram 1-18   Changes in layer height, multipath delay and notch frequency

In another experiment on a 50km hop the effects of multipath were found to be greatest when the transmitting and receiving antennas are at the same height [34].

2.4   Surface reflections

Radio paths which pass over reflective surfaces can cause constructive and destructive multipath interference at the receiving antenna [35]. Highly reflective surfaces in flat

humid areas, or over large bodies of water, can cause more fading than atmospheric

multipath, especially on short paths [35]. Snow, particularly after it has been melted and

frozen several times, is a very reflective surface[36]. Horizontally polarised microwave

signals are more likely to be reflected than vertically polarised signals [36]. Areas with

poor drainage may be subject to flooding and the potential for providing a highly reflec-

tive surface [1].

Weak surface reflection

Strong surface reflection
after rain / flooding
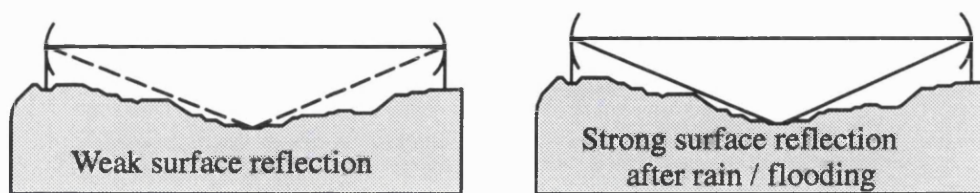
Diagram 1-19   Changes in reflected signal strength following rain or flooding

Severe fading occurs when the amplitude of the direct and reflected signals are similar

in amplitude, and are in antiphase [30]. When dealing with reflections from a highly

reflective surface a critical consideration is the grazing angle since this is related to the

reduction in received and transmitted power, relative to the direct signal, caused by an-

tenna discrimination [1]. The magnitude of the reflected signal depends upon the the

relative permittivity and conductivity of the reflecting surface, for the frequency con-

cerned, and the polarisation used [37]. Research has shown that there is 100% reflection

from sea water at 3GHz for both polarisations when the grazing angle is 0.001 degrees,

but when the grazing angle is increased to 5 degrees only 13% of the vertically polarised

signals power is reflected, but 100% of the horizontally polarised signals power is

reflected [37]. Thus a vertically polarised signal is less susceptible to destructive inter-

ference from ground reflections. For a vertically polarised signal the angle which corre-

sponds to the minimum reflected power amplitude is called the Brewster angle, and it is sometimes used to combat reflections over a highly reflective surface. However, the angles made at most reflective surfaces are less than two degrees, so that the use of the Brewster angle in hop design is rare. The phase shift associated surface reflection is polarisation dependent, but the total phase difference at the receiver also depends on the path length difference between the direct and reflected signals [37]. The loss in power at a reflective surface is also affected by surface roughness [30]. The ITU–R Report P.1008–1 [37] gives a measure of surface roughness, g. The surface is considered smooth when, g, is less than 0.3 [37]

$$g \;=\; 4\pi \left(\frac{S}{\lambda}\right) \sin \phi$$

Formula A-15   Surface roughness

where, λ, is the wavelength used, ϕ, is the grazing angle, and, S, represents the standard deviation of surface height about a local mean within the first Fresnel zone. If a surface is rough it has two components, one which is coherent with the incident signal, and one component which fluctuates with a Rayleigh distribution [37]. If no power is lost at the reflecting surface then the reflections from a rough surface can have a resultant secondary signal which is greater in amplitude than the main signal, depending on how the reflected components add together [2]. The position of the notch will continuously move, and depends on the resultant phase shift of the secondary signals [2]. When a surface is smooth there is only one reflected signal which can have a maximum amplitude equal to that of the main signal, if there is no loss in reflected power or divergence loss

[2]. The notch position is therefore stationary [2].
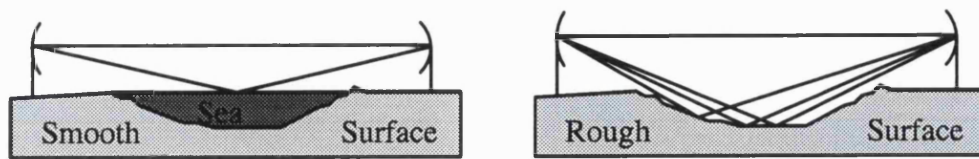
Diagram 1-20   Reflections from smooth and rough surfaces

Changing the antenna tilt can improve the performance of the radio when path geometry shows that the reflection point is on a highly reflective surface [17]. It may also be possible to use natural obstacles to prevent the reflected ray reaching the receiving antenna [35]. In the case of reflections from sea water tidal changes in the height of the water should be considered [1]. However care should be taken since meteorological changes can effect the refractivity gradient, and allow a reflected signal to avoid objects that would normally be obstacles under standard conditions [30].

Normal atmospheric conditions   Abnormal atmospheric conditions
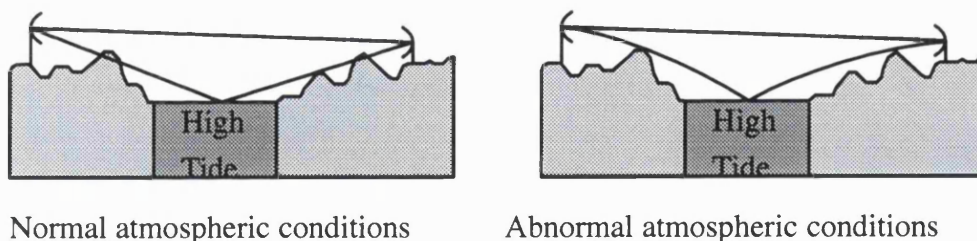
Diagram 1-21   Unobstructed surface reflections during abnormal conditions

2.5   Scintillations

Scintillations are caused by small scale inhomogeneities in the refractivity gradient [38]. Eddy currents are responsible for a turbulent atmosphere which can scatter microwave energy [39]. Convection currents create turbulence which allow pockets of air, at a temperature and humidity characteristic of their origin, to ascend into the atmosphere [135]. Since these pockets contain air with a different temperature and humidity the refractive

index is also different to the surrounding air [135]. At millimetric and microwave frequencies a signal which passed though these pocket might suffer from fluctuations in the received signal level, phase and angle of arrival at the receiver[135]. The intensity of turbulence can be related to the structure parameter of the refractive index $Cn2$, which is directly proportional to turbulent variations of the refractive index [135].
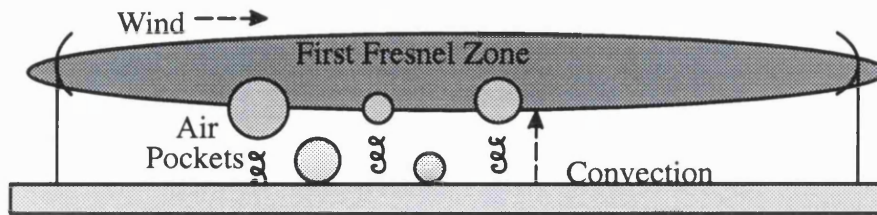
Diagram 1-22   Scintillations caused by air pockets crossing a radio path

Studies of turbulence have revealed that eddy currents range in size between an inner scale lo, and an outer scale Lo [135]. The inner scale is related to the dissipation of energy and the viscosity of air, while the outer scale depends on the input energy (usually solar) and the corresponding stability of the air [135]. In the troposphere the inner scale of turbulence is about 1mm and the outer scale varies between 10 metres and 100 metres [135].

The slow non–selective fading created by small scale inhomogeneities in the refractivity gradient is particularly evident above 10GHz [35]. These fluctuations are due to pure scattering, or a mixture of pure scattering and reflections [40]. In London, England, it was discovered that, in the absence of rain, maximum scintillation activity occurred at midday, with minimum activity between midnight and the early hours [41]. The difference in mean signal level depends on the variation of water vapour, the wavelength used, the path length, and the outer scale of turbulence [41][42]. Depending on the relative size of the outer scale of turbulence the scintillation variance on a line of sight path can

be expressed as

$$\sigma_X^2 = 23.17 \ k^{7/6} C_n^2 \ L^{11/6} \qquad \left(dB^2 \right) \quad L_o \gg \sqrt{\lambda L}$$

Formula A-16   **Scintillation variance related to the outer scale of turbulence (case 1)**

or alternatively as [135].

$$\sigma_X^2 = 29.49 \ k^2 \ C_n^2 \ L \quad L_o^{5/3} \quad \left(dB^2 \right) \quad L_o \ll \sqrt{\lambda L}$$

Formula A-17   **Scintillation variance related to the outer scale of turbulence (case 2)**

Where L is the path length in metres and k is the wave number

$$k = \frac{2\pi}{\lambda}$$

Formula A-18   **The wave number**

In temperate climates scintillation activity is usually maximum in the summer, and minimum in the winter, and may increase in regions of abundant water vapour [8]. However, in Riyadh, Saudi Arabia, scintillations and multipath occurred simultaneously, and were more common in the winter, when temperatures are typically around 15 degrees Celsius with a relative humidity between 50% to 70%, as opposed to the summer when temperatures can reach 48 degrees Celsius [43]. In addition to the commonly described dry scintillations, which occur in clear air conditions, scintillations have also been recorded in Riyadh, Saudi Arabia, during rainfall, and between rainfall events [43]. Between rain events the sun heats the Earth rapidly, which results in a steep change in the temperature and humidity profiles, and a greater variation in refractivity air pockets crossing the path, which cause scintillation [43]. During thunderstorms strong updrafts, and down-

51

drafts create turbulence which scatters microwave energy, and may cause scintillations

[43].
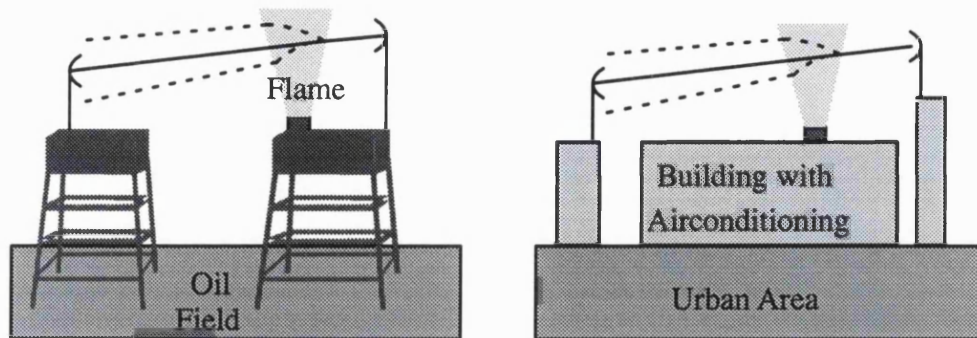
Diagram 1-23   Scintillations caused by a flame and by air conditioning plants

The affects of microwave propagation though a flame has been investigated for a range

of frequencies between 37GHz and 210GHz [44]. In the experiment, with the flame fill-

ing the first Fresnel zone, the heat envelope extended well beyond the visible flame. The

scintillations recorded for 37GHz, 57GHz, 97GHz, 137GHz, and 210GHz, were ,<0.1,

0.8, 1.5, 2.4 and 4.0 dB respectively on a 500m test site, demonstrating that the affects

of the flame were negligible below 40GHz. [44]. On a 4km link in London scintillation

caused a 1dB change at 36GHz, and a 3dB fluctuation at 110GHz [41]. However, it was

discovered that one airconditioning plant would increase fluctuations to 1.28dB at

36GHz, and to 4.56dB at 110GHz [41]. Scintillations between 0.5 and 6dB were found

on a 14km path operating at 40GHz in Riyadh [43].

2.6   Ducting

A horizontally launched microwave signal will have a radius of curvature equal to the

average radius of the Earth when the refractivity gradient of the atmosphere is −157N

units per kilometre. When the gradient is less than −157N/km the radius of curvature

is less than the average radius of the Earth, causing ducting [11]. Subsidence, advection,

and radiative cooling tend to stratify the lower atmosphere causing layers with a refractivity gradient less than −157N/km to be immersed in a broader region having a refractivity gradient greater than −157N/km [5]. Elevated ducts are caused by layers in the atmosphere with refractivity lapse rates less than −157N/km, which allows a microwave signal to be trapped, by alternatively bending the signal down at the top of the duct, and then bending the signal up at the bottom of the duct [4]. Ducts can also be found at the base of a weather front, caused by subsidence [31]. Surface ducts are caused by a layer in the atmosphere with refractivity gradient less than −157N/km will cause microwave signals to be bent down towards the surface of the Earth, where they may be reflected back towards the atmospheric layer again.[20].
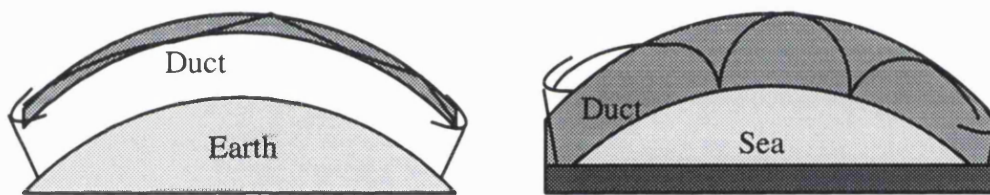
Diagram 1-24   Propagation in elevated and surface ducts

Frontal systems can create regions of superrefractivity in which ducting can occur [31]. Ducts can be expressed in terms of a modified refractivity, M, which is equal to radio refractivity gradient, dN/dh, plus 157 [25], where the modified refractivity will have a negative value whenever ducting conditions are present. Elevated and surface ducts can be described in terms of the change in modified refractivity gradient, M, with height, h, [5]

h ⟋
         d] D
   ΔM
m
Elevated duct

h ⟋
        d] D
  ΔM
m
Surface duct

h ⟋
       d|D
  ΔM
m
Surface duct
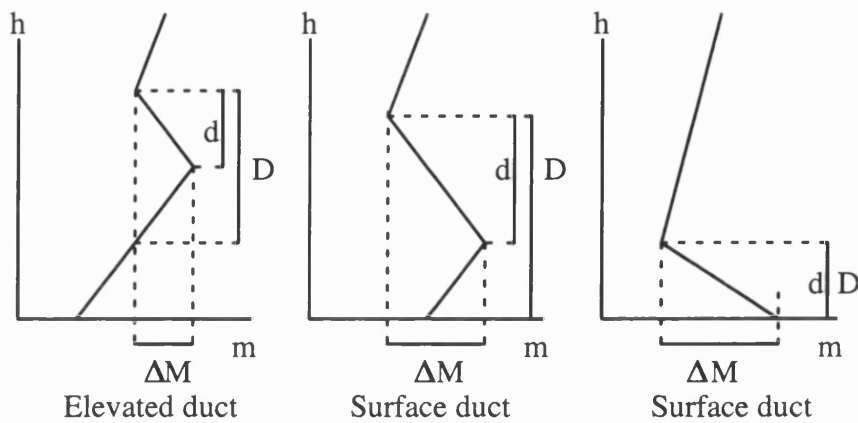
Diagram 1-25   Refractivity gradients in a duct

where, d is the ducting thickness, D is the ducting layer thickness, and ΔM is the duct intensity. Ducts are particularly common over the sea, or over flat humid land which is highly reflective, and last for several hours at a time [35]. Low wind velocity favours ducting conditions [23]. Ducts regularly form over areas of warm water, and the extent of ducting conditions over the sea may be related to ocean depth or currents, while their penetration inland depends on the direction of the wind, and coastal topography [5], as hills tend to break up layers as ducts move inland from the coast [3]. Some ducts allow several rays to be trapped, while other ducts can prevent the propagation of a given microwave signal, creating 'radio holes' which may cause fading greater than 30dB which can last for several hours [35]. When a signal is trapped in a duct, the radio horizon has no meaning and that microwave signals can travel over the radio horizon and may be a source of interference [22]. Ultra high and very high frequency television signals transmitted in Qatar arrive in Bahrain, after passing over the Earth's bulge, causing regulatory problems [23]. In free space the power density of a microwave signal is proportional to the reciprocal of the distance squared, but that when a microwave signal propa-

gates in a duct, the vertical spread of power is restricted causing the reduction in power

to be proportional to the reciprocal of distance [4]. However, the increase in amplitude

experienced in a duct, relative to free space propagation, is rarely greater than 30dB [20].

The transmission loss, L, experienced in a duct has been approximated by the express-

ion

$$L = L_{fs} - 10 \log d + A$$

Formula A-19   Loss experienced in a duct

where Lfs is the free space loss, d is the distance in kilometres, and A is an offset to ac-

count for attenuation mechanisms such as leakage due to irregularities, loss due to

ground reflection, and loss from the coupling of energy into the duct [15]. However, the

type of duct, the number of ducting layers, duct thickness, duct height, and turbulence

within a duct also influence propagation [15]. Ducts are not uniform in dimension, but

vary in height along their length [4]. Only paths with low elevation angles are subject

to ducting, that is paths with elevations less than half a degree [35], or one degree in cer-

tain conditions [3], are subject to ducting. However, ducts can be tilted by radiative heat-

ing [20], and the height of an elevated duct can move up and down depending on thermal

heating during the day [25]. If the terrain is flat the duct will follow the slope of the land

[15], and for ducting to occur, the angle of incidence, ϕ, should be less than a critical

angle, ϕc. For a simple case of a transmitting antenna situated within a horizontally

stratified surface duct with a normal refractivity profile above the duct, which has a fixed

refractivity gradient, the critical angle ϕc (rad) below which rays to be trapped, is [11].

$$\phi \quad < \quad \phi_c \quad - \quad \sqrt{2 \ |\Delta M| \ x \ 10^{-6} \ \Delta h}$$

Formula A-20   **Angles of incidence which allow signal to be trapped in a duct**

Where ΔM, is the gradient of modified refractivity across the surface ducting layer, and where, Δh is the thickness of the duct, which is the duct top above the transmitting antenna. For efficient coupling of energy into a duct the wavelength, λ, should be less than the critical wavelength, λc, [11]. However, there in no sharp cut–off frequency for a duct, only a slow transition between low and high leakage [4]. The energy coupled into a duct is not necessarily the main signal, and is a source of interference to other systems. Coupling by diffraction, and scattering should also be considered [20], and sidelobe coupling is also a potential source of interference [15].

2.7   Diversity

The effects of multipath propagation can be reduced by employing diversity. Since multipath is a function of frequency and path length two signals of different frequency which are subjected to multipath will experience different fading [13]. Performance can therefore be improved by simultaneously transmitting two different frequencies, and then selecting the best signal at the receiver [7]. However frequency diversity is not spectrally efficient since two frequencies are transmitted simultaneously and this should be avoided whenever possible [17].
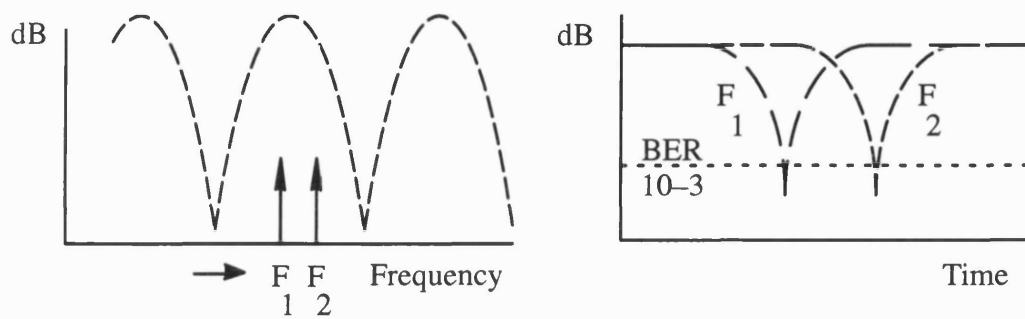
Diagram 1-26   Frequency diversity shown in the frequency and time domains

Space diversity operates by spacing two receiving antennas. When multipath is expected

from a highly reflective surface on a path, the antenna spacing should be based on path

geometry [35]. For frequencies above 3GHz the receiving antennas may be selected so

that one antenna is at the centre of an odd Fresnel zone while the other is at the centre

of an even Fresnel zone, when the edge of the Fresnel zone touches the point of reflection

[2].
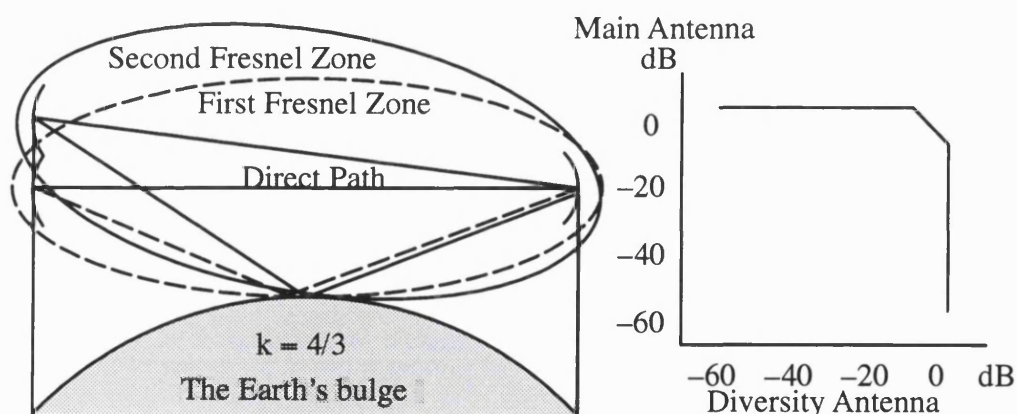
Diagram 1-27   Ideal space diversity separation

For reflection from a smooth surface this will provide the optimum antenna spacing.

Fading caused by reflections from a rough surface will depend on the relative phase of

the resultant secondary signals at the receiving antennas [2]. The secondary signals arriving at two space diversity antennas located at the centre of adjacent Fresnel zones will be very similar, but 180 degrees out of phase [2]. As the distance between the antennas increases the secondary component signals arriving at the two receiving antennas become increasingly dissimilar, and locating the antennas at the centre of even and odd Fresnel zones no longer guarantees 180 degree phase shift between the secondary signal [2]. However, although this techniques does provide a high diversity improvement it requires the antennas to be sited higher than would be necessary for diffraction fading.

When considering atmospheric multipath at frequencies above 3GHz it is common to separate the antennas by 150 to 200 wavelengths in the vertical plane [7], but a considerably larger separation is required in the horizontal plane [18]. An improvement in performance is achieved because the probability that both antennas receive signals of similar amplitude in antiphase to the main signal is less than the probability of just one antenna being in this situation [7]. However, strong superrefractive layers tend to form at the same height within a given region [2]. It has therefore been suggested that space diversity antennas should be located at the centre of adjacent odd and even Fresnel zones, assuming similar reflection/refraction of one secondary component from a superrefractive layer would leads to the secondary signals being shifted in phase by 180 degrees at the receiving antennas [2]. This approach assumes knowledge of the strength and height of the superrefractive layer, and that the refractivity profile of a standard atmosphere is present below the superrefractive layer [2]. It also assumes a single secondary signal, since two or more secondary signals of similar amplitude arriving at one receiving antenna would have a phase which depends on their superimposition, and this

resultant phase would no longer be 180 degrees out of phase with the other receiving antenna. With space diversity the receiving radio should select the best signal. When multipath interference is expected from both atmospheric layers and surface reflections a compromise spacing should be used[35]. In such a situation, and when the phase difference between the signals is not 180 degrees, the better signal may be selected, or the received signals may be combined.
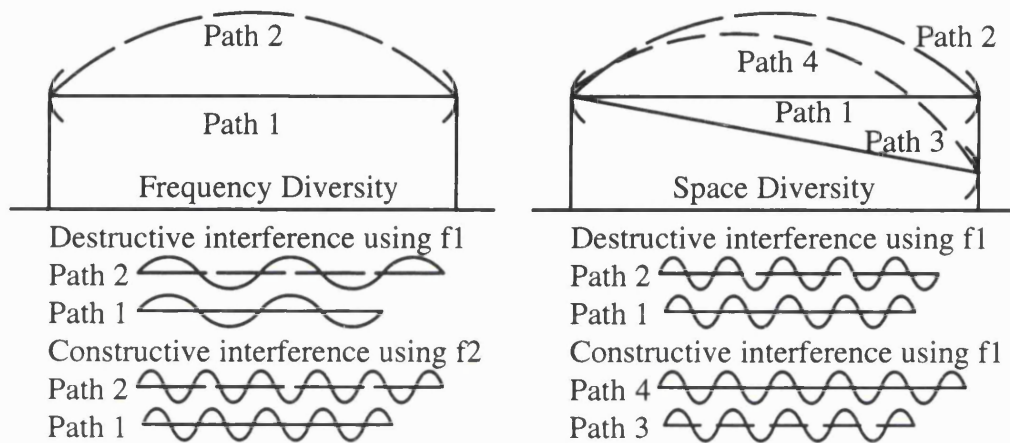
Diagram 1-28   **The principle behind the use of frequency and space diversity**

When the direct signal and an interfering signal arrive at the antenna with angular separation, it may be beneficial to tilt the antennas so that the difference in antenna discrimination is maximised [1]. By tilting the antenna, the main signal will be reduced in amplitude, but the interfering signal will be reduced in amplitude to a greater degree [7].
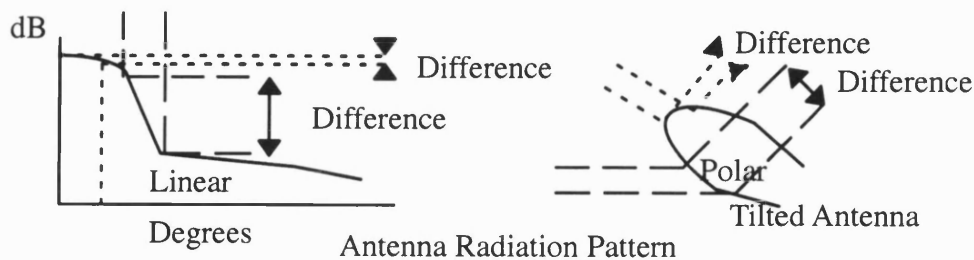
Diagram 1-29   **The principle behind the use of antenna tilting**

A diversity improvement similar to that of space diversity with 150 wavelength separation can be obtained from angle diversity, by placing two antennas side by side with a one degree difference in elevation [13]. Angle diversity provides an improvement because of the different angles of arrival. The multipath components add up differently in the two beams resulting in different frequency selective fading in the two beams [7]. By using one antenna with two beams separated by a small angle the wind loading on a tower can be reduced [7].
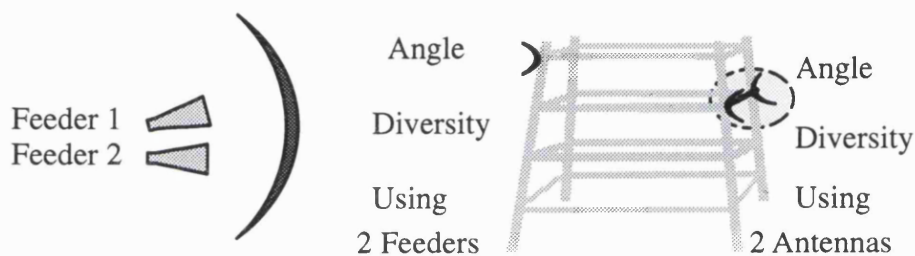
Diagram 1-30   Angle diversity using two antennas or one dual feed antenna

A small diversity improvement can also be achieved on digital radio systems by transmitting the same frequency with both vertical and horizontal polarisation, using different scrambling polynomials [1]. Vertical and horizontal signals are subjected to different phase shifts when reflected by a medium [37]. However, polarisation diversity is rarely used, and when it is employed it is usually combined with either frequency, space or angle diversity [1]. Polarisation diversity can be implemented using separate antennas or a dual polarised antenna to reduce tower loading.

To be effective a diversity switch should maintain frame alignment during switching, and ideally be error free [13]. Error free switching can be achieved by using parity bits within the radio frame structure to check the quality of the signal ahead of an elastic

buffer and diversity switch [1]. Some diversity switches select the stronger signal, while some wideband systems combine the two received signals to reduce the effects of dispersion caused by a multipath notch.

In general, antennas which are tilted towards the ground experience deeper fading, for a given percentage of time, when compared with those which are tilted upwards [35]. A combination of space and angle diversity, where the upper antenna is untilted and the lower antenna is tilted upwards, provides better fading and cross polar discrimination performance [35]. However, on paths over the sea where there is a strong stationary standing wave, a space diversity system can be improved by tilting the lower antenna towards the sea floor [35]. Finally, severe ducting can be tackled using two transmitting antennas which are separated by a large vertical distance [35], but this approach requires high, expensive towers.

2.8   The isotropic model

When a microwave signal leaves the radio it is subjected to losses, which can be expressed as

$$L_s = L_{bf} + L_z - (G_t + G_r) + F_t + F_r + A_t + A_r + L_{ct} + L_{cr} + L_a$$

Formula A-21   System loss
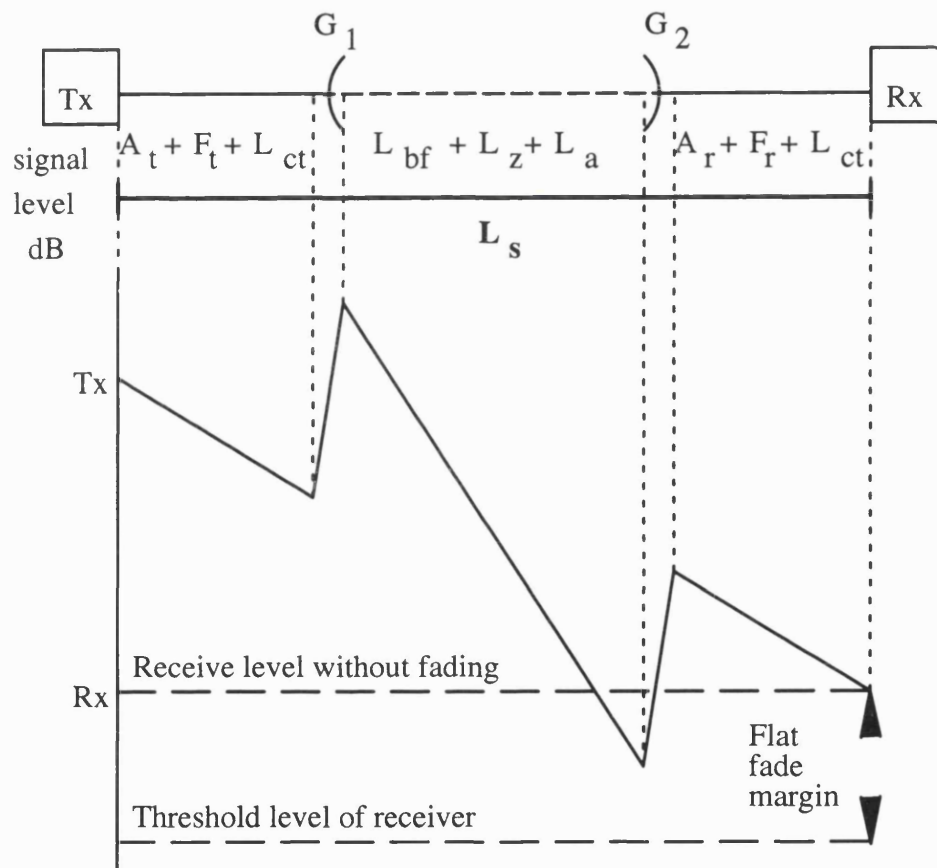
Diagram 1-31   The power budget and resulting fade margin

where, L_s is total system loss, L_{bf} is the free space loss in the far field, L_z is additional obstruction loss, G_t and G_r are isotropic antenna gains at each end, F_t and F_r are feeder losses at each end, A_t and A_r are antenna branching losses at both ends, L_{ct} and L_{cr} are connector loss at each end, L_a is atmospheric absorption at frequencies above 15GHz

[1]. Although it is possible to calculate the received power from the power flux density, with a knowledge of antenna beamwidth and path distance, received power can also be calculated using an isotropic reference, where the free space loss, Lbf is given by
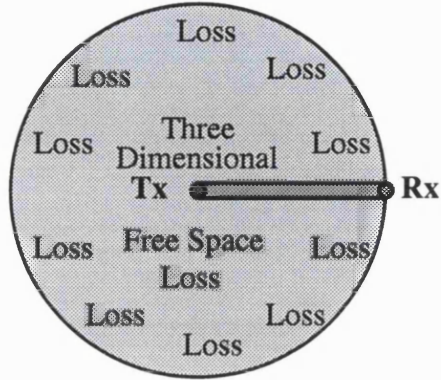
Free Space Loss L_{bf}

$$L_{bf} = 20 \log_{10}\left(\frac{4 \pi d}{\lambda}\right)$$

Using the Isotropic Model

Formula A-22   Free space loss

where, λ is the wavelength and d is the distance are in metres [45]. A more practical expression for free space loss, using frequency, f in GHz, and distance, d in kilometres is

$$L_{bf} = 92.45 + 20 \log_{10} d + 20 \log_{10} f$$

Formula A-23   A practical expression for deriving free space loss

When the transmission loss is defined in terms of the isotropic model, the free space loss and antenna gain must be considered together [46]. The gain, G, of a perfect antenna, relative to an isotropic antenna, is

$$G = 10 \log_{10}\left(\frac{4 \pi A_e}{\lambda^2}\right)$$

Formula A-24   Gain of a perfect antenna relative to an isotropic antenna

where A_e is the effective area of a uniformly radiating aerial [16]. However, the effective area of a parabolic antenna is a compromise between maximising the illuminated

63

area or the reflector, and minimising interference caused by microwave energy spilling over the edge of the reflector [7]. The efficiency of a parabolic antenna is also effected by surface irregularities, the shadow cast by the feeder on the reflector, and connector losses [45]. The maximum gain of an antenna, relative to an isotropic antenna, can be expressed as

$$G = 10 \log_{10}\left(\eta\frac{4\pi A}{\lambda^2}\right)$$

Formula A-25   Gain of a practical antenna relative to an isotropic antenna

where, A is the area of the antenna aperture, η, is the efficiency of the antenna [16], with typical values between 0.5 and 0.7 [1]. The maximum gain, and the radiation pattern is identical in the transmit and receive directions, which is in agreement with practice and the theory of reciprocity [16]. Finally, it should be noted that free space loss loss, L_{bf}, calculated for a path will only correspond to the real loss experienced by the system if the antenna is isotropic, and the power is radiated isotropically in three dimensions in a perfectly dielectric, homogeneous, isotropic, unlimited environment [46]. Similarly, an antenna gain specified in dBi for a given angle of radiation is an antenna gain in decibels relative to an isotropic radiating source [45]. Consequentially the isotropic model is only valid for real systems when at least 60% of the first Fresnel zone is clear from obstruction [17], and both antennas and the free space loss are considered together [45].

2.9   Signal outage

Modulators vary the amplitude, frequency or phase (or a combination of these) of a carrier signal according to the polarity of an incoming baseband signal. At the far end of the radio hop a demodulator converts these changes in the carrier signal back into a

copy of original baseband signal. A common method of modulation / demodulation used in radios systems is 4PSK, that is phase shift keying where two incoming binary bits are represented as one of four possible phases relative to the carrier signal. The incoming baseband signal is split into two parallel binary bit streams which control the phase of two generated waveforms. One of the signals is inphase with the local oscillator, is labelled 'I' and referred to as the cosine wave, the other has a ninety degree phase shift relative to the local oscillator so that its phase is in quadrature, labelled 'Q' and referred to as the sine wave [128]. In the absence of interference the bit error rate at the demodulator depends on the flat signal–to–noise ratio of the received signal relative to thermal noise, and on any distortion of the transmitted spectrum caused by the propagation medium [19].
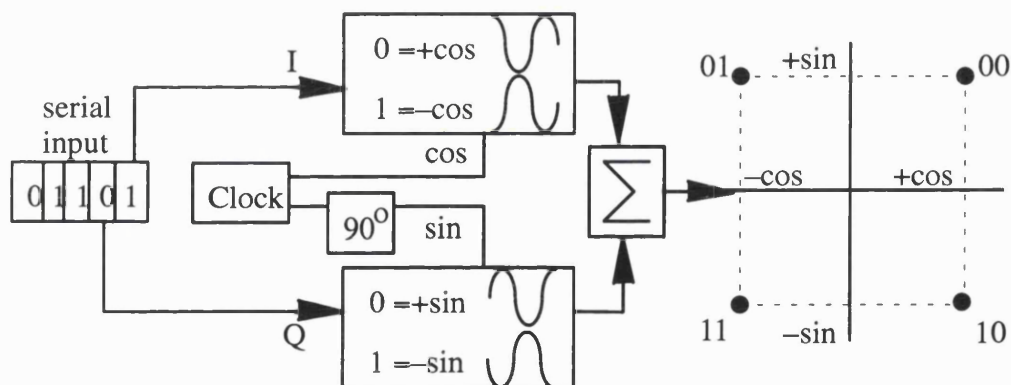
Diagram 1-32   A 4PSK modulator

Diffraction fading caused by obstructions on the path and attenuation caused by rain and other forms of precipitation are considered to be uniform across the transmitted spectrum [1]. Flat multipath fading is defined as flat across the transmitted spectrum [1]. Assuming linear amplifiers at the transmitting and receiving ends of the radio hop, these forms of fading will not distort the spectrum transmitted from the modulator, and in the

absence of interference, the bit error rate caused by these forms of fading is only a function of signal level relative to the thermal noise floor [1]. A 4PSK radio system typically has a signal–to–noise ratio of ten to one, that is the received signal is ten decibels stronger than the noise signal, for a bit error rate of one error in a thousand.

Changes in the phase of the carrier are created in the modulator by changing the period of the transmitted signal, and changes in the period of the waveform in the time domain correspond to a transmitted line spectrum in the frequency domain. The demodulator is designed to reproduce the original data stream from the received signal, which has been transmitted from the modulator. However, if the spectrum (which corresponds to a series or waves of varying period) at the demodulator has been distorted by selective multipath fading the original bit stream may not be reproduced at the receiving end [130]. Received power is integrated over the received bandwidth in a unit of time, and although a notch caused by selective multipath may not attenuate the received signal significantly the dispersion caused to the baseband signal may cause the radio link to perform below specified performance levels [1][19].
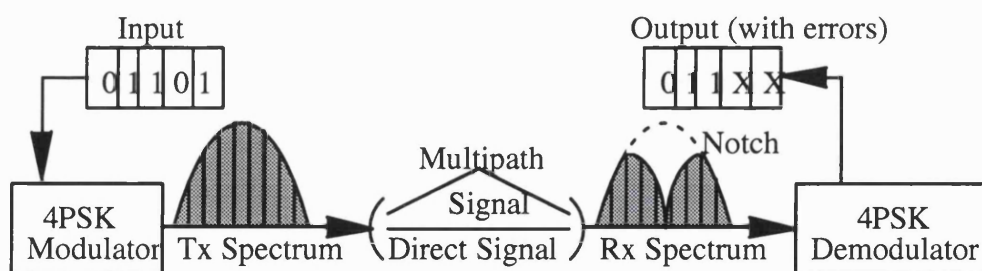
Diagram 1-33   Bit errors caused by selective multipath fading

The distortion introduced in the received signal can be compensated for by devices which produce complementary distortions such as space diversity combiners and time varying adaptive equalizers [130]. Forward error checking code add extra coding bits

to the incoming data stream at the transmitter which are used to enable the receiver to

identify errors, and correct these errors whenever possible [130][129].

2.10　Flat multipath fading model

ITU–R P530–7 [17] presents an expression which predicts the percentage of time,Pf,

that a large fade depths of A dB, is exceeded on a narrow band system during the worst

month of multipath activity. The formula is considered valid for hops between 7km and

95km for frequencies between 2 GHz and 37 GHz, and path inclinations between 0 to

24 milliradians [1][17], and fade depths greater than 15 dB [1].

$$P_f = K\ d^{3.6}\ f^{0.89}\ (\ 1 + |E|\ )^{-1.4}\ 10^{-A\ /\ 10}$$

Formula A-26　　**ITU–R P.530–7 worst month flat multipath outage prediction**

The formula is based on hop length, d in km, frequency, f in GHz, path inclination, E

in milliradians, and a geoclimatic factor, K. The lower frequency limit of validity, f(min)

is inversely proportional to the hop length, and can be estimated from the expression

[17]
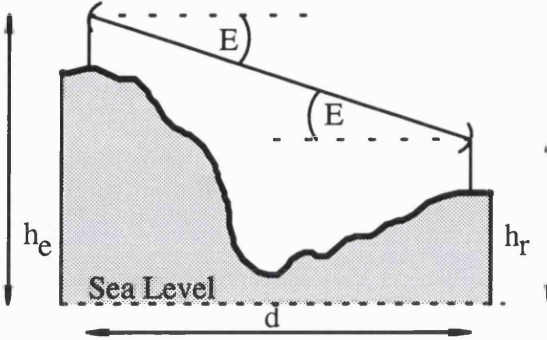
$$f(min)\ =\ \left(\frac{15}{d}\right)\ GHz$$

Formula A-27　　**Lower frequency limit of ITU–R P.530–7 flat multipath model**

where the hop length, d is in kilometres.

When the path length, d, in kilometres is known, and the antenna heights, hr and he, in

metres above a reference level are known, the path inclination, E, is given in milliradians

by the expression

$$|E| = \frac{|h_r - h_e|}{d}$$

Formula A-28   The path inclination

The geoclimatic factor, K depends on latitude, longitude, altitude, terrain, and the PL

value, which is the percentage of time that the refractivity in the lowest 100m of the

atmosphere is less than −100N/km [17].

$$K = 5.0 \times 10^{-7} \times 10^{-0.1(C_0 - C_{Lat} - C_{Lon})} PL^{1.5}$$

Formula A-29   The geoclimatic factor

Where the coefficient for longitude , C(Lon) are +3, −3, and 0, for Europe and Africa,

North and South America, and other longitudes, respectively. The coefficient for lati-

tude C(Lat) are given in the table [17].
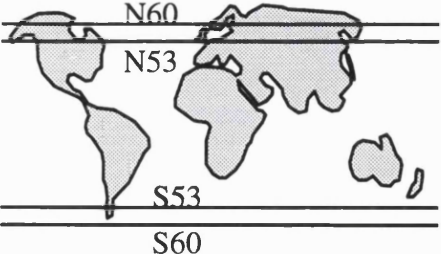
C_{lat}	Latitude
0	Between N53 and S53
−53 + Lat	Between 53 and 60 N or S
7	Greater than 60 N or S

Table 1-1   Latitude coefficients for flat multipath prediction, ITU model

For initial planning when the type of land is not known the coefficient for land type C(0),

depend on the height of the lower antenna, and when this antenna is below 400m above

sea level, between 400m and 700m, and more than 700m above sea level, the coefficients are 1.7, 4.2, and 8 respectively. [17]. When the type of land is known the corresponding coefficient C(0) can be found from ITU–R P.530–7[17]. The value of the climatic variable PL can be estimated by taking the highest value from the seasonal maps in the recommendation ITU–R P.453–6 [6].

On coastal links near or over large bodies of water such as The English Channel or the North Sea, where no measured data exists for the geoclimatic factor, K, it can be estimated from the expression.

$$K = 10^{(1-r_c)\log K_i + r_c \log K_{cl}}$$

Formula A-30   The geoclimatic factor used near or over large bodies of water

where r_c is the fraction of the path below 100m in altitude within 50km of coastline, assuming that there is no land above 100m between the coastline and the path, and the value K_i is the same as the K value calculated for paths over land. The parameter K_{cl} is given by the expression.

$$K_{cl} = 2.3 \times 10^{-4} \times 10^{-0.1C_0 - 0.011|\text{Lat}|}$$

Formula A-31   The K_{cl} parameter required near large bodies of water

If the parameter $K_{cl} < K_i$, the geoclimatic factor, K is taken to be K_i.

On coastal links near or over medium sized bodies of water such as The Gulf of Finland the geoclimatic factor, K, can be estimated from the expression (if no reliable measured data is available).

$$K = 10^{(1 - r_c) \log K_i + r_c \log K_{cm}}$$

Formula A-32   **The geoclimatic factor used near medium bodies of water**

and

$$K_{cm} = 10^{0.5(\log K_i + \log K_{cl})}$$

Formula A-33   **The K_{cm} parameter required near medium bodies of water**

In an area which is not coastal but there are a large number of lakes, such as inland areas

of Finland, the geoclimatic value should be calculated from the formula.

$$K = 10^{0.5[(2 - r_c) \log K_i + r_c \log K_{cm}]}$$

Formula A-34   **The geoclimatic factor used near large inland lakes**

2.11   Selective multipath fading model

The time delay of the secondary signal may be assumed to have a a negative exponential

distribution with a mean value, τm which depends on the path length and can be esti-

mated in nanoseconds from the formula [17]

$$\tau_m = 0.7 \left(\frac{d}{50}\right)^{1.3}$$

Formula A-35   **Mean time delay (nanoseconds) of a secondary signal**

where 0.7 is the mean relative delay for a standard 50km path, and the hop length, d,

is given in kilometres. The multipath activity factor η can be evaluated from [17]

$$\eta = 1 - e^{-0.2\,(P_O)^{0.75}}$$

Formula A-36   The multipath activity factor

and where

$$P_O = \left(\frac{K\,d^{3.6}\,f^{0.89}\,(1 + |E|)^{-1.4}}{100} \right)$$

Formula A-37   Parameter Po used to determine the multipath activity factor

The values for the geoclimatic value K, the path length d, frequency f, and path inclination are the same as those used in the flat multipath fading model. The probability, Ps, that a bit error rate is greater than a given threshold is caused by selective fading is given be the product of the multipath activity factor η, and the probability P(s/mp), that the bit error rate threshold was exceeded due to intersymbol interference during multipath fading [125] as shown

$$P_s = \eta\,P_{s/mp}$$

Formula A-38   ITU–R F.1093–1 worst month selective multipath prediction

If a system signature exists for the radio Ps can be found from the expression [17]

$$P_s = 2.15\,\eta \left(W_M \times 10^{-B_M/20} \frac{\tau_m^2}{|\tau_{r,M}|} + W_{NM} \times 10^{-B_{NM}/20} \frac{\tau_m^2}{|\tau_{r,NM}|} \right)$$

Formula A-39   ITU–R P.530–7 worst month selective multipath prediction

where W_M and W_{NM} are the minimum phase and non minimum phase signature widths in GHz, B_M and B_{NM} are the minimum phase and non minimum phase signature depths in dB, τ_M and τ_{NM} are the delays in nanoseconds used to obtain the signatures for minimum phase and non minimum phase signatures, and τ_m is the mean time delay in nanoseconds for the hop.

If system signatures are not available an estimate of selective multipath fading during the worst month can be obtained from the formula [125].

$$P_s = 2.16\eta \left(\frac{2\,\tau_m^2}{T^2} \right) K_n$$

Formula A-40   ITU–R F.1093–1 worst month selective multipath estimation

where T is the system baud period in nanoseconds, and K_n is an approximation for the normalised signature area. When no forward error checking codes or adaptive equalizers have been used K_n values of 1.0, 7.0, 5.5, and 15.4 may be used for 4PSK, 8PSK, 16QAM and 64QAM modulation methods respectively [125]. Adaptive baseband transversal equalizers improve system performance, and typically reduce the K_n to roughly one tenth of the values indicated above [125].

It is generally assumed that on radio paths longer than 40km, without strong surface reflections, that during deep fading the minimum phase notches and nonminimum phase notches are equally common [127]. On shorter hops, with more shallow fading, minimum phase notches are roughly four times more important than nonmimimum phase notches [127].

2.12 Total multipath fading

The total probability P of outage caused by multipath during the worst month of fading

can be calculated if the outage due to flat multipath fading, Pf , and the outage due to

selective multipath fading, Ps, are known from the following relationship[125]

$$P = \left(P_s^{\alpha/2} + P_f^{\alpha/2} \right)^{2/\alpha}$$

Formula A-41   ITU–R F.1093–1 worst month total multipath prediction

where α has a value between 1.5 and 2.

2.13 Fading due to hydrometeors

2.13.1 Variability of statistics

One of the most striking features of rainfall is its variability with time and location [49].

Dutton and Dougherty [49] used thirty years of data to improve the rainfall model devel-

oped by Rice and Holmberg [50]. However, both authors used round figures like total

annual rainfall, or total number of thunderstorm days to predict the percentage of time

that an area would have rainfall exceeding a given intensity. This approach is fairly accu-

rate for rainfall rates exceeding 0.1%, but for smaller percentages of time these models

overestimate rainfall [51]. The accuracy of the cumulative rainfall distribution depends

on how rapidly the rainfall was recorded and how stable the cumulative distribution re-

mains over time [52]. It has been suggested that long term records should be averaged

over 11 years , as records are cyclical in behaviour, and this is probably related to the

11 year sunspot activity cycle [134]. However, Crane [53] pointed out that when Suzuki

[S2] used 64 years of data for one site in Japan to identify a trend in rainfall activity

which was found to have a 10% to 20% root mean square variation about the trend.

Mooley and Crutcher [S3] used 130 to 150 years of rainfall data from eleven sites and

80 to 100 years of data were needed to smooth out long term variations [53]. Long term

records use data gathered from pulviometer float rain gauges, and since these gauges

utilize a pen and rotating drum the fine structure is lost and resolution is limited to 5 to

10 minutes. The long integration period used by pulviometers in Lae, Papua New

Guinea, underestimated the peak rainfall activity by a factor of 0.6 [54]. Cumulative

rainfall distributions averaged over different numbers of years will show slight changes

[55]. To estimate the attenuation distribution caused by rainfall with a 10% error, 1 year

of rainfall data is required for 0.1%, 2 years of data for 0.01%, and 10 to 15 years for

0.001% attenuation probability, for data gathered from one site [53]. In the absence of

suitable locally measured rainfall data, the ITU–R rainfall maps may be used [56].

2.13.2   Attenuation by rain

Ippolito [51] considers a plane wave, Pt, which has been transmitted from a point, T,

and is incident upon a volume of uniformly distributed raindrops of identical radius,

extending over a length L. The received power, Pr, is defined as

$$P_r = P_t \, e^{-\alpha L}$$

Formula A-42   **Received power after propagation through uniformly distrib
uted drops of identical radius extending over a length L**

where α is the attenuation coefficient. Attenuation, A, can be expressed in terms of decibels as

$$A = 10 \log_{10} \frac{P_t}{P_r} = 10 \log_{10} e^{\alpha L}$$

Formula A-43   Attenuation in dB produced by uniform, identical rain drops

or in natural logarithms as

$$A = 10 \log_{10} e^{\alpha L} = 10 \log_{2.718} e^{\alpha L} \left(\log_{10} 2.178 \right) = 4.343 \; \alpha L$$

Formula A-44   Attenuation in natural logarithms

The attenuation coefficient, α, is

$$\alpha = p \, Q_t$$

Formula A-45   Attenuation coefficient for a uniformly distributed raindrops of identical radius

where, p, is the drop density per unit volume and, Q_t, is the attenuation cross section of the drops. The total cross section Q_t is the sum of Q_a and Q_s, where Q_a is equivalent to the power absorbed by the drops when they are irradiated by a plane wave of unit power per unit area, and Q_s is equivalent to the power scattered in all directions from the drops, when irradiated by the same unit plane wave. Q_t is a function of the drop radius r, the wavelength of the incident wave λ and the complex refractive index of the water drop, m. Since real rain does not have a uniform drop radius, the attenuation coefficient, α, must be determined by integrating over the entire range of drop sizes.

$$\alpha \ = \int Q_t \ (\ r, \ \lambda, \ m \ ) \ n \, (r) \, dr$$

Formula A-46   **Attenuation coefficient for homogeneous rain filled medium consisting of a range of drop sizes**

where n(r) is the drop size distribution, with n(r) dr the number of drops per unit volume

with radii between, r, and, r + dr.

Oguchi [57], expresses specific attenuation in decibels per kilometre is as.

$$A \ = \ 4.343 \ x \ 10^3 \int Q_t \ (\ r, \ \lambda, \ m \ ) \ n \, (r) \, dr \ (dB \, / \, km)$$

Formula A-47   **Specific attenuation for a homogeneous rain filled medium consisting of a range of drop sizes**

This equation can be solved using the classical scattering theory of Mie, which requires Q_t and n(r) in terms of drop size. Mie theory assumes that each drop is illuminated by a plane wave, drops of equal size are uniformly distributed, and that the distance between the drops is large enough to avoid interaction [58]. The relationship between the attenuation cross section Q_t, and the forward scattering function, Re {S(0)} is [38].

$$Q_t \ = \ \left(\frac{\lambda^2}{\pi} \right) \ Re \ \{ \ S(0) \}$$

Formula A-48   **Total attenuation cross section in terms of the forward scattering function**

The complex forward scattering function, S{0}, is given by

$$S(0) = \frac{1}{2} \sum_{k=1}^{\infty} (2k+1)(a_k + b_k)$$

Formula A-49   The complex forward scattering function

where ak, and bk are the Mie coefficients which depend upon frequency, sphere radius, and the complex refractive index of water [58]. The resulting series expansion solution for Q_t is[51].

$$Q_t = \left(\frac{\lambda^2}{2\pi}\right) \sum_{k=1}^{\infty} (2k+1) \ \text{Re} \ (a_k + b_k)$$

Formula A-50   Total attenuation cross section in terms of Mie coefficients

Olsen, Rogers, and Hodge [114] presented a power law approximation for specific attenuation in terms of rainfall intensity R,

$$A = a R^b$$

Formula A-51   Power law approximation for specific attenuation

and defined the parameters, a and b, for spherical drops. However, since these parameters were defined for spherical drops they are polarisation independent. Fedi [59] presented the values of, a and b, [S4] for vertical and horizontal polarisation, assuming a Laws Parsons [122] drop size distribution, the terminal drop velocity developed by Gunn and Kinzer [115], refractive index of water at 20 degrees Celsius according to Ray [116], and oblate drops defined by Oguchi and Hosoya [S5]. Fedi [59] reports that these values agree with the experimental values developed by Harden, Norbury, and White

[S6]. The values of the parameters, a and b, may also be derived for a mixture of spherical and oblate drops [60]. Values of, a and b, for vertical and horizontal polarisations can also be found in ITU–R Recommendation 838 [61]. Watson, Ahmed, and Papaioannou [62] write that the power law approximation is only valid for a uniform rain medium and that net path attenuation An, can be derived from the integration of specific attenuation expressed in terms of position x, along the path length L.

$$A_n = a \int_0^L R(x)^b \, dx$$

Formula A-52   Attenuation derived from integration of the specific attenuation along the path

Such detailed knowledge is rarely available, so a common approach is to multiply the result from the power law equation by an effective path length, Le, to take account of spatial averaging [17].

$$A_n = a R^b L_e$$

Formula A-53   Attenuation derived by multiplying the specific attenuation at one point by an effective path length

Spatial averaging could also be achieved by applying a reduction coefficient to the measured point rainfall rate [7].

2.13.3   Drop size distribution

During 1938 and 1939 Laws and Parsons [122] measured the drop size distribution of rainfall in Washington D.C. by exposing 25cm diameter pans containing a 2.5cm deep base of flour to the rain for periods of a fraction of a second to several minutes, depend-

ing on the intensity of the rainfall. The flour pellets which formed were passed through a series of sieves, after they were dried in an oven, and organised in a number of classes. The classes where weighed and the weight was divided by the number of pellets in the group in order to find the average weight. By creating a number of drops of known diameter, and finding their average weight, it was possible to convert the cumulative distribution of pellets into a cumulative distribution for the volume of rain contributed by a given interval of drop sizes at different rainfall rates [122]. Unfortunately the relationship between the mass of the drop and the mass of the pellet varied with the mass of the drop. The authors present a graph showing the relationship between drop mass and pellet mass, but the smallest reliable drop they were able to reproduce had a mass of approximately 1.3325mg, a pellet mass 1.3mg and a spherical diameter of 1.36528mm. However the authors presented the drop size distribution for drops as small as 0.5mm diameter, by extrapolating the measures ratio of drop mass to pellet mass down to a ratio of 1:1 which should have occurred for drops with a 1.24mm diameter, and then further assuming that ratio of 1:1 for drops with a diameter less than 0.5mm. Data for drops smaller than this were derived by prediction.

In temperate climates the Laws and Parsons distribution is adequate, when dealing with frequencies below 40GHz [20] [5], but it does not model diameters less than 1mm well. [5]. Good agreement with the Laws and Parsons distribution was found for widespread rainfall on a 4km path in London [41]. Research carried out in Germany using an electrostatic method to measure the drop size distribution found similar results to those of Laws and Parsons for rainfall rates greater than 1.25 mm per hour [117], and this distribution is normally used as a good average for both widespread and convective rainfall [57]. However, evidence suggests that in tropical climates the Laws and Parsons distribution

79

may overestimate both small and large drops [65].

Marshall and McK Palmer developed a negative exponential equation to describe the raindrop size distribution, based on their own research, which was similar to the Laws and Parsons distribution [137]. However, the Marshall Palmer and Laws and Parsons distribution are only accurate for a drop size distribution above 1mm [64]. Marshall and Palmer gathered their data in Ottawa, Canada using a filter paper technique [137]. Similar studies deriving drop size distributions from filter paper have found that the thickness of the dried blots varies with different size drops and that paper should be stored at a controlled humidity [122]. The sensitivity of the filter paper also limits the accuracy of results for drops below 0.4mm diameter [66]. Since the Marshall Palmer distribution is exponential there is a rapid increase in the number of small drops as the diameter tends to zero, which causes errors in the rainfall rate [57][58]. Therefore it is only valid for a specified range of diameters [67]. The Marshall and Parlmer distribution is simple but it overestimates both large and small drops[68].

Joss, Thams and Waldvogel [118] reported a considerable variation in the drop size distribution for different types of rain. Their results indicate that drizzle and widespread rain are stratiform in nature and are characterised by small drops, while thunderstorms are convective in nature and are characterised by a higher percentage of large drops [57]. As a result of their finding they defined three different raindrop size distributions [118]. However, some research suggests that the Joss thunderstorm distribution overestimates small and large drops, and is inadequate for tropical thunderstorms [65].

Harden, Norbury and White [63] proposed the lognormal distribution for describing the raindrop sizes. The ability of the lognormal distribution to limit the number of small drops increases the accuracy of rainfall attenuation models at frequencies above 30

GHz, compared to the Marshall Palmer distribution [58]. One study in tropical climates showed that the lognormal distribution behaved well, when describing showers, thunderstorms, and widespread rainfall, and outperformed the Laws Parsons, Marshall Palmer, and Joss distributions [65]. Another report showed that in tropical climates the lognormal distribution performed well, and better than the Marshall Palmer distribution [68].

Distributions which are used less often include the gamma distribution, the Ajayi Olsen distribution, and Weibull distribution.

2.13.3.1 Processes affecting the drop size

The type of precipitation leaving the cloud base depends on the conditions within the cloud. Clouds can be classified as glaciated clouds, cold clouds and warm clouds [69]. The temperature in glaciated clouds is below minus forty degrees Celsius with ice crystals in high cirrus clouds producing precipitation which rarely reaches the surface, but the glaciated part of a cumulus cloud may act as a nuclei. The temperature in cold clouds is between minus forty degrees and zero degrees Celsius and condensation produces both water droplets and ice crystals. When the cloud is close to saturation, ice crystals grow at the expense of water droplets. The ice crystals then collect together to form snowflakes which fall and may melt, depending on temperature of air layers between the cloud base and and the ground. Warm clouds have temperatures above zero degrees Celsius and condensation produces water droplets. When the drops have sufficient mass they will overcome the lift supporting the cloud and fall. Larger drops have a greater terminal velocity than smaller drops and collision occurs if a small drop is close to the axis of fall of a larger drop. After collision the drop will grow in size if the two drops

coalesce, which happens most readily if the two drops are of considerably different size and this is related to the range of cloud condensation nuclei. In addition to condensation and coalescence, the breakup of large unstable drops and also binary drop encounter, where several small drops are created with no noticeable change to the parent, also effect the drop size distribution [57]. The humidity of air layers determines the evaporation that will take place, while that fall velocity effects the time that the air layers have to act on the particles [63][69][70]. Both these processes effect the drop size distribution, especially the number of small drops. Sand and dust from land and salt crystals from sea spray can act as cloud condensation nuclei and this explains why marine clouds have a wider range of droplets but fewer droplets per unit volume compared to continental clouds [69]. Atmospheric turbulence is another mechanism which effects the drop size distribution [53][63]. Joss, Cavalli and Crane [S7] noticed that in an updraft area there was a relative increase in the number of small drops [53]. However, wind sorting of this nature is transient, existing horizontally over a distance of around 100 metres, and these effects are rare and can be neglected [53]. Atlas and Plank [123] noticed a relative increase in the number of large drops at the leading edge of a shower in Washington, Massachusetts. They suggest that the larger drops had originated from the centre of the cloud when the cloud was closer to the measuring station on the ground, and that the smaller drops originated from the edge of the cloud a greater distance away. The small drops had therefore been airborne outside the cloud–base for a longer period of time and subjected to evaporation for a longer period. The drop size distribution at the ground consisted of raindrops released from the cloud–base at different times and points in space, with trajectories which terminated at the measurement station at a given time.

2.13.4   Drop shape

Jones [136], arranged two orthogonal cameras in the horizontal plane and found that the ratio of vertical diameter to horizontal diameter ranged between 0.6 and 1.2 [57]. Ugai, Kato, Nishijima, Kan and Tazaki [S8] used one camera, and found that the ratio of vertical diameter to horizontal diameter ranged between 0.75 and 1.0 [57]. The shape of falling drops can be calculated from an equation describing the balance of internal and external pressure on the surface of a drop [57][126]. Pruppacher and Pitter [126] modified existing pressure measurements on rigid spheres, and existing balance equations, to develop a model which describes drop shape as a function of drop radius. They acknowledged in their work that the internal circulation within drops effects their curvature and deforms the drops, and further pointed out that the original balance equations, which they had modified, had not taken this into account. However, they compared their theoretical results with their own photographs of drops in a wind tunnel and photographs taken by Pruppacher and Beard [131] and found good agreement with all but the largest drops, whose deformation they had slightly underestimated. Pruppacher and Pitter [126] found that drops with radii less than approximately 0.17mm were very slightly deformed but could be considered spherical, however drops between about 0.17mm and 0.5mm radii where asymmetric oblate spheroids, and drops with a radius greater than 2mm developed a concave depression in the base.

While spherical drop shapes were used in early work, the electrical characteristics of larger drops are different in the vertical and horizontal planes [67] and the shape defined by Pruppacher and Pitter [126] or the oblate shape defined by Oguchi [S9], which are easier to model, are more accurate when modeling microwave propagation [51]. Although the work of Pruppacher and Pitter [S20] was carried out in the laboratory and

did not take account of internal circulation, the results are accurate [5][57].

Drops with a radius greater than 4.0mm are hydrodynamically unstable and will break up [57]. However, before they break up large drops assume a variety of shapes [58].

2.13.5   Canting angle

The axis of symmetry of a non spherical rain drops is always parallel to the airflow around the drop, and the direction of the airflow can be defined with vertical and horizontal vectors [119]. The vertical vector referred to the fall of the drop, and the horizontal vector referred to the horizontal wind speed, which is a laminar, and may be expressed in the lowest 300 metres of the atmosphere in terms of height above the ground and the roughness of the terrain [119]. The important point is that the horizontal vector changes with height, if it was constant the drop trajectory would be inclined but the airflow relative to the drop would be vertical. The canting angle increases with drop size and also with proximity to the ground [119][57]. Wind has been identified as the main cause of raindrop axis inclination [71], with the distribution of canting angles determined by wind gusting [57]. The affect of the canting angle on depolarisation will be covered later in the material.

2.13.6   Terminal velocity

The terminal fall velocity of rain drops depends on air pressure, humidity and temperature [57]. If the terminal velocity is known, the drop size distribution in a three dimensional volume can be calculated from the drop size distribution on the ground. Most research work assumes a terminal velocity based on the work of Gunn and Kinzer [115] or Kerr [120]. In fact the terminal velocity figures attributed to Kerr [120] are presented in chapter eight, on page 679 of that excellent book, which was edited by Kerr (Kerr was

also one of the co–authors), in a section written by Herbert Goldstein, who acknowl-edged that the figures were reproduced from the figures presented by Best [S17] seven years earlier. Gunn and Kinzer [115] conducted their research in quiet conditions in the laboratory. The air pressure and temperature were constantly changing during the experiment, modifying the density of the air though which the drops were falling. There-fore a correction for density variation was made, and the results were published for stag-nant air at a pressure of 1013 milliBars, with 20 degrees Celsius ambient temperature and 50% relative humidity [115].

2.13.7   Dielectric properties of water, snow, ice

Dielectric properties depend on temperature and frequency and at microwave fre-quencies electrolytes in the water are not significant [57]. When the wavelength being used is greater than 1mm, the dielectric properties are due to the polar nature of the water molecule, but when the wavelength used is less than 1mm, the dielectric properties de-pend on the resonant absorption in the molecule [57]. The complex refractive index of water, and consequentially the attenuation coefficient, are effected by temperature changes [73]. A falling drop, at a given ambient temperature, pressure and humidity, will have a temperature which approximates to the wet bulb temperature [5]. However, the variation of specific attenuation with temperature is only noteworthy below 15GHz and significant between 4GHz and 6GHz where attenuation is low [57]. The dielectric constant of snow is quite variable and depends on the water content [57].

2.13.8   Shape, velocity, size of snow and ice

Pruppacher and Klett [S10] found the maximum diameter of a snowflake to be 15mm and most flakes to be between 2mm and 5mm, with a fall velocity that increased with

mass [57]. Magono and Nakamura [S11] used a camera to check the ratio of vertical diameter to horizontal diameter and found that for diameters less than 10mm the ratio was unity, while for snowflakes with a diameter greater than 10mm the ratio was 0.9 [57]. Fall velocity was shown to depend on water content and could reach 5 or 6 metres per second.

2.13.9 Rain types

When air becomes saturated water vapour condenses and clouds are formed, but the type of clouds depend on the processes which have brought the air to saturation [69]. Rain found around the world is of two basic types, stratiform and convective [74], although some researchers have sub–categorised rain as drizzle, widespread rain, showers, and thunderstorms [67]. Convective rain is seen by radar as a column of enhanced reflectivity, and stratiform rain is characterised by a bright band around the zero degree Celsius isotherm [5]. Monsoon activity is seen as bands of intense convection followed by bands of stratiform rain [5] and need to be treated with caution when considering attenuation caused by monsoon rainfall at frequencies as low as 7GHz [7].

2.13.9.1 Stratiform

Stratiform rain is widespread, covering thousands of square kilometres and always start from snow crystals [73]. The vertical motion supporting the cloud is weak and the particles start to fall to the ground almost from their formation [74]. Particles initially grow by joining together. When supercooled water droplets come into contact with the crystals they immediately freeze around the crystal, a process known as 'rimming'. Finally, when the ambient temperature is above minus five degrees Celsius and the surface of the crystal is moist, the crystals grow by aggregation [69]. The transitional height, which

is typically 300m thick around the zero degree Celsius isotherm, is a mix of water snow and ice [5]. This band is reflective when observed by radar and is often called the 'bright band'. This transitional layer is characteristic of stratiform rainfall [5].
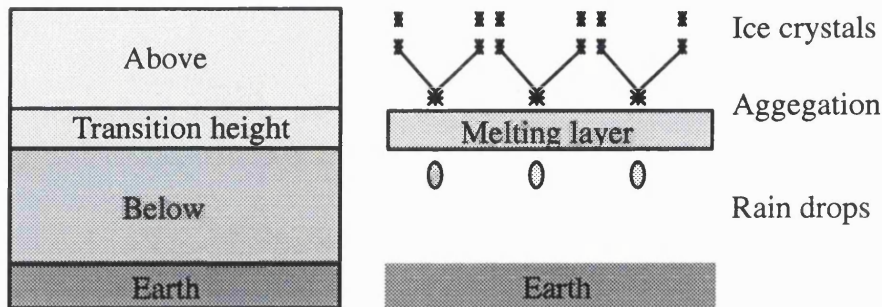
Diagram 1-34   Stratiform rainfall

2.13.9.2   **Convective**

Thunderstorms are violent examples of convective rainfall which develop in an unstable and humid atmosphere and can be described in terms of a life cycle which includes the developing, mature and dissipating stages [69][74]. During the developing stage condensation takes place in the buoyant air in the interior of the cloud which releases latent heat, providing additional lift. Particles are formed in the early stages at the cloud base and these particles are carried well above the freezing level as supercooled water droplets, in updrafts that can reach ten metres a second. After about forty minutes the drag from the particles initiates a downdraft in the lower portion of the cloud. The downdraft causes rain, which in turn increases the downdraft. In the dissipation stage the downdraft suppresses the updraft completely and a weak downdraft causes the remaining precipitation to fall as light rain or evaporate.
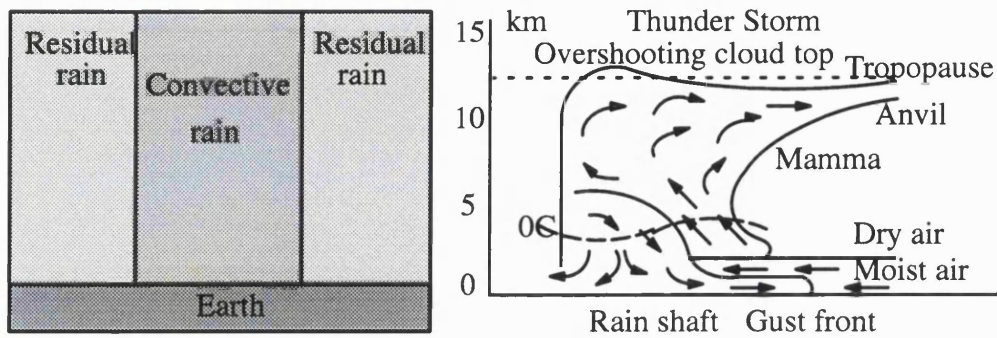
Diagram 1-35   Convective rainfall

2.13.10   Horizontal structure of rain

Moupfouma, Martin, Spanjaard, and Hughes [72] observed extreme variability in the simultaneously recorded rainfall from two rain gauges 2.5km apart in Cameroon. This showed that two types of rain were recorded during the same fading event. They concluded that convective showers existed for short durations, embedded in wide spread stratiform rainfall. Since the rainfall was not homogeneous, a correction factor was required to calculate the attenuation. When they compared the results of four different rain gauges, it was evident that the rainfall was greater inland compared with the coast. Individual rain cells, which tended to last a few minutes, were buried in a larger rainfall region which could last for between 5 and 20 minutes [53]. A model for this type of rainfall could be a circular uniform cells, surrounded by residual rainfall, with the diameter of the core depending upon its intensity [73].
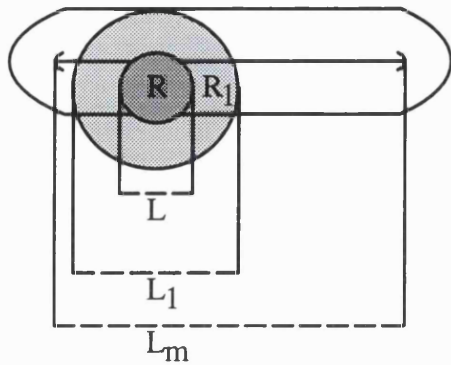
A   Is the resulting attenuation

$$A = k \left(L\, R^{\alpha} + (L_1 - L)\, R_1^{\alpha} \right)$$

Formula A-54   Attenuation model assuming uniform core and residual rain

However models which attempt to account for the inhomogeneous nature of rain, by treating rain cells as cylinders between the zero degree Celsius isotherm and the ground, may overestimate radio fading since real rain cells have leading and trailing edges [5]. Some researchers have tried to take this into account by treating rain cells as having an exponential profile with rotational symmetry, surrounded by residual rainfall in the region 4mm to 10mm per hour [62][75].

Research on a satellite link with a 72 degree elevation in Lae, Papua New Guinea, discovered that the slope of the cumulative rainfall distribution changed at rainfall rates of about 70 mm/h [76]. This is believed to be caused by a second rain cell on the link when the rainfall rate exceeded 70 mm/h [76]. More than one cell on a microwave path affects the accuracy of rainfall models [62][77].

Goldhirsh [78] found that individual cells in the Wallops Islands were elongated and that statistically there was a preferred azimuth. He found that cells on a northeast – southwest axis were 7.5km on average, while cells on a northwest – southeast axis were 5.6 km on average. An average difference of 2km, with a difference of 4km for 20% of the time. Goldhirsh [78] points out that normally the direction of rain clouds and the direction of

the wind are within plus or minus ten degrees of each other.
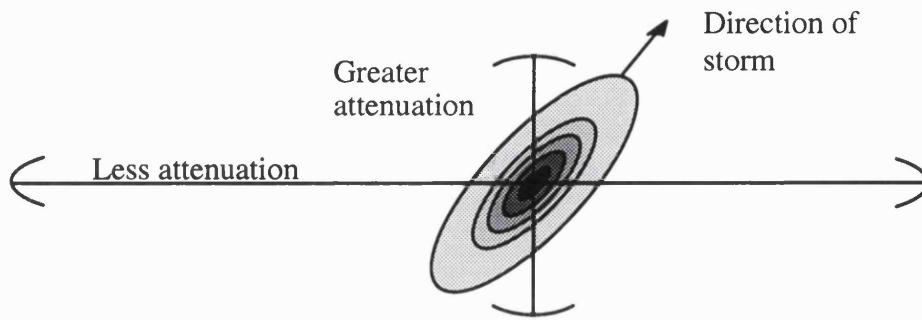
Diagram 1-36   **Elongated rain cells causing greater attenuation in one plane**

ITU–R P.530–7 [17] suggests that if ten links of 20, 10, and 5km each are connected together in the direction of the storm motion, the overall outage would be approximately 80%, 65%, and 40% of the uncorrelated expected outage respectively, at a probability of 0.03%. If four hops of 4.6km were connected together perpendicular to the direction of the storm, the overall outage at 0.01% would be approximately 0.8 of the uncorrelated expected outage probability [17].

Capsoni, Fedi, Magistroni, Paraboni and Pawlina [79] used radar near Milan during 1980 to investigate rain cell ellipticity. They defined two moments of inertia for biaxial cells, a minimum and a maximum, which had gyrational radii Px(min) and Py(max). Cell asymmetry was found to be substantially uncorrelated with cell size and peak rain-fall activity, with an average value of Px(min) / Py(max) of approximately 0.56.
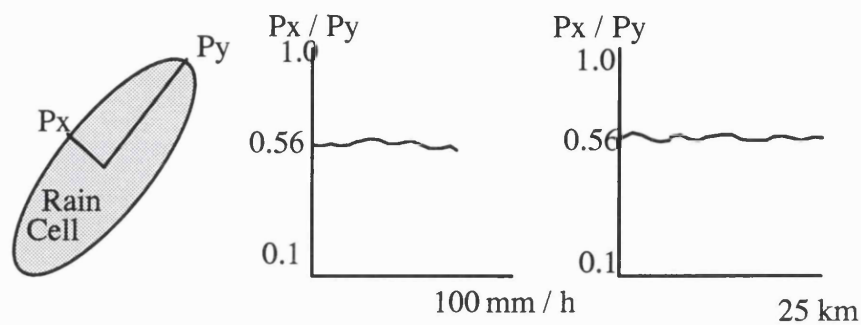
Diagram 1-37   **The ratio of minimum / maximum axes for elongated rain cells**

They also checked cell size in terms of monoaxial cells and found that the cell diameter decreased slowly with increasing rainfall intensity above10mm per hour, and were about 2.9km at 10mm/h, and about 1km at 100mm/h, but that cell diameter increases rapidly with decreasing rainfall below 10mm per hour. This supports the idea of convective and and stratiform rainfall mechanisms in operation. However, only cells completely contained within the radars 30km radius, with areas greater than 5 square kilometres were analysed, giving rise to a quantization error of about 6% [79]. Crane [53] used radar to study 1700 cells in coastal Virginia, he found the average cell size to be 2.9km, with typical cells between 2km and 6km, surrounded by residual rainfall.

2.13.11   Scattering by rain

Energy is lost when raindrops absorb or scatter microwave signals [57].The energy loss can be modelled by two populations of raindrops, one which scatters and one which absorbs energy [80]. Scattering occurs when a wave impinges on an obstacle without being absorbed and the effect of scattering is to change the direction of travel [69]. When the particle is small compared to the incident wavelength the product may be described by Rayleigh scattering, but when the particle is of a similar size to the incident wave-

length the scattered radiation should be described using Mie scattering theory [69]. Below 10GHz scattering can be approximated by the Rayleigh Law, but above 10GHz real scattering deviates from the Rayleigh curve and Mie theory must be used [81]. However, the precise directivity can only be approximated due to the inhomogeneous nature or rain [82]. Since non–spherical scatterers are polarisation dependent the drop size distribution is important [3], because large oblate drops can be considered as having different electrical sizes when irradiated by vertically and horizontally polarised signals [57].

2.13.12   Effective path length

The power law approximation is only valid for a uniform rain medium and net path attenuation, A_n, can be derived from the integration of specific attenuation, expressed in terms of position x, along the path length, L [62]

$$A_n = a \int_0^L R(x)^b \, dx$$

Formula A–52   **Attenuation derived from integration of the specific attenuation along the path**

This information is not normally available, but statistical averaging of the rainfall rate along the path can be achieved by applying a reduction coefficient to rainfall measured at one point, or by applying a reduction factor to the actual path length [7]. There is a relationship between the net path attenuation and the rainfall measured at one point, which depends upon the drop size distribution, the spatial structure of the rainfall, the drop temperature, the local wind direction and the resulting orientation of the drops [55]. A five minute integration time for rainfall corresponds to a spatial averaging of approximately 2.1 km for vertically variable rain, assuming an average terminal velocity of 7m/s

for the raindrops [55]. Historical records existed for the measurement of rainfall inten-

sity, averaged over a five minute period, which is why this period of integration was

adopted [55]. Using a five minute integration period R5, for data from nine hops in the

U.S.A. between 5km and 43km, all operating at 11GHz, Lin [55] proposed that the stat-

istical attenuation, A, on a hop was

$$A = a R_5^b \left(\cfrac{1}{1 + \left[\cfrac{L}{\bar{L}(R_5)} \right]} \right)$$

Formula A-55   The Lin attenuation model

where

$$\bar{L}(R_5) = \frac{2636}{R_5 - 6.2}$$

Formula A-56   Path length correction parameter for the Lin model

ITU–R P.530–7 [17] recommends that the rainfall rate, integrated over one minute, ex-

ceeded for 0.01% of the time R0.01, up to a maximum rainfall rates of 100 millimetres

per hour, should be applied to the power law equation. The resulting specific attenuation

being multiplied by the path length, which is in turn multiplied by a reduction factor

r,as shown.

$$r = \frac{1}{1 + \left(\frac{L}{L_o} \right)}$$

Formula A-57   Reduction factor for the ITU–R P.530–7 attenuation model

Where

$$L_o = 35 \, e^{-0.015R_{0.01}}$$

Formula A-58   **ITU–R P.530–7 path length correction parameter**

and attenuation A0.01, exceeded for 0.01% of a statistically valid time, is expressed as

$$A_{0.01} = a\left(R_{0.01}\right)^b L_r$$

Formula A-59   **ITU–R P.530–7 predicted attenuation exceeded 0.01% of time**

where the path length, L, multiplied by the reduction factor, r, is the effective path length, Le

$$A_{0.01} = a\left(R_{0.01}\right)^b L_e$$

Formula A-60   **Predicted attenuation**

This is a general formula which is considered to be valid for frequencies as high as 40GHz and path lengths up to 60km. The attenuation value given by these models is only valid when a rainfall rate is provided and the correct integration time is used. If the rainfall intensity, integrated over one minute and exceeded for 0.01% of the year (R0.01), is greater than 100 mm per hour, a value of 100 should be used for R0.01 in the equation [17].

Measured rainfall rates depend upon the integration time used, and therefore different

integration times can only be compared if a conversion factor k is known [83]. If rainfall

records exist, it is possible to calculate the conversion factor k from the following rela-

tionship [84],

$$\frac{P_1(R)}{P_{10}(R)} = k \, a \, R^b$$

Formula A-61   Conversion factor for different integration times

where P1 represents the probability of exceeding a rainfall intensity of R, which is inte-

grated over one minute period, and P10 represents the probability of exceeding a rainfall

intensity of R, integrated over a period of ten minute.

Another approach for finding the net path attenuation on a path made up from N sections

of equal length with average rainfall Ra, has been reported [60]

$$A_n = \frac{L}{N} \sum_{i=1}^{N} a \, (R_a)^b$$

Formula A-62   One method of finding the average attenuation on a path

By using three rain gauges, R1, R2, R3, it has also been suggested that the net path at-

tenuation on a path of length L could be expressed as [86]

$$A_h = L\,a\left(\frac{\left(R_1^b + 2R_2^b + R_3^b\right)}{4}\right)$$

Formula A-63   A second method of finding the average attenuation on a path

2.13.13   Errors in measuring rain rate

Errors made in measuring rainfall intensity depend upon the sensitivity of the rain gauge, its accuracy, and its saturation point [72]. The ratio of water fallen to water collected is termed the captivation power[87]. Wind changes the trajectory of raindrops from the perpendicular plane and this effects the captivation power of the rain gauge. This change in trajectory is termed the Jevon Effect [87]. A wind speed of 12, 25, and 50 miles an hour can result in an error of 20%, 40% and 50% respectively [87].
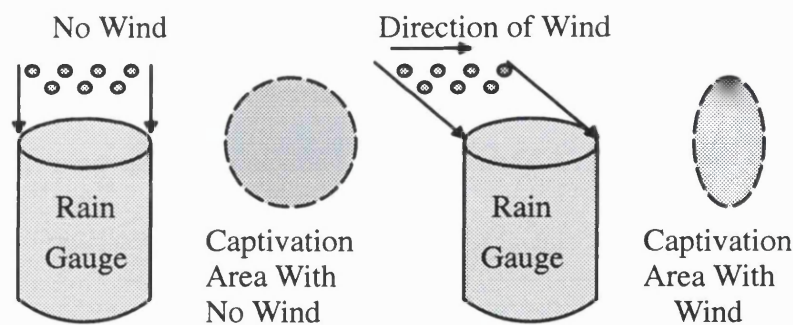
Diagram 1-38   A reduction in the rain gauge capture area caused by wind

The rain gauge introduces a disturbance into the environment which effect air currents and this disturbance is proportional to the dimensions of the gauge [87][88]. Wind speed is effected by the obstruction and drag caused by buildings and in built–up areas tall buildings can create tunnelling of air currents [89]. Rainfall peaks can be missed if the integration time is too long[59], but rapid response rain gauges, with a sensitivity as low as 0.004mm, need to be integrated over at least ten seconds to avoid errors from air

turbulence [54]. Fine airborne particles which are trapped in raindrops can pass though the protective filter on the rain gauge and be deposited in the rocker mechanism of tipping bucket rain gauges, affecting its accuracy [85][90]. If a rain gauge is installed on the Earth's surface, large leaves may be blown onto the gauge effecting the captivation power [90].

Wet radomes can cause additional attenuation which is caused by reflection, absorption and scattering [100]. For a given frequency the loss varies with the hydrophobic state of the material. A hydrophobic radome forms beads of water rather than allowing water to form a thin film. However the ability of PVC and polyester coated materials to form beads of water is reduced with exposure to sunlight and pollution [100]. Tests in Austalia in 1998 on a 38GHz link employing 0.6 metre antennas revealed that when the antennas were new beads of water formed. Simultaneously soaking both antennas with a spray–gun on a sunny day only created 2dB of attenuation. When the test was repeated six months later on the same link, under identical conditions, water formed films on the 'aged' radome which were responsible for 15dB of attenuation [85]. However, the attenuation obtained by simultaneously soaking both radomes with spray–guns was extreme, and much greater than the attenuation produced by natural rainfall .
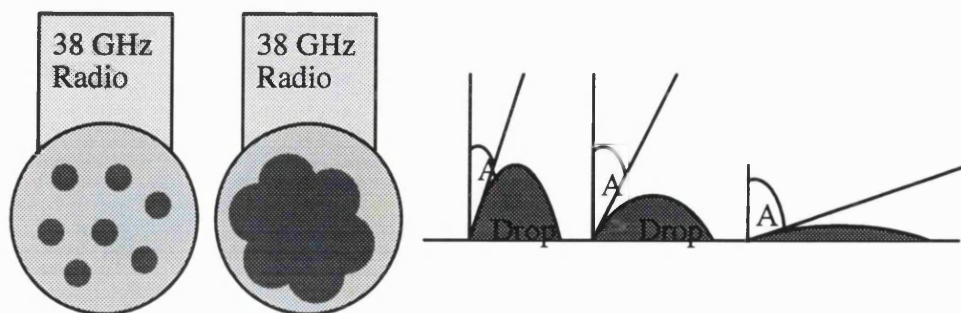
Diagram 1-39   **Rain forming either beads or a film depending on the radome**

When using radar to measure rainfall intensity accurately, the calibration and sampling errors need to be evaluated [53].

2.13.14 Scaling

If the long term average attenuation caused by rainfall intensity, which is exceeded for 0.01% of the time, is known, the long term attenuation values for other percentages of time, for frequencies up to 40GHz and path lengths up to 60km, can be approximated from [17]

$$A_P = A_{0.01} \, 0.12P^{-(0.546 + 0.043 \log P)}$$

Formula A-64   **Attenuation predictions for different percentages of time**

This formula gives factors of 0.12, 0.39, 1, and 2.14 for 1%, 0.1%, 0.01% and 0.001% respectively.

Where long term attenuation statistics exist for one polarisation on a given link, attenuation on the same link, but with a orthogonal polarisation, can be estimated from the expression [17]

$$A_V = \frac{300A_H}{355 + A_H} \qquad A_H = \frac{355A_V}{300 - A_V}$$

Formula A-65   **Attenuation predictions for one polarisation based on measured attenuation on the orthogonal polarisation**

for frequencies up to 40GHz on path lengths up to 60km.

For the frequency range 7GHz to 50GHz frequency scaling may be applied to long term rain attenuation statistics to obtain a rough estimate of attenuation for hops of the same length in the same climate region, and ITU–R P.530–7 [17] presents a formula for this purpose.

2.14 Attenuation by other hydometeors

Snow is difficult to analyze because of its varying shape and dielectric constant. Referring to the work done at 34GHz by Nishitsuji and Matsumoto [S12], Oguchi [57] shows that moist snow has a specific attenuation less than the equivalent rainfall, while wet snow has nearly double and watery snow triple the specific attenuation of the equivalent rainfall. Oguchi [57] also states that Oomori and Aoyagi [S13] reported snow attenuation six to seven times greater than the attenuation from the equivalent rainfall. Oguchi [57] states that attenuation depends upon the water content of the snow and that classification of snow is fundamental to developing accurate attenuation models. Measurements conducted in Helsinki, Finland at 38GHz [85] showed a large variability in attenuation between an ambient temperature of zero degrees Celsius and minus three degrees Celsius, with very low attenuation measured at temperatures below minus three degrees Celsius. The attenuation due to snowfall at 38GHz was not as high as the attenuation caused by rainfall [85] in the summer. However, snow which settles on an antennas reflector, can effect that antennas performance [85].

Hail is only important for a few minutes a year in most areas. It is usual to measure attenuation against equivalent water content of the hail because this does not depend upon terminal fall velocity [53]. The dielectric constant of hail can be averaged in terms of the ratio of ice:water:air composition, and several types of hail can be identified depending upon the composition [91]. When hard ice melts it forms a layer of surface water, but particles formed from loosely packed ice crystals melt internally and externally, with the external water drawn within the particle to fill the air voids created by melting ice [91]. For millimetre wave attenuation in the presence of hard ice spheres there is little difference whether the spheres are wet or dry, but for granular hail it was ob-

served that there was a significant increase in attenuation, at all frequencies, as the particle became fully wet [91]. Wet or dry hard hail, with an equivalent rainfall rate of 150 mm per hour would have about the same attenuation on a 34GHz signal, the specific attenuation being about 6 dB per km, but spongy hail would have significantly different attenuation, depending upon its composition [92].

Cloud and fog droplets with less than a 0.1mm diameter allow the Rayleigh approximation to be used for specific attenuation on frequencies as high as 200GHz [93], and cloud droplets are normally less than 0.1mm diameter[8][51]. The liquid water density in fog is typically about 0.05 grams per cubic metre for medium fog with a visibility of about 300m, and 0.5 grams per cubic metre for thick fog with visibilities around 50m [93]. For fog with a visibility of about 300m and a liquid water water density of 0.05 grams per cubic metre the specific attenuation would be approximately 0.3 dB per km at 40GHz, and less at lower frequencies [93]. The measured attenuation will depend upon the temperature [93] and whether the fog is patchy [41].

2.15   Attenuation due to sand and dust

A distinction should be made between sand particles which generally have a diameter greater than about 0.2mm [133], and are never less than 0.04mm [121], and dust particles. A sand storm is a low flying cloud which rarely exceeds a height of two metres above the Earth's surface, whereas dust particles can rise in dense clouds to a height of one kilometre or more [121][133]. Sand storms are therefore unlikely to effect millimetric or microwave links which have antennas located at a reasonable height.

Bashir and McEwan [94] refer to the work of Cihlar and Ulaby [S14] to indicate that the chemical composition of dry soil has little effect on microwave propagation, unless

magnetic or metallic minerals are present. A medium of dry soil with 0.1mm radii and

a visibility of 15 metres would produce a specific attenuation of 0.027, 0.058, 0.25, 0.42

and 1.37 dB per km at frequencies of 3, 10, 14, 24 and 37 GHz respectively [121]. In

humid climates dust particles absorb water molecules, which effects the specific attenu-

ation of the medium [121]. At 3GHz and 10GHz a moisture content of 16.8% increases

the specific attenuation of the 0.1mm filled medium with 15 metre visibility, to 0.18 and

1.75 dB per km respectively, while at 14, 24, and 37 GHz the specific attenuation for

20% moisture content increases to 4.45, 12.9 and 16.5 dB per km respectively [121].

The effect seems to saturate, with little difference between 20% and 30% moisture con-

tent [121]. Attenuation experienced by linearly polarised waves in a dust storm in negli-

gible, unless the storm is severe with visibilities of a few metres or less, and the attenu-

ation experienced by circularly polarised microwave signals is negligible at visibilities

greater than 200 metres. [95]. Optical visibility is proportional to [94]

$$\int_0^\infty N\,(a)\,a^2\,da$$

Formula A-66   Optical visibility proportionality factor in a dust storm

whereas microwave attenuation was proportional to

$$\int_0^\infty N\,(a)\,a^3\,da$$

Formula A-67   Microwave attenuation proportionality factor in a dust storm

where N(a) is the number of particles per cubic metre per unit radius range and a is the

particle radius. Ghobrial, Ali, and Hussein [S15] found that for Khartoum sandstorms

there was an upper particle size limit of 150 microns, and that below this size the particle

size distribution was given by the expression [94]

$$N(a) = \frac{1}{a_o} e^{-(a/a_o)}$$

Formula A-68   Particle size distribution in Khartoum

Where a_o is the mean radius, of about 8 microns. Ahmed [96] states that the Rayleigh

approximation is valid, for dust and sandstorms, for frequencies up to 100GHz.

$$\frac{2\pi a}{\lambda} \ll 1$$

Formula A-69   Validity of Rayleigh scattering

Goldhirsh [S16] showed that a particle density of 100 million particles per cubic metre

corresponded to a visibility of about four to five metres [94].

2.16   Attenuation by atmospheric gases

Oxygen, and water vapour cause microwave signals to be attenuated [3]. Nitrogen absorption becomes noticeable at frequencies above about 150GHz [97]. The oxygen molecule has a permanent magnetic moment with rotational absorption lines between 50GHz and 70GHz, and at 118.8 GHz and at 367GHz, while the water molecule is an electric dipole, which causes molecular absorption at 22.2 GHz and at 183.3GHz, and 325GHz [3][97]. The magnetic moment of the oxygen molecule interacts with the magnetic field of microwave signals, while the water vapour molecule interacts with the electric field [51]. At frequencies above 310GHz, or within 10GHz of 183GHz, the attenuation due to water vapour will often be greater than attenuation due to rainfall [3]. Below 300GHz, except for frequencies around 60GHz and 183GHz, the attenuation due

to gases is less than the attenuation caused by 5 mm per hour of rainfall integrated over one minute [97]. Attenuation at 60GHz is about 15dB per km at twenty degrees Celsius, sea level, and is about 25dB per km at 183GHz, for the same conditions [97]. Oxygen density remains fairly constant, but water vapour density varies rapidly [5][8][98]. Oxygen and water vapour should be considered above 10GHz and on long paths at frequencies above 20GHz statistical variation of water vapour density and temperature should be considered [17].

2.17 Reduction in cross polar discrimination

Cross polarisation occurs when a portion of the transmitted microwave signal is converted into the orthogonal polarisation [8]. Cross polarisation discrimination (XPD), is a measure of wanted signal to the unwanted orthogonal signal, expressed in decibels.

$$ XPD = 20 \log_{10} \left(\frac{\text{Received co--polarised signal}}{\text{Received cross--polarised signal}} \right) $$

Formula A-70   Cross polar discrimination

Depolarisation can be caused by rain, ice crystals, snow, hail, and when linear polarisations are used antenna tilt should also be taken into consideration [8]. Multipath propagation is a main cause of depolarisation on hops longer than 50 kilometres [35]. Non spherical rain drops have different attenuation and different phase shift coefficients in the vertical and horizontal polarisations [51]. Differential phase shift is important at low frequencies where attenuation is low, but differential attenuation is important at higher frequencies [38]. When considering the cross polarisation discrimination caused by non spherical rain drops in a rain filled medium at frequencies below 10GHz differential

phase shift dominates, while at frequencies above 10GHz differential attenuation domi-

nates [67]. The drop size distribution is important when considering the number of large

non spherical drops in a rain filled medium since spheroidal and Pruppacher Pitter [126]

drop shape models produce slightly different cross polarisation results [65]. Both differ-

ential attenuation and differential phase shift vary with type of rain [67]. The mean cant-

ing angle describes the medium, which is influenced by the wind [71], but the affect of

different orientations tend to cancel each other [38]. Depolarisation caused by rainfall

does not significantly increase outage time on dual polarised systems, as rainfall induced

depolarisation tends to occur at the same time as severe rain attenuation [35]. On satellite

paths depolarisation coincides with lightning discharges, which suggests the alignment

of ice crystals to electrical fields [51]. Depolarisation in sand and dust storms could be

due to particle alignment caused by electrostatic fields generated by lightning, or the

dust itself, or the aerodynamic forces could produce particle alignment [94]. Ahmed

[96] suggests that dust and sand particles, which are small compared to signal wave-

length, should not, in general, have a significant effect on depolarisation. Ansari and

Evans [121] found that when the moisture content of dry dust is increased to 20% the

cross polarisation of both linear and circular waves dropped by 10dB [121]. They found

that varying the axial ratio from 1.1:2 to 2:1 reduced discrimination by about 20dB, but

a further increase to 5:1 only reduced discrimination by another 8dB [121]. Linear cross

polarisation values in dry regions would not be significant with visibilities of 15m and

very eccentric particles, with the same true of humid areas up to 20GHz [121]. In addi-

tion, circular polarisation would be unsuitable in dry regions with visibilities of about

100 metres [121].

2.18 Interference

In the absence of interference the receiver threshold of the radio is determined by thermal noise, but when interference is present the threshold and fade margin can be affected [19]. To prevent radios at one location causing mutual interference, links are designed so that the frequencies transmitted at one station, within a given frequency band, are all either high or low [1]. When a radio link consists of a chain of hops, the hops are normally arranged in a 'zig–zag' pattern to prevent interference from distant stations [1].
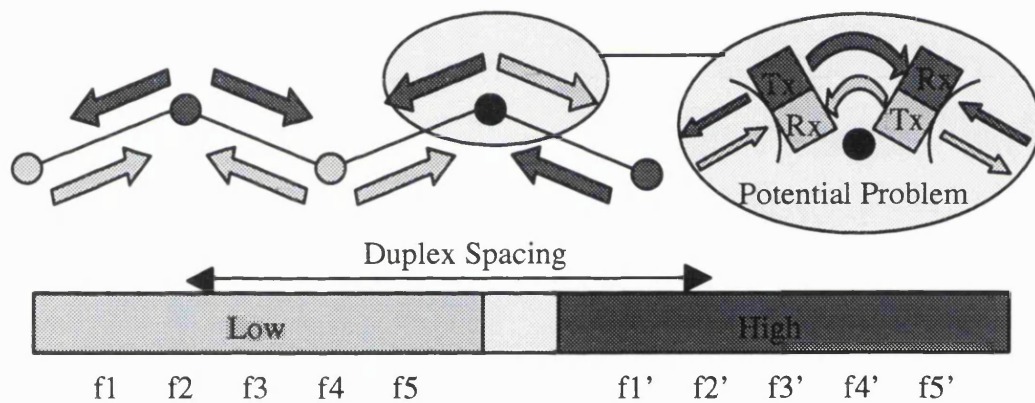
Diagram 1-40   Potential interference caused by poor frequency planning

The level of interference that can be tolerated depends on the type of modulation and the bandwidth of the interfering and victim radio system as these parameters effect the spectrum density of the signals concerned [1]. As a general rule modern four phase shift keyed modulated radios are unlikely to have a reduction in fade margins when the interfering signal is 25dB, or more, below the threshold value of the victim radio [1]. Interference between radio systems can take place through line of sight propagation, tropospheric scattering, diffraction by terrain and buildings, ducting layers, and hydrometeor

scatter ing[47] [48].
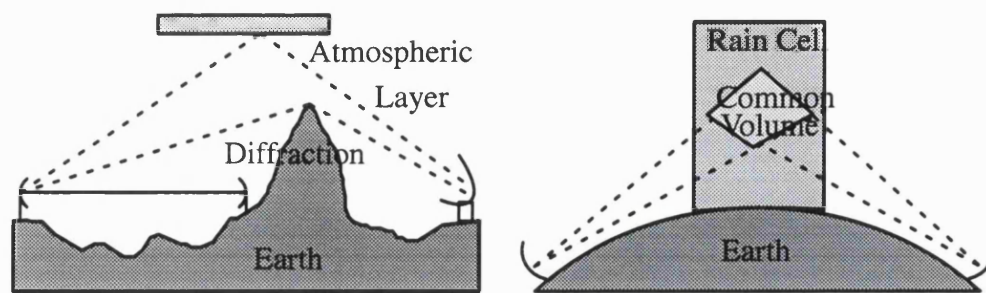
Diagram 1-41   Sources of interference

The most significant form of interference on terrestrial microwave links is usually from

other radios with line of sight. Coupling of radio systems though line of site can be

reduced by network planning, since the interference power I, relative to the carrier

power C, depends on the antenna discrimination of the transmitting interference source,

the antenna discrimination of the receiving victim and the decoupling provided by the

victim radios filters, when the interfering and victim radio are not operating on exactly

the same frequency [1].
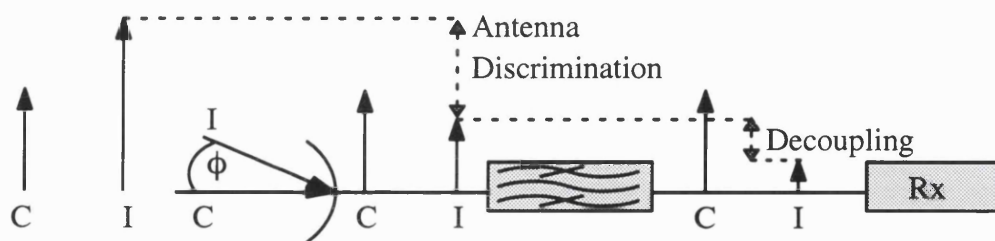
Diagram 1-42   Antenna discrimination and decoupling

A reduction in the effects of interference from known terrestrial sources can be achieved

by using higher gain antennas with greater discrimination in the direction of the interfer-

ing system. Possible sources of interference can be shown graphically using a 'keyhole'

template. The dimensions of the template depend upon the gain and discrimination of

the antenna used and the transmit power and receive sensitivity of the radios used [1].
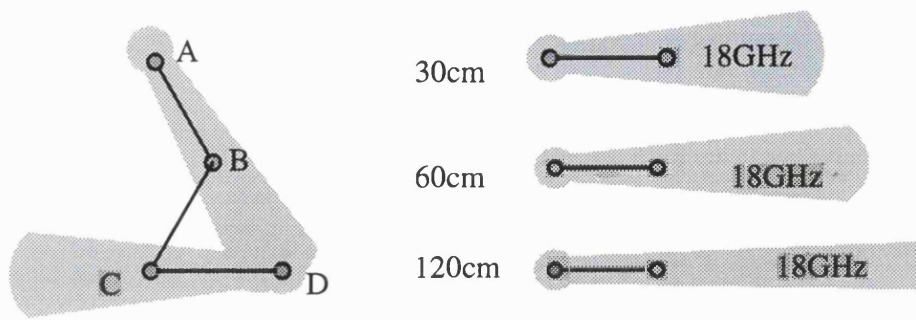
Diagram 1-43   **Keyhole template showing potential sources of interference**

Once a potential source of interference has been identified its effect on the victim radio can be reduced by selecting a frequency which allows the victim radios channel filters to decouple the signals, and/or by using different polarisations. A reduction in the bandwidth could reduce interference power and even allow an increase in the channel separation. This is possible when an operator has been allocated a frequency bandwidth for its sole use. It may be possible to attenuate the transmit power of the interfering radio. Star points can create serious interference problems since there is no antenna discrimination provided by the interfering sources. When all the radios at a star point have the same bandwidth and similar modulation and receiver sensitivities, the best system performance can usually be achieved when the receive power of the radios at the star are all the same. This can be done by attenuating the transmit power of the interfering sources. For a particular victim radio the interference power from different sources will vary with angle, frequency separation and polarisation. The interfering signals can be summed together logarithmically, but the strongest signal will dominate. If two interfering signals have the same power there is an approximate increase of 3dB in the interference power level.
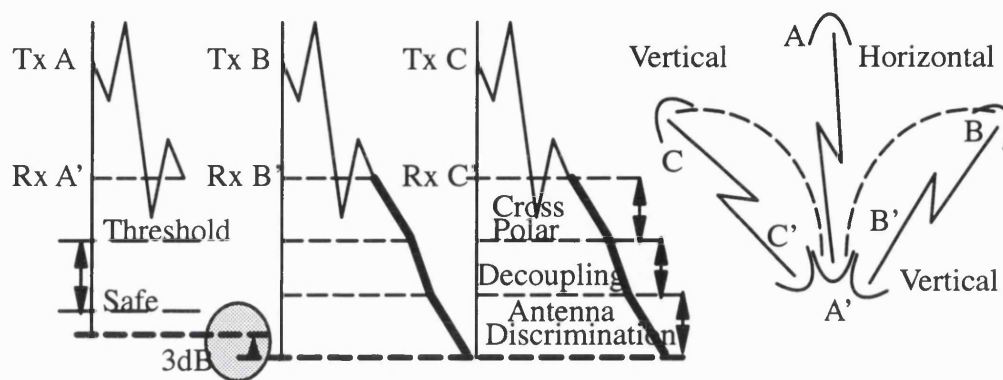
Diagram 1-44   Establishing safe interference levels using a power budget

If the level of interference power is too high it will be responsible for a reduction in the flat fade margin. Measured values for Nokia's 4 x 2Mbit/s DMR 38GHz continuous phase modulated radio, CPM, used as both victim and interference source shows that a reduction of half a decibel in flat fade margin, to the one error per thousand threshold level, when the received carrier power C is only 20.2dB greater than the received interference power I [101]. The reduction in the received interference power due to the decoupling by the channel filters allows the interference power to be 44.5 dB greater than the received carrier power (after antenna discrimination) for the radios described above, with a 21MHz separation and 0.5 dB reduction in the flat fade margin.

16.6 dB	−6.5 dB	Separation in MHz (Nokia DMR38)						
		0	3.5	7	10.5	14	17.5	21
		20.2	16.6	−6.5	−32.3	−42.6	−44.4	−44.5
3.5MHz	7MHz	Interference Level in dB Responsible for a 0.5 dB Reduction in Flat Fade Margin						
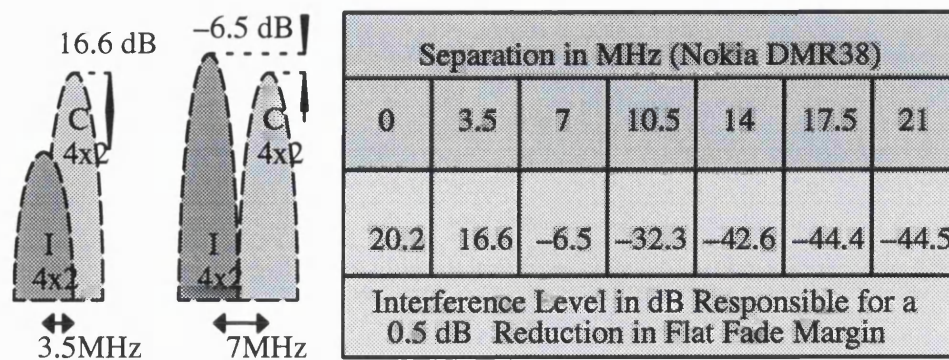
Diagram 1-45   Filter decoupling for the Nokia 4x2Mbit/s DMR38 radio

Natural obstacles may also be used to block the direct path of known interfering sources [35]. However, refractivity gradients are affected by changing meteorological conditions and these changes may change the apparent height of obstacles compared with standard atmospheric conditions [30]. If these measures fail to reduce the interference power, it may be necessary to change the frequency band or the selected site [1].

The threshold to interference T / I, ratio is the ratio of carrier power to interference power on a digital system which is necessary to degrade the performance from one error in a million to one error in a hundred thousand bits [132]. It can be measured by fading the received power level to a point where the error rate is one bit in a million, and then injecting interference until the error rate drops to one error in one hundred thousand bits [132].

2.19 Summary

The power which is received at the end of a microwave hop is affected by variations in the gradient of refractivity along the hop and by particles which may pass thought the line of sight. The normal value of radio refractivity is −40N/km in the lowest part of the atmosphere, which corresponds to a k value of 4/3. Subrefractivity occurs when the

gradient is greater than –40N/km. A gradient of 0N/km has a k value of 1 and a positive

gradient of refractivity corresponds to k value less than 1. Antenna heights should

initially be planned to allow clearance of 50% of the first Fresnel zone for frequencies

below 3GHz, and 100% clearance of the first Fresnel zone for frequencies greater than

7GHz. However, clearance of the direct ray should also be planned for subrefractive

conditions, when the k value is reduced and the Earths bulge increases. ITU–R P.530–7

presents a graph of effective k values which are exceeded for 99.9% of the time for dif-

ferent hop lengths in a continental temperate climate.

When the gradient of radio refractivity is reduced to considerably less than –40N/km

super refractive conditions occur. A gradient of –157N/km corresponds to a k value of

infinity, which is represented as a flat Earth. Further reductions in the gradient of radio

refractivity correspond to ducting conditions and a negative value of k, which is com-

monly represented with an Earth's surface which is concave.

ITU–R P.530–7 presents a formula which predicts the percentage of time that a fade

depth caused by multipath is exceeded on a hop which is not subjected to strong surface

reflections. The prediction is based on hop length, frequency, path inclination, latitude,

longitude, altitude, terrain, and the percentage of time that the refractivity is less than

–100N/km. However on 16x2 and 8x2 Mbit 4PSK modulated radios on hops longer than

40km and also QAM radios, the dispersive effects of multipath fading should also be

taken into account. ITU–R P.530–7 presents a formula which predicts the percentage

of time that a a predefined bit error rate is exceeded based on measured signature values.

Variation in the gradient of radio refractivity can also cause variation in the angle of

launch and the angle of arrival, which is may become important on coastal paths which

use high gain antennas. Localised turbulence can cause pockets of air with a different

refractive index to the surrounding air to cross a line of sight path scattering and reflecting the microwave energy and producing a slow non–selective fading known as scintillation. Layers of air with a different refractive index to the surrounding air may cross the radio path and defocus the signal. In extreme cases these layers may be produce radio holes. Particles such as hail, snow, rain, sand, dust, on the radio path can also affect the signal. However hail is normally only present for a few minutes a year and snow is not significant compared with the attenuation caused by rain. Sand and dust storms are only important when the visibility is in the order of a few metres and the moisture content is around 20%.

Attenuation caused by rain should be considered above 7 GHz, in areas with very heavy rainfall. ITU–R P.530–7 presents a method for calculating the attenuation due to rainfall by first finding the rainfall intensity which is exceeded for 0.01% of the time and then evaluating the specific attenuation caused by such rainfall. The specific attenuation in dB per km is multiplied by the path length and this product is then multiplied by a reduction factor which accounts for the non uniform rainfall intensity. The result is the attenuation which is exceeded for 0.01% of the time, for the polarisation in question. ITU–R P.530–7 also presents a method converting this value to other percentages of time. This method requires rainfall intensity values which have been integrated over one minute. Antennas should be located at positions which prevent highly reflective surfaces from causing multipath. Obstacles may be used to prevent reflected signals reaching the receiving antenna.

The attenuation due to rainfall at 5 mm/hour is greater than the attenuation due to atmospheric gases at frequencies less than 300 GHz, with the exception of the bands at 60GHz and 183GHz.

3 Application to a new GSM network

3.1 Introduction

This section looks at the phases and growth of a new network, capacity issues, the choice of the transmission medium and site surveys. Availability objectives, network architecture, traffic carried and network topology are discussed. The problems associated with path which cross water are assessed and frequency planning and interference is also introduced. Finally passive and active repeater solutions are considered.

3.2 The phases in a new GSM network

When the GSM 900MHz spectrum is opened, business investors bid for one of the new licences. Once the new GSM operators are selected they compete against each other, fixed line operators, and any analog cellular operators which may exist in the market place.

When the new operators compete in a new digital cellular market place it is usual to establish objectives to be met in a number of phases. In the first phase the operator would aim to cover the business areas in the main city centres, the main shopping centres, airports, busy railway stations, and the roads leading to these areas. The revenue generated by new cellular subscribers helps to finance the growth of the network. In the second phase the coverage in the main city centres would be increased and the other cities and towns centres, busy shopping centres and main roads into these areas would be provided with coverage. While the first phase was being built, measurements would be taken to establish areas where capacity provided by the operator was not sufficient to meet subscriber demand. Extra capacity would be added to these busy areas during the second phase. In the third phase the coverage of the cities, towns and connecting roads would

be completed and extra capacity provided where necessary. In the fourth phase the operator continues to provide coverage, and aims to increase the quality of the service provided by optimising the network. The income generated by the new subscribers supports the massive investment required by the operator at all the phases, and it is critical that the operator attracts the new GSM900 users to their network by providing the coverage, quality and tariffing equal to, or better than, their competitors.

Country To Be Covered

Phase 1 GSM900
Main City Centres and
Busy shopping centres
International Airports
Busy Railway Stations
Roads Leading to Busy Areas

● Capital City
● Main Cities
● Smaller Cities
○ International Airport
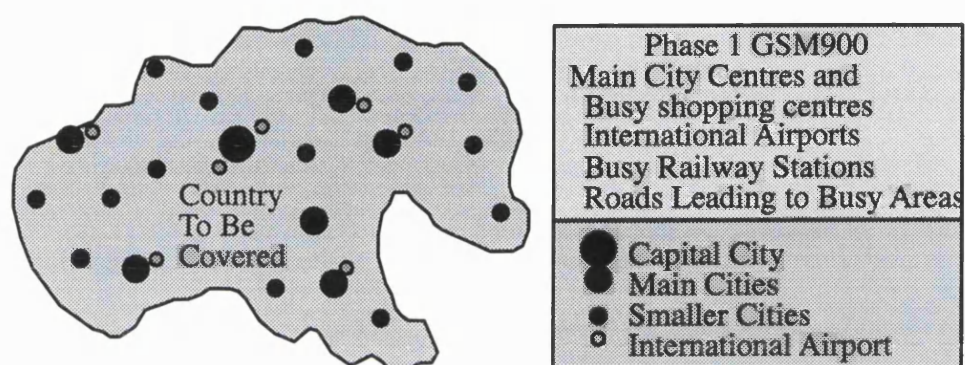
Diagram 1-46   Coverage planning in phase 1 for a new GSM operator

The digital cellular licences for 1800MHz, referred to here as GSM1800, are usually auctioned after the GSM900 operators have established a sizable network with an established subscriber base. The strategy for network growth used in GSM900 systems may not therefore be the best approach for GSM1800 network growth. It is difficult to attract subscribers to a new digital cellular network if it can not provide the coverage offered by the existing digital cellular operators. A different approach is to provide complete coverage for the big cities and the roads leading into these cities, and airports, first phase. Then in a second phase providing extra capacity to busy areas in the existing network, and increasing the coverage of the network to other cities, big towns and connecting roads. In the third phase coverage is increased and further capacity is provided in areas where measurements have shown that demand exceeds the current capacity.

3.3   Estimating capacity

Whether an area is to be provided with a digital or an analog cellular network, the initial stages are the same. The operator must establish the number of potential cellular users in the area, and what their share of the market will be. The density of users will be different in different parts of the area to be covered, and the traffic generated by subscribers will change from area to area. In a city area the cellular radio planning engineers will divide the city into different clutter types such as dense urban, urban, suburban, industrial, rural, forest, water, and other. From experience with other networks in that area the cellular radio planning engineer will assign a value of expected traffic to be generated per unit area during the busiest hour of the week. Telephone traffic channels are then assigned to these areas to carry, typically, 98% of the traffic generated in the busiest hour. Typically during the busiest hour of cellular traffic, in a given area, 2% of the attempted calls will not be connected because the network is busy. This is referred to as 2% blocking, and blocking objectives in cellular networks are usually between 1% and 5%. The area covered by a cellular base station will depend on the transmitted power from the cellular antenna, the antenna height and type, the type of terrain and clutter.
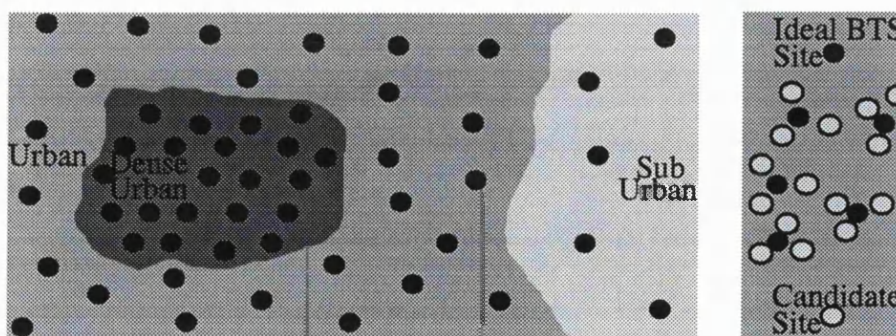
Diagram 1-47   Identification of ideal BTS sites and possible site candidates

Based on a combination of experience and software simulation of cellular propagation at the frequency in question, the cellular designer will decide on the number of cells to be used, their capacity, and the approximate location of the base station, BTS. Three possible base station sites are selected per cell, and site visits are arranged. After the cellular radio planning engineer, the microwave planning engineer, and the implementation engineer have visited the sites they are arranged in order of preference. The site acquisition team then try to secure a rental agreement with the landlord of the preferred site location. Once the location and capacity of the base stations is known, detailed transmission planning can begin. When designing digital GSM900 or GSM1800 networks, the area to be covered should be subdivided into base station controller, BSC, areas. The size of the BSC area generally depends on the amount of traffic generated in an area, how many transceiver, TRX, units are required to carry that traffic, how many TRX units a BSC can control, and how much of the total TRX capacity is reserved for future expansion inside the BSC area. The number of TRX units that can be controlled by one BSC depends on the type of base station controller which is used . In 1997 BSC's generally had a capacity of 128 base TRX's, in 1998 this figure rose to 256, and in 1999 it will be 384. The cellular radio planner, in consultation with the transmission planning engineer, defines the BSC areas. The borders to a BSC area should not straddle a road as this may cause an excessive amount of traffic to be generated by mobiles handing over from one BSC area (location area) to another. Cellular transmissions broadcast from a base station can propagate much further than expected over rivers and lakes and parkland. For this reason it is best to enclose such areas within one BSC area to prevent unnecessary handovers.

3.4   Transmission capacity

The radio cellular planning engineer provides the transmission planning engineer with a plot showing the position of the sites and the number of traffic channels which will be broadcast from those sites. For GSM900 and GSM1800 the traffic will be presented as the number of TRX's to be used at the BTS. Each TRX is provided with two time slots of capacity back to the BSC, and in addition each TRX used in a network requires two bits allocated for its signalling. The BTS will require between two bits and eight bits for signalling. As a rule of thumb a 2Mbits/s transmission link can carry twelve TRX's. The signalling requirement of twelve TRX's is twenty–four bits, or three time slots. One time slot is reserved for special loop protection use, leaving three time slots from the thirty–one time slots available in a standard 2Mbit/s frame for base station signalling.

The transmission requirements of a network between the BSC and the BTS in a GSM900 or GSM1800 system is usually provided by digital radio wherever possible. The typical solution is to use 4x2Mbit/s radios with a capacity of 48 TRX's, or 8x2Mbit/s radios with a capacity of 96 TRX's, operating at a frequency of 18, 23, 26 or 38GHz. The difference in purchase price between a 4x2Mbit/s radio and an 8x2Mbit/s model is not significant, compared to the costs of planning and implementing the network, but bandwidth requirement of the 8x2Mbit/s radio is double. One approach used by operators is to use 8x2Mbit/s with half the capacity held in reserve for future expansion. However, for a given network configuration and corresponding interference levels, approximately twice the available bandwidth would be required for the identical solution using 8x2Mbit/s radios with the same interference levels as those which could have been achieved using a 4x2Mbit/s solution.
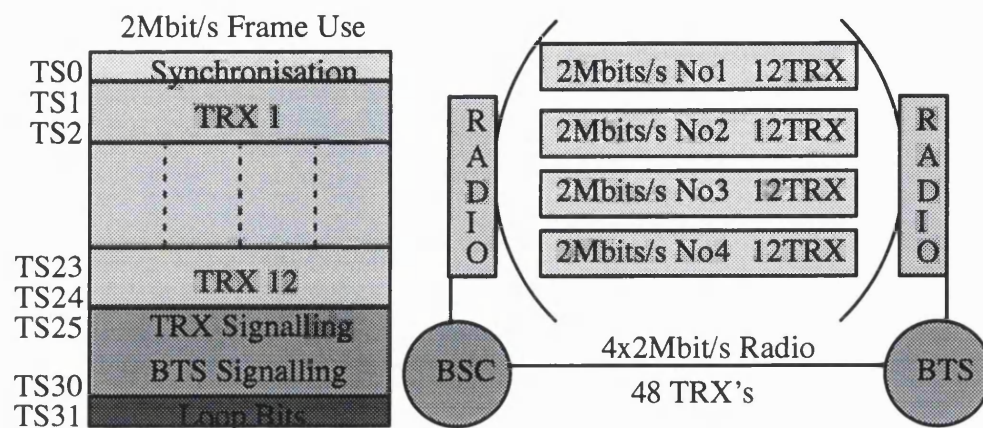
Diagram 1-48   Typical full rate capacity of a Nokia 4x2Mbit/s DMR38

3.5   Transmission medium

After the BTS sites have been fixed and the BSC areas have been defined, the transmission planning engineer can begin to plan the network in detail. The connections between sites can be made with leased lines or, if there is line of sight, by millimetric or microwave radio. If radios are used to connect the sites together the operator has control of the transmission cost, repair time, transmission quality and implementation time. It is therefore normal practice to use millimetric or microwave radio wherever possible. The frequency used to carry the point–to–point traffic between the base stations is generally greater than 17GHz and therefore network design is heavily influenced by the rainfall climate, and the transmission planner must check to make sure that the availability figures are acceptable. If the frequency used is between 10GHz and 17GHz error performance and availability may need to be considered, and below 10GHz the error performance objective is usually the main concern. In dry climates, multipath may create error performance problems above 20GHz, since a dry climate would allow longer

paths, and at the other extreme monsoonal rainfall may affect the availability objective at frequencies as low as 7GHz.

3.6   Line of sight surveys

The cellular planning engineer will establish an ideal location for the base station sites, after which three possible candidates for the site will be chosen. During site survey the cellular planning engineer, the transmission planning engineer, the implementation engineer and possibly a member of the site acquisition team will visit all the sites to establish the best candidate for each base station.

In the planning room the transmission planning engineer will have created an outline report, in electronic or paper form depending on the operator's requirements, for each candidate. The report will contain the approximate latitude and longitude of each candidate and the compass bearing and distance to the other candidates in the area with a space for comments about the possibility for line of sight. Space on the form will also be available for comments relating to the key holder to the building, the power supply and earthing/bonding, space and ease of radio installation. When conducting site surveys in countries where language is likely to present a problem the report should also contain a brief letter of introduction in the local language.

On arrival at the candidate site the exact location and height should be determined using a global positioning satellite system, GPS. Some operators like to receive reports containing the height indicated by an altimeter, but care should be taken to calibrate the altimeter to a known height before using it. Using binoculars and a compass, line of sight should be established wherever possible with the candidates in the surrounding area. Steel towers and steel reinforcing in buildings will effect the compass bearing. In areas

where a structure is to be built on the roof of a building to establish line of sight it may

be necessary to use helium–filled balloons which are allowed to rise to a height where

they can be seen by a planning engineer at an adjacent site. At green field sites where

a tower is to be erected to support the transmission network a mobile hoist will be

required. Note is taken of the height at which the adjacent sites become visible, with

sufficient clearance for the radio signal. An alternative and cheaper solution at a green

field site is to erect a light weight quick–assembly tower with a video camera at its apex.

These mobile towers are towed in a trailer and can reach heights between 30 and 40

metres.

Mobile Hoist   Mobile Tower

New Site   Forest   New Site
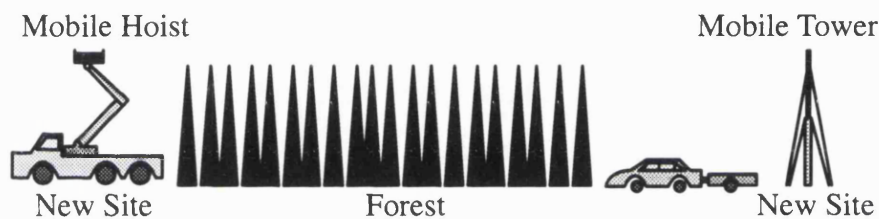
Diagram 1-49   **Line of sight radio site survey**

High–powered light sources used by line of sight crews who work in two groups enable

quick identification of adjacent sites in poor visibility or over longer distances. Photo-

graphs should be taken in the direction of adjacent sites showing whether there is line

of sight or not, and these photographs should be included in the final report. A good cam-

era with a zoom lens is therefore required. Reports, including photographs, should be

written within two days of the survey, while the details of the survey are still fresh in

the memory of the engineer who is responsible for the survey. The report should also

include instructions on how to find remote sites.

During the site survey allowances must be made for the future growth of trees in young

forests. Paths which cross potential building sites or areas where frequent flooding could

cause multipath problems should be avoided.
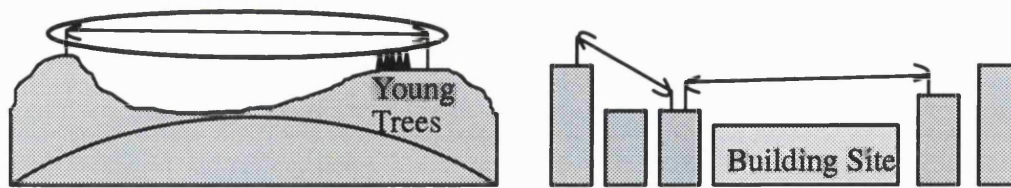
Diagram 1-50   **Potential obstructions to future line of sight**

3.7   Availability objectives

The transmission configuration between the base stations in urban areas will depend on the availability objective, as well as the capacity requirements and the bandwidth constraints. Loops provide a diversity route when one path has been attenuated by rain beyond its fade margin, or when one radio fails or is decommissioned temporarily by the operator, either deliberately or accidentally. However, there are no availability objectives issued by the International Telecommunications Union which cover cellular systems in a mobile environment. There is a suggestion of 99.9% availability for fixed users in a wireless local loop, who are considered as part of the local grade network, but nothing that relates to mobile cellular systems. Mobile operators fix their own objective, and an availability figure of 99.85%, and better, between the last base station and the mobile switching centre is typical.

Unavailability can be caused by adverse propagation, equipment failure, and operator error. The transmission planning engineer is free to allocate the unavailability allowance as he sees fit, but typically propagation is assigned between 30% and 50% of the total figure. The unavailability due to equipment failure can be calculated if the mean time between failure, MTBF, and the mean time to restoration, MTTR is known. For example assuming that the MTTR figure is six hours, and the MTBF for a radio is nine years, then

the unavailability, U, caused by the failure of the radio is 0.00761%

$$U \;=\; \left(1 - \left(\frac{MTTR}{MTBF + MTTR}\right)\right)$$

$$U \;=\; \left(1 - \left(\frac{(6\text{Hours})}{(9\text{Years} \times 365\text{Days} \times 24\text{Hours}) + (6\text{Hours})}\right)\right)$$

$$U \;=\; 0.0000761 \;=\; 0.00761\%$$

Formula A-71   Unavailability due to equipment failure

If three hops were chained together, the unavailability caused by equipment failure at the end of the chain would be sum of the unavailability figures for each of the six radios used in the chain, which is 0.04566%. Further, if each of the hops had a fade margin which yielded an unavailability figure of 0.01% for the rainfall climate in question, and also assuming that each hop was at least the size of the typical rain cells which provided the heaviest 0.01% rainfall, then the unavailability at the end of the chain caused by rain-fall would be approximately 0.03%.

$$U \;=\; (\,[0.00761 \times 6] + [0.01 \times 3]\,) \;=\; 0.07566$$

Equipment + Propagation Only
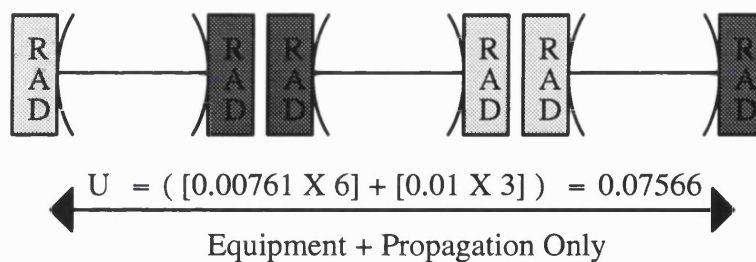
Diagram 1-51   Unavailability at the end of a chain

Therefore the unavailability at the end of the three–hop chain, due to equipment failure and propagation, would be 0.07566%. Unavailability due to the operator's deliberate or accidental actions could easily take the unavailability figure at the end of the chain

to 0.09%, ie an availability of 99.91%. This figure is only for the three hops, and does

not include any equipment at the end of the chain such as a base station.

3.8   Architecture

The MSC provides standard 2Mbit/s signals which contain 31, 64kbit/s channels, which

may contain traffic channels and common channel signalling channels. These 2Mbit/s

signals are connected to transcoders which employ an efficient coding method to reduce

the traffic channels from 64kbit/s to a 13kbit/s traffic channel, with an additional 3kbit/s

inband signalling channel. The 64kbit/s common channel signalling channels which

may be part of the 2Mbit/s link are not affected by the transcoders and pass through as

64kbit/s channels. The output from several transcoders are connected to a submulti-

plexer which maps the compressed signals into a standard 2Mbit/s which passes though

transmission equipment and terminates at the BSC. This process of coding and sub-

multiplexing may be done by separate units or one integrated piece of equipment.

Each TRX broadcasts eight channels into the area which it covers. If only one TRX is

used to cover an area, one of the broadcast channels must be reserved for signalling and

synchronisation of the mobile telephones, however the second, third and fourth TRX's

which cover the same area may broadcast seven or eight traffic channels, depending on

their configuration. Each traffic channel requires 16kbit/s transmission capacity back

to the BSC. Software limitations dictate that in a standard configuration each TRX is

allocated 128kbit/s of traffic capacity whether it broadcasts seven or eight traffic chan-

nels. In addition, each TRX requires a 16kbit/s signalling channel, and each BTS

requires at least a 16kbit/s signalling channel for network management.

When a mobile telephone is switched on in an area covered by a network it searches for

the signalling and synchronisation channel broadcast by a TRX covering that area, and via this signalling channel and the TRX signalling channel it informs the BSC of its presence. The BSC informs the MSC about the mobile telephone by using one of the common channel signalling connections. The MSC checks the home location register, HLR, or the visitors location register, VLR. The MSC acknowledges the mobile telephone via the common channel signalling channel to the BSC, the TRX signalling link between the BSC and the TRX, and the synchronisation channel between the TRX and the mobile telephone. When a valid mobile telephone makes or receives a call, the same signalling channels are used. In addition, once the MSC has allocated a traffic channel and the BSC has made the connection to the TRX, the 3kbit/s inband signalling link between the transcoder and the TRX is used to set up and synchronise the 13kbit/s transmission link.
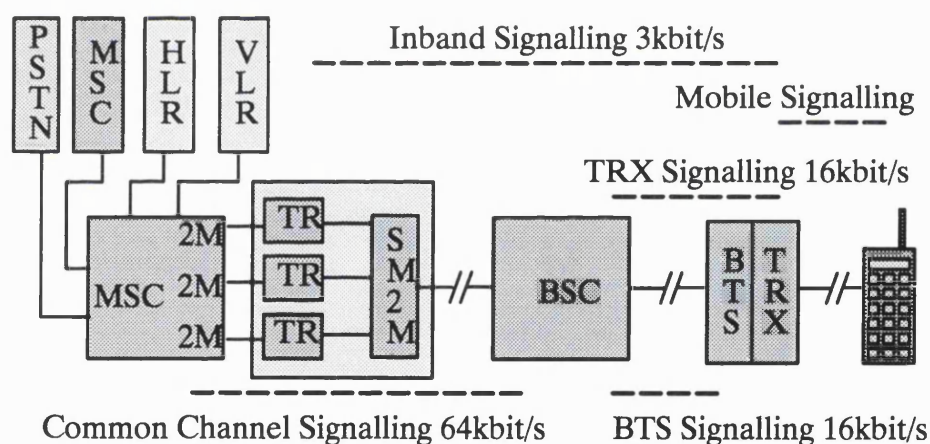
Diagram 1-52   Signalling channels in a GSM network

3.9   Traffic carried

During dimensioning, the cellular network planning engineer establishes the amount of traffic which is expected to be generated by an area in the busiest hour of the week. It would be economically unrealistic to provide enough capacity to carry all the calls during the busiest hour or the week, so the cellular planning engineer usually provides

enough capacity in the individual cells to carry 98% of the traffic during 'busy hour'. Therefore in the busiest hour 2% of the attempted calls in a cell will not be successful because the cellular planning engineer deliberately, for economical reasons, did not provide enough capacity in the cells to carry all the possible traffic. The transmission planning engineer will design the transmission network in such a way that there is enough transmission capacity to carry all allocated capacity in the cells from the BTS to the BSC. If it is assumed that the BSC is located in the area it controls, the transmission planning engineer must arrange for enough capacity to carry all the active traffic channels from the BSC to the MSC. A BSC usually controls between 20 and 50 BTS's. If during busy hour all the cells and sectors were at full capacity, that is carrying 98% of all the call attempts during that hour, it is clear that the full capacity of the BSC would have to be carried back to the MSC. However, even if all the BTS's under one BSC were in the same 'type' of area it is unlikely that each base station would be at full capacity during busy hour, and therefore a small reduction in the transmission capacity between the MSC and BSC can be made. On the other hand, if an area covered by a BSC is made up of different 'types' of land, for example dense urban, urban, suburban, industrial etc, this could significantly reduce the transmission capacity required between the BSC and MSC. Although the cellular planning engineer may have designed the base stations to carry 98% of the offered traffic in a cell or sector during busy hour, different 'types' of areas will probably have different busy hour periods, that is busy hour in a suburban area will probably occur at a different time to busy hour in a dense urban area.
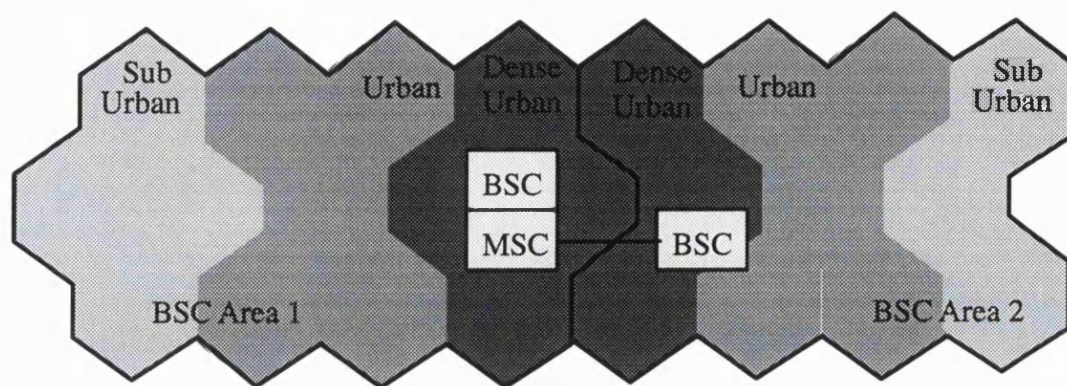
Diagram 1-53   The lucrative dense urban area split between two BSC's

The dense urban part of the city contains the business users. These subscribers generate a great deal of revenue, and for this reason the area is often split into at least two BSC areas to provide some protection against BSC failure. Before 1998 a break in the common channel signalling connection between the MSC and the BSC of more than one second would loose all calls, however since 1998 it has been possible to keep the existing calls connected for a break of up to five seconds in the common channel signalling link (between the BSC and MSC). To protect against loss of the common channel signalling link, and of traffic itself, the BSC's in a city area are normally connected to the MSC in a protected loop. The transmission capacity of this loop is large and normally carried on an optical fibre, although it may be necessary to use radios to carry the transmission capacity initially, while waiting for the local fixed service operator to provide the optical links.
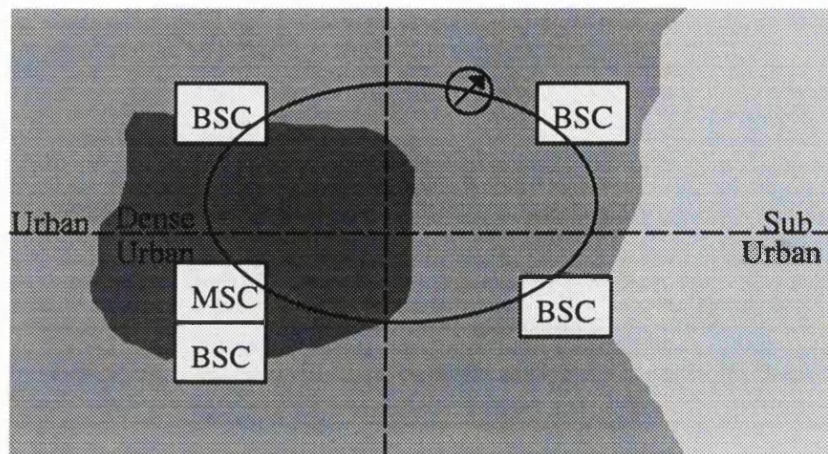
Diagram 1-54   A typical fibre transmission solution between the BSC's

Some operators gather the BSC's under one MSC together in one location. This solution

reduces the cost of maintenance but increases the vulnerability of the network to natural

disasters such as fire and also requires extra transmission capacity . For example, assume

that the area covered by a BSC using 25 BTS's and 200 TRX's. If the BSC was remotely

located in the region to be covered and it is assumed that the area is urban with all the

BTS's experiencing busy hour at the same time, then 400 64kbit/s time slots for traffic

channels and about five 64kbit/s common channel signalling links would be required.

If the BSC was colocated with the MSC then an additional 50, 64kbit/s time slots for

TRX signalling channels and 6.24, 64kbit/s time slots for BTS signalling channels

would be required. If the areas controlled by the BSC were different with different busy

hours then an even greater reduction in transmission capacity could be achieved by using

a remote BSC, as opposed to a BSC which has been colocated with the MSC. Therefore

at least an extra 12% transmission capacity is required when the BSC is colocated with

the MSC, and this type of solution favours operators who own their own transmission

network and have no capacity limitations.

Maximum 5 Time Slots for Common Channel Signalling
200 TRX's x 2 Time Slots = 400 Traffic Time Slot

| MSC |————————————————————————| BSC | Urban

BTS 25
TRX 200

Maximum 5 Time Slots for Common Channel Signalling
200 TRX's x 2 Time Slots = 400 Traffic Time Slots

| MSC | BSC |————————————————————| Tx Point | Urban

200 TRX's x 0.25 = 50 TRX Signalling Time Slots
25 BTS's x 0.25 = 6.25 BTS Signalling Time Slots

BTS 25
TRX 200
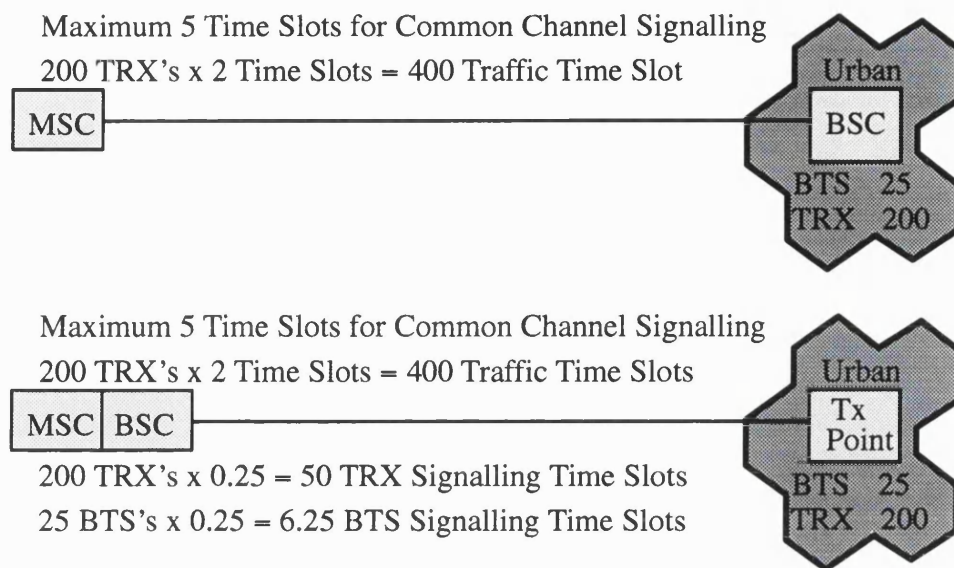
Diagram 1-55   Comparing distributed and colocated BSC networks

3.10   Loops topology

If a loop is designed using one frequency band it should be constructed with an even number of stations in the loop. This approach will ensure that all the transmitters at one site are transmitting either the high end of the band or the low end of the band. If an odd number of sites are included in a loop, and only one frequency band is used to construct the loop, at one of the sites one radio will be transmitting high and receiving low, while the other radio will be transmitting low and receiving high. If these radios are in close proximity to each other there may be an interference problem. If the network topology demands that an odd number of sites should be included in a loop and that only one fre-quency band can be used, the transmission planning engineer must identify a site that will allow the radios to be separated by a distance which will allow interference–free operation. However this may limit the future expansion of that site by restricting the possible location of other radios operating in the same band. Another way of solving the

problem of an odd number of sites in a loop would be to use two frequency bands so that

at one site both 18 and 23GHz are used, one transmitting high and one transmitting low.

This is the preferred way of dealing with an odd number of sites in a loop, but to give

the planner the greatest freedom an even number of sites should be included in the loop

wherever feasible. It should be borne in mind that future interference–free expansion

of an existing network will be easier if the original plan was constructed using the mini-

mum number of frequencies.
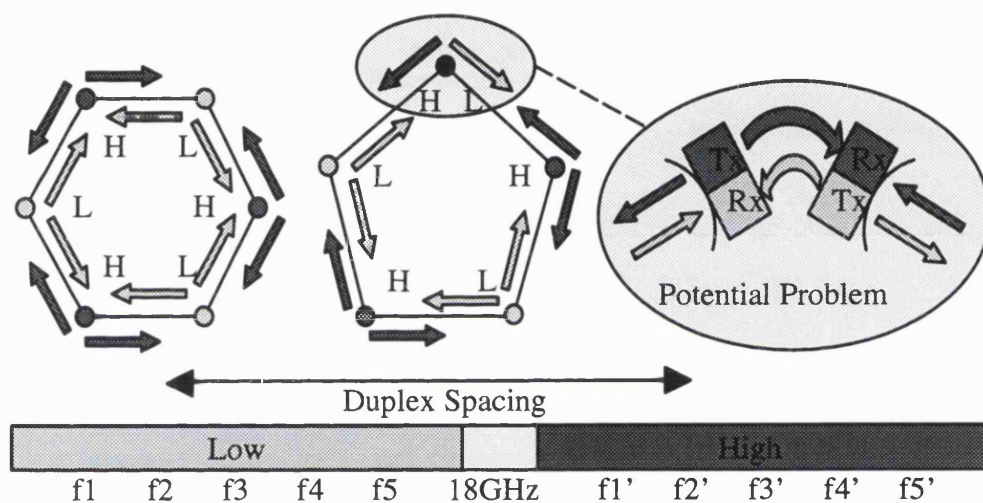
Diagram 1-56   Frequency planning in a loop topology

The availability offered to sites which are connected in a loop is improved because it

is less likely that equipment failure, operator action, or excessive fading will effect both

sides of the loop simultaneously. When considering rain induced attenuation, the avail-

ability figure can be maximised by making the loop as wide as possible, up to a limit

of 8km after which there is very little further improvement. The general goal is to have

a loop with a minimum 3km diameter wherever possible, although this figure can be

refined with a knowledge of the frequency bands to be used in the local climate and top-

ography.
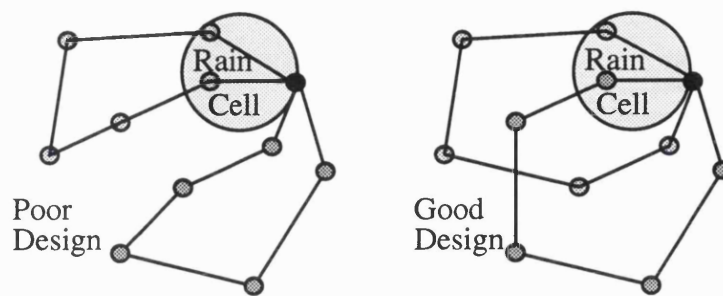
Diagram 1-57   Loop design for radios operating above 13GHz

Under normal circumstances the individual radio hops which make up an individual loop should not cross. However in difficult terrain it may not be possible to design a loop which does not have any hops that cross each other's path. In these situations the weakest part of the loop is where the two hops cross, and at least one of these hops should be 'over–engineered' to ensure propagation in much heavier rainfall than would normally be considered necessary in an ordinary loop.
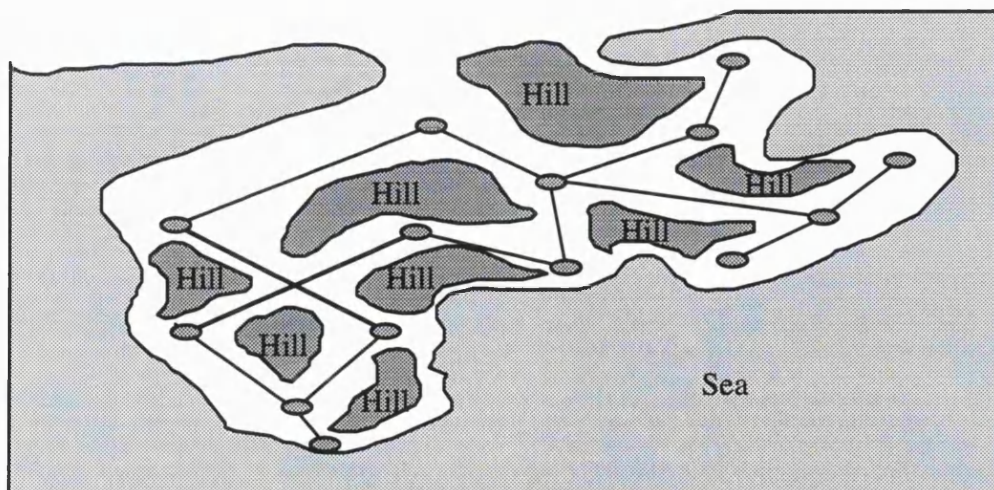
Diagram 1-58   Loops with hops which cross use large fade margins

Employing loops in the design of a system greatly improves the availability of the transmission network. Assuming that the mean time between failure is nine years and that

the mean time to restoration is six hours and that the unavailability due to rain fading

is 0.01% on each hop, it can be seen that the approximate unavailability, without con-

sidering deliberate or accidental decommissioning by the operator, between points 'A'

and 'D' falls from 0.07566% in the chain, to 0.00005724% in the loop. This approxima-

tion is simplistic and assumes that the unavailability of each hop is statistically indepen-

dent from the other hops. This may not be totally true but there is usually insufficient

data to calculate the unavailability in millimetric or microwave transmission radios in

a loop in any other way, and this method serves as a useful approximation.

$$(\, [0.00761 \times 6] + [0.01 \times 3])$$

$$100 \times \Bigl(\bigl(\, [0.0000761 \times 6] + [0.0001 \times 3] \bigr)^{2} \Bigr)$$
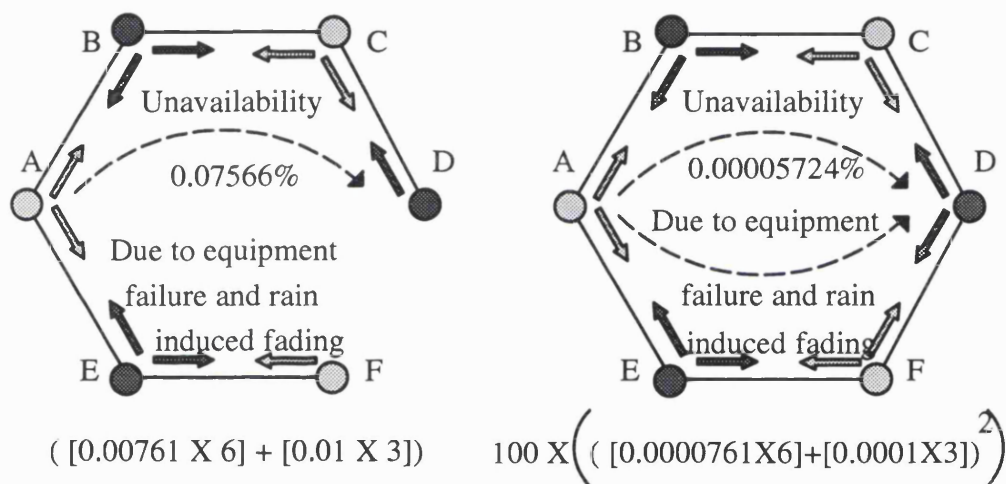
Diagram 1-59   **Low unavailability in a properly designed loop**

Although loops improve the availability of the transmission network and therefore the

availability of the base stations connected to this transmission network, an extra trans-

mission link is required to close the loop. When conducting site surveys it is more diffi-

cult to find locations which allow a loop configuration to be built. If 4x2Mbit/s radios

are used to build a loop, capacity limitations may restrict future expansion. Consider a

loop consisting of six sites A to F. Site A is the central point and does not require capacity

from the loop. If sites B,C,E,F all have nine TRX's installed and site D has six TRX's

installed, the capacity requirement is 42 TRX's. Since the normal capacity of a 4x2Mbit/s radio is 48 TRX's, the loop will not support a great deal of future expansion. However a chain configuration consisting of two branches, A–B–C–D with 24 TRX's, and A–E–F carrying 18 TRX's could easily support future growth, at the expense of availability.

4x2Mbits/s Capacity

9 TRX's for B	3 TRX's for D	No1
9 TRX's for C	3 TRX's for D	No2
9 TRX's for F	3 TRX's Spare	No3
9 TRX's for E	3 TRX's Spare	No4
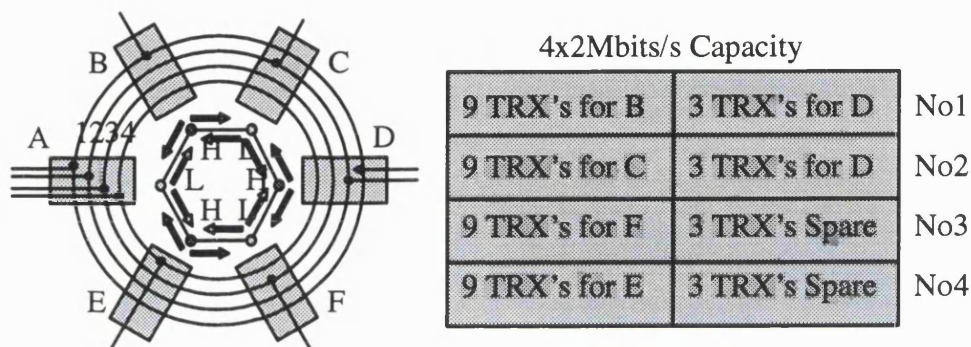
Diagram 1-60   **Typical allocation of TRX's in a loop in an urban environment**

In a city centre the radio interference at 900 or 1800MHz would normally be high, therefore the loss of a BTS would reduce the capacity but not necessarily the coverage of the area since the neighbouring and normally interfering BTS's would be capable of carrying the extra traffic.

3.11   Paths over water

Cellular signals which are broadcast from a BTS can propagate with relatively low attenuation across water surfaces compared to signals broadcast from neighbouring BTS's which propagate though buildings. To prevent unnecessary extra traffic being generated by handovers between one BSC in one location area and another BSC in a different location area, it is usual practice to keep rivers and lakes within one BSC area wherever possible. This practice usually involves millimetric or microwave radios providing transmission links across water surfaces.

Water surfaces can reflect a millemetric or microwave radio signal towards the receiving antenna. If an antenna receives a reflected signal which is similar in power to the direct signal, but in antiphase, then the reflected signal may destructively interfere with the direct signal, causing a degradation of performance or unavailability. The angle between the direct signal and the reflected signal, and the antenna discrimination at the transmitting and receiving ends, will define the relative power of the reflected signal to that of the direct signal. This angle will depend on the length of the path, the height of the transmitting and receiving antennas and the height of the water. It is best to site at least one of the radios so that the water is not visible, but if this is not possible the antennas should be as high as possible and the path as short as possible, in a city environment. If problems are anticipated then the use of larger antennas with greater discrimination, and slight upward tilting of the antenna helps to reduce the amplitude of the reflected signal relative to the desired signal.
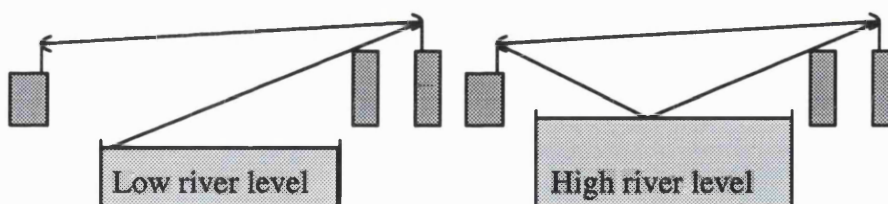
Diagram 1-61   A potential source of multipath at high tide

As the path length increases beyond 5km the angle between the reflected signal and the direct ray reduces. Natural obstacles should be used wherever possible to prevent a reflected signal reaching the antenna. However, during non–standard atmospheric conditions a signal may be bent around such obstacles.

3.12 Interference

An area to be provided with GSM900 or GSM1800 coverage must first be divided into BSC areas. These areas are agreed upon between the cellular planning engineer and the transmission planning engineer. Ideally the transmission planning engineer would like to have the tallest building in the area ,which is willing to allow installation of GSM equipment on its roof, at the centre of the BSC area. This will increase the probability of having line of sight to potential BTS sites. The four sides of a tall building can not normally be seen by sites at a much lower level, and high diffraction losses therefore limit the possible sources of interference to transmitting antennas with line of sight to receiving antennas located on one or two sides of the building.
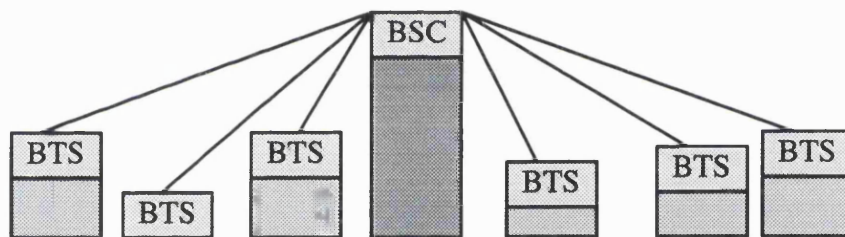
Diagram 1-62   Transmission solution using the tallest building to site the BSC

The objective is to use as few frequencies as possible in the initial planning since it is easier to expand a network at a later date by employing frequencies not originally used. Star points cause the worst interference problem, particularly when the star point is a mast and all the receiving antennas are close together, indicating that all the transmitting radios pointing at the mast have line of sight to all the receiving antennas. Starting with one frequency band, and assuming all the radios in that frequency band are the same type, with the same antenna size, capacity and threshold level, a judgement must be made regarding the fade margin required in the rain climate concerned for the maximum

distance which is likely to be required. Once this fade margin has been established the attenuators of all the transmitting radios connected to radios at the star point should be attenuated to ensure that all radios in a band have the same the receive level, as this will ensure the optimum interference performance. Next the maximum interference power level at the demodulator must be established. This maximum level is normally considered to be a level which does not reduce the radio's performance when it is operating close to the threshold level in an interference–free environment. These levels have been tested and depend on the bandwidths of the victim and interfering radios, transmitted spectrum density, antennas, polarisation, frequency separation and decoupling performance of the filters. In general, after antenna discrimination and filter decoupling, an interference power level which is 25dB below the threshold level of the victim radio would not cause a problem on a 4PSK modulated radio. Therefore, assuming all the receiving radios have a 40dB fade margin at a star point, the object is to reduce the combined interference level, in this example, to 65dB below the normal received carrier power level.
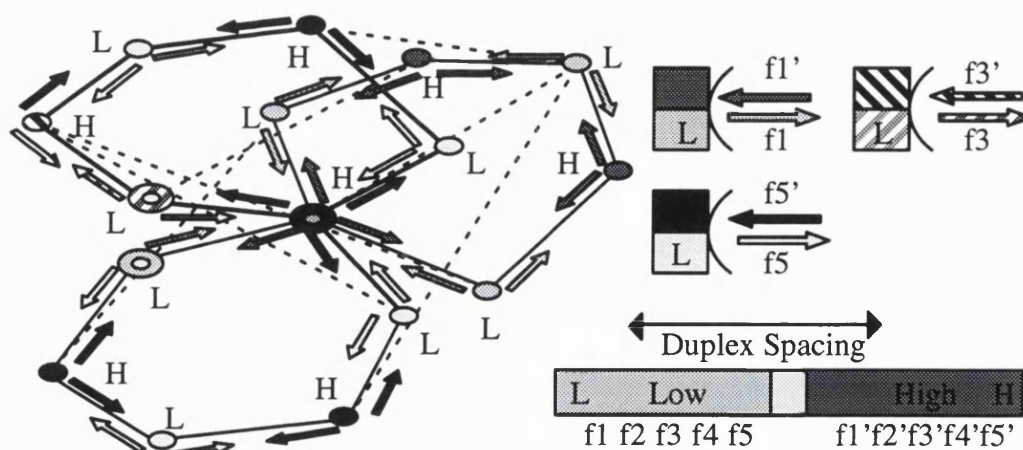
Diagram 1-63   Identifying sites with high or low frequency transmitters

When considering interference at a star point no reduction is made for antenna discrimination from the transmitting radios, but a reduction can be made at the receiving antenna. The angle between each hop is established, and if the antenna discrimination is greater than 65dB, in this example, the same frequency can be used. Where the discrimination is less than 65dB a frequency separation which will result in the combined filter decoupling and antenna discrimination greater than 65dB is desirable. If this is not possible then it may be necessary to use different polarisations, and if this is not possible a different frequency band may have to be used.
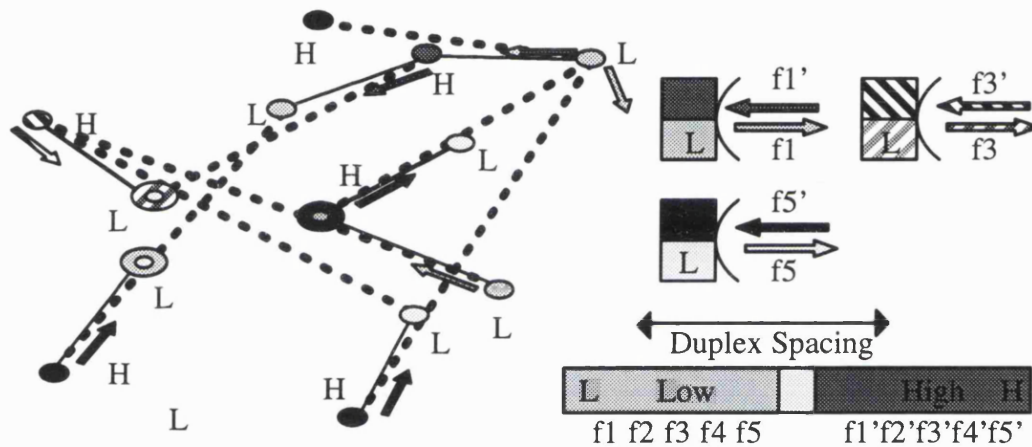
Diagram 1-64   Sites requiring careful channel selection and filter decoupling

Once the frequencies have been selected for the radios at the star points the other radio frequencies can be chosen. However, care should be taken when allocating a frequency to a hop which transmits at the low end of a frequency band when it is transmitting in the direction of a station which transmits at the high end of the same frequency band, and vice versa. In these cases there might be an interference problem. The transmission planning engineer should identify such potential problems and calculate the received interference power, assuming that there is line of sight and that the same frequency is used. If after calculating the received power using the isotropic model, and taking into

account the antenna discrimination at the transmitting and receiving ends, the received power is 25dB below the 4PSK victim's receive threshold power there is no problem. If the interference power level is too high, an appropriate channel spacing or different polarisation should be used, or a different frequency band used if necessary.

After the frequencies at the star point and at the hops with potential interference problems have been allocated, the remaining hops can also be assigned frequencies, which should be selected to provide interference levels at least 25dB below the one error in a thousand bit error threshold level of the victim 4PSK radio.

The distance over which an interfering signal can travel depends on the antenna heights, the refractivity and hence the value of k, and the height of obstacles. The distance over which the signal can be a potential problem depends on the transmit power, the gain of the antennas and the discrimination, the frequency, the polarisation, the receive threshold of the victim radio and the modulation technique used, the modulation technique used by the interfering signal and its spectrum density, and the bandwidth of the interfering and victim radios.

3.13   Repeater sites

Repeater sites can be used to redirect microwave signals over the top of obstacles or around them. It may be more economical to install a mast on the top of a hill in order to connect two stations together when the cost is compared to that of erecting two taller masts to provide line of sight. In city centres repeater sites may allow the point–to–point connection of two sites which do not have line of sight at a crossroads.
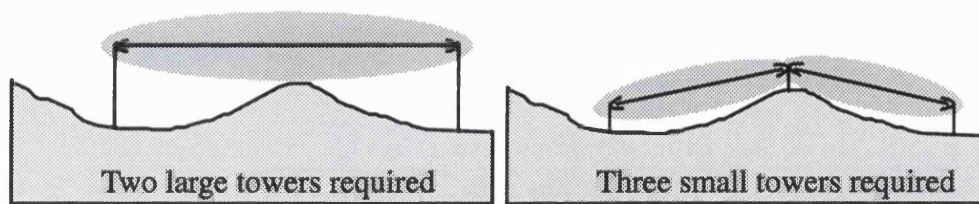
Diagram 1-65   Transmission solution using three smaller cheaper towers

Repeaters may be active or passive. An active repeater receives the signal and passes it from the antenna to an amplifier before retransmitting the signal. Usually two radios are connected back–to–back at the repeater site and the signal is demultiplexed into the constituent 2Mbit/s signals and cross connected to the other radio before being multi-plexed and retransmitted. Alternatively the radio frame may be passed to the other radio on a copper repeater bus, and then retransmitted. Active repeaters require power and a suitable transmission room or shelter.
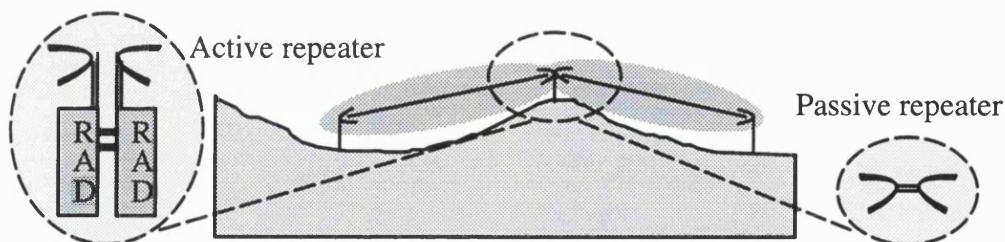
Diagram 1-66   Use of active or passive repeaters

Passive repeaters are usually two antennas connected back to back by a short waveguide. They do not require power, and can be fixed in any location that provides line of sight. The received power is the sum of the four antenna gains, G, the two isotropic free space path losses, FSL, and the original transmit power, Tx, and any waveguide losses, F. The two path loss components dominate, and distances are much shorter than could normally

be achieved by the radios in normal operation.
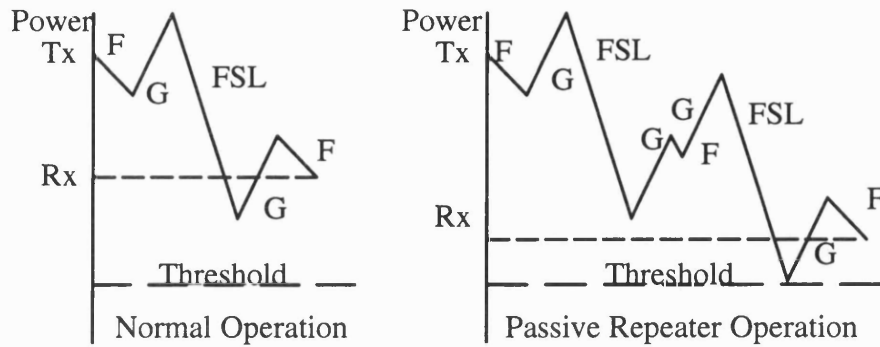
Diagram 1-67   **The reduced fade margin associated with a passive repeater**

Passive reflectors are metallic boards with dimensions greater than the size of the first Fresnel zone. These metallic structures reflect the transmitted signal in the direction of the receiving antenna. However the spread of electromagnetic energy from the reflector can cause an interference problem, and for this reason some frequency administration authorities forbid their use.
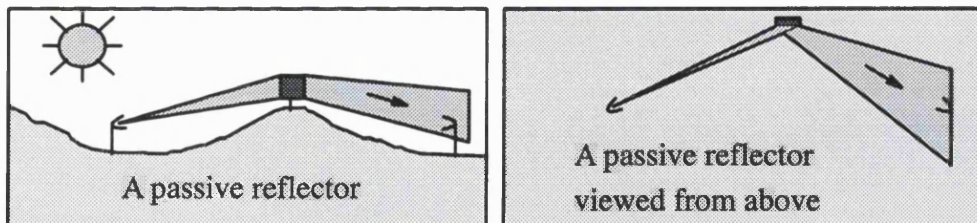
Diagram 1-68   **The use of passive reflectors**

4 The method

4.1 Introduction

To allow network operators to meet the availability and performance requirements defined by the International Telecommunications Union, or by their own organisation, mathematical propagation models are used to predict the performance of the link during the worst month of available time and to predict unavailable time caused by adverse propagation conditions over a period of at least one year. Empirical measurements are used to check the accuracy of existing mathematical models and to develop such models when they do not exist or are too inaccurate.

The International Telecommunications Union presents in recommendation ITU–R P.530–7 formulae for predicting the performance of millimetric and microwave links in the presence of multipath activity and link availability during rainfall. Flat and selective multipath outage for links without strong surface reflections are modelled assuming atmospheric multipath activity. Fixed links at 38 GHz are usually too short to be affected by atmospheric multipath and these formulae are therefore of limited use. The rainfall attenuation model presented in ITU–R P.530–7 assumes a Laws Parsons drop size distribution and is considered to be valid for rainfall fading predictions up to a frequency of 40GHz. The spatial averaging used in that rainfall model may not be appropriate at 38GHz , where the hop length is only a few kilometres.

During normal unfaded operation the power at the receiver will depend on the transmitted power, the gain of the transmitting and receiving antennas, the free space loss and atmospheric absorption. For a given method of modulation, and in the absence of interference, the receive 'threshold' power for a bit error rate of one error in a thousand will

depend on the signal–to–noise ratio, which is influenced by the temperature of the radio and the bandwidth of the received signal. The difference between the normal received power level and the flat fade 'threshold' level is called the flat fade margin. This flat fade margin can be used to predict the performance and availability of a link.

For a given rain intensity, in a homogeneous rain–filled medium, the fading will depend on the drop size distribution, the drop shape, the polarisation used and the drop tempera-ture. Assuming an average drop size distribution, drop shape and drop temperature, it should be possible to relate the cumulative distribution for fading on a vertically pola-rised link to the cumulative distribution for rainfall intensity. The cumulative distribu-tion for rainfall intensity can be measured with a rain gauge. The cumulative distribution for fading can be measured with a personal computer which logs the incoming power level at the receiver. Placing a rain gauge at each end of the hop provides two sets of cumulative distribution, and reduces the chance of missing data due to rain gauge fail-ure. By synchronising the rain gauge clocks the homogeneity of rain cells can be exam-ined. Fading caused by rainfall changes over a period of several seconds and it is there-fore reasonable to time–stamp the received level every three seconds.

The radio transmit power level is temperature dependent and will vary over time. The thermal noise power will change with temperature, affecting the signal–to–noise ratio at the receiver, and thereby changing the flat threshold level. There is a difference be-tween the true received power and the indication of received power provided by the receiver, which is based on the automatic gain control voltage. This error varies with both fade depth and temperature. There is also a small resolution error introduced since small changes in the received power level are not capable of being measured and logged at the receiver. For high receive power levels, that is flat fade margins above 60 dB, the

automatic gain control amplifier will saturate.

To account for these variables the transmit power, receiver sensitivity, indicated power and true power were measured in 1dB steps over the entire power range, repeated at different temperatures. The data should be recorded before and after the research project, over the expected ambient air temperature range. This will allow compensation for inaccuracies in recorded data caused by temperature variation during the project.

On short point–to–point installations at 38GHz the antennas will be located in a position which prevents permanent reflections from being harmful. These paths might be too short to be affected by atmospheric multipath. However, moving objects such as vehicles may cause secondary signals which interfere with the direct signal. Secondary signals can cause bit errors by a combination of fading and distorting the received spectrum or by just fading the received signal down to a low signal–to–noise ratio. The transmitted radio frame contains parity bits in the overhead and the radio is capable of displaying the average bit error rate over a ten, thirty or sixty second period. If the personal computer logs both the received power level and the bit error rate, averaged over ten seconds, it is possible to produce a cumulative distribution for bit error rate and relate it to multipath activity, assuming that the radio itself does not introduce errors due to faulty components. Fading caused by moving vehicles will be transient in nature. Multipath activity can therefore be identified by short periods where a bit error rate is recorded but the received power level, which is recorded every three seconds, is at an acceptable level. If the bit error rate information provided by the radio has been set to provide an averaged error rate over a ten second period, there will be at least three recorded bit errored entries in the log. If the corresponding power levels are above the bit error rate threshold and the rain gauges show no evidence of rainfall, the errors will have been

created by multipath activity or equipment failure.

The unavailability requirements for a single link is likely to be around 0.01% a year or less, which corresponds to 52.6 minutes a year or less. This unavailability should result from rainfall, with possibly a few minutes a year caused by hail. For unavailability, the task is therefore to model the attenuation caused by rainfall. The relationship between rainfall intensity and the attenuation caused by rainfall, can be seen by comparing the cumulative distribution for rainfall and the cumulative distribution for rain induced attenuation. These curves have a characteristic shape which is shown below.
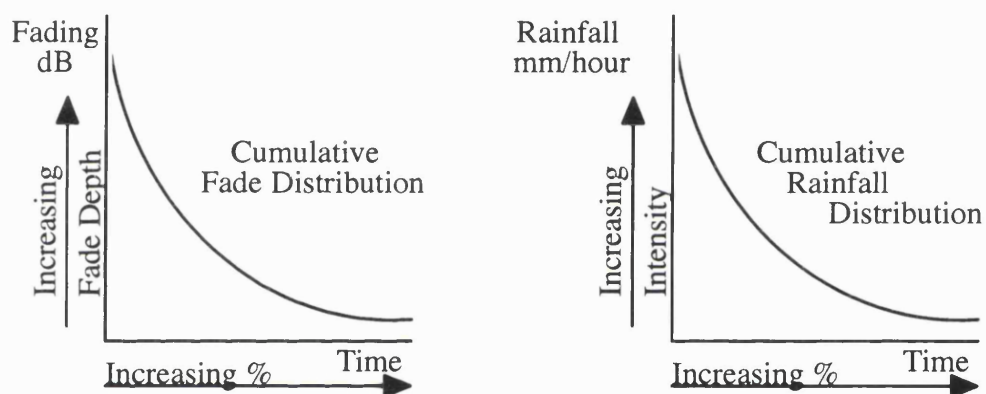
Diagram 1-69   Characteristic cumulative distributions of fading and rainfall

In general, between three and ten thunderstorms per year are typically responsible for the worst 0.01% of fading during the year. The accuracy of any model which relates these cumulative distributions will depend on the number of convective thunderstorms contained within the study. The accuracy will decrease with increasing fading and increasing rainfall rates. The worst 0.001% of fading corresponds to approximately the worst five minutes of the year, and this would be caused by the worst convective cell of the year. To develop an accurate model for the worst five minutes of the the year would require ten to fifteen years of data.

On a radio path of several kilometres the heaviest 52.6 minutes of fading during the year will not necessarily correlate with the heaviest 52.6 minutes of rainfall measured at a single rain gauge at the receiving end of a hop. Attenuation also depends on how much of the path was contained within the significant rain cells as they crossed the path, the size of those cells, the frequency used, the polarisation, the drop size distribution and drop shape within these cells. However even if the worst 52.6 minutes of rainfall and fading occurred at different times, statistically there is a relationship. On a path of two kilometres the worst 52.6 minutes of fading and the worst 52.6 minutes of rainfall measured by rain gauges at the transmitting and receiving ends of the hop may occur at the same time.

4.2   Method used in Australia

Between December 1996 and February 1999 measurements were recorded in Brisbane, Australia to evaluate the effect of rainfall on the availability of a radio signal operating in the 38GHz band. The hop was commissioned in December 1996 to measure the effects of rain between the Optus offices and the Royal Brisbane Hospital. A twelve month measurement period was selected at the beginning of this project, between 1February 1997 and 31 January 1998, to allow for any initial start–up problems. This hop was 2.1 km in length, vertically polarised with an azimuthal angle relative to true north of 212.91 degrees from the Optus building towards the Royal Brisbane Hospital, which is 32.91 degrees towards the Optus building from the Royal Brisbane Hospital.
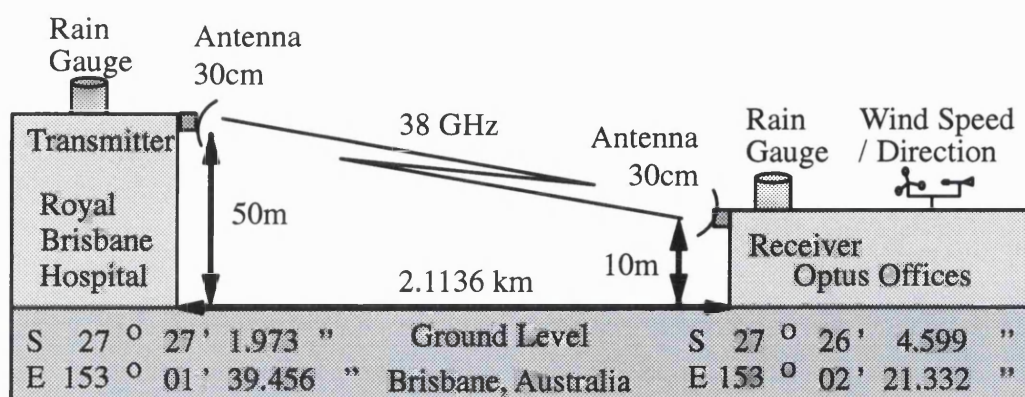
Diagram 1-70   The research hop

A laptop computer with an Intel 286 microprocessor was connected to the NokiaQ1 network management interface of the 38GHz radio at the Optus (receive) end. This personal computer recorded the received radio power, the automatic gain control voltage and demodulator temperature of the receiver. Rainfall, wind speed and direction were measured on separate data loggers. The average ambient temperature over four hour periods was supplied by the local meteorological laboratory. Rain gauges with a 20cm aperture were installed on the roof at the Royal Brisbane Hospital (transmit end) and on the roof at the Optus (receive end) office, within twenty metres of the antennas. These rain gauges were purchased from Hydrological Services PTY., Australia. A dual wind speed/direction monitor and data logger was installed at the Optus (receive) end of the hop. This equipment was purchased from Campbell Scientific Ltd., England. Andrew's 30cm diameter precision antennas with radomes were sited on the roof of the two story Optus (receive end) building, and the roof of the seventeen story Royal Brisbane Hospital (transmit end).

Although the hop crossed a river the geometry prevented surface reflection from the

river causing a multipath problem. A busy railway track crossed the path within 20 metres of the outdoor radio unit at the Optus (receive) end of the hop, which was fixed 10 metres above the ground. The curved metal roof of the carriages which crossed the path presented a reflecting surface which was a possible source of multipath.

The first Fresnel radius at the centre of the hop was 2.03 metres. The Earth's bulge at the centre of the hop, for a k value of 1.33, was 0.06 metres. Clearance between the first Fresnel zone and the ground was 27,91 metres, including the Earth's bulge. Since the average building height on the path was 10 metres the path was free from obstruction.

4.3   The equipment used

4.3.1   Radio

The radios used in Brisbane were prototype versions of the Nokia DMR 38 C model radio with a transport capacity of four 2Mbit/s signals plus a management overhead. This radio consists of an indoor baseband unit and an outdoor radio unit. The units are connected together by two coaxial cables which carry the traffic in both directions and a 48 volt direct current to power the outdoor radio unit. The indoor baseband unit is designed for installation in a 19 inch mechanical rack, while the outdoor radio unit is designed for pole mounting.
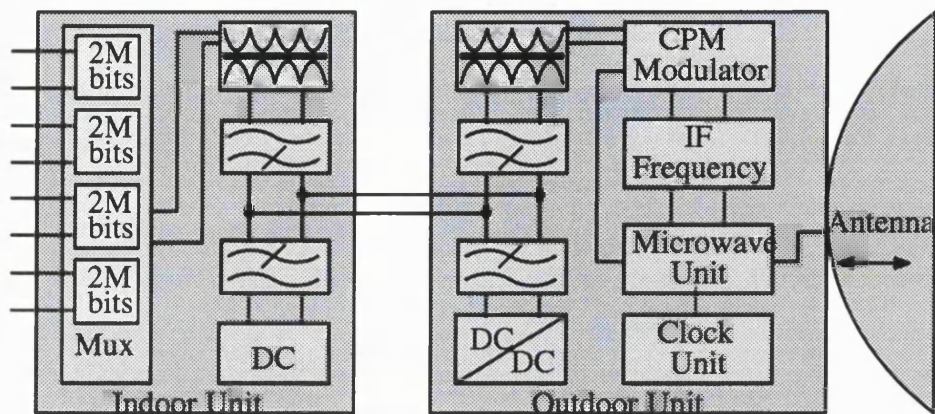
Diagram 1-71   **The Nokia DMR38 C model radio used on the research hop**

The antennas at each end were 30cm parabolic high performance antennas with collar,

radome and boresight gain of 39dBi and a beamwidth at the half power point of two

degrees. These antennas have a Nokia specific fitting and were supplied by Andrew.
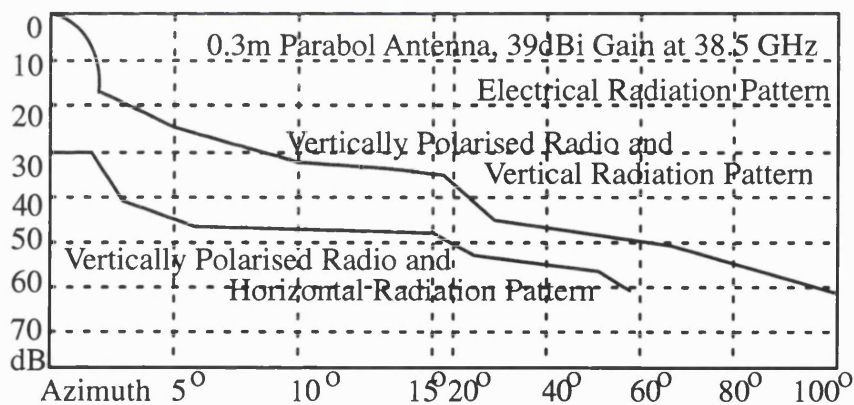
Plot A-1   **The radiation pattern of the 0.3m antenna used on the hop**

The transmit power of the Nokia DMR 38 C radio used at the Royal Brisbane Hospital

(transmit) end of the hop was +11 dBm with a variation of plus or minus 1.5 dB depend-

ing on the frequency used within the band. Additionally there is a maximum variation

of transmit power with temperature of plus or minus 1.5dB over the outdoor unit's speci-

fied ambient operating temperature range from minus 30 degrees Celsius to plus 40

degrees Celsius. The four 2Mbit per second signals and the management overhead were transmitted using continuous phase modulation within a 7MHz bandwidth. The receive sensitivity for a bit error rate of one error in a thousand bits is guaranteed to be less than −81dBm, and when measured it was found to be −83 dBm. This threshold will typically vary by less than 2dB over the specified ambient temperature range between minus 30 degrees Celsius and plus 40 degrees Celsius.
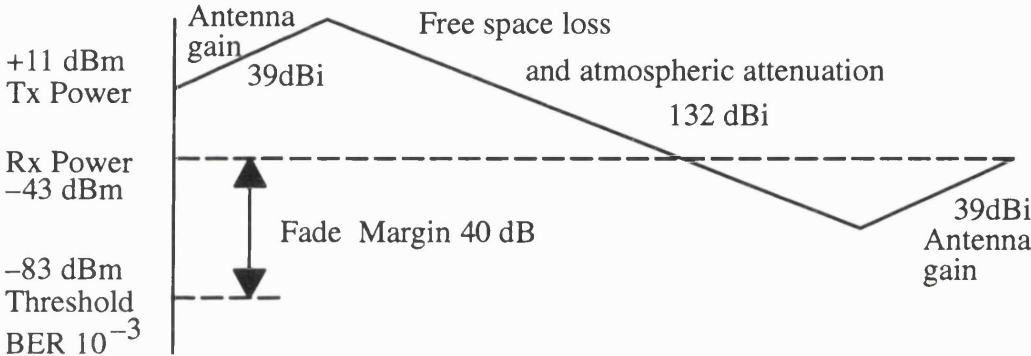
Diagram 1-72   The power budget of the research hop

The radio frame which was transmitted between the two buildings contained the four 2Mbit/s signals and a Nokia specific overhead, which consisted of four data channels and a service telephone channel. In addition to the payload and overhead a number of parity bits are added. By counting the number of erroneous parity bits over a ten, thirty and sixty second period the radio is capable of reporting the bit error rate when polled by a personal computer.
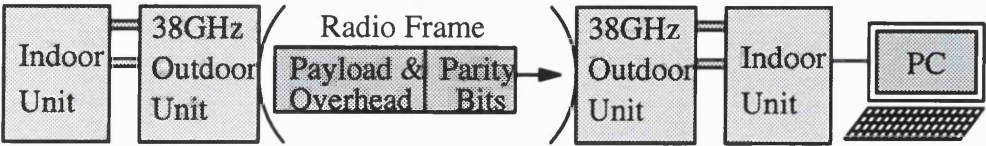
Diagram 1-73   Use of parity bits in the radio frame to calculate bit error rate

At one end the outdoor radio unit was fixed to a secure mounting frame on the roof of a two story building where the Optus (receive end) offices were located. The other outdoor radio unit was fixed to a secure 20cm mounting pole on the roof of the seventeen story Royal Brisbane Hospital (transmit end).

Both ends of the hop were commissioned with a personal computer and Nokia proprietary software, the DMR Manager. The NokiaQ1 network management connector on the indoor radio unit uses an asynchronous, electrically balanced V.11 serial interface, which was set up to work at 9600 bits per second. However, since the personal computer uses an asynchronous, electrically unbalanced V.28 serial interface, a 'black box' was required for converting between the electrically balanced V.11 and electrically unbalanced V.28 serial interfaces.
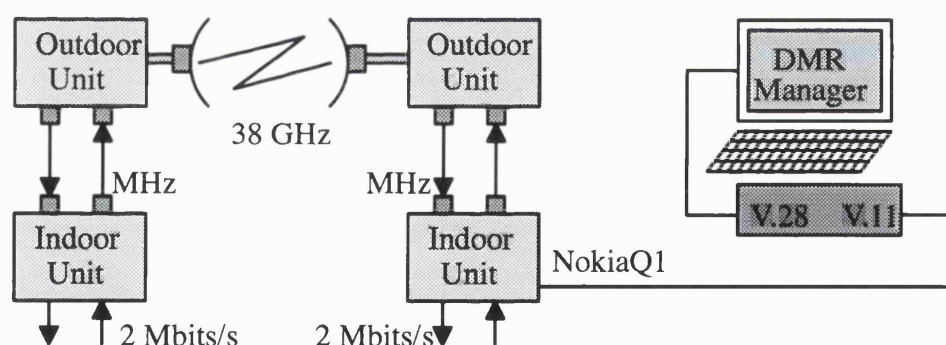
Diagram 1-74   Commissioning the Nokia radios

After commissioning, the personal computer was permanently connected to the indoor unit at the Optus (receive) end of the hop to log the receiver's performance. The personal computer monitored the radio's performance by running the Nokia DMR Manager software in a 'performance window'. The log files produced recorded the incoming power level in dBm. The log files were typically checked daily and reset every five to ten days.
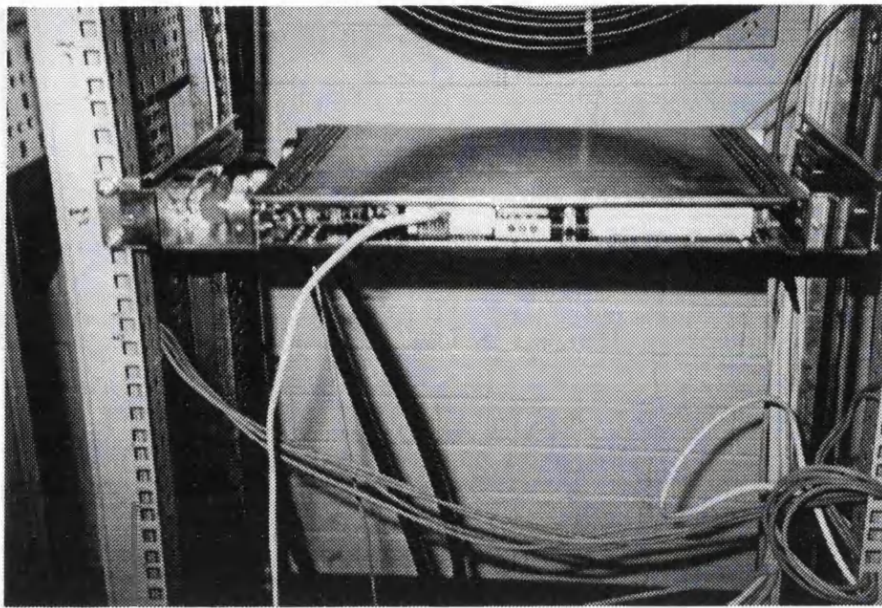
Diagram 1-75   The indoor radio unit at the Royal Brisbane Hospital (tx) end

4.3.2   Wind monitor

Horizontal wind speed and direction were measured in Brisbane with a model 03001–5,

Campbell Scientific, wind anemometer and vane. This instrument uses a 12cm diameter

cup wheel assembly, with hemispherical cups of 4cm diameter to generate an alternat-

ing current sine wave signal with a peak–to–peak voltage and a frequency which is pro-

portional to the wind speed. The wind speed range is 0 to 50 metres a second, with a

threshold of 0.5 metres a second and a gust survival rating of 60 metres a second. The

wind direction is measured using a precision potentiometer with a 355 degree electrical

range, which is attached to a vane with a 360 degree mechanical range and a 16cm turn-

ing radius. The potentiometer is excited via an external direct current, with a maximum

voltage of 15volts. The analogue direct current output voltage from the potentiometer

is proportional to the wind direction, with regard to the excitation voltage applied across

the terminals of the potentiometer.
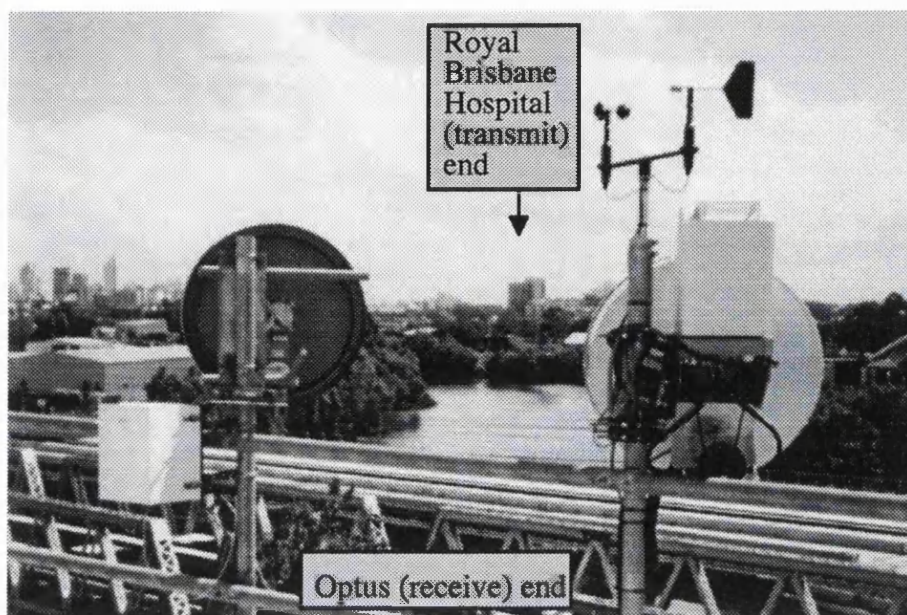
Diagram 1-76   The research hop and wind monitor

The wind anemometer and vane were connected to a CR500 data logger supplied by Campbell Scientific. The data logger was installed inside the Optus (receive end) office next to the indoor radio unit and connected to the sensors via a 20metre, 0.4mm cross sectional area, screened multicore cable. Once every minute the data logger would time stamp the instantaneous wind speed and direction. The data logger used 64kbytes of non volatile flash EEPROM memory to store up to 32000 events. Every minute seven events were recorded: the day, month, year, hour, minute, wind speed and wind direction. The information recorded by the data logger was downloaded to a personal computer and saved every three days to prevent it from being overwritten. The data logger was commissioned and the data was downloaded and saved by using a personal computer, which ran the proprietary CR500 software. The connection between the data logger and the

personal computer was made via the serial V.28 cable interface.
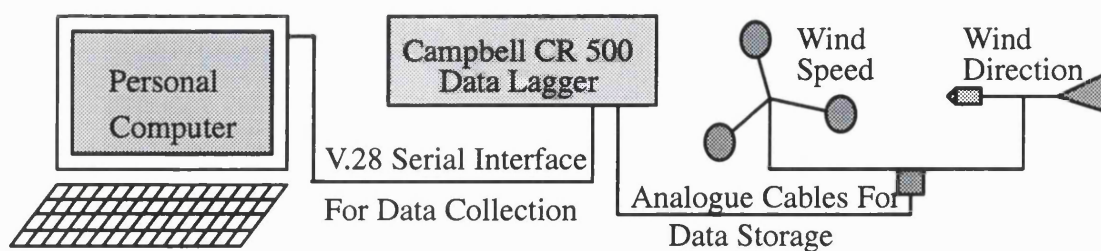
Diagram 1-77   Wind monitor commissioning and subsequent data collection

4.3.3   Rain gauge

The rain gauges used for measurement were supplied by Hydrological Services Pty. Ltd

of Sydney, Australia. These instruments operate based on the tipping bucket principle.

Rainfall is collected in the capture area at the top of the gauge and fed to the tipping

bucket mechanism, after being strained by a metal gauze. The flow of water, which is

fed to the tipping bucket reservoir, is regulated by a valve which limits any measurement

error that could be introduced by water spilling over the full bucket, between tips during

heavy rainfall.
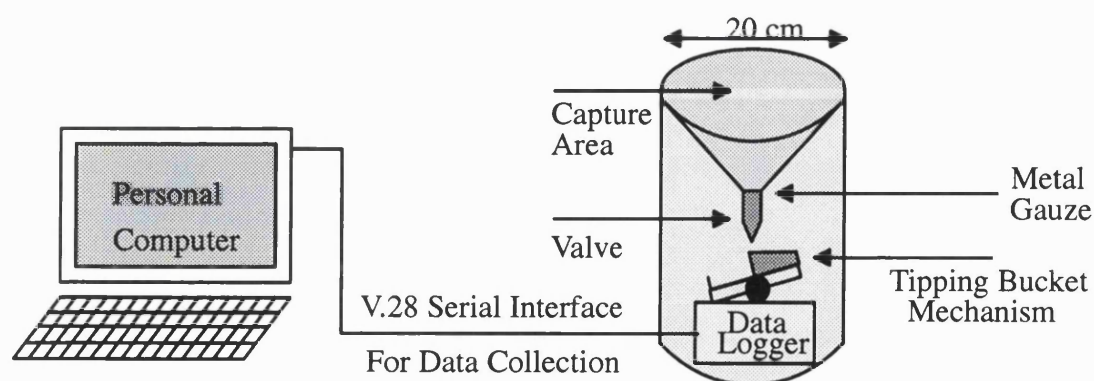
Diagram 1-78   Rain gauge commissioning and subsequent data collection

The rain gauges used had a circular capture area with a diameter of 0.2 metres, which

caused the bucket to tip when a depth of 0.2mm of rain water had fallen. The bucket's

tipping action causes the closure of a normally open dual reed switch. One side of the switch was connected to a local data logger, while it was possible to connect the other side of the dual reed switch to a remote data logger. The closure of these contacts causes the data logger to time stamp the event. Only the local internal data logger was employed. The effects of switch bounce are eliminated by the internal circuit design of the data logger.

The internal data logger is housed within the body of the rain gauge and is powered by six AA 1.5 volt alkaline finger batteries. These batteries were replaced every three months to ensure against loss of data.

The data logger was commissioned with a personal computer which ran the proprietary menu–based software supplied. The personal computer's serial port was connected to the data logger's electrically unbalanced, asynchronous V.28 maintenance port with a proprietary interface cable.

4.3.4 Data processing

There is a variation between the true received power at the end of the radio waveguide and the power indicated by the radio on the NokiaQ1 bus, the value which was recorded in the log files. This variation between the true received power and indicated received power level changes with both the received power level and with changes in ambient temperature.
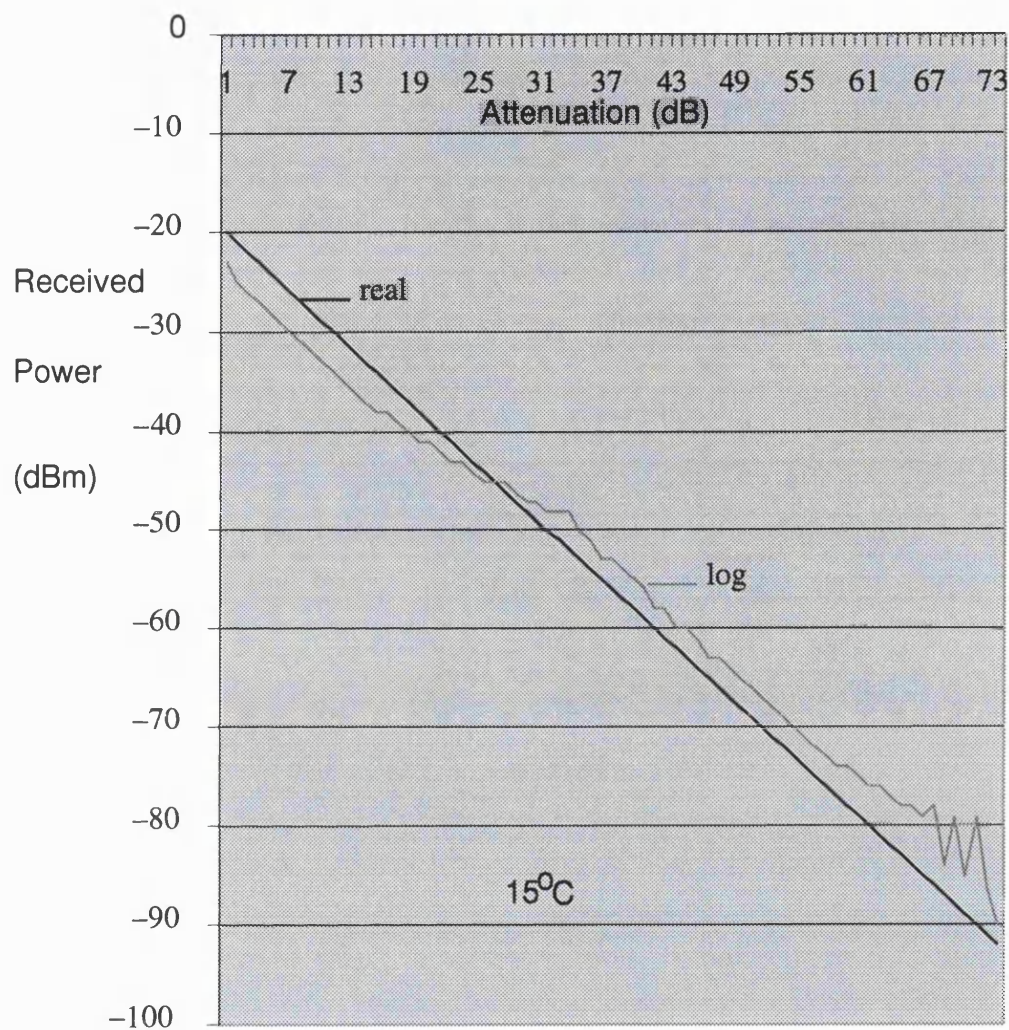
Plot A-2   **Real and indicated received power levels at 15 degrees Celsius**

To account for this variation between the logged received power level and the true

received power level, measurements were made at four different temperatures before

commissioning the radio. This was achieved by varying the air conditioning settings at

the Optus office complex. Several fixed attenuators and a 50dB variable attenuator were

used to sweep the power range between –20dBm and –90dBm in 1dB steps at 15, 20,

26 and 30 degrees Celsius using a hand–held Marconi 6970 power meter with 6914

power sensor, which had been calibrated in the Nokia Calibration Centre in Finland in

November of 1996, five weeks earlier. However, it was expected that once commissioned the radiation from the Sun would have an effect equivalent to an additional 5 degrees Celsius.
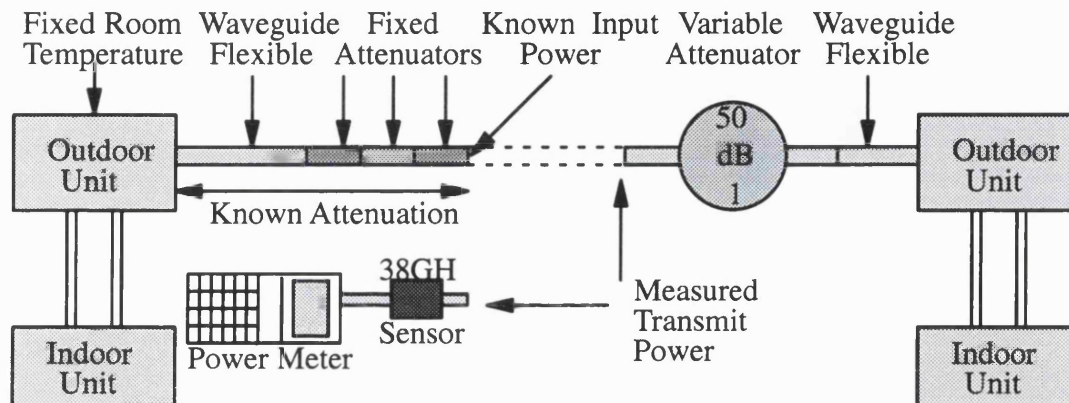
Diagram 1-79   Temperature calibration measurements

The DMR Manager software provided by Nokia polled the radio at the Optus (receive end) office every three seconds and time stamped any changes in the received power level. The report produced shows the date, hour, minute, second, and the received power level.

Date	Hour	Min	Sec	Rx (dBm)
1 Jul	16	40	00	−52
1 Jul	16	40	10	−55
1 Jul	16	40	40	−52

Table 1-2   Example of the received power level log

The indicated received power level in the log report must be adjusted to display the correct received power level. The correction depends on the received power level and upon the ambient temperature. Adjustments were made to take account of the differences in indicated received power and true received power level at the receiver. These adjustments were based on measured data which was recorded before the project began. This

allows the identification of the number of seconds that the receive power level was at

a specified level, or a little less than that value, to be recorded.

Time Min	Time Sec	Logged Rx (dBm)	Adjustment dB	Compensated Rx (dBm)	Time Sec	Minimum dBm
40	0	−52	+2	−50		
40	10	−55	+2	−53	10	50
40	40	−53	+2	−51	30	51

Table 1-3   **Received power level temperature compensation**

The creation of a cumulative distribution for fading requires a knowledge of the variation in transmitted power, which for a fixed frequency will vary with temperature. However, over the temperature range of interest the transmit power only varied by half a decibel.

Nominal Tx (dBm)	Temperature ^oC	Compensated Tx (dBm)	Unfaded Rx (dBm)	Time Sec	Less than dBm	Fade dB
+11	+15 to 30	+10	−43			
+11	+15 to 30	+10	−43	10	50	7
+11	+15 to 30	+10	−43	30	51	8

Table 1-4   **Transmit power level temperature compensation**

For each rain storm the fade levels are tabulated in one decibel steps. The number of seconds that the receiver was at a particular fade level are recorded in the table.

Fade Level Exceeded in dB (for a rain storm)													
17	18	19	20	21	22	23	24	25	26	27	28	29	30
10	10	15	5		10		10	5	15	20	10	5	25
15	30	25			15						15	10	15
30	25	20											
20	10				Time in Seconds								
15													
15													
105	75	60	5	0	25	10	10	5	15	20	25	20	40
Total Time Fade Level Exceeded in Seconds													

Table 1-5   **Typical fading measurements caused by rainfall**

After the fade distribution for each storm has been identified, the annual cumulative distribution is created by summing the times for each fade level in each rain storm throughout the year.

Each time that the bucket mechanism in the rain gauge tips the event is time stamped in the log. Each time stamp recorded by the data loggers in Brisbane represents a rain depth of 0.2mm. The International Telecommunications Union models fading based on rainfall intensity in millimetres per hour when integrated over one minute. Therefore the number of time stamps in a one minute period are multiplied by 0.2mm and this figure is then multiplied by 60 to yield the rainfall intensity in millimetres per hour. By varying the integration time it is possible to average rainfall intensity over any period of interest.

Time Date	Time Hour	Time Min	Time Sec	Number of 0.2mm Tips	Intensity mm / hour
1 Sep	18	29	50		
1 Sep	18	30	10		
1 Sep	18	30	35	3	36
1 Sep	18	30	55		
1 Sep	18	31	10		

Table 1-6   **Identification of rainfall intensity for a given integration time**

The cumulative distribution for rainfall intensity in each storm, at a specified integration time, is obtained by summing the durations that particular rainfall threshold was exceeded. The cumulative distribution for the entire year is obtained by summing the cumulative distributions for each individual rain storm.

The data logger purchased from Campbell Scientific provided a report which shows the instantaneous wind speed and wind direction relative to true north at one minute intervals.

Date Year	Day of Year	Time Hour:Min	Wind Direction True North + Degrees	Wind Speed metres / second
1998	25	20:16	1.895	4.625
1998	25	20:17	44.44	5.525
1998	25	20:18	38.95	3.975

Table 1-7   **Example of the wind speed / direction log**

By creating an Excel sheet with entries for year, month, day, hour, minutes, seconds, fade depth, bit error rate, 0.2mm tips, wind speed, wind direction, and temperature it was possible to produce graphs which compared the variables over a common time base. Adding entries for a rolling rainfall average, integrated over 30 seconds, 1, 2, 3, 4, and 5 minutes allowed a visual comparison between fading and rainfall with different

integration periods to be made.

If it is assumed that the 38GHz radio operates without errors being introduced from electronic and radio frequency components, in an obstruction free environment, then the bit errors recorded must result from multipath or rainfall activity. Rainfall which is capable of fading the received power to levels which produce bit errors will have a duration of some tens of seconds. If the bit error rate supplied by the radio, as an average over ten seconds, is compared with the received power level, a relationship between rainfall and bit errors should be clearly seen. A high receive power level and a simultaneous bit error rate would indicate the presence of multipath on the path.

Time Min	Time Sec	Power Rx (dBm)	Bit Error Rate 10s Average
10	0	−84	3.3×10^{-3}
10	3	−83	4.5×10^{-4}
10	6	−80	5.1×10^{-5}
Example of rain fading			

Time Min	Time Sec	Power Rx (dBm)	Bit Error Rate 10s Average
40	0	−43	3.3×10^{-8}
40	3	−74	4.5×10^{-4}
40	6	−60	5.1×10^{-5}
Example of multipath fading on a different day			

Table 1-8   Characteristic rain induced fading and multipath fading

5 Australian data

5.1 Introduction

This chapter looks at the most significant data collected over a one year period. To begin with the rain events containing at least one minute of rainfall with an intensity greater than 60 mm per hour are identified at each end of the hop. This was done using a one minute integration period and this integration time was used to create all the tables in this chapter. The cumulative distribution recorded at each end of the hop is then presented in tabular form. The possibility of a wind induced error is then considered by comparing the total rainfall at each end of the hop over the year, and additionally by comparing the results from two rain gauges 15 metres apart at the Optus (receive) end during a storm on 27 December 1997 between 1507 and 1600 .

The temperature induced error at the receiver was compensated by comparing the indicated received power level with a known power level at four different ambient temperatures between 15 and 30 degrees Celsius. Based on these temperature compensated values the fading events greater than 6dB are presented in tabular form and the cumulative fade distribution for the worst 53.5 minutes of fading is presented. The impact of wind speed and direction on the cumulative rain and fade distributions is considered, the missing or lost data is also considered and the absence of multipath fading is noted. Correlation between the worst 0.01% of fading and rainfall activity is examined. Finally, availability objectives are considered and a comparison is made between measured data and predicted fading based on ITU–R P.530–7.

5.2 Rainfall data

Between 1 February 1997 and the 31 January 1998 a tipping bucket rain gauge measured

the rainfall intensity at the Optus (receive) end of the hop. These results are presented

on a monthly basis along with a cumulative rainfall distribution for the twelve month

period. The rain gauge supplier offered three different sizes of tipping bucket mechan-

isms with either a 0.1mm, 0.2mm or 0.5 mm bucket. The 0.2 mm bucket was selected,

with each tip corresponding to 12mm of rainfall per hour when a one minute integration

period is used. The 0.2mm bucket therefore limits the resolution to 12mm per hour

(when a one minute integration period is used) but also limits the amount of water which

spills over the full bucket while it is in the process of tipping from one side to the other.

A 0.1mm bucket would have increased the resolution to 6mm per hour but the bucket

mechanism would tip at twice the rate and there would be a reduction in accuracy. The

0.5mm bucket would have reduced the error caused by water spillage but the resolution

would have also been reduced to 30mm per hour.

5.3 Rainfall events

The period of time over which measured rainfall is integrated has a significant impact

on the recorded rainfall rate, as can be seen from Appendix B. The method presented

for approximating rain induced attenuation in ITU–R P.530–7 requires the rainfall

exceeded for 0.01% of an average year using a one minute integration period. According

to ITU–R P.837–1 the rainfall exceeded for 0.01% of the time is 63 mm per hour when

a one minute integration period is used. At the Optus (receive) end of the hop twenty

six rainfall events were registered which contained at least one minute where the rain

intensity was 60 mm per hour or greater. At the Royal Brisbane Hospital (transmit) end

of the hop twenty seven rainfall events were recorded with at least one minute where the intensity was 60 mm per hour or greater. In both cases a sixty second integration time was used to measure the rainfall intensity.

O P T U S 1 F e b u a r y 199⁷ To 31 J a n u a r y 199⁸	Date	Time	Max intensity (60s)	Duration (minutes)
	16 Feb	2234 – 2242	96	9
	18 Feb	0953	60	1
	26 Mar	1312	60	1
	31 Mar	1613 – 1216	60	4
	29 Apr	1215	60	1
	16 May	1847 – 1850	96	4
	16 May	2036	60	1
	30 May	1919 – 1933	120	15
	7 July	1343	60	1
	24 Sep	1350 – 1354	72	5
	25 Sep	1439	60	1
	7 Oct	2005	60	1
	7 Oct	2121 –2124	84	4
	7 Oct	2140 – 2141	108	2
	8 Oct	0001 – 0005	180	5
	17 Nov	1748	60	1
	18 Nov	0855	60	1
	30 Nov	1741 – 1751	96	11
	23 Dec	2157 – 2158	72	2
	23 Dec	2258 – 2302	132	5
	27 Dec	1518 – 1529	108	12
	11 Jan	0659	60	1
	28 Jan	1207 – 1214	132	8
	28 Jan	1224 – 1316	168	53
	31 Jan	0307 – 1308	72	2
	31 Jan	0345 – 0348	84	4

Table 1-9   **Rain rates of 60mm/hour or more measured at the Optus end**

	Date	Time	Max intensity (60s)	Duration (minutes)
R B H	18 Feb	0130	72	1
	22 Mar	1957	72	1
	26 Mar	1212	60	1
	29 April	1336 – 1339	72	4
	16 May	1856	60	1
1	16 May	2039	60	1
F	30 May	1926 – 1930	84	5
e	24 Sep	1349 – 1357	120	9
b	7 Oct	1925	60	1
u	7 Oct	2121	72	1
a	7 Oct	2358	96	1
r	16 Nov	1832	84	1
y	17 Nov	2025	60	1
1997	30 Nov	1736 – 1739	96	3
	30 Nov	1743 – 1749	72	7
To	10 Dec	0915	72	1
	10 Dec	0919	60	1
31	23 Dec	2203	60	1
	23 Dec	2301	60	1
J	11 Jan	0826	60	1
a	13 Jan	0920 – 0921	60	2
n	28 Jan	1225 – 1229	72	5
u	28 Jan	1244 – 1310	216	27
a	31 Jan	0310	60	1
r	31 Jan	0312	60	1
y	31 Jan	0349	84	1
1998	31 Jan	1646	60	1

Table 1-10   **Rain rates of 60mm/hour or more measured at the RBH end**

5.4   Cumulative rainfall distribution

The ITU model used to predict fading on a millimetric or microwave radio link requires a knowledge of the heaviest rainfall for 0.01% of an average year, which is the heaviest 52.6 minutes of rain in an average year. At the Optus (receive) end of the hop 96 mm per hour and 84 mm per hour rainfall intensities were exceeded for 45 and 64 minutes respectively over the measurement period. Linear interpolation suggests that 91 mm per hour was exceeded for 0.01% of the year at the Optus (receive) end. At The Royal Brisbane Hospital (transmit) end of the hop a rainfall intensity of 72 mm per hour was exceeded for 0.01% of the twelve month measurement period.

Rain (60s)	Rainfall duration in minutes for months February 97 to January 98 Measured at the Optus end of the hop												Cumulative
mm/h	Feb	Mar	Apr	May	Jun	Jul	Aug	Sep	Oct	Nov	Dec	Jan	Minutes
24	45	54	13	164	28	31	2	45	143	127	81	61	1143
36	25	6	4	32	2	5	0	8	34	24	20	16	350
48	1	5	1	6		0	2	3	2	7	0	4	174
60	2	3	1	4		1		3	3	5	5	8	143
72	7			6				3	4	4	3	17	108
84	0			2					1	1	5	10	64
96	1			2					0	1	3	7	45
108				3					1		1	4	31
120				1					0		0	6	22
132									1		1	5	15
144									0			2	8
156									0			2	6
168									0			3	4
180									1				1

Table 1-11   Cumulative rainfall distribution at the Optus end of the hop

Rain (60s) mm/h	Rainfall duration in minutes for months February 97 to January 98 Measured at the RBH end of the hop												Cumu-lative Minutes
	Feb	Mar	Apr	May	Jun	Jul	Aug	Sep	Oct	Nov	Dec	Jan	
24	34	31	10	119	15	21	3	42	121	107	68	56	867
36	7	12	4	18	1	2		7	14	19	19	13	240
48	4	6	2	10		3		4	0	6	4	8	124
60	0	1	2	3				2	1	4	3	9	77
72	1	1	1	3				2	1	4	1	3	52
84				1				0	0	2		4	35
96								1	1	1		3	28
108								0				3	22
120								2				0	19
132												3	17
144												2	14
156												3	12
168												2	9
180												4	7
156												2	3
168												0	1
180												1	1

Table 1-12   **Cumulative rainfall distribution at the RBH end of the hop**

5.5   Total rainfall

At the Optus (receive) end of the hop between midnight on 1 February 1997 and mid-

night on January 30 1998 there were 4772 tips of the rain gauge representing 954.8 mm

of rainfall. There were 132 days where at least one tip of the gauge was recorded. At the

Royal Brisbane Hospital (transmit) end of the hop over exactly the same period there

were 3881 tips representing 776.2 mm of rainfall. The rain gauge recorded at least one

tip on 103 days. Since the gauge at the Royal Brisbane Hospital (transmit) end of the

hop was removed before midnight on the 31 January 1998 the comparison was carried

out up to midnight on 30 January. Less rainfall was recorded during the year at the Royal

Brisbane Hospital (transmit) end and this may have been due to the effects of wind at

the top of the building, 50 metres above ground level compared to the Optus (receive)

end where the gauge was 10 metres above ground level. This may also explain why the

heaviest 52.6 minutes of rainfall were 72 mm per hour or more at the Royal Brisbane

Hospital (transmit) end compared with 91 mm per hour or more at the Optus (receive)

end.
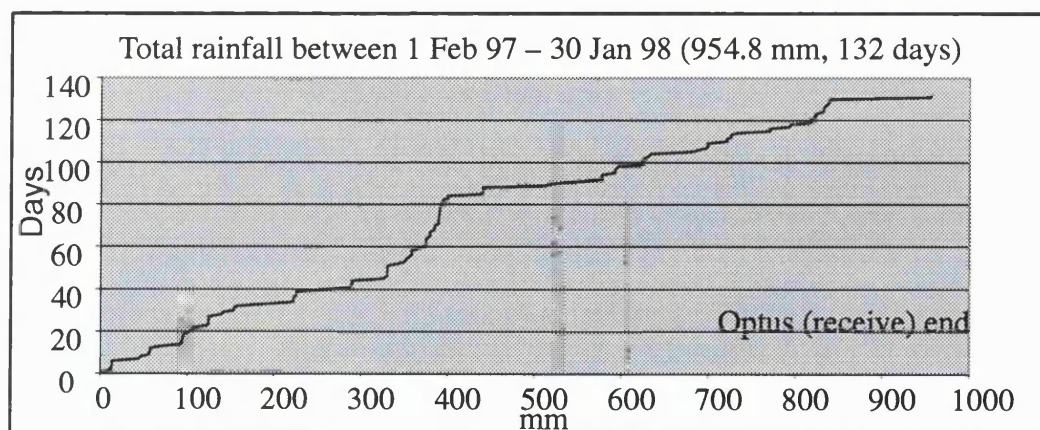
Plot A-3   **Total rainfall at the Optus end between 1.Feb.97 and 30.Jan.98**

Total rainfall between 1 Feb 97 – 30 Jan 98 (776.2 mm, 103 days)
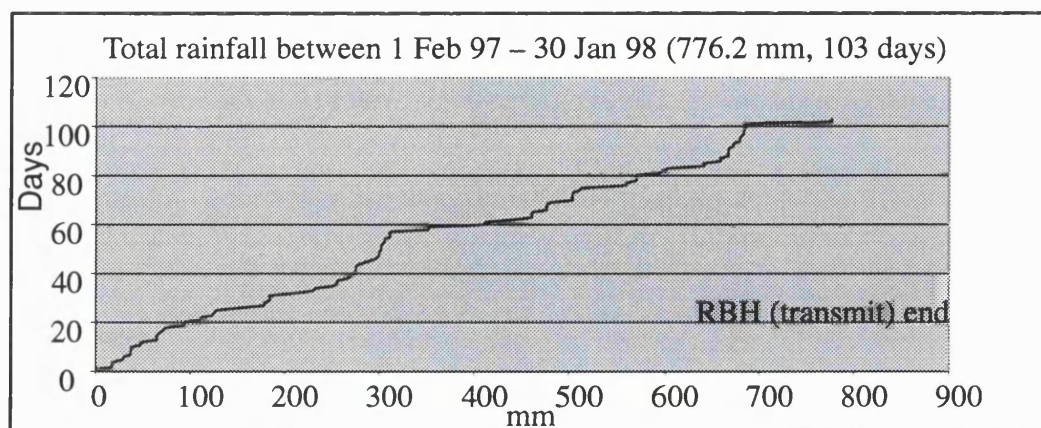
Plot A-4   **Total rainfall at the RBH end between 1.Feb.97 and 30.Jan.98**

5.6   Second rain gauge

Between 1 April 1997 and 31 January 1998 two identical rain gauges were used at the

Optus (receive) end of the hop. A comparison was made between the rain gauges to

check the accuracy of the recorded rainfall. Both of the rain gauges used in the compari-

son had been calibrated on site with a three percent error for a rainfall intensity of 100

mm per hour, integrated over one minute, in December of 1996 and February 1998. The

records produced by the rain gauges were nearly identical over the nine months the com-

parison was made. This suggests that the error produced by the tipping bucket mechan-

ism did not exceed the three percent error noted during calibration. However, the two

gauges would have been simultaneously exposed to the same wind intensity since they

were separated by fifteen metres on the flat roof at the Optus (receive) end of the hop.
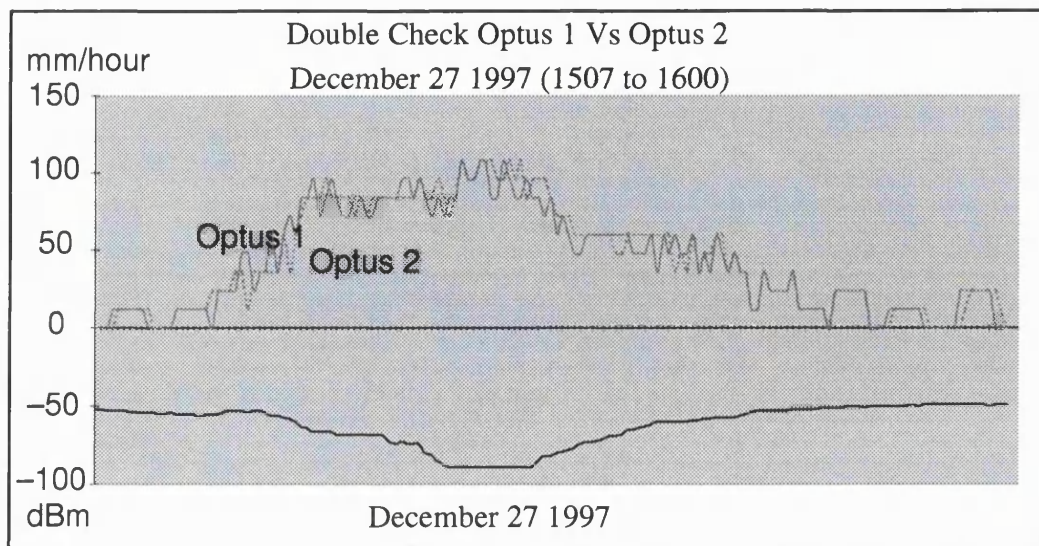
Plot A-5   **Rainfall comparison between two rain gauges located at Optus**

5.7   Calibration of received power level

The radio hop used in Brisbane operated with a vertically polarised electric field at a frequency of 38GHz over a 2.1km hop. Between 1 February 1997 and 31 January 1998 the received power level was logged at the Optus (receive) end of the hop. The normal received signal power level during non fading conditions was –43 dBm. The receive power level for a sensitivity of one bit error in a thousand bits was measured and found to be –83 dBm.
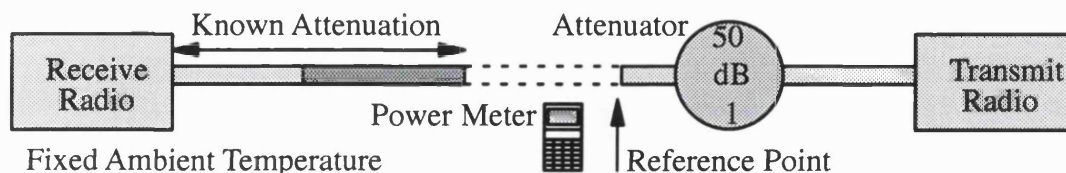
Diagram 1-80   **Comparison between actual and indicated receive power**

In December 1996 a comparison was made between the actual received power level and the received power level indicated by the radio, which was to be installed at the Optus

(receive) end of the hop. The measurements were conducted in one decibel steps between input power levels of –20dBm and –90 dBm, at ambient temperatures of 15, 20, 26 and 30 degrees Celsius. The first set of measurements were made at 15 degrees. However, the reference power level measured with the Marconi 6970 power meter and 6914 power sensor (before the fixed attenuators at the input to the radio receiver) was allowed to fall to a level below –18dBm where the measurements were unreliable. The power meter had been calibrated one month earlier down to a level of –30 dBm. This mistake was not repeated and the reference power level measured at temperatures of 20, 26 and 30 degrees was always greater than –18dBm and these measurements were therefore considered to be reliable. For power levels at the radio receiver which were greater than –78 dBm the measurements made at 15 degrees are also considered to be reliable. This was because the reference power level did not fall below –18dBm when these measurements were made.

The difference between indicated and measured power is shown below.
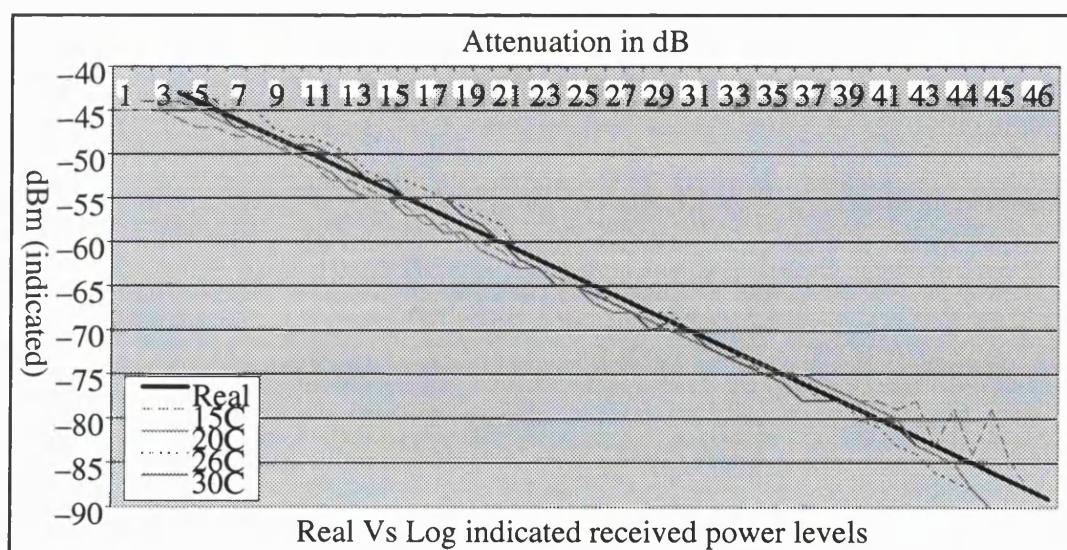
Plot A-6   **Temperature induced uncertainty in the received power level**

The relationship between the power level indicated by the personal computer and the real received power level at temperatures of 15, 20, 26 and 30 degrees Celsius is shown in the table below. The cumulative distributions created in this thesis assume a minimum receive power level .

Indicated power	Uncertainty	Real value range
–50dBm to –59 dBm	+ – 2dB	–48 dBm to –61 dBm
–60 dBm to –70dBm	+2dB	–58 dBm to –68 dBm
–71 dBm to –74 dBm	+1dB	–70 dBm to –73 dBm
–75 dBm to –80 dBm	+ – 1dB	–74 dBm to –81 dBm
–81 dBm to –84 dBm	+2dB	–79 dBm to –82 dBm
–85 dBm to –89 dBm	+4dB	–81 dBm to <–84 dBm

Table 1-13   Temperature induced uncertainty in the received power level

The research hop was decommissioned in February 1998. It had originally been planned to measure and record the real received power level and the receive power level indicated by the receiver at the Optus end at 15, 20, 26 and 30 degrees Celsius and compare these values with the original measurements from December 1996. However the power meter which was to be taken to Australia in 1998 had a faulty 38GHz sensor, and it proved to be impossible to obtain a replacement sensor at short notice in England, Finland or Australia. It was therefore impossible to measure and confirm the variation of real and logged (indicated) power levels at the end of the experiment.

5.8   Fading at the receiver

The temperature compensated receive power level had faded by more than 6dB on 31 occasions between 1 February 1997 and 31 January 1998, for a total duration of ten hours and 22 minutes. However, because of data loss no fading measurements were

available for the periods between 2 May and 6 May and 8 October and 18 November

1997. No fading events were recorded between 22 June and 6 August 1997 due to the

failure and subsequent repair of the Gunn–diode transmitter unit used in the transmit

radio at the Royal Brisbane Hospital end of the hop.

Fades greater than 6 dB measured at the Optus end			
Date	Time Fade > 6 dB	Maximum Fade dB	Minutes
18 Feb	0053 – 0057	25	5
18 Feb	1403 – 1405	15	3
22 Mar	1919 – 1923	18	5
26 Mar	1124 – 1138	15	5
26 Mar	1235 – 1237	15	3
31 Mar	1527 – 1558	25	32
29 Apr	1145 – 1202	31	18
29 Apr	1258 – 1303	24	6
30 Apr	1210 – 1213	19	4
1 May	0028 – 0039	27	12
16 May	1808 – 1819	34	12
16 May	1946 – 1949	21	4
16 May	1959 – 2002	19	4
30 May	1836 – 1904	>41	29
21 Jun	1051 – 1058	18	8
24 Sep	1341 – 1426	>41	46
7 Oct	1902 – 2032	34	91
7 Oct	2059 – 2159	34	61
7 Oct	2221 – 2229	20	9
7 Oct	2355 – 0001	>41	7
30 Nov	1734 – 1810	>41	37
10 Dec	0923 – 0954	25	32
23 Dec	2155 – 2210	24	16
23 Dec	2251 – 2309	36	19
27 Dec	1511 – 1537	>41	27
11 Jan	0823 – 0828	15	6
16 Jan	2106 – 2113	15	8
28 Jan	1207 – 1328	>41	82
31 Jan	0305 – 0314	36	10
31 Jan	0345 – 0349	>41	5
31 Jan	1644 – 1659	21	16
Missing data	2 May – 6 May	22 Jun – 6 Aug	8 Oct – 18 Nov

Table 1-14   **Fading events greater than 6 dB**

There were three hours and fifty three minutes of recorded fading between 1 February

1997 and 31 January 1998 where the received power faded by 15 dB or more. The

recorded fading activity has been examined on a monthly basis and a cumulative fading

distribution shown for fading between 15 dB and 41 dB, and fades greater than 41 dB can be found in Appendix 3. The worst 0.01% of recorded annual fading is shown below. These fading distributions are based on the personal computer recording an unfaded signal at the Optus (receive) end of −43 dBm.

Worst 53.483 minutes of fading between 1 February 1997 and 31 January 1998								
Min Fade dB	30 May 1836 1904	24 Sep 1341 1426	7 Oct 2355 0001	30 Nov 1734 1810	27 Dec 1511 1537	28 Jan 1207 1328	31 Jan 0345 0349	Cumul– ative Minutes
37	47	0	0	23	12	35	0	53.483
38	0	46	0	13	0	23	0	51.533
39	34	139	0	285	22	69	35	50.167
40	12	34	12	36	12	12	0	40.433
41	23	58	0	69	0	103	0	38.467
>41	207	0	34	0	138	1676	0	34.25

Table 1-15   **The worst 53 minutes of measured fading**

5.9   Wind speed and direction

Heavy rain fading is associated with convective rain cells in the mature stage of development. Mature convective rain cells are characterised by strong downdrafts. It was assumed at the beginning of the research that these downdrafts would be responsible for a reduction in the capture area of the rain gauges during thunderstorm activity by blowing the drops across the top of the instrument. However after examining the wind speed log during heavy fading activity it was observed that the wind speed was typically four metres per second. This would not be strong enough to introduce a significant error into the measured rain intensity during heavy rain fading. This was examined by plotting wind speed and fading on the same plot. The worst storm of the year is shown below

as an example. The wind speed here is typical of wind speed recorded during other thunderstorms.
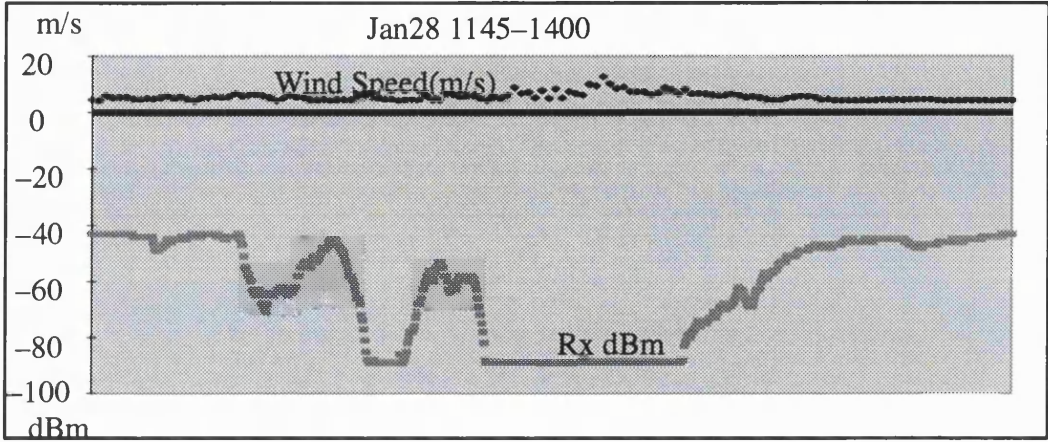
Plot A-7   Wind speed during the worst fading of the year

No preferred wind direction was found when different thunderstorms were compared with each other and even during a single thunderstorm there were changes in wind direction.
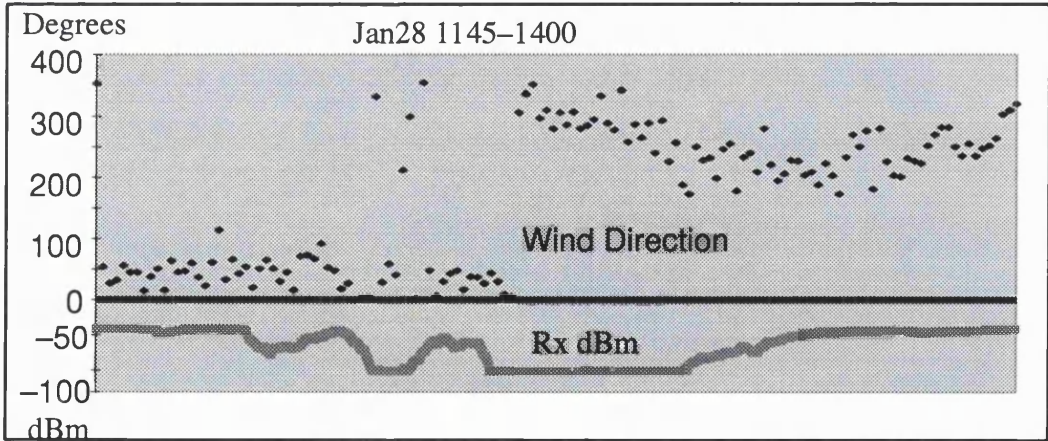
Plot A-8   Wind direction during the worst fading of the year

5.10 Missing data

Between 1 February 1997 and 31 January 1998, information on fading activity was not available for the periods from 2 May to 6 May, 22 June to 6 August and 8 October to 18 November. The data recorded from 2 to 6 May and from 8 October to 18 November were corrupted and could not be recovered. At the beginning of June the radio at the Royal Brisbane Hospital (transmit) end of the hop began to produce microwave unit alarms on occasions. The alarms produced were a known symptom of eventual transmitter failure and so the decision was made to repair the radio during the Australian winter rather than risk failure in the spring and summer months when significant fading was expected. The link was therefore decommissioned between 22 June and 6 August to allow the radio to be shipped to Finland for repair. Fortunately the faulty radio was at the transmitting end and the repair did not affect the calibration measurements performed on the radio at the receiving end. No data was ever lost from the rain gauges which were used.

Between 2 May and 6 May no significant rainfall measurements, at or above 60mm per hour, were made at either end of the hop. Between 22 June and 6 August there was one period of significant rainfall at 1433 on 7 July when the intensity was 60 mm per hour at the Optus (receive) end of the hop. Between 8 October and 18 November there were four occasions where there was significant rainfall. On 17 and 18 November at 1748 and 0855 respectively, there were two one minute periods of rainfall with an intensity of 60 mm per hour at the Optus (receive) end of the hop. On 16 and 17 November at 1832 and 2025 there were two one minute periods of 84 and 60 mm per hour respectively at the Royal Brisbane Hospital (transmit) end of the hop.

5.11 Multipath

The path profile prevented reflections from the river from causing a multipath problem, and the antenna discrimination on a 2.1 km path prevented atmospheric multipath from presenting a problem. At the start of the project it was felt that the curved metal surface of trains which passed within 20 metres of the Optus (receive) end of the hop could create a multipath problem. Fading caused by the passage of a train across the hop would have a duration of seconds rather than minutes associated with rain fading.

After analysing the received power level it was noted that all observed fades of 15 dB or more occurred on rainy days. There were no unexplained bit error bursts during the year. All the error bursts were associated with heavy rain fading when the receive power had been attenuated to a power level of −79 dBm or less.

5.12 Worst 53 minutes of fading

Using an integration period of one minute the ITU model finds the rainfall intensity exceeded for 0.01% of the time to determine the fading exceeded for 0.01% of an average year. Conversely the heaviest 0.01% of fading is related to the heaviest 0.01% of rainfall. The worst 53.483 minutes of fading during the twelve month observation period, that is 0.01017% of the year, was caused by five rain storms in 1997 on 30 May, 24 September, 7 October, 27 December 1997 and two rain storms during 1998 on 28 January and 31 January. The received power at the Optus end of the hop and the rainfall intensity at each end of the hop have been plotted on a common time axis for each of these storms. These plots can be found in Appendix F. The storm which caused the worst fading and heaviest rainfall is shown here.
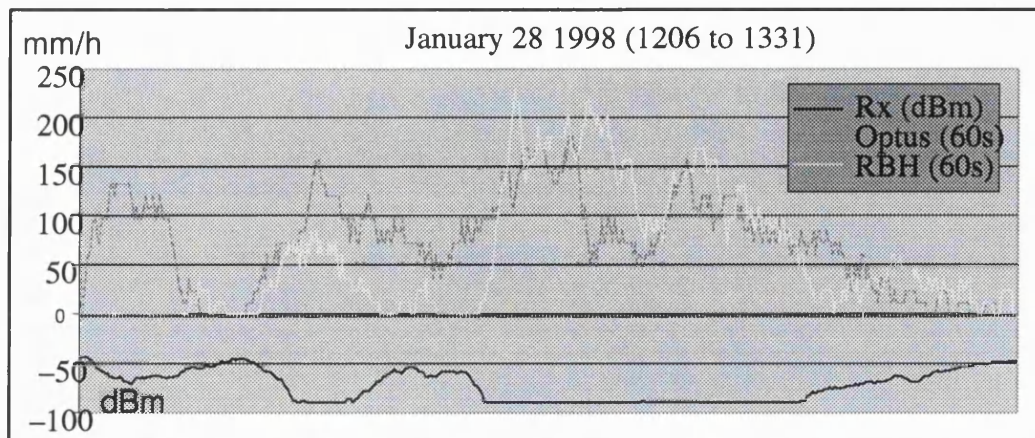
Plot A-9 **Rain rate at Optus and RBH 1206 – 1331 on 28.Jan.1998**

When comparing the recorded rainfall at the Optus (receive) and Royal Brisbane Hospital (transmit) ends of the hop with the seven heaviest fading events of the twelve month period it can be seen that the storms which caused this fading also caused rainfall intensities of 72mm per hour or more. Generally, the rain storms causing the heaviest fading also caused the heaviest rainfall.

Correlation of the worst 53 minutes of fading with rainfall intensity									
	Radio	Duration Fade 5dB or less		Optus	Duration Rain 60mm/h or more		RBH	Duration Rain 60mm/h or more	
Date	Min dB	Start	Finish	mm/h	Start	Finish	mm/h	Start	Finish
30 May	>41	1836	1904	120	1919	1933	84	1926	1930
24 Sep	41	1341	1426	72	1350	1354	120	1349	1357
7 Oct	>41	2355	0001	180	0001	0005	96	2358	
30 Nov	41	1734	1810	96	1741	1751	96	1736	1739
								1743	1749
27 Dec	>41	1511	1537	108	1518	1529			
28 Jan	>41	1207	1328	132	1207	1214	72	1225	1229
				168	1224	1316	216	1244	1310
31 Jan	39	0345	0349	84	0345	0348	84	0349	

Table 1-16 **Correlation of the worst 53 minutes of fading with rainfall rate**

The heaviest rainfall recorded at one rain gauge does not necessarily coincide with the heaviest fading because fading depends upon the structure of the rainfall along the path. At the Optus (receive end) rain gauge on 16 February and on 16 May a peak rainfall intensity of 96mm per hour was recorded. On 7 October 108mm per hour was recorded at Optus, and on 23 December 132 mm per hour was recorded at Optus. These events were amongst the heaviest fortyfive minutes of rainfall recorded at the Optus (receive) rain gauge, but did not contribute to the heaviest 53 minutes of fading.

At the Royal Brisbane Hospital (transmit end) on 18 February, 22 March, 29 April, 7 October and 10 December the rainfall intensity was recorded at 72 mm per hour. These were amongst the heaviest fifty two minutes rainfall recorded at the Royal Brisbane Hospital end of the hop but they did not contribute to the heaviest 53 minutes of fading recorded during the year.

5.13 Planning

Objectives are set for quality and availability between the mobile switching centre and the last base station in the network. The overall objective is then subdivided and allocated to the individual circuits which make up the network. At 38GHz the hop is subject to rain fading and it is important to have a large enough fade margin to allow the availability objectives for the link to be satisfied. However, the larger the fade margin the greater the chance of interference reducing the threshold sensitivity of other 38GHz links. This is particularly true at star points in dense urban networks. Unnecessary fade margins therefore increase the number of frequency channels which the operator needs. At best this is an unnecessary expense, and at worst these extra channels may not be available, and the network objectives are therefore difficult to meet.

5.14   The ITU model

In ITU–R P.530–7 the International Telecommunications Union outline a method for

predicting the long term unavailability caused by rainfall. The first step is to obtain the

rainfall intensity, integrated over a period of one minute, which is exceeded for 0.01%

of the time, which is termed R0.01. An estimation of this value can be obtained from

the global rainfall maps in ITU–R P.837–1 if reliable local data is not available. Once

R0.01 is known the specific attenuation Y, in dB per kilometre, caused by this rainfall

rate can be approximated by using a power law approximation provided in ITU–R P.838.

$$Y = a\left(R_{0.01}\right)^b$$

Formula A-72   Specific attenuation in decibels per kilometre

The coefficients a and b are provided for frequencies between 1 and 400GHz in ITU–R

P.838. These values are frequency and polarisation dependent and are considered to be

reliable at frequencies below 40 GHz. The coefficients for 38 GHz must be obtained by

interpolation, according to ITU–R P.838.

Frequency	a_v	b_v
38	0.27617	0.94385

Table 1-17   ITU–R P.838 coefficients for vertical polarisation at 38GHz

The specific attenuation obtained is valid for a uniform rain medium. To take account

of the non uniform nature of rain a reduction factor r is used, which takes the hop length

and rainfall intensity at R0.01 into consideration.

$$r = \frac{1}{1 + \left(\dfrac{L}{L_o}\right)}$$

Formula A–58   Reduction factor for the ITU–R P.530–7 attenuation model

Where L is the hop length in kilometres and Lo is given by

$$L_o = 35\ e^{-0.015R_{0.01}}$$

Formula A–59   ITU–R P.530–7 path length correction parameter

When $R_{0.01}$ is less than 100 mm per hour, Lo should be calculated using the real rainfall value, but when $R_{0.01}$ is greater than 100 mm per hour the value 100 should be used in place of the $R_{0.01}$ figure, since this limits the effect of the reduction factor with increasing rainfall intensity.

The path attenuation $A_{0.01}$ exceeded for 0.01% of the time can therefore be calculated from the expression

$$A_{0.01} = a\left(R_{0.01}\right)^b L r$$

Formula A–60   ITU–R P.530–7 predicted attenuation exceeded 0.01% of time

This is considered to be valid for frequencies as high as 40GHz.

Rainfall mm/h Exceeded 0.01% $R_{0.01}$ (60s)	Specific Attenuation aR^b (dB/km)	Reduction Factor r	Attenuation Exceeded 0.01% $A_{0.01}$ (2.1km)
60	13.167	0.8714	24.09
65	14.200	0.8628	25.63
70	15.229	0.8596	27.49
75	16.254	0.8440	28.81
80	17.275	0.8339	30.25
85	18.292	0.8232	31.62
90	19.306	0.8121	32.93
95	20.317	0.8003	34.15
100	21.324	0.7881	35.29
105	22.329	0.7881	36.96
110	23.332	0.7881	38.61
115	24.331	0.7881	40.27
120	25.329	0.7881	41.92

Table 1-18   **Rain rate and expected attenuation according to ITU–R 530–7**

Once the attenuation figure exceeded for 0.01% of the time is known other percentages within the range 1% to 0.001% can be approximated from the expression

$$A_P = A_{0.01} \, 0.12P^{-(0.546 + 0.043 \log P)}$$

Formula A–64   **Attenuation predictions for different percentages of time**

Where P is the percentage in question. For example, if $A0.01$ is 37 dB then according to this method $A0.015$ is 31.64 dB.

$$A_P = A_{0.01} \, 0.12(0.015)^{-(0.546 + 0.043 \log 0.015)} = 31.64 \, dB$$

Formula A-73   **Attenuation predictions for 0.015% of time on the test hop**

It is possible to approximate the rainfall exceeded for 0.015% of the time by assuming

a power law for the new rain rate

$$A_{0.015} = a\left(R_{0.015}\right)^b L_r = 31.64\, dB$$

Formula A-74   **Attenuation predicted for 0.015% of the time on the test hop in terms of the predicted rainfall exceeded for 0.015% based on the ITU–R P.530–7 attenuation model**

therefore

$$R_{0.015} = \sqrt[b]{\frac{\left(\dfrac{A_{0.015}}{L_r}\right)}{a}}$$

Formula A-75   **Predicted rainfall exceeded for 0.015% based on the ITU–R P.530–7 attenuation model**

This approximation uses the same values for a and b that were used for the R0.01 power

law. The R0.01 rainfall of 85 mm per hour should cause 31.64 dB of attenuation, using

a reduction factor of 0.8232. This approach uses this reduction factor r when approxi-

mating the R0.015 rainfall rate.

The ITU model would suggest that attenuation of 37 dB, exceeded for 0.01% of an aver-

age year, would require a rainfall rate of 106 mm per hour to be exceeded for 0.01% of

an average year. Using the ITU model it is possible to estimate the attenuation exceeded

for other percentages of time within the limits 0.1 to 0.001%, and that attenuation

exceeded for 0.015% of the year would be approximately 31.64 dB. By modifying the

formula it is possible to estimate that a rainfall intensity of 85 mm per hour exceeded

for 0.015% of the time would produce 31.64 dB attenuation for 0.015% of an average

year.

This extension of the ITU model can be used to estimate the rainfall which should have
been present to produce the fading distribution measured during the year.

Rainfall intensity required to produce attenuation shown in an average year			
Measured Fade dB	Cumulative Distribution Minutes	Cumulative Distribution Percentage	Rainfall Required for Attenuation % (ITU) mm/h
15	233.017	0.044334	70
16	217.517	0.041385	73
17	203.467	0.038711	76
18	188.9	0.035940	79
19	168.483	0.032055	80
20	150.517	0.028637	80
21	138	0.026256	82
22	123.333	0.023465	82
23	118.933	0.022628	85
24	107.55	0.020462	85
25	97.6	0.018569	86
27	92.75	0.017647	93
28	87.817	0.016708	95
29	84.917	0.016156	98
30	77.4	0.014726	98
31	72.85	0.013860	99
32	70.717	0.013455	102
33	68.783	0.013087	104
34	64.733	0.012326	104
35	59.8	0.011378	104
36	56.633	0.010775	105
37	53.483	0.010176	106
38	51.533	0.009805	107
39	50.167	0.009545	109
40	40.433	0.007693	103
41	38.467	0.007319	104
>41	34.25	0.006516	102

Table 1-19   Rain rate required for measures fading based on ITU–R 530–7

Rain climate zones from ITU–R PN.837–1															
%	A	B	C	D	E	F	G	H	J	K	L	M	N	P	Q
0.3	0.8	2	2.8	4.5	2.4	4.5	7	4	13	4.2	7	11	15	34	49
0.1	2	3	5	8	6	8	12	10	20	12	15	22	35	65	72
0.03	5	6	9	13	12	15	20	18	28	23	33	40	65	105	96
0.01	8	12	15	19	22	28	30	32	35	42	60	63	95	145	115
0.003	14	21	26	29	41	54	45	55	45	70	105	95	140	200	142
0.001	22	32	42	42	70	78	65	83	55	100	150	120	180	250	170
Rainfall intensity in mm/hour (integrated over one minute) as % of one year															

Brisbane is contained within climate zone M.
When the rainfall is integrated over a one minute period the
intensity exceeded for 0.01% of an average year should be
63 mm per hour.
According to ITU–R PN.837–1

Table 1-20   **Rain zones and their rain rates according to ITU–R PN.837–1**

5.15 Comparisons

Brisbane is located in rainfall region M and is approximately 500km south of the border with rainfall region N. The rainfall rate which is exceeded for 0.01% of the time in the M and N regions are 63mm per hour and 95 mm per hour respectively, according to ITU–R PN.837–1. The K rainfall region which borders the M region inland has a rainfall intensity of 42 mm per hour which is exceeded for 0.01% of an average year. The rain intensity exceeded for 0.01% of the year was measured at the Optus (receive) and the Royal Brisbane Hospital (transmit) ends of the hop were 72 and 91 mm per hour respectively. The measured data which exists for the radio shows that a 37 dB fade margin was exceeded for approximately 0.01% of the year, and using the ITU Model outlined in ITU–R P.530–7 it would appear that a rainfall rate of 106 mm per hour, exceeded for 0.01% of the time, should produce this fading in an average year.

ITU–R PN.837–1		mm per hour (60s integration)					
%	Minutes	Optus	RBH	Fade	K	M	N
0.03	157.7	54	44	80	23	40	65
0.01	52.6	91	72	106	42	63	95
0.003	15.6	131	137		70	95	140

Table 1-21   Comparison of measured data with ITU–R PN.837–1

The rainfall values provided by ITU–R PN.837–1 for rainfall regions K, M, and N have been compared with the measured rainfall figures for 0.03, 0.01, and 0.003% of an average year which is 157.7, 52.6, and 15.8 minutes a year. The ITU–R P.530–7 Model was used to predict the rainfall required to produce measured attenuation for 0.01 and 0.03% of the time, but a figure for 0.001% was not possible because the system measurement threshold of 41 dB was exceeded for 34.25 minutes during one storm. It can be seen that

the rainfall required to produce the fading observed was greater than that expected for region M, in which Brisbane is located, or the measured rainfall recorded by the rain gauges at each end of the hop.

5.16   Hop design

The method for predicting attenuation on a path, outlined in ITU–R P.530–7, requires the rainfall rate, integrated over one minute, which is exceeded for 0.01% of an average year. In the absence of reliable long term measurements made over the correct integration period, the ITU recommendation states that an estimate can be obtained from the rainfall maps presented in ITU–R PN.837–1. These maps show Brisbane to be in rainfall zone M with a rainfall intensity of 63 mm per hour being exceeded for 0.01% of the time. Using the ITU method, the attenuation exceeded for 0.01% of the time in this rainfall climate is 25.1dB. However, the rain gauge at the Royal Brisbane Hospital (transmit) end of the hop recorded 52.6 minutes when the rainfall was 72 mm per hour or greater. The rain gauge at the Optus (receive) end of the hop indicates that a rainfall intensity of 91 mm per hour or more was exceeded for 53 minutes a year. Working backwards from the 53.48 minutes of fading on the hop it would appear that the ITU model would require a rainfall rate of 106 mm per hour to be exceeded for 0.01% of the time to produce this fading.

It should be noted that while the rain gauges operated for the entire year several weeks of fading data were lost due to corruption or equipment failure. Naturally, it should also be borne in mind that one year's data is not statistically a very long observation period.

Source of data 1 Feb 97 to 31 Jan 98 Exceeded 0.01% of time	Period Exceeded Minutes	Rainfall (60s) mm/h	Attenuation caused by rainfall exceeded 0.01% dB (2.1km, 38GHz, Ver)
ITU–R PN.837–1	52	63	25.1
RBH rain measurement	52	72	27.9
Optus rain measurement	52	91	32.7
Radio fade measurement	53	106	37

Table 1-22   **Expected fades (0.01% time) using ITU and measured data**

The availability target for this hop depends on the end–to–end availability target adopted by Optus, the unavailability of the circuits which connect this hop to the MSC and whether this hop will eventually connect another hop to the MSC. For argument's sake it is assumed that the availability of this hop is to be 99.98% and that 0.01% has been allocated to equipment failure, human error and testing, and that the remaining 0.01% has been allocated to rain fading. Using 30cm antennas the received signal power level is –43 dBm and the receive sensitivity for a bit error rate of one error in a thousand was measured as –83 dBm, providing a 40 dB flat fade margin.
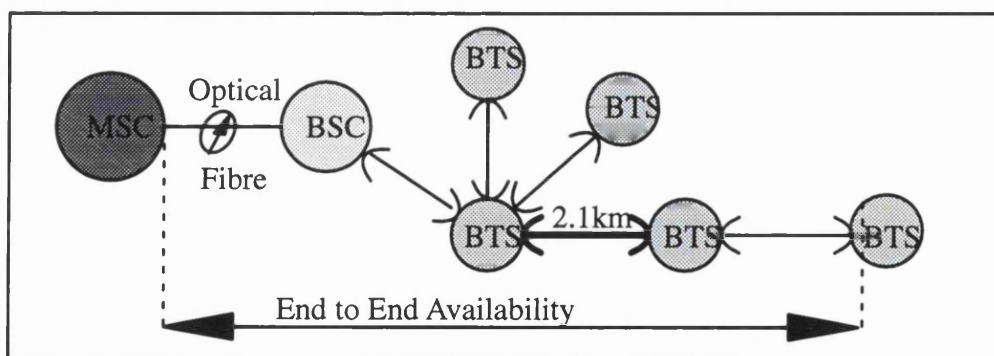
Diagram 1-81   **Consideration of end–to–end availability requirements**

To reduce interference in the city centre and allow maximum frequency reuse a waveguide attenuator has been included in the Nokia radio which allows up to 30dB of attenu-

ation to be applied to the transmitted signal. Since the rain fading objective is 0.01%, in this example, which corresponds to 25 dB of fading in ITU rainfall zone M, the attenuator would be used during installation to ensure that the flat fade margin is no larger than necessary. Based on the ITU rainfall figures the transmitting radio on this link should attenuate the transmitted signal by 15 dB to reduce the flat fade margin from 40dB to 25 dB . Although several weeks of records are not available the fading records which do exist show 53.48 minutes of fading of 37dB or more. Using the procedure outlined by ITU–R P.530–7, this amount for fading should have been produced by rain intensity, exceeded for 0.01% of the time, of 106 mm per hour. This corresponds to 142 minutes of unavailability or 0.027% of unavailability for a hop designed with a 25 dB fade margin.

Fade Margin, V 2.1km, 38GHz	Minutes fade margin exceeded per year based on the rainfall value shown, which is exceeded 0.01% of the year			
dB	63 mm/h	72 mm/h	91 mm/h	106 mm/h
25	52	70	105	142
28	39	52	79	107
33	25	33	52	71
37	17	24	37	53

Table 1-23   **Number of minutes per year that the fade margin shown should be exceeded for the rain rates shown (exceeded for 52.6 minutes a year) according to ITU–R P.530–7**

Number of minutes the fade level was exceeded on the Optus – RBH hop			
25 dB	28 dB	33 dB	37 dB
97.6 Min	87.8 Min	68.8 Min	53.5 Min

Table 1-24   **Number of minutes the indicated fade level was exceeded**

5.17 El Nino

The ocean temperatures in the Equatorial Pacific deviate from the mean seasonal average. There are periods of unusually cold ocean temperature known as La Nina and periods of unusually warm ocean temperatures known as El Nino. The United States Department of Commerce have reported the presence of El Nino between April 1997 and July 1998, and noted that it was abnormally strong between July 1997 and April 1998. As a result of the strong El Nino Northern Australia was dryer than normal during the research period, as can be seen from Appendix H.

5.18 Average rainfall

The ITU model uses the rainfall value at a particular point to calculate the attenuation. It achieves this by applying a reduction factor to take account of the non uniformity of the rainfall across the hop. According to theory it should be possible to place a large number of rain gauges along the hop and calculate the specific attenuation at these points based on the rainfall intensity. Integration would then reveal the instantaneous attenuation experienced at the receiver. An attempt was made to gain permission from the owners of the property below the path to locate rain gauges on their land, but without success. However, it was possible to take the rainfall measurements from one of the rain gauges at the Optus (receive) end of the hop and the gauge at the Royal Brisbane Hospi-

tal (transmit) end of the hop and take an average rainfall value for the hop and compare this with the fading experienced.

Since the ITU model predicted fading on this hop should exceed 25dB for 52.6 minutes in an average year, measurements were restricted to rain storms which created more that 25dB of fading. There were eleven days when the fading exceeded 25dB. These days were 29 April, 1 May, 16 May, 30 May, 24 September, 7 October, 30 November, 23 December, 27 December, 28 January and 31 January. Samples were taken every ten seconds when a fading threshold of 5dB was exceeded. At both the Optus (receive end) and the Royal Brisbane Hospital (transmit end) rain gauges a rolling sixty second average was calculated every ten seconds. These two rainfall values were then added together and divided by two. This value was recorded every ten seconds along with the average fade level in dB at that sampling time. A value was not recorded for fades greater than 41dB since the equipment sensitivity had been exceeded at this point.

The average rainfall level required to fade the receiver to the levels shown are considerably less than the rainfall intensity expected according to ITU–R P.530–7. However, the rain gauges used to generate the average were 2.1km apart and these results were generated from only 1744 ten second samples, or four hours fifty minutes and forty seconds. More information can be found in Appendix I.

ITU figures based on a 2.1 km hop operating at 38 GHz with a vertical electrical field Samples taken from rain events causing fading greater than 25 dB			
Minimum Fade dB	Number of Samples 10s	Averaged over the year $\left(\dfrac{\text{Optus + RBH}}{2}\right)$ mm / hour	Rainfall intensity required to produces fading according to the ITU model mm / hour
5	43	12	
6	92	13.3	
7	64	14.3	15
8	90	16.3	
9	92	16.2	20
10	74	18.8	
11	62	18.1	25
12	138	21	
13	85	25.8	30
14	68	24	
15	92	27	35
16	50	24.4	
17	46	28.3	40
18	89	30.8	
19	74	33.3	45
20	39	37.8	
21	56	36.2	50
22	19	33.5	
23	58	37.2	
24	44	36.8	60
25	26	39.5	
27	29	39.3	70
28	14	48.4	
29	48	43.5	75
30	26	45.2	
31	20	42	
32	16	52.9	
33	17	54.7	90
34	38	60.3	
35	18	61	100
36	18	60.7	
37	10	61.2	105
38	7	72	
39	47	69.2	
40	13	65.5	115
41	22	63	

Table 1-25   **Comparison of measured fade levels with the average rain rate**

6 Summary and conclusions

6.1 Introduction

Between 1 February 1997 and 31 January 1998 a personal computer was used to poll a Nokia DMR C model radio and record the received power level every three seconds. The radio which was polled operated at 38 GHz using vertical polarisation on a 2.1 km path in Brisbane. The normal unfaded received power level was −43 dBm and the receive sensitivity allowed fading of up to 41 dB to be recorded. A rain gauge was located at each end of the hop and wind speed and direction was recorded at the receive end. A full description of the research method can be found in chapter 4.

This chapter contains plots showing the cumulative rain distributions at each end of the hop and a bar chart showing the storms which contributed to the heaviest rain at each end of the hop The attenuation model outlined in ITU–R P.530–7 has been applied to the research hop and a plot shows the attenuation exceeded for 0.01% of the time which should result from rainfall exceeded for 0.01% of the time. In another plot rain rates exceeded between 15.6 (0.003%) and 157.7 (0.03%) minutes a year have been plotted for measured rainfall, the rainfall which according to ITU–R P.530–7 should have produced the measured fading and the predicted rainfall according to ITU–R PN.837–1. The ITU–R predictions are all based on an average year. The final plot in this section compares the rainfall rate necessary, according to ITU–R P.530–7, to cause the measured fading and compares this with the average rainfall on the hop.

6.2 Cumulative rainfall distributions

Between 1 February 1997 and 31 January 1998 the heaviest 64 minutes of rainfall recorded at the Optus (receive) end of the hop resulted from 11 rain storms. The heaviest

190

64 minutes had an intensity of 84 mm per hour when integrated over one minute. Inter-

polating the data suggests that the intensity of the heaviest 52.6 minutes of rainfall was

in the region of 91 mm per hour.
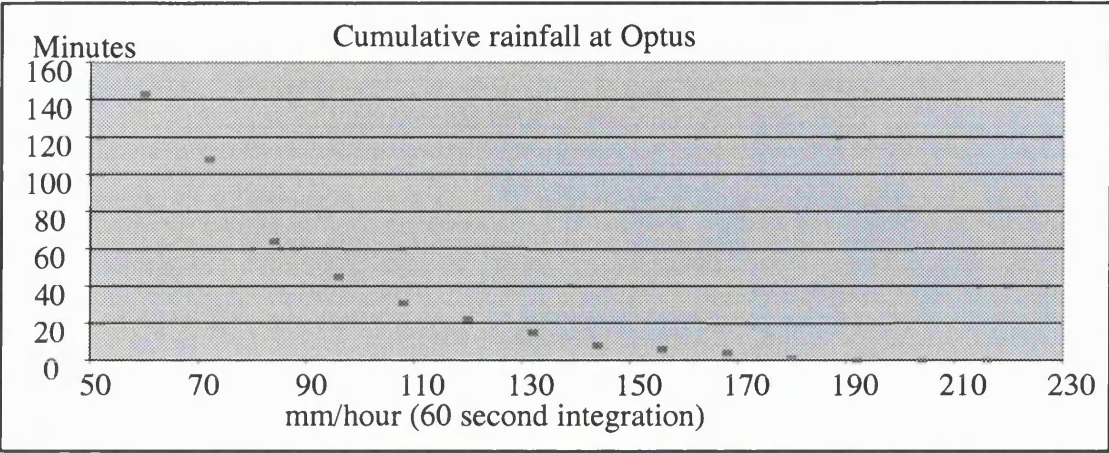
Plot A-10 **The cumulative rainfall distribution at the Optus end**

At the Royal Brisbane Hospital (transmit) end of the hop the heaviest 52.6 minutes of

rainfall had an intensity of 72 mm per hour. This was measured during the heaviest 12

rain storms at the Royal Brisbane Hospital (transmit) end of the hop.
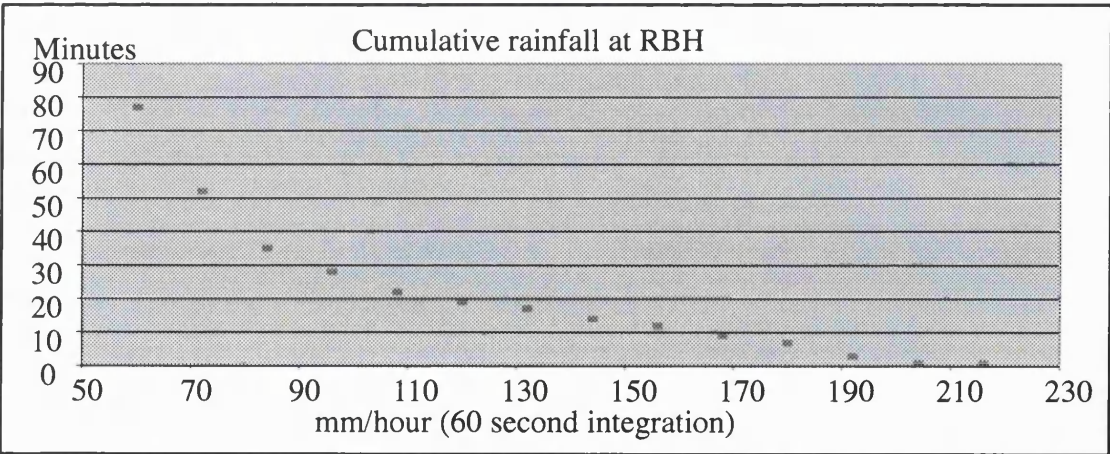
Plot A-11 **The cumulative rainfall distribution at the RBH end**

Although the rain gauges were only 2.1 km apart the heaviest rainfall data was not col-

lected at the same time. On 16 February, 18 February, 22 March, 29 April, 16 May, 24

September, 16 November, 10 December, 23 December and 27 December the heaviest

52 / 64 minutes or rainfall was recorded at one, but not both rain gauges. On 30 May,

7/8 October, 30 November, the heaviest rainfall was recorded at both ends of the hop.

The difference of about 19 mm per hour for the heaviest 52 minutes of rainfall a year

is mainly due to spatial separation, but may also be influenced by wind sorting at the

Royal Brisbane Hospital (transmit) end, where the rain gauge was located 50 metres

above ground level compared with 10 metres above ground level at the Optus (receive)

end. When comparing the total rainfall recorded between 1 February 1997 and 30 Jan-

uary 1998, midnight to midnight, it can be seen that 954.8 mm was recorded over 132

days at the Optus (receive) end while only 776.2 mm was recorded over 103 days at the

Royal Brisbane Hospital (transmit) end. Any wind sorting which would have occurred

would have been a function of height above the ground and the associated reduction of

drag. No funnelling of wind currents would have been produced at either end and the

airconditioning plants were too far away to influence the data. Although the rain gauge

had been fixed on a slightly sloping roof at the Royal Brisbane Hospital (transmit) end,

a wedge had been used to ensure it was nearly level, and the tipping mechanism was at

right angles to the slope. All the rain gauges used in the project had similar performance,

with less than three percent error at a rainfall rate of 100 mm per hour, with a one minute

integration time.
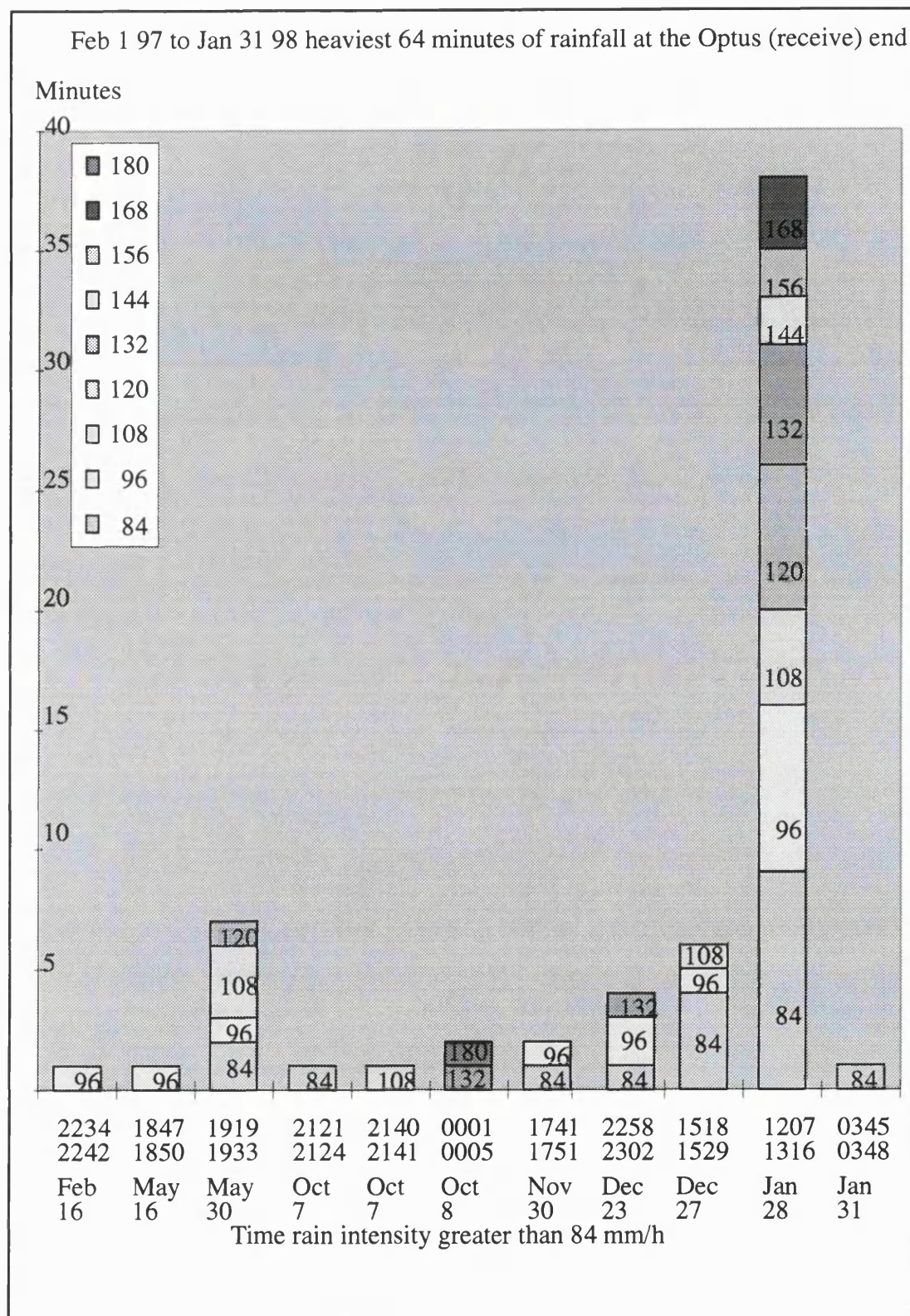
Diagram 1-82   The worst 64 minutes of rainfall at the Optus (receive) end
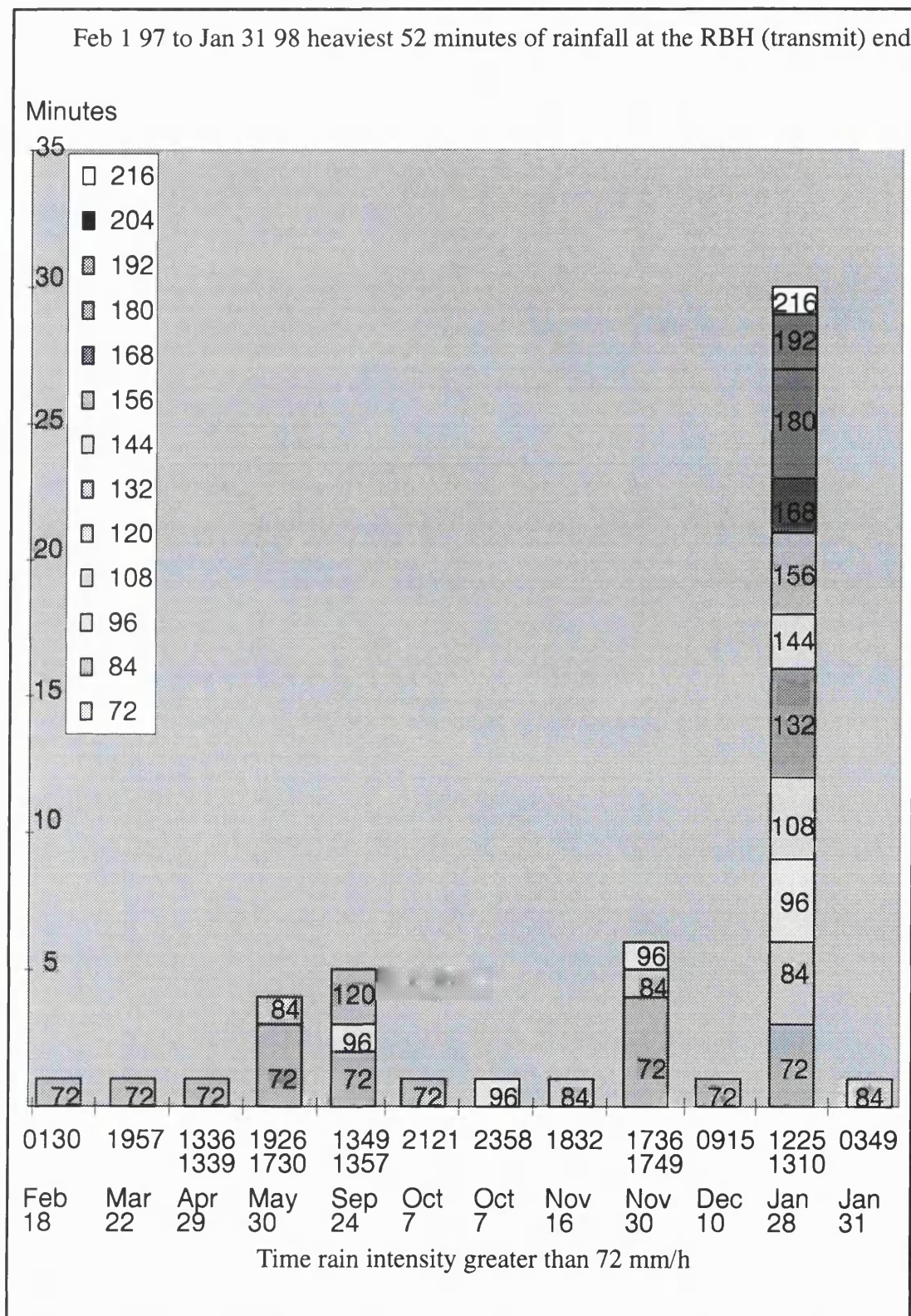
Diagram 1-83   The worst 52 minutes of rainfall at the RBH (transmit) end

6.3   Cumulative fade distribution

The received power level was recorded on a 2.1 km path in Brisbane operating at 38 GHz with vertical polarisation between 1 February 1997 and 31 January 1998. The receive power levels logged over this period were adjusted to compensate for the changes in the relationship between the real and indicated power level, which varied with temperature. Adjustments were based on measurements which were made at four different temperatures before the hop was commissioned in order to produce a minimum fade distribution for the radio.
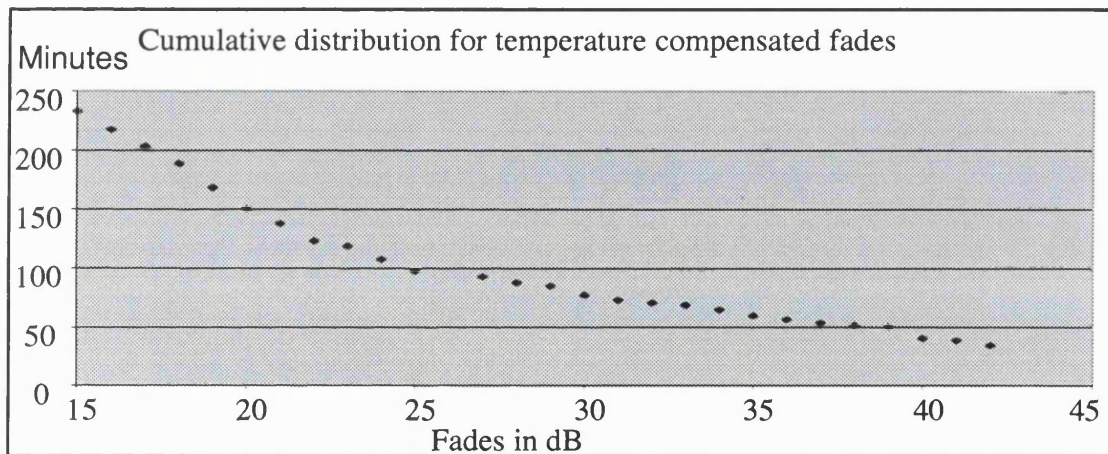
Plot A-12   **The cumulative fade distribution recorded at the Optus end**

The distribution produced shows that the radio experienced fades of at least 37dB for 53.48 minutes. However because data was lost between 2 and 6 May 1997, 8 October to 18 November 1997 and because the radio was being repaired between 22 June and 6 August 1997 the fade distribution is optimistic. The rainfall intensity of 60 mm per hour was recorded at the Optus (receive) end of the hop on 7 July, 17 and 18 of November, and 84 and 60 mm per hour was recorded at the Royal Brisbane Hospital (transmit end) on 16 and 17 of November respectively. No fade data exists for these events.

6.4   The ITU model

The ITU Model was applied to a 2.1 km hop operating at 38 GHz with vertical polarisation. The rainfall input was varied between 15 and 150 mm per hour in 5 mm steps to produce a range of expected attenuation values. The rainfall figure used is for the heaviest 0.01% of an average year and the attenuation value produced is for 0.01% of an average year. It can be seen from the graph that a rainfall intensity of 106mm per hour exceeded for 0.01% of the time produce attenuation of 37 dB, on a 2.1 km hop with vertical polarisation operating at 38 GHz, for 0.01% of the time.
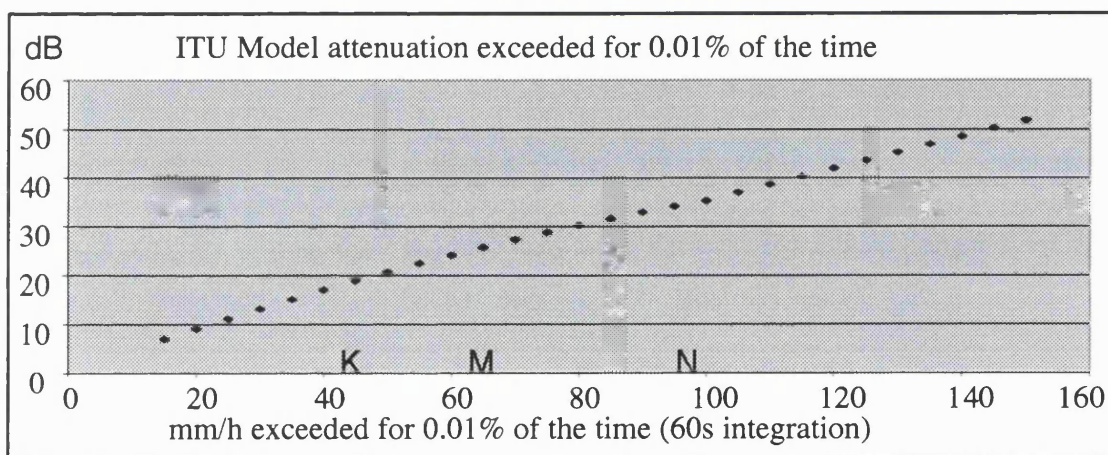
Plot A-13   **Attenuation exceeded for 0.01% of an average year (according to ITU–R P.530–7 for a 2.1km vertically polarised 38GHz hop) based on rainfall rates exceeded for 0.01% of an average year**

The ITU–R Recommendation PN.837–1 placed Brisbane in rainfall region M. The rainfall rate which is exceeded for 0.01% of the time in this region should be 63mm per hour, which suggests that if an unavailability figure for rainfall of 0.01% was acceptable then a 25 dB flat fade margin would be suitable. However the fading measured on the radio was 25 dB or more for 97.6 minutes and not 52.6 minutes, 0.01%, as would be expected according to the ITU method, a difference of 45 minutes. Rainfall region N has a rainfall rate of 95 mm per hour exceeded for 0.01% of the time according to ITU–R PN..837–1.

This rainfall zone would produce attenuation of about 34 dB for 0.01% of the time. The fading experienced on the radio was 34 dB or more for 64.7 minutes over the measurement period.

6.5 Rainfall comparisons

The rainfall values for regions K, M, and N and the measured rainfall for 0.03, 0.01, and 0.003% of an average year have been compared with the rainfall necessary, according to ITU–R P.530–7, to produce the measured attenuation for 0.01 and 0.03% of the time. For durations less than one hour, which is the area of interest, the rain gauge at the Optus (receive end) has similar values to the rainfall region N. However the average annual rainfall required to produce the fading observed is much higher.

Fading data was not available on the 7 July or 16, 17 and 18 November when there was a significant amount of rainfall. If the data had not been lost the fading distribution for the heaviest hour of fading might have been affected. This would have depended on what proportion of the rain cells, recorded at the rain gauges in November, would have crossed the radio path.

It is possible to remove the rainfall data recorded while the fading data was not available in order to compare the rainfall and fading data over the same period of time. However this was not done since it would have reduced the accuracy of the rainfall data.

Comparison of region N, M, the rain gauges and fade measurements
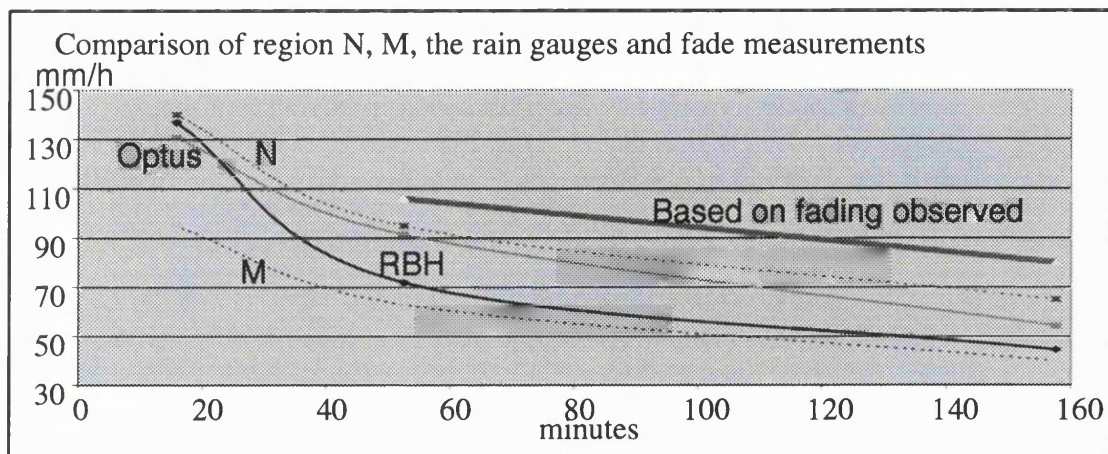
Plot A-14 **A comparison between recorded rainfall rates, predicted rain fall rates (ITU–R PN.837–1) for an average year in rain zones N and M and the rainfall rates necessary in an average year to produce the fading observed**

6.6 Non uniformity of rainfall

The ITU model predicts the attenuation exceeded for 0.01% of the time by first finding the rainfall rate exceeded for 0.01% of the time. Since rainfall is not uniform in nature a reduction factor is used to statistically compensate for a non homogeneous rain medium. However an attempt was made to take account of the rain filled medium by averaging the measured rainfall intensities at each end of the hop, integrated over a rolling one minute period at each end. This allowed a comparison of the average rainfall intensity with the fading observed. This evaluation was carried out on the 14 rain storms which were responsible for all the fading events greater than 25 dB. The 1744 ten second samples were averaged to produce a comparison of average rain intensity against fading over the range 15 to 41 dB.
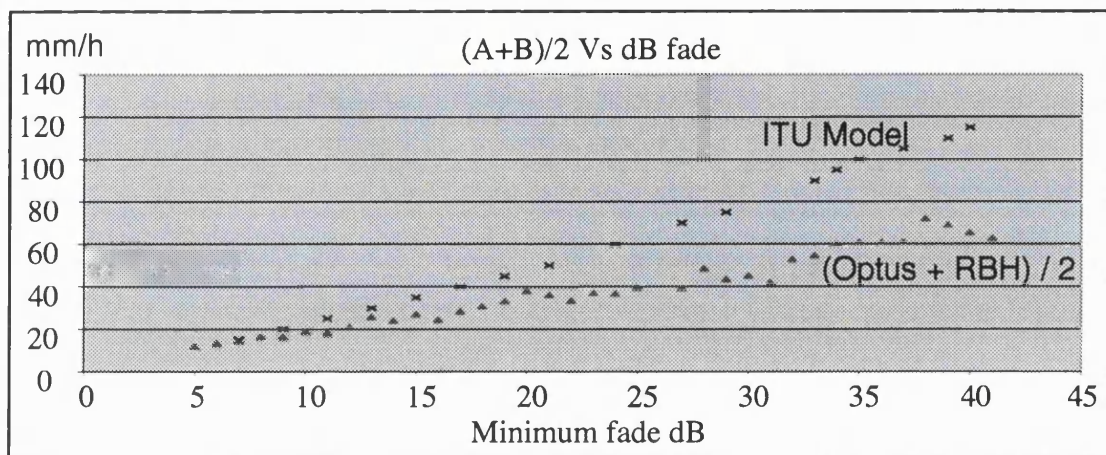
Plot A-15   **The average rainfall intensity across the hop, the recorded fading and the predicted rain rate based on ITU–R P.530–7**

The ITU model predicts that a fade of 37 dB will be exceeded for 0.01% of the time if the rainfall intensity of 106 mm per hour is exceeded for 0.01% of the time. The measured data shows that 37 dB fades were produced by an average intensity of about 70 mm per hour. If these measurements are statistically representative, then an average intensity of about 62mm per hour for 0.01% of the time would produce fading of 37dB or more for 0.01% of the time. However, with a limited number of samples and gauges 2.1 km apart there is great uncertainty surrounding the average rain filled medium.

6.7 Conclusions

As the coverage and capacity of the Optus Network grew it became difficult to add new radio links to the network without causing interfere. Therefore a decision was made in 1996 to start using the 38GHz band in the Brisbane area in 1998 in order to accelerate the fixed radio network planning process in areas where frequency crowding had become a problem.

A radio hop needs to be designed with a fade margin that is large enough to meet the

objectives set for the hop, but fade margins which are too large can cause interference. Maximum frequency reuse can be achieved by attenuating the transmitted signal to a suitable level. However, the planning tools used by Optus are based on ITU–R P.530–7 and some links which had previously been designed for maximum frequency reuse at 15, 18 and 23 GHz had experiencing unacceptable levels of unavailability.

The method presented in ITU–R P.530–7 for predicting attenuation caused by rainfall is for global use. It has been designed to predict the rain induced attenuation with a minimum error on path lengths up to 60 km and at frequencies up to 40 GHz. It is in common use around the world. The object of this thesis is to improve the accuracy of the attenuation predictions within the Brisbane area at a frequency of 38 GHz.

Software planning tool based on this model require data on path length, operating frequency, transmitted power, polarisation, antenna gain, connector and waveguide losses, and rainfall intensity exceeded for 0.01% of the time when integrated over a one minute period. Tuning this model can be achieved by varying the rainfall figure used.

Long term rainfall intensity records are not available with a one minute integration period in Brisbane and therefore rainfall intensity figures presented in ITU–R PN.837–1 were initially used as a guide for fixed radio network planning. ITU–R PN.837–1 places Brisbane in rain region M, and using an integration period of one minute, it estimates rainfall intensity, for 0.01% of the time, to be 63 mm per hour or greater in this region. Using the same integration period the measures rainfall intensities were found to exceed 91 and 72 mm per hour at the Optus (receive) and Royal Brisbane Hospital (transmit) ends respectively. The difference between the measured rainfall distributions is due the spatial separation and may also be due to wind sorting.

The rain gauge at the Royal Brisbane Hospital (transmit) end was located 50 metres

above the ground where strong wind currents were observed. However no wind speed data exists for this end of the hop. The rain gauges at the Optus (receive) end were located 10 metres above the ground and the wind speed was sampled at this end every minute throughout the year. During the significant rain events the wind speed was typically around 4 metres per second. This would not be strong enough to generate large rainfall intensity errors by blowing the drops across the rain gauge.

All the rain gauges were calibration on site at the beginning and end of the research period and found to have a 3% error at a simulated rainfall rate of 100 mm per hour. Both rain gauges at the Optus (receive) end (the original rain gauge and the rain second gauge which was installed in April 1997) recorded identical rainfall activity.

The rainfall recorded at the Optus (receive) end is considered to be reliable. There is a possibility that the wind may have influenced the recorded rainfall at the Royal Brisbane Hospital (transmit) end. The total rainfall recorded between 1 February 1997 and 30 January 1998 was 954.8mm at the Optus (receive) end but only 776.2mm at the Royal Brisbane Hospital (transmit) end.

When considering the heaviest rainfall for 0.01% of the time it is clear that the distribution at both ends are dominated by one storm on the 28 January 1998. The obvious question is what would the rain intensity distribution have been if the observation period had been between 1 January 1997 to 31 December 1997? There is no answer to this question since rainfall data was not gathered in January 1997 because the observation period, decided upon in 1996 by common agreement, was between 1 February 1997 and 31 January 1998. A strong El Nino event was recorded between April 1997 and July 1998, which made Northern Australia drier than normal. The recorded rainfall data may therefore by less than usual and further measurements should be made to resolve this issue.

Unfortunately no data was available on rainfall intensities over a one minute or five minute integration period from the local Meteorological Authority.

The fade distribution presented in this thesis is optimistic since the temperature compensation mechanism, which attempts to corrected differences between the real and indicated receive power levels always assumed the minimum fade level. However, the temperature correction values used are based on calibration measurements performed in December 1996 and there may have been some variation over the year. The fade distribution is compared with the predicted fading for an average year but no fading measurements were made between 2 May and 6 May 1997, or between 22 June and 8 October 1997, or between 8 October and the 18 November 1997. There was significant rainfall on 16, 17 and 18 November 1997 and this rainfall might have influenced the fade distribution. However, the file containing this fading data was corrupted. On 7 July the radio at the Royal Brisbane Hospital (transmit) end was being repaired when the rain gauge at the Optus (receive) end recorded 60 mm per hour. This rain event might also have influenced the fading distribution.

The ITU–R P.530–7 rainfall attenuation method predicts that the 2.1km vertically polarised 38GHz test link will experience fading greater than 25.1 dB for 52.6 minutes in an average year if a rainfall figure of 63 mm per hour is used. However, the link experienced fading of 37 dB for 53.48 minutes. A difference of 12 dB which is considerable. According to ITU–R P.530–7 106 mm per hour is required to produce 37 dB of fading on this hop, and this is a great deal higher than the 63 mm per hour predicted in ITU–R PN.837–1.

Fading of 37dB was experienced on the hop for 53.48 minutes over a one year period. According to the attenuation prediction method presented in ITU–R P.530–7, in an aver-

age year a rainfall intensity of 106 mm per hour, integrated over a one minute period, would need to be exceeded for 52.6 minutes to produce this level of attenuation. However, interpolation of the rainfall measurements recorded by the Optus (receive end) rain gauge show that only 91 mm per hour was exceeded for 52.6 minutes during the one year observation period. Additionally the 37 dB of fading was recorded in a period rather less than a year. Why is there a difference? One possibility possibility is that the 7 rain storms which created this fading are not statistically representative of an average year in the Brisbane area. Another possibility is that the global rain attenuation prediction method presented in ITU–R P.530–7 produces an error in subtropical rainfall. A slight change in the specific attenuation created by rainfall with an intensity of 91 mm per hour, and / or a slight change in the reduction factor used to account for non linear rainfall could account for the differences. However, the software which has been written for Optus's planning tools calculates the reduction factor and the specific attenuation based on ITU–R P.530–7, and the only way that the software can be tuned to the local climate is by choosing an appropriate rainfall figure.

The rainfall intensity of 91 mm per hour recorded at the Optus end is similar to the 95mm per hour predicted for the heaviest 52.6 minutes of rainfall in rainfall region N. The ITU–R P.530–7 rainfall attenuation method predicts that a rainfall rate of 95 mm per hour exceeded for 52.6 minutes in an average year would produce a fade of 34 dB or more for 52.6 minutes in an average year. The measured fade distribution shows that the test hop experienced fades of 34 dB or more for 64.7 minutes a year. More rainfall and fading data is required but based on data measured between 1 February 1997 and 31 January 1998 a rainfall figure of 95 mm per hour is not unreasonable and may be optimistic.

Appendix A

7 Performance and Availability

Error performance requirements for an international digital connection have been presented by the International Telecommunication Union in Recommendation G.821 in the 'Yellow Book' from 1980, amended in the 'Blue Book' from 1988, and reprinted in 1993. ITU–T Recommendation G.821 [102] defines the performance requirement for a 64kbits/s international connection in terms of high, medium and low grade connections. While measurements made at higher transmission rates can be normalised to 64kbits/s, errors which effect the frame alignment or justification bits at higher levels may introduce a measurement error.

To meet the needs of future digital networks a new recommendation was introduced in 1993, ITU–T Recommendation G.826 [103]. This recommendation is independent of the transport medium and specifies the error performance objectives for digital paths which operate at or above the primary rate of either 2Mbits/s or 1.54Mbits/s. This recommendation does not identify high, medium, and low grade portions of a network. Instead it refers to the national portion of a network and the international portion of a network. Error performance measurements for ITU–T G.826 are based on monitoring blocks of bits.

Both ITU–T G.821 and ITU–T G.826 identify two categories of time, namely available time and unavailable time, and state that error performance should be measured during the available time over a suggested period of one month.

It should be noted that the two recommendations [102][103] define availability differ-

ently. ITU–T G.821 states that the unavailable period begins when ten consecutive seconds have a bit error rate, in 'both' directions, which is greater than one error in a thousand or ten consecutive seconds with no signal. The available time begins with the first second of a period of ten consecutive seconds where the bit error rate in both directions is less than one error in a thousand. ITU–T G.826 states that the unavailable period begins when ten consecutive seconds have a bit error rate in 'either or both' directions greater than one error in a thousand, or ten consecutive seconds with no signal. The available time begins with the first second of a period of ten consecutive seconds where the bit error rate in both directions is less than one error in a thousand.

The error performance objectives for radio relay systems are covered by a number of objectives, which are based on ITU–T G.821, if the radio operates below the primary rate and by ITU–T G.826 if the radio operates at or above the primary rate.

When a radio relay system operates below the primary rate it should meet the objectives for high grade, medium grade and low grade as defined in ITU–R recommendations F.634–4 [104], F.594–4 [105], F697–2 [106], and F.696–2 [107], which were all published in 1997 and based on ITU–T G.821, but refer to ITU–R F.557–4 [108] for the definition of available time and unavailable time. ITU–R F.557–4 was published in 1997 and has the same definition as ITU–T G.826 with regards to available and unavailable time.

When a radio relay system operates a constant bit rate, at or above the primary rate, it should meet the objectives for the national or international portion of the network, as defined in ITU–R recommendations F.1189–1 [109] and F.1092–1 [110], which were both published in 1997.

Availability objectives are set for a period of time greater than one year, and are defined

in ITU Recommendation 695 [110], which was published in 1990, and in ITU–R Recommendations F.557–4, F.697–2 and F.696–2, which were published in 1997. The availability objectives for radio relay systems which operate below the primary level in the local and medium grade portions of the network are defined in ITU–R Recommendations F.697–2 and F.696–2 respectively. Both Recommendation 695 and F.557–4 define availability objectives in terms of a 2500km high grade hypothetical reference digital path, HRDP, which was defined in the 1986 Recommendation 556–1 [112] as operating above the second hierarchical plesiochronous multiplexing level. There are not any current recommendations which define objectives for radio relay systems which operate at or above the primary rate in the national or international portion of an international connection.

7.1   ITU–T G.821   1993

ITU–T Recommendation G.821 defines the error performance objectives of an end–to–end circuit switched line in terms of errored seconds, 'ES', severely errored seconds, "SES', and degraded minutes, 'DM'. A errored second is a one second period which contained at least one error. A severely errored second is a period of one second where the bit error rate is worse than one error in a thousand bits. A degraded minute is a block of sixty contiguous seconds, which contains no severely errored seconds and has a bit error rate worse than one error in a million. When considering the end–to–end connection, the objectives for errored seconds is less than 8%, with severely errored seconds less than 0.2% and degraded minutes less than 10%.

Objectives are apportioned in a networks which have the potential to be part of an end–to–end international connection, by employing the concept of a 27 500 km hypothetical

reference connection, which consists of local grade, medium grade and high grade sections. The local grade section represents the connection between the subscriber and the local switching centre, but the boundary between medium grade and high grade sections will depend on the administration authority concerned. However, the combined local grade and medium grade sections should not exceed 1 250 km at either end, while the high grade section is defined as 25 000 km.
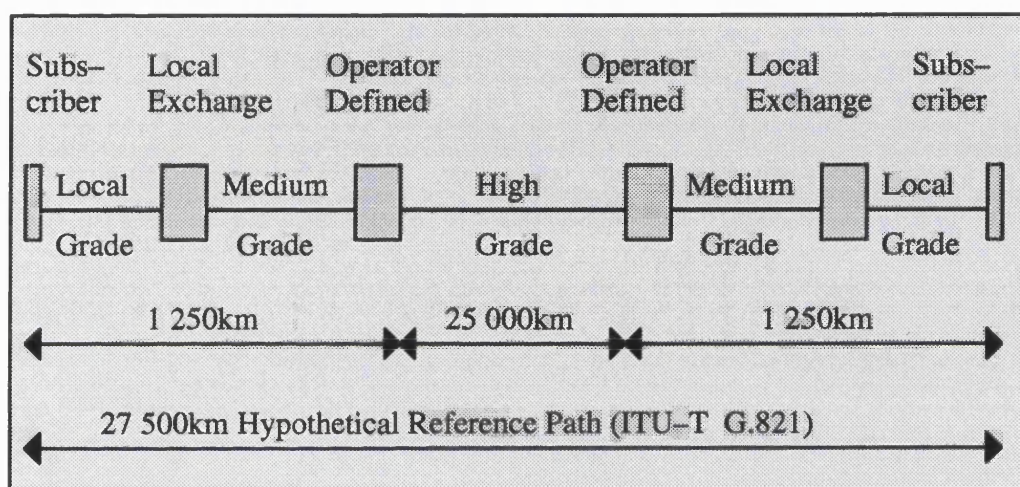
Diagram 1-84   Hypothetical reference path defined by ITU–T G.821

Each local grade part of the hypothetical reference connection is allocated 15% of the performance allowance, regardless of length. Each medium grade part is allocated 15% of the performance allowance, regardless of length. However administration authorities may combine the local and medium grade allowances with 30% of the total performance allocation up to a maximum distance of 1 250km. The 25 000 km high grade portion of the network is allowed 40% of the performance allowance, which works out at 0.0016% of the allowance per km. A single satellite link which forms part of the high grade portion of the network is allowed 20% of the high grade block allowance.

The total performance allowance for errored seconds and degraded minutes is 8%, and

10%, as stated above, with the local, medium and high grade sections receiving 15%, 15% and 40% of this allowance.

The total allowance for severely errored seconds is 0.2%, which is broken down into two 0.1% blocks. One 0.1% block is allocated to local, medium and high grade sections in the ratio 15%, 15% and 40% respectively. Therefore an allowance of 0.04% for severely errored seconds is allocation to a 25 000 km high grade link, although for practical terms it is usually considered to be 0.004% per 2 500 km. The remaining 0.1% is a special allowance for adverse weather conditions on high grade and medium grade connections. However 0.05% of this special allowance is allocated to a 2500 km high grade hypothetical reference digital path, HRDP.

Circuit Classification ITU-T G.821	64 kbits/s Objectives				
	Degraded Minutes Ratio	Errored Seconds Ratio	Severely Errored Seconds Ratio		
Total	0.1	0.08	0.001	+	0.001
Local Grade	0.015	0.012	0.00015	0	0
Medium Grade	0.015	0.012	0.00015	0	0.0005
High Grade	0.04	0.032	0.0004	0.0005	

Table 1-26   **Objectives for a 64kbit/s circuit**

7.2   ITU–T G.826   1993

The ITU–T recommendation G.826 defines the error performance objectives for each direction of a constant bit rate digital path which operates at the primary rate, or at a higher bit rate. The path may be part of a plesiochronous digital hierarchy, 'PDH', or a synchronous digital hierarchy, 'SDH', network and the objectives are independent of

the physical transport medium. Compliance with these objectives will usually ensure compliance with ITU–T G.821. Performance objectives should be satisfied during the available time, which is suggested to be evaluated over the worst month.

The performance objective is defined in terms of error blocks. The number of bits in a measurement block may vary within a defined range, the upper and lower limits of the measurement block size depending upon the transmission rate of the radio link. An errored block, 'EB', is a block with at least one error. An errored second is a second which contains at least one errored block, that is a second with at least one error. A severely disturbed period, 'SDP', is defined as one millisecond where the bit error rate is one error in a hundred bits or greater, or where four contiguous blocks have an error rate of one error in a hundred or greater. A severely errored second, 'SES', is a one second period which contains 30% or more errored blocks or at least one severely disturbed period. A background block error, BBE, is a block of bits which contain errors but which is not part of a severely errored second.

When considering a 27 500 km hypothetical path operating at the primary rate or at a higher bit rate, the ratio of errored seconds to available time, ESR, depends on the bit rate used. However the ratio of severely errored seconds to available time, SESR, is a fixed value of 0.002. The end–to–end objective for background block errors is set at three blocks in ten thousand for transmission rates below 5 million bits a second, and at two blocks in ten thousand blocks for higher capacity links.

The end–to–end objective set by ITU–T G.826 is allocated to the national section of an international path and to the international section. The national portion is allocated 17.5% of the the objective, with an additional 1% for every 500 km. The international allocation is 1% for the terminating country plus 1% per 500 km, and 2% for intermedi-

ate countries with 1% per 500 km. A satellite hop is allowed 35% of the end–to–end objective regardless of whether it is part of the national or international path.

Classification ITU–T G.826	1.5 – 5 Mbit/s	>5 – 15 Mbit/s	>15 – 55 Mbit/s	>55–160 Mbit/s
Bits / Block	2 000 – 8 000	2 000 – 8 000	4 000 – 20 000	6 000 – 20 000
ESR	0.04	0.05	0.075	0.16
SESR	0.002	0.002	0.002	0.002
BBER	$3\text{x}10^{-4}$	$2\text{x}10^{-4}$	$2\text{x}10^{-4}$	$2\text{x}10^{-4}$

Table 1-27   Objectives for a link operating at or above the primary rate

7.3   Radios operating above the primary rate

ITU–T Recommendation G.826 establishes the error performance objectives for constant bit rate digital paths which operate at the primary rate, or above. The end–to–end objectives are set in terms of the national network and the international network. Further guidance for the allocation of error performance objectives to radio relay systems which operate at a constant bit rate at or above the primary rate, within the national portion of a 27500km hypothetical reference path, can be found in ITU–R Recommendation F.1189–1. Digital radio relay systems operating at a constant bit rate at or above the primary rate, which for part of the international portion of a 27500km hypothetical reference path are covered by ITU–R Recommendation F.1092–1.

The national portion of a network can be broken down into three sections, namely access, short haul, and long haul [109]. The access network section includes the connec-

tions between the path end–point and the local switching centre. The short haul inter–exchange network section includes the connections between the local switching centre and a defined switching level within the national architecture. The long–haul inter–exchange network section includes connections between the international gateway and an operator defined switching level within the national architecture.

ITU–R Recommendation F.1189–1 has provisionally allocated between 7.5% to 8.5% of the error performance objectives stated in ITU–T G.826 for use in the access portion of the national network, and between 7.5% to 8.5% of the objectives for use in the short haul inter–exchange portion of the national network. However, the provisional values for the combined access and short haul sections should be between 15.5% and 16.5% [109]. Depending on the allocation to the access and short haul parts of the network the long haul inter–exchange portion of the national network will receive between 1% and 2% [109] of the national allocation, plus 1% of the end–to–end objectives for every 500km, rounded up to the next 500km [109].
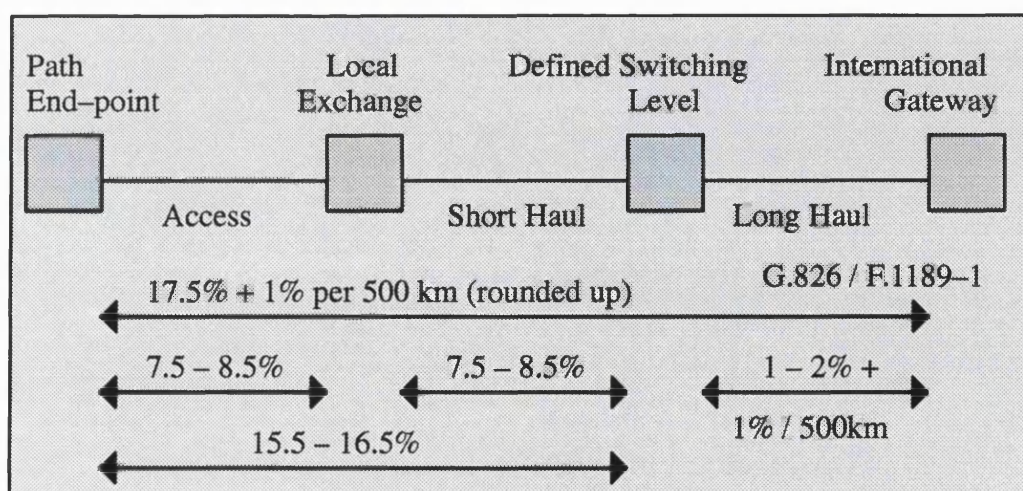
Diagram 1-85   Hypothetical reference path defined by ITU–T G.826

The international portion of a constant bit rate path at or above the primary level, will be allocated a distance allowance of 1% of the G.826 objectives per 500km, plus at least part of a country allowance. The full terminating country allowance of 1% will be allocated if the path between the international gateway and the country border is greater than 500km [110]. If the distance is less than 500km, which is a provisional figure, the 1% allowance will be allocated based on the ratio of the path length to the 500km reference. The full intermediate country allowance of 2% will be allocated if the path between the country borders is greater than 1000km. If the distance is less than 1000km, which is a provisional figure, the 2% allowance will be allocated based on the ratio of the path length to the 1000km reference path [110].

7.4   Radios operating beiow the primary rate

ITU–T G.821 defines objectives for a 64kbit/s international circuit in terms of a high grade, medium grade and local grade path. The error performance objectives for radio relay systems operating below the primary rate should be assessed in terms errored seconds and severely errored seconds as defined in ITU–T G.821 [105][106][107]. On the 25000 km high grade portion of an international connection the ratio of errored seconds to available time, ESR, should not exceed 0.032 in any month and the ratio of severely errored second to available time, SESR, should not exceed 0.0004, plus a special allowance for adverse conditions in any month [102]. The special allowance of 0.001 (0.1%) is for use in high grade and medium grade portions of the network, but half of this allowance 0.0005, is allocated to a 2500km hypothetical reference digital path, HRDP [102]. Scaling the SESR allowance for the 25000km high grade network down to a 2500km HRDP yields an allowance of 0.00004, and the special allowance of 0.0005. This means

that the SESR allowance for the first 2500km HRDP is 0.00054 [105]. Therefore the first 2500km HDRP the ESR should not exceed 0.0032 in any month [105] and the SESR should not exceed 0.00054 in any month [105].

In the local grade portion of a network the ESR should not exceed 0.012 in any month and the SESR should not exceed 0.00015 in any month [106].

The medium grade portion of a network can be subdivided into four quality classifications. Class 1, which is equivalent to high grade, and class 2 sections have a maximum distance of 280 km, while classes 3 and 4 have a maximum distance of 50 km [107]. There is no reduction in the error performance allocation if the radio link is shorter than either a 50 km or a 280 km section [107]. If the overall radio link is longer than 50 km or 280 km then the allocation for classes 2, 3, or 4 will be an integer number of allowances for 50 km sections or 280 km sections [107]. Since class 1 is equivalent to the high grade, if the radio link is longer than 280 km the performance objective should be derived from a pro–rata approach [107]. Although the medium grade link may comprise of a number of 50 km or 280 km digital radio sections, the ESR may not exceed the end–to–end allowance of 0.012 in any month [107]. The SESR should not exceed the 0.00015 of end–to–end objective for any month [107]. However ITU–T G.821 allows an additional 0.001 for adverse conditions in the medium and high grade sections, and in the case of class 3 and 4 the administration concerned may allow an additional 0.00025 to the medium grade section, in which case the SESR should not exceed the 0.0004 of end–to–end objective in any month [107].

Bit Rate Below 2Mbits/s (or 1.54)			Allowance Per Unit Length		
Grade	Class	Length	ESR	SESR	ITU Rec
High	High	Total	0.032	0.0009	G.821
High	HRDP(1st)	2500km	0.0032	0.00054	F.594–2
Medium	Class 1,2	Total	0.012	0.00015	F.696–2
Medium	Class 3,4	Total	0.012	0.0004	F.696–2
Medium	Class 1	280km	0.00036	0.00006	F.696–2
Medium	Class 2	280km	0.0016	0.000075	F.696–2
Medium	Class 3	50km	0.0016	0.00002	F.696–2
Medium	Class 4	50km	0.004	0.00005	F.696–2
Local	Local	Total	0.012	0.00015	F.697–2

Table 1-28   **Objectives for radios operating below the primary rate**

The SESR for a high grade 2500km path is 0.00054 according to ITU–T recommendation G.821, but at bit rates greater than the primary rate the end–to–end objective for SESR is 0.002 according to ITU–T recommendation G.826. For real radio links operating below the primary rate, on radio links between 280km and 2500km, the SESR allowance should be allocated by linear scaling, ie (length in km / 2500 km) x 0.00054 [104]. Likewise on radio links between 280km and 2500km which operate below the primary rate, the allowance for the ESR,should be calculated by linear scaling, as follows (length in km / 2500 km) x0.0032 [104].

7.5   Availability

A hypothetical reference digital path, HRDP, is defined by the 1986 ITU Recommendation 556–1, as a 2500km path operating at a bit rate above the second plesiochronous

digital hierarchical level, which is made up of nine sets of digital multiplexing equipment. This path is defined as high grade, and the 1986 Recommendation makes reference to G.821, Geneva 1980. Availability objectives for a HRDP are described in the 1997 ITU–R F.557–4, as 99.7%, when measured over a statistically valid period which is probably greater than one year. It is noted in ITU–R F.557–4 that the availability figure of 99.7% is provisional and that in practice objectives may fall into the range 99.5% to 99.9%. It is also noted in ITU–R F.557–4 that high grade objectives for real radio link are covered in ITU–R F.695.

Referring to real HRDP, the 1990 ITU Recommendation 695 states that the provisional availability figure is 99.7%, and that for links between 280km and 2500km the unavailability of 0.3 should be linearly allocated according to the link length. The recommendation also states that in practice the availability figure may range between 99.9% and 99.5%.

Availability objectives for radio relay systems operating at a bit rate below the primary rate, in hypothetical reference digital sections, HRDS, of 50km and 280km are given in the 1990 ITU–R Recommendation F.696–2. Classes 1, 2, 3 and 4 are allocated 0.033%, 0.05%, 0.05% and 0.1% respectively for sections of 280km, 280km, 50km and 50km. ITU–R F.696–2 proposes an overall medium grade availability objective of between 99.8% and 99.5%.

ITU–R F.697–2, which was published in 1997, describes the performance and availability objectives for the local grade portion of a network which uses digital radio relay systems at a bit rate below the primary rate. This recommendation states that the ITU–T and ITU–R have not set standards for local grade availability, however, the values being considered range between 0.01% and 1.0%.

Proposed Unavailability in %				
Grade	Class	Length	Unavailability	ITU Rec
High	HRDP	2500km	0.3%	F.557-4
High	HRDP	280 to 2500km	0.3x(path/2500)	Rec 695
Medium	Medium	Medium	0.2% to 0.5%	F.696-2
Medium	Class 1	Up to 280km	0.033%	F.696-2
Medium	Class 2	Up to 280km	0.05%	F.696-2
Medium	Class 3	Up to 50km	0.05%	F.696-2
Medium	Class 4	Up to 50km	0.1%	F.696-2
Local	Local	Local	Not Defined	F.697-2

Table 1-29   **Availability objectives**

7.6   Prediction of unavailability and SESR

ITU–R P.530–7 [17] provides a method for determining antenna heights, in order to

limit unavailability due to diffraction, based on measured effective k values exceeded

for 0.1% of time. In addition this document provides a method for predicting unavail-

ability due to rain based on rainfall intensity, frequency and polarisation of operation,

and path length. ITU–R P.530–7 also provides a model for predicting the percentage of

time, during the worst month of fading activity, that flat multipath fading would cause

the received power level to fade below a defined fade margin, corresponding to a par-

ticular bit error rate being exceeded. A model, bases on measured signatures at the bit

error rate of interest, is provided by ITU–R P.530–7 for predicting the percentage of time

during the worst month of fading activity that selective multipath fading will cause dis-

tortions in the received spectrum to cause the predetermined bit error rate to be

exceeded. The outage periods caused my multipath activity normally last for less than ten seconds, and can be considered to be part of available time, and therefore influence the performance objectives. If the fade margin and signatures have been determined for a bit error rate of one error in a thousand, the predicted time that this error rate will be exceeded during the worst month can be used to check the SESR objective according to ITU–T G.821. Since ITU–R G.826 defines SESR in terms of errored blocks, the predicted outage values provided by the ITU–R P.530–7 method no longer correspond exactly to SESR, according to ITU–R G.826. However, since the ITU–R have not provided a method of calculating SESR according to ITU–T G.826, the method defined in ITU–R P.530–7 has been used to provide an approximation.

Appendix B

8 Rainfall integration time

mm/h   Dec23   2243–2319 (one minute integration period)

150
100
50
0
−50
−100
dBm

60s Optus
60s RBH
Rx dBm
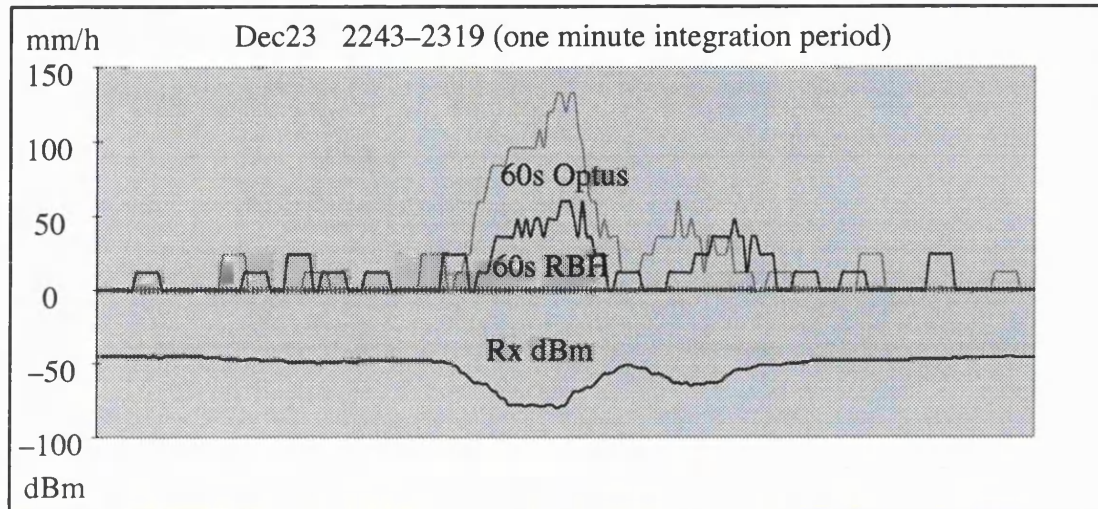
Plot A-16   Rain rate using one minute integration (2243–2319 23.Dec.97)

mm/h   Dec23   2243–2319 (five minute integration period)

120
100
80
60
40
20
0
−20
−40
−60
−80
−100
dBm

5m Optus
5m RBH
Rx dBm
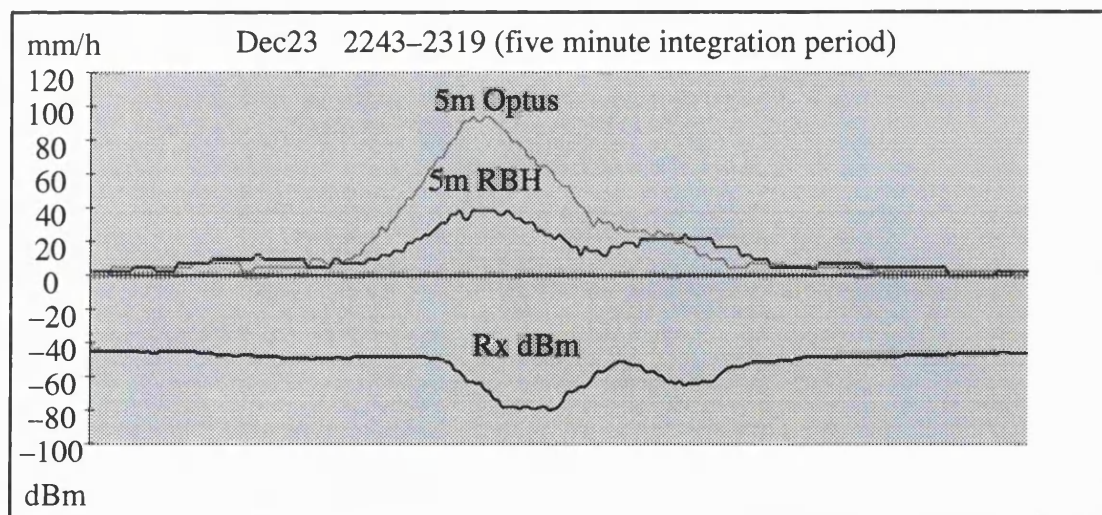
Plot A-17   Rain rate using five minute integration (2243–2319 23.Dec.97)

Appendix C

9   Fade distributions

Log Fade dB	Fade duration in seconds for months February 97 to January 98 Measured at the Optus end of the hop (based on indicated rx levels)												Cumulative Minutes
	Feb	Mar	Apr	May	Jun	Jul	Aug	Sep	Oct	Nov	Dec	Jan	
17	22	23	23	168	23			79	313	23	151	105	233.017
18	0	57	45	175	12			183	111	0	122	138	217.517
19	0	57	69	114	46			217	185	12	34	140	203.467
20	0	172	92	196				126	217	0	149	273	188.9
21	12	150	80	114				68	218	11	184	241	168.483
22	23	102	46	46				80	70	39	264	81	150.517
23	0	58	44	138				11	185	11	318	115	138
24	0		58	46				11	69	0	34	46	123.333
25	23		103	91				35	125	0	136	170	118.933
26			0	128				148	58	11	184	68	107.55
27			12	68				35	35	12	70	59	97.6
28			11	81				11	45	12	44	92	92.75
29			0	23				0	23	68	12	48	87.817
30			23	35				12	93	162	57	69	84.917
31				79				0	0	11	58	125	77.4
32				11				12	47	22	0	36	72.85
33				47				0	0	46	0	23	70.717
34				81				11	34	12	12	93	68.783
35				46				26	0	51	127	46	64.733
36				23				22	47	26	23	49	59.8
37				22				0	0	0	27	12	56.633
38				12				58	11	0	12	35	55.617
39				47				0	0	23	12	35	53.483
40				0				46	0	13	0	23	51.533
41				23				35	0	0	0	12	50.167
42				11				81	0	170	22	22	49
43				0				23	0	115	0	70	43.9
44				12				34	12	36	12	12	40.433
45				23				58	0	69	0	103	38.467
>45				207					35		138	1676	34.25

Table 1-30   Fade distribution based on indicated received power levels

Real fade distribution based on measurements at 15, 20, 26 and 30 degrees Celsius					
Logged Fade dB	Log Power Level –dBm	Adjustment Required dB	Maximum Power Level –dBm	Minimum Fade dB	Cumulative Distribution Minutes
17	60	+2	58	15	233.017
18	61	+2	59	16	217.517
19	62	+2	60	17	203.467
20	63	+2	61	18	188.9
21	64	+2	62	19	168.483
22	65	+2	63	20	150.517
23	66	+2	64	21	138
24	67	+2	65	22	123.333
25	68	+2	66	23	118.933
26	69	+2	67	24	107.55
27	70	+2	68	25	97.6
28	71	+1	70	27	92.75
29	72	+1	71	28	87.817
30	73	+1	72	29	84.917
31	74	+1	73	30	77.4
32	75	+1	74	31	72.85
33	76	+1	75	32	70.717
34	77	+1	76	33	68.783
35	78	+1	77	34	64.733
36	79	+1	78	35	59.8
37	80	+1	79	36	56.633
38	81	+2	79	36	
39	82	+2	80	37	53.483
40	83	+2	81	38	51.533
41	84	+2	82	39	50.167
42	85	+4	82	39	
43	86	+4	82	39	
44	87	+4	83	40	40.433
45	88	+4	84	41	38.467
>45	89	+4	<84	>41	34.25

Table 1-31   Temperature compensated cumulative fade distribution

Appendix D

10   Wind speed during fading
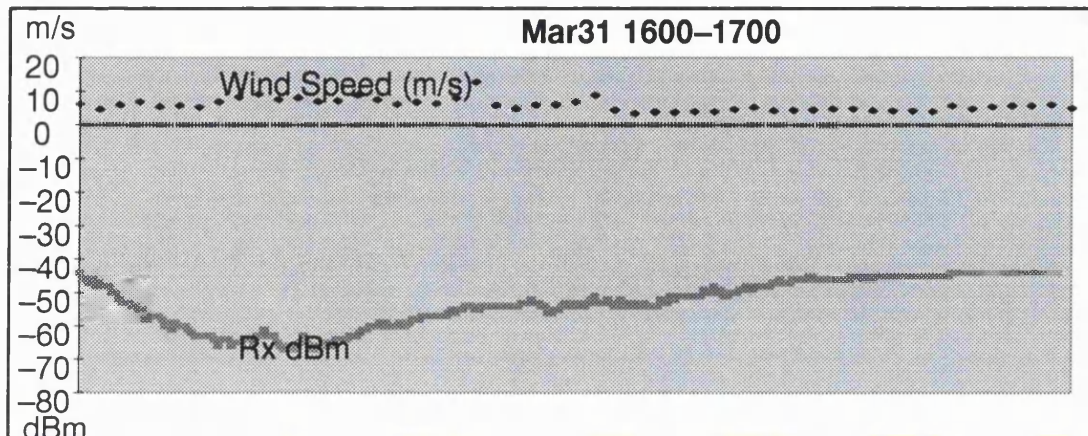
Plot A-18   **Wind speed between 1600 and 1700 on 31.Mar.1997**
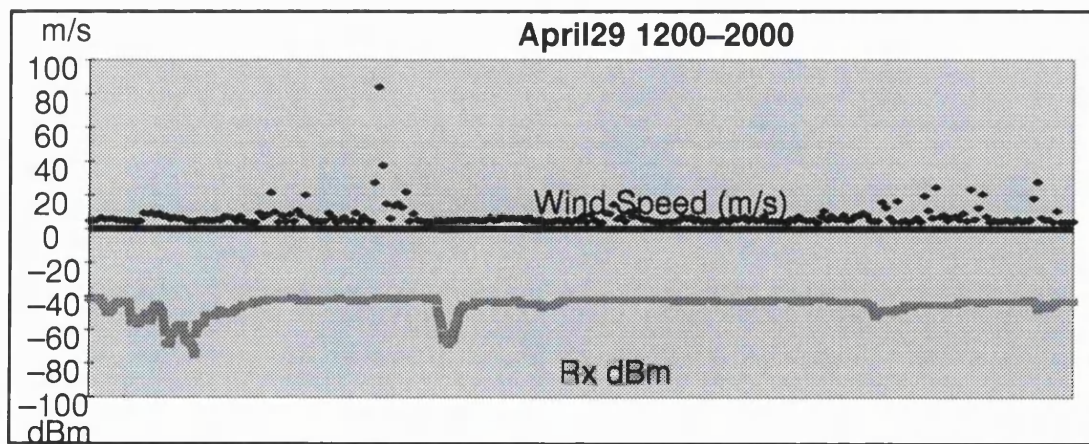
Plot A-19   **Wind speed between 1200 and 2000 on 29.Apr.1997**
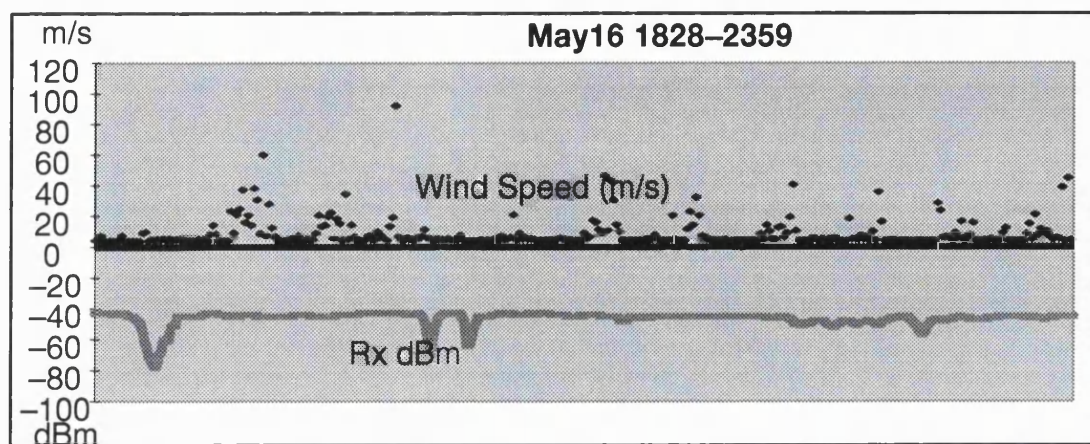
Plot A-20   **Wind speed between 1828 and 2359 on 16.May.1997**
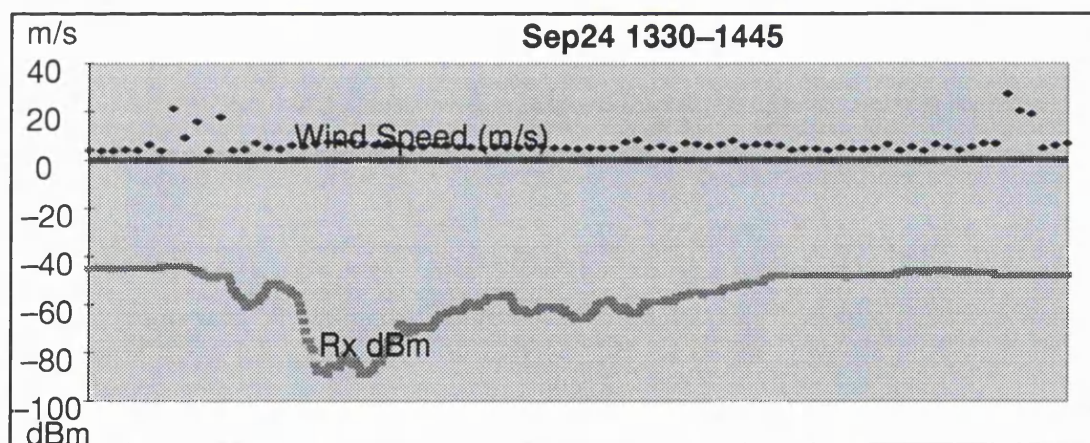
Plot A-21   **Wind speed between 1330 and 1445 on 24.Sep.1997**
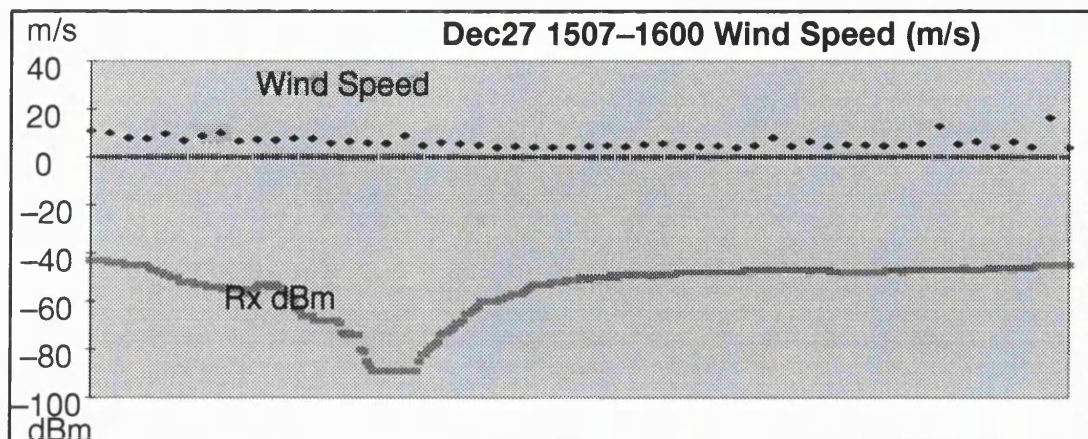
Plot A-22   **Wind speed between 1507 and 1600 on 27.Dec.1997**
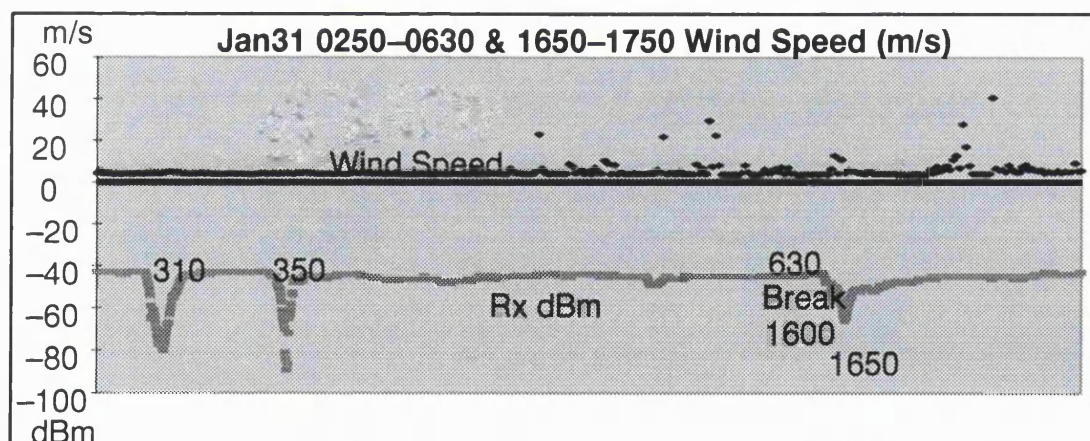
Plot A-23   **Wind speed between 0250 and 1750 on 31.Jan.1998**

Appendix E

11 Wind direction during fading
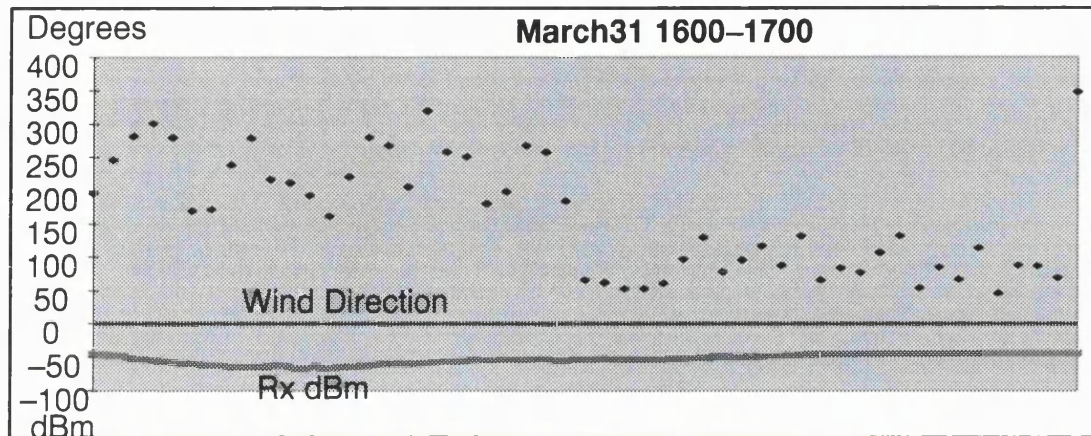
Plot A-24   **Wind direction between 1600 and 1700 on 31.Mar.1997**
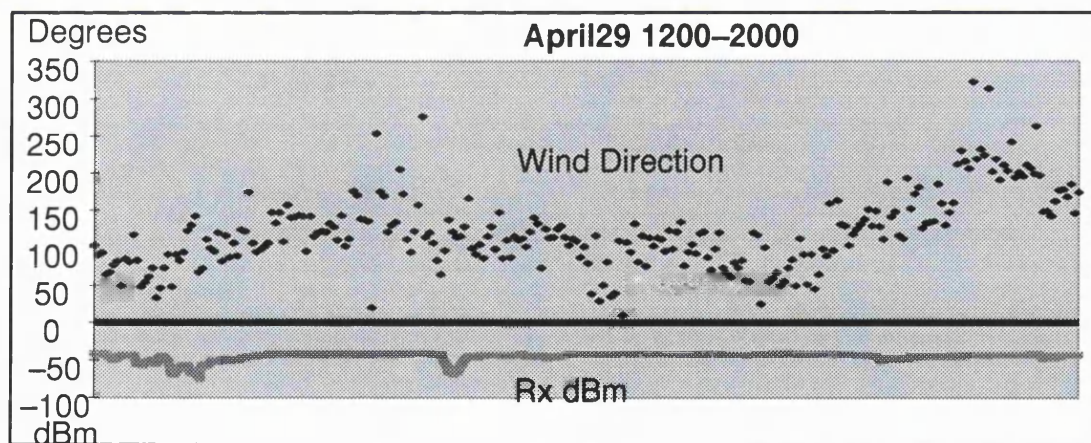
Plot A-25   **Wind direction between 1200 and 2000 on 29.Apr.1997**
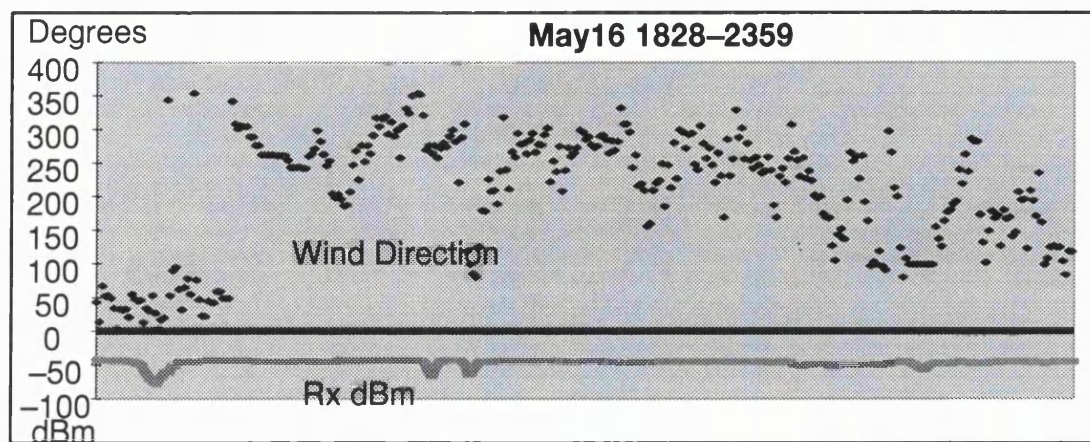
Plot A-26   **Wind direction between 1828 and 2359 on 16.May.1997**
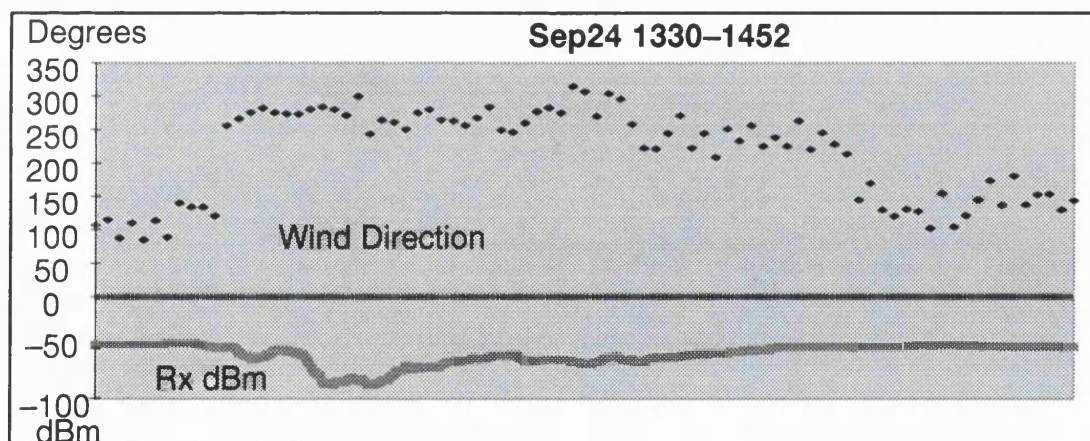
Plot A-27   **Wind direction between 1330 and 1445 on 24.Sep.1997**
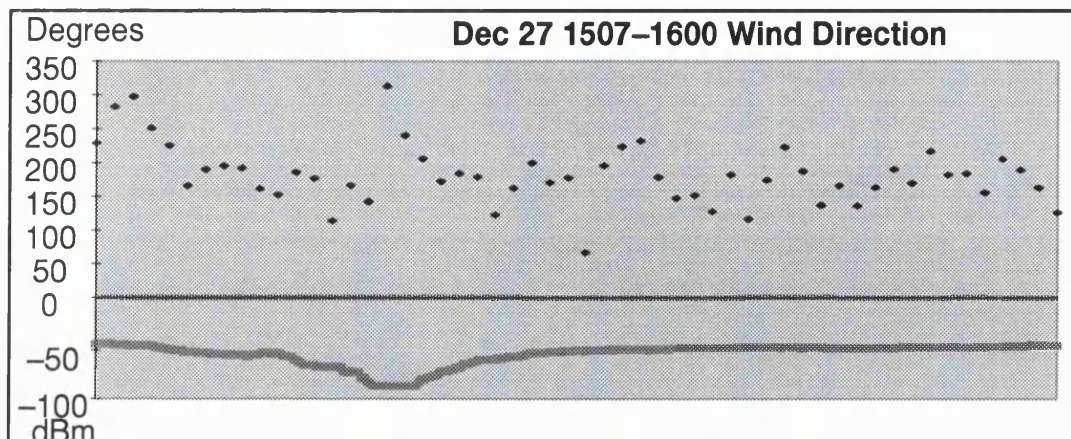
Plot A-28   **Wind direction between 1507 and 1600 on 27.Dec.1997**
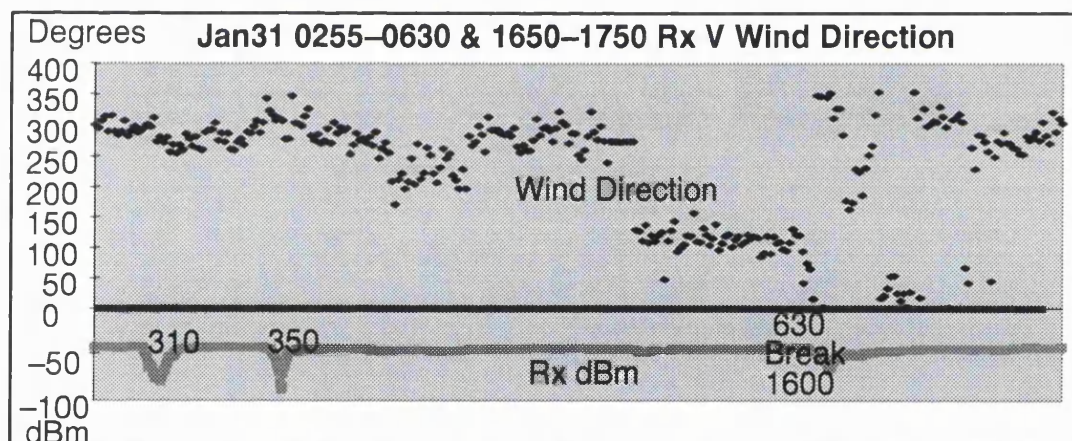
Plot A-29   **Wind direction between 0250 and 1750 on 31.Jan.1998**

Appendix F

12 Rainfall causing the worst fading
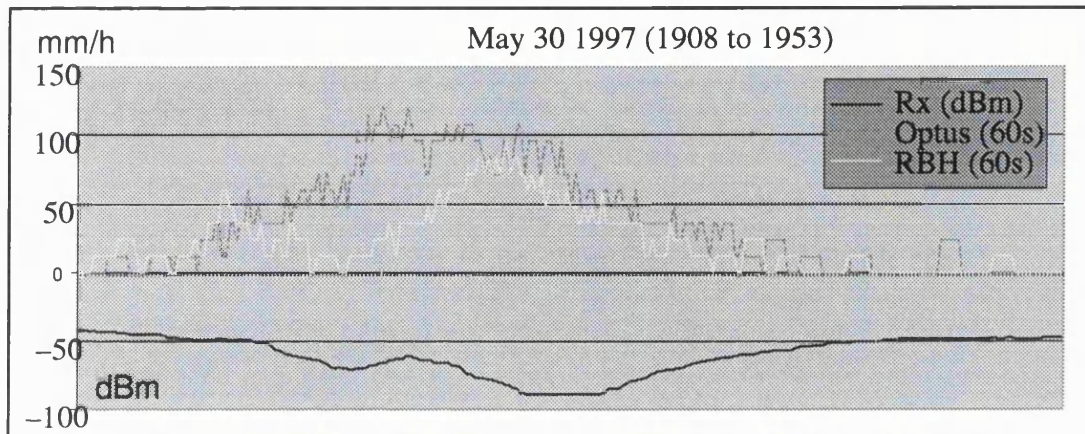
Plot A-30   **Rain rate at Optus and RBH 1908 – 1953 on 30.May.1997**
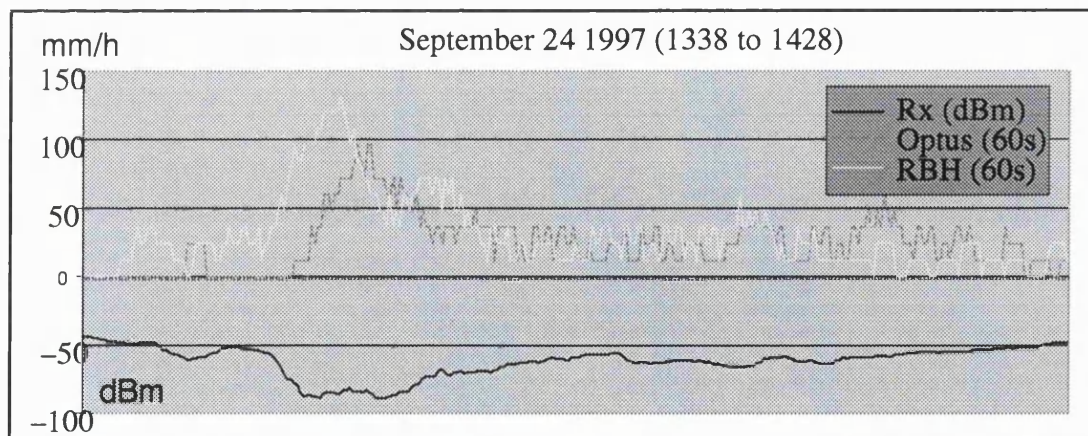
Plot A-31   **Rain rate at Optus and RBH 1338 – 1428 on 24.Sep.1997**
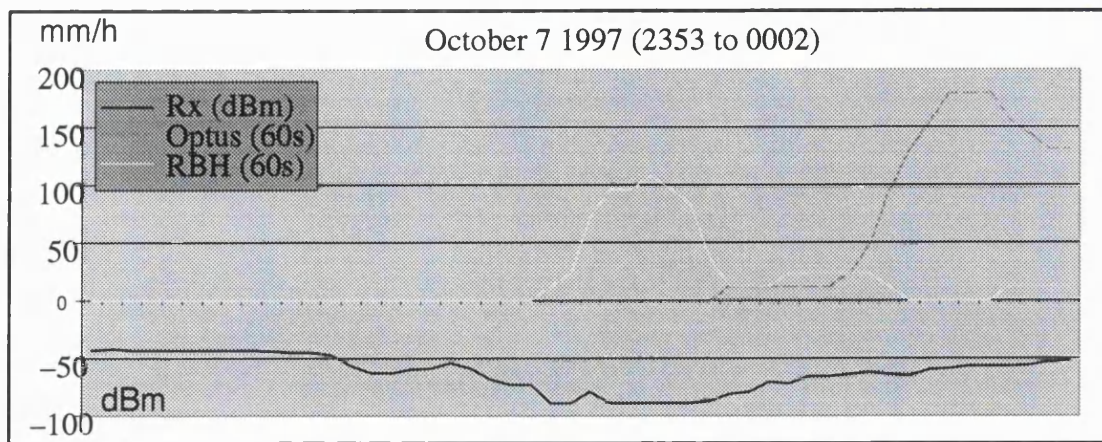
Plot A-32   **Rain rate at Optus and RBH 2358 – 0002 on 7/8.Oct.1997**
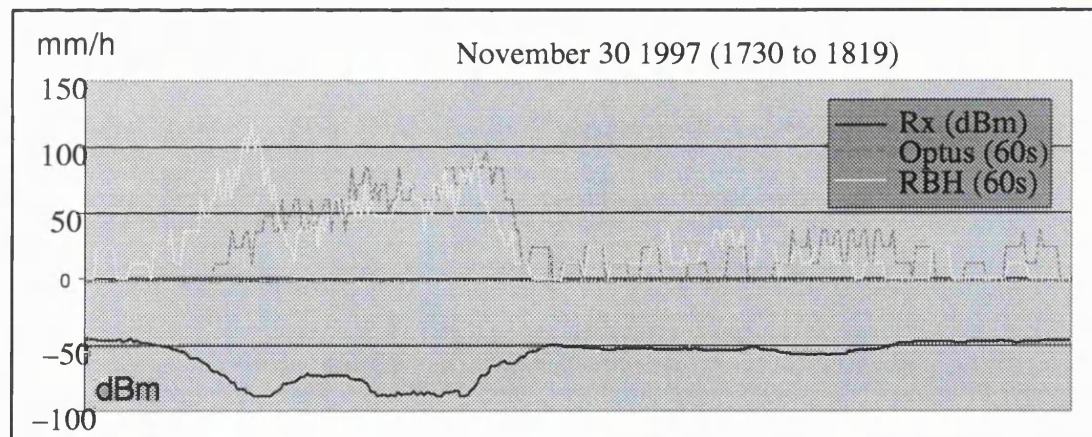
Plot A-33   **Rain rate at Optus and RBH 1730 – 1819 on 30.Nov.1997**

dBm
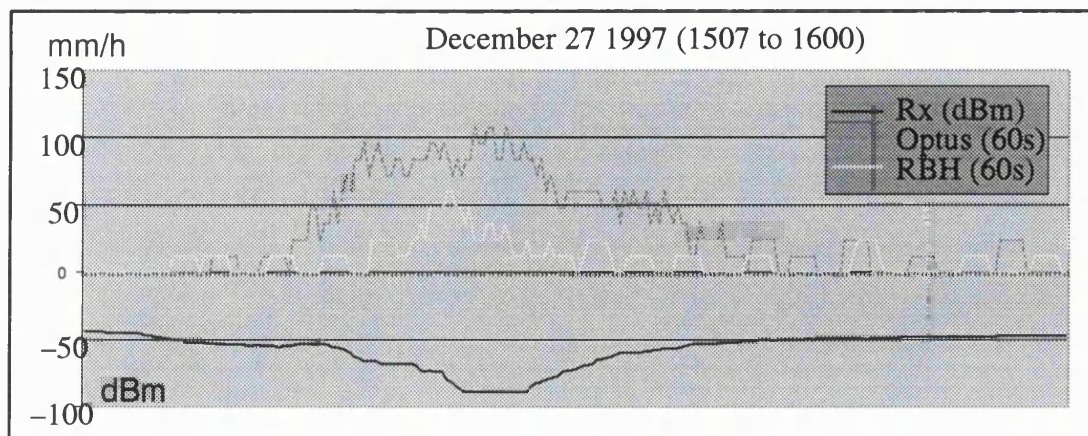
Plot A-34 **Rain rate at Optus and RBH 1507 – 1600 on 27.Dec.1997**
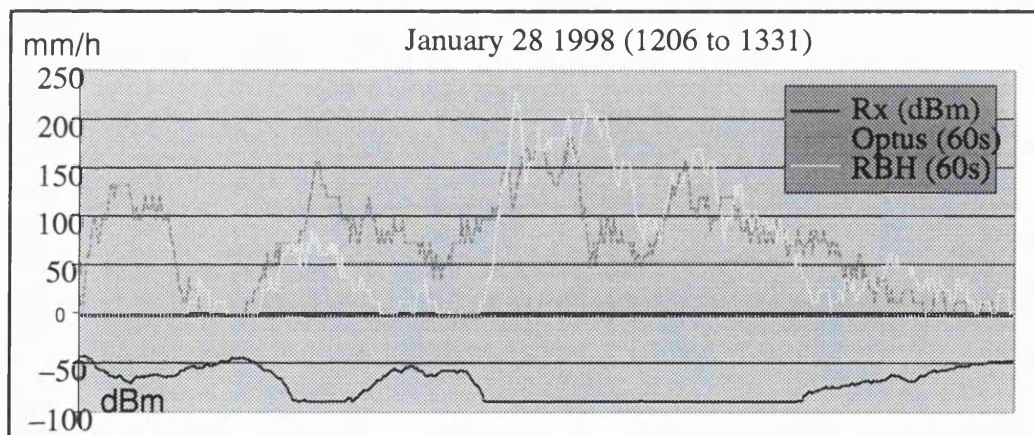
Plot A–9 **Rain rate at Optus and RBH 1206 – 1331 on 28.Jan.1998**
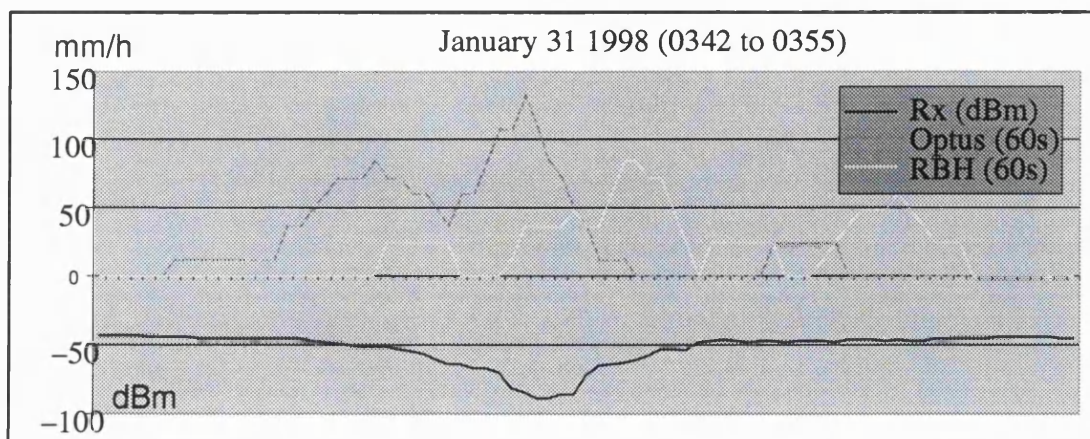
Plot A-35   **Rain rate at Optus and RBH 0342 – 0355 on 31.Jan.1998**

Appendix G

13   Significant rainfall and fading events

During February there were five significant events caused by four rainfall systems.

February 1997							
Event	Start	Finish	Log Fade	Real Fade	Optus (60s)	RBH (60s)	Duration
Date	Time	Time	dB	dB	mm/h	mm/h	Minutes
16 Feb	2234	2242			96		9
18 Feb	0053	0057	−27	−25			5
18 Feb	0130					72	1
18 Feb	0953				60		1
18 Feb	1403	1405	−17	−15			3

Table 1-32   **Fades 15dB or more or rain 60mm/h or more in February 97**
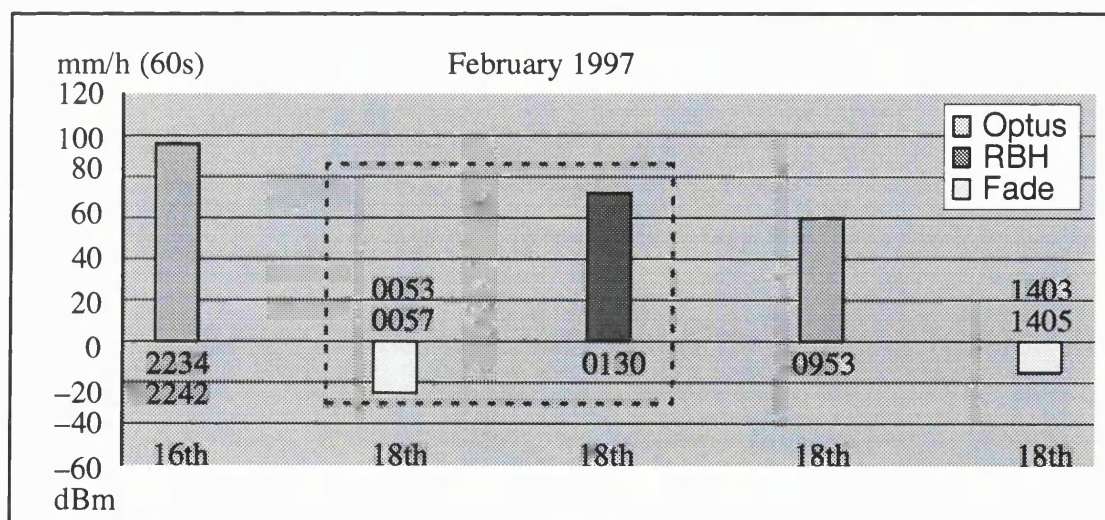
Diagram 1-86   **Fades 15dB or more or rain 60mm/h or more in February 97**

During March there were eight significant events caused by three rainfall systems

			March 1997				
Event	Start	Finish	Log Fade	Real Fade	Optus (60s)	RBH (60s)	Duration
Date	Time	Time	dB	dB	mm/h	mm/h	Minutes
22 Mar	1919	1923	−20	−18			5
22 Mar	1957					72	1
26 Mar	1124	1138	−17	−15			5
26 Mar	1212					60	1
26 Mar	1235	1237	−17	−15			3
26 Mar	1312				60		1
31 Mar	1527	1558	−24	−22			32
31 Mar	1613	1616			60		4

Table 1-33   Fades 15dB or more or rain 60mm/h or more in March 97
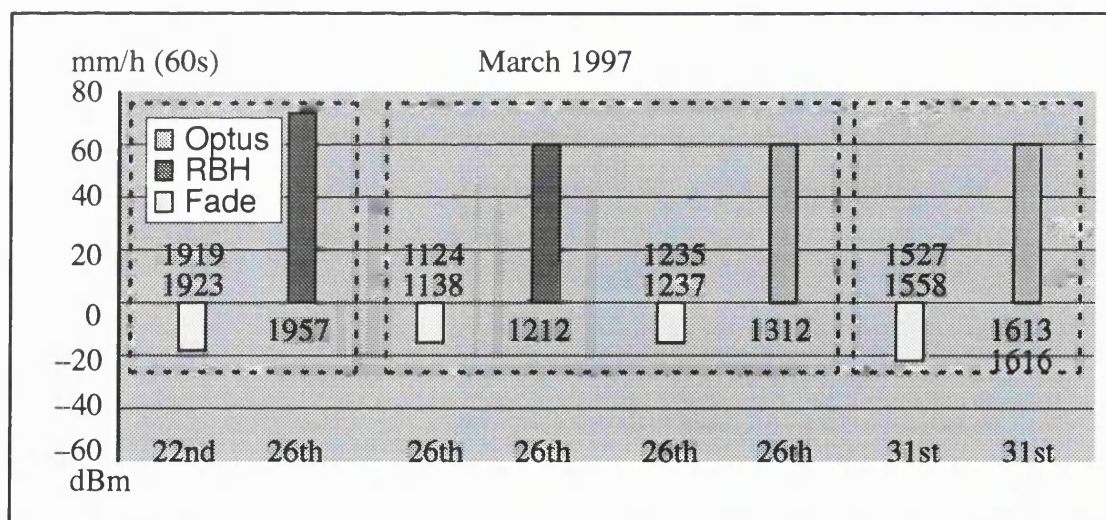
Diagram 1-87   Fades 15dB or more or rain 60mm/h or more in March 97

In April there were five significant events caused by three rainfall systems

April 1997							
Event	Start	Finish	Log Fade	Real Fade	Optus (60s)	RBH (60s)	Duration
Date	Time	Time	dB	dB	mm/h	mm/h	Minutes
29 Apr	1145	1202	−32	−31			18
29 Apr	1215				60		1
29 Apr	1258	1303	−26	−24			6
29 Apr	1336	1339				72	4
30 Apr	1210	1213	−21	−19			4

Table 1-34   **Fades 15dB or more or rain 60mm/h or more in April 97**
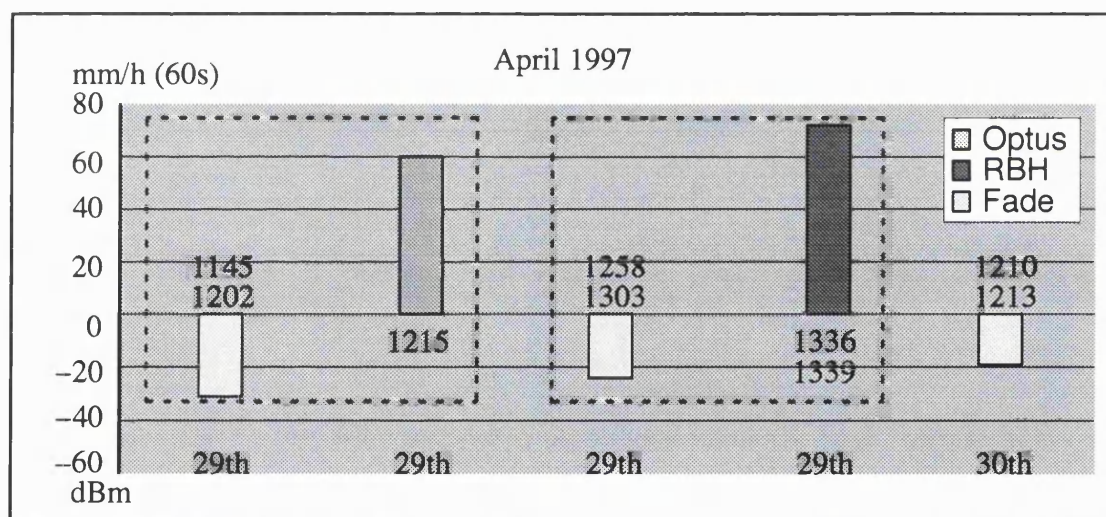
Diagram 1-88   **Fades 15dB or more or rain 60mm/h or more in April 97**

In May there were eleven significant events caused by three rainfall systems.

		May 1997					
Event	Start	Finish	log Fade	Real Fade	Optus (60s)	RBH (60s)	Duration
Date	Time	Time	dB	dB	mm/h	mm/h	Minutes
1 May	0028	0039	−28	−27			12
16 May	1808	1819	−35	−34			12
16 May	1847	1850			96		4
16 May	1856					60	1
16 May	1946	1949	−23	−21			4
16 May	1959	2002	−21	−19			4
16 May	2036				60		1
16 May	2039					60	1
30 May	1836	1904	<−45	<−41			29
30 May	1919	1933			120		15
30 May	1926	1930				84	5

Table 1-35   Fades 15dB or more or rain 60mm/h or more in May 97
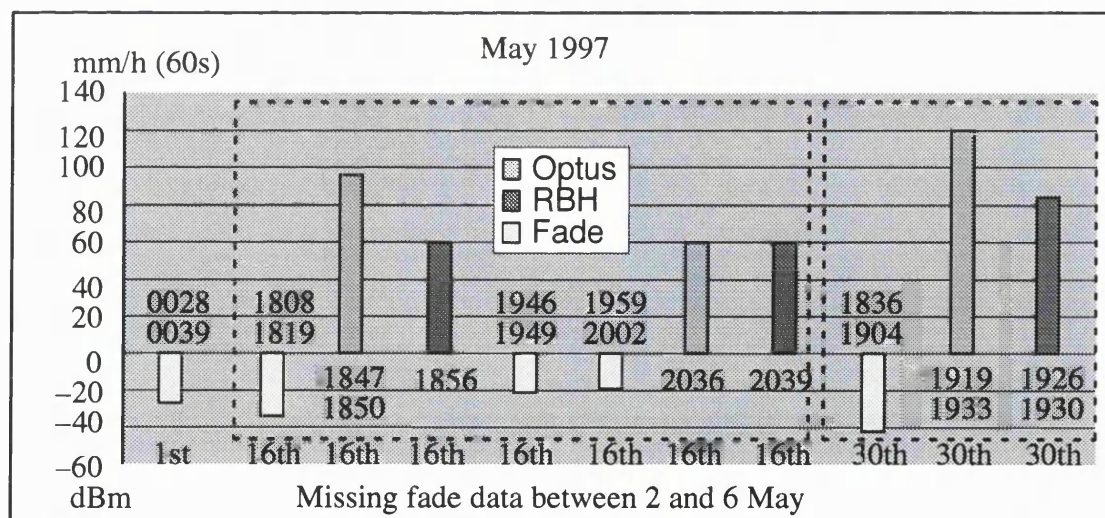
Diagram 1-89   Fades 15dB or more or rain 60mm/h or more in May 97

During June, July and August there was one significant rainfall event and one significant fading event. However non fading information was available between 22 June and 6 August while the transmit end from the Royal Brisbane Hospital (transmit) end was being repaired.

June July 1997							
Event	Start	Finish	Log Fade	Real Fade	Optus (60s)	RBH (60s)	Duration
Date	Time	Time	dB	dB	mm/h	mm/h	Minutes
21 Jun	1051	1058	−20	−18			8
7 Jul	1343				60		1

Table 1-36   **Fades 15dB or more or rain 60mm/h or more in June/July 97**
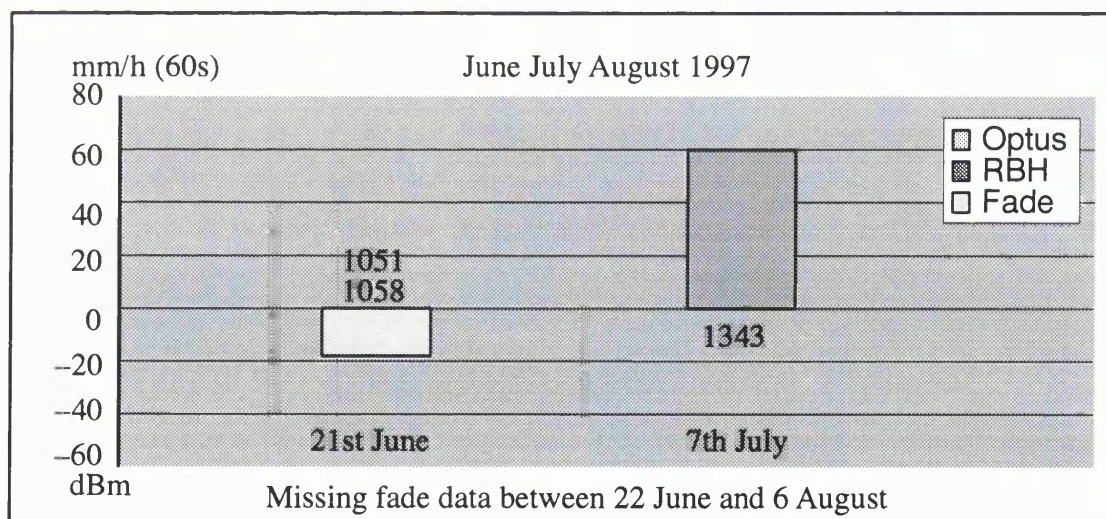
Diagram 1-90   **Fades 15dB or more or rain 60mm/h or more in June/July 97**

During September four significant events were caused by two rainfall systems.

			September 1997				
Event	Start	Finish	Log Fade	Real Fade	Optus (60s)	RBH (60s)	Duration
Date	Time	Time	dB	dB	mm/h	mm/h	Minutes
24 Sep	1341	1426	<–45	<–41			46
24 Sep	1349	1357				120	9
24 Sep	1350	1354			72		5
25 Sep	1439				60		1

Table 1-37   **Fades 15dB or more or rain 60mm/h or more in September 97**
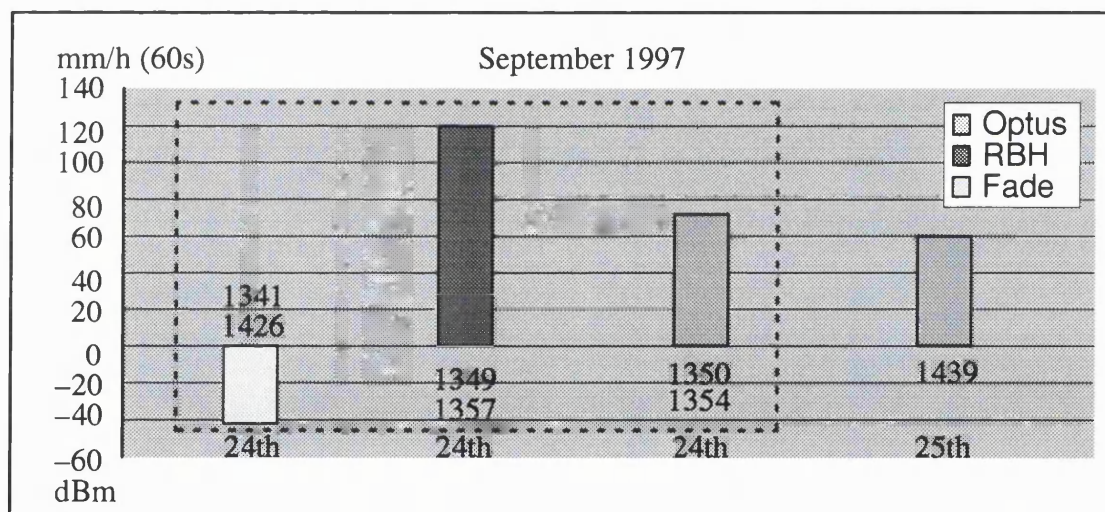
Diagram 1-91   **Fades 15dB or more or rain 60mm/h or more in September 97**

During October eleven significant rainfall events were caused by four rainfall systems. However no fading information was available from 8 October onwards due to data corruption.

October 1997							
Event	Start	Finish	Log Fade	Real Fade	Optus (60s)	RBH (60s)	Duration
Date	Time	Time	dB	dB	mm/h	mm/h	Minutes
7 Oct	1902	2032	−35	−34			91
7 Oct	1925					60	1
7 Oct	2005				60		1
7 Oct	2059	2159	−35	−34			61
7 Oct	2121					72	1
7 Oct	2121	2124			84		4
7 Oct	2140	2141			108		2
7 Oct	2221	2229	−22	−20			9
7 Oct	2355	0001	<−45	<−41			7
7 Oct	2358					96	1
8 Oct	0001	0005			180		5

Table 1-38   **Fades 15dB or more or rain 60mm/h or more in October 97**
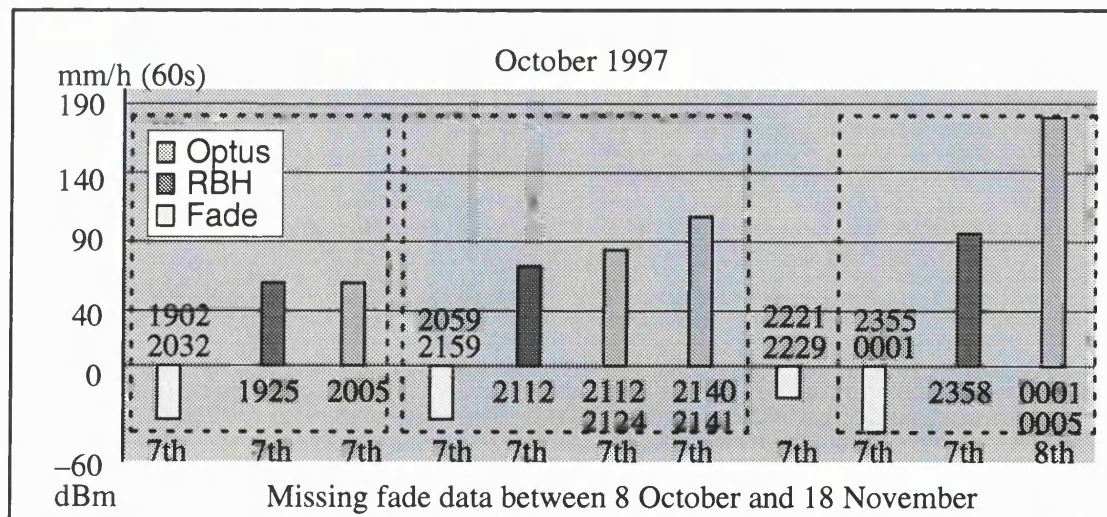
Diagram 1-92   **Fades 15dB or more or rain 60mm/h or more in October 97**

238

In November eight significant rainfall events were caused by five rainfall systems.

However no fading data was available until 18 November due to data corruption.

November 1997							
Event	Start	Finish	Log Fade dB	Real Fade dB	Optus (60s) mm/h	RBH (60s) mm/h	Duration
Date	Time	Time					Minutes
16 Nov	1832					84	1
17 Nov	1748				60		1
17 Nov	2025					60	1
18 Nov	0855				60		1
30 Nov	1734	1810	<–45	<–41			37
30 Nov	1736	1739				96	4
30 Nov	1741	1751			96		11
30 Nov	1743	1749				72	7

Table 1-39   **Fades 15dB or more or rain 60mm/h or more in November 97**
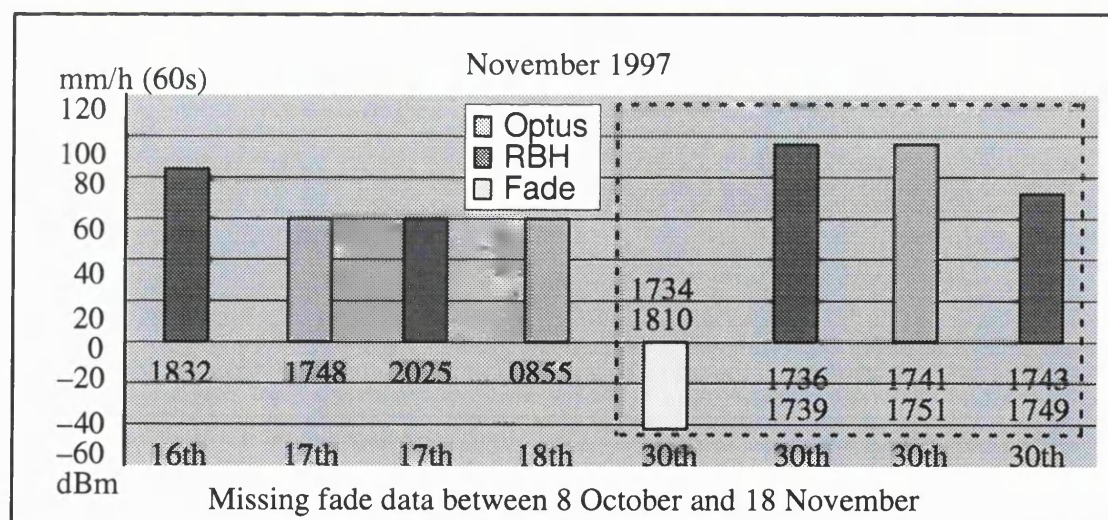
Diagram 1-93   **Fades 15dB or more or rain 60mm/h or more in November 97**

During December eleven significant rainfall events were caused by four rainfall systems.

December 1997							
Event	Start	Finish	Log Fade	Real Fade	Optus (60s)	RBH (60s)	Duration
Date	Time	Time	dB	dB	mm/h	mm/h	Minutes
10 Dec	0915					72	1
10 Dec	0919					60	1
10 Dec	0923	0954	–27	–25			32
23 Dec	2155	2210	–26	–24			16
23 Dec	2157	2158			72		2
23 Dec	2203					60	1
23 Dec	2251	2309	–37	–36			19
23 Dec	2258	2302			132		5
23 Dec	2301					60	1
27 Dec	1511	1537	<–45	<–41			27
27 Dec	1518	1529			108		12

Table 1-40   Fades 15dB or more or rain 60mm/h or more in December 97
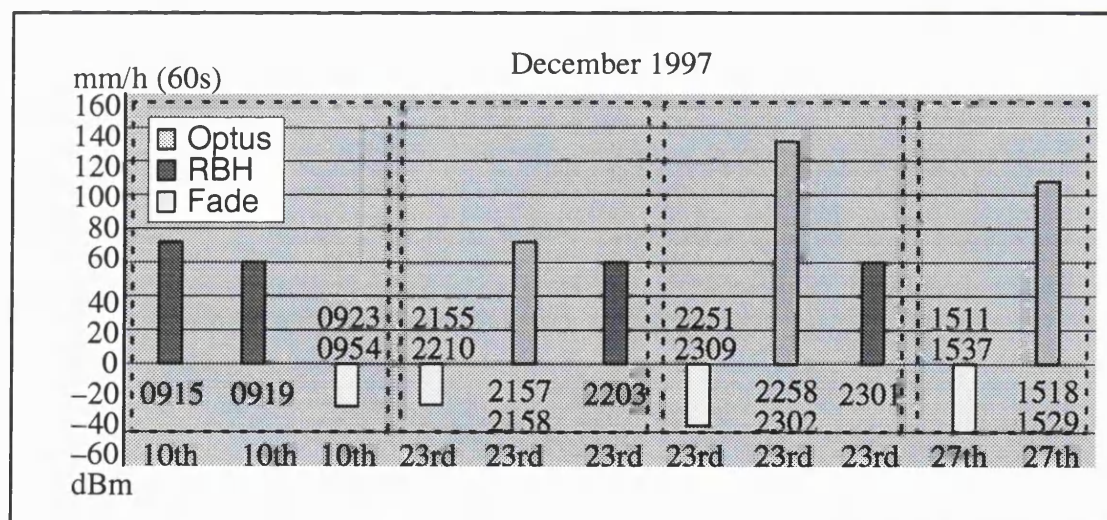
Diagram 1-94   Fades 15dB or more or rain 60mm/h or more in December 97

240

During January nineteen significant rainfall events were caused by eight rain systems.

January 1998							
Event	Start	Finish	Log Fade	Real Fade	Optus (60s)	RBH (60s)	Duration
Date	Time	Time	dB	dB	mm/h	mm/h	Minutes
11 Jan	0659				60		1
11 Jan	0823	0828	−17	−15			6
11 Jan	0826					60	1
13 Jan	0920	0921				60	2
16 Jan	2106	2113	−17	−15			8
28 Jan	1207	1328	<−45	<−41			82
28 Jan	1207	1214			132		8
28 Jan	1224	1316			168		53
28 Jan	1225	1229				72	5
28 Jan	1244	1310				216	27
31 Jan	0305	0314	−37	−36			10
31 Jan	0307	0308			72		2
31 Jan	0310					60	1
31 Jan	0312					60	1
31 Jan	0345	0349	<−45	<−41			5
31 Jan	0345	0348			84		4
31 Jan	0349					84	1
31 Jan	1644	1659	−23	−21			16
31 Jan	1646					60	1

Table 1-41   **Fades 15dB or more or rain 60mm/h or more in January 98**
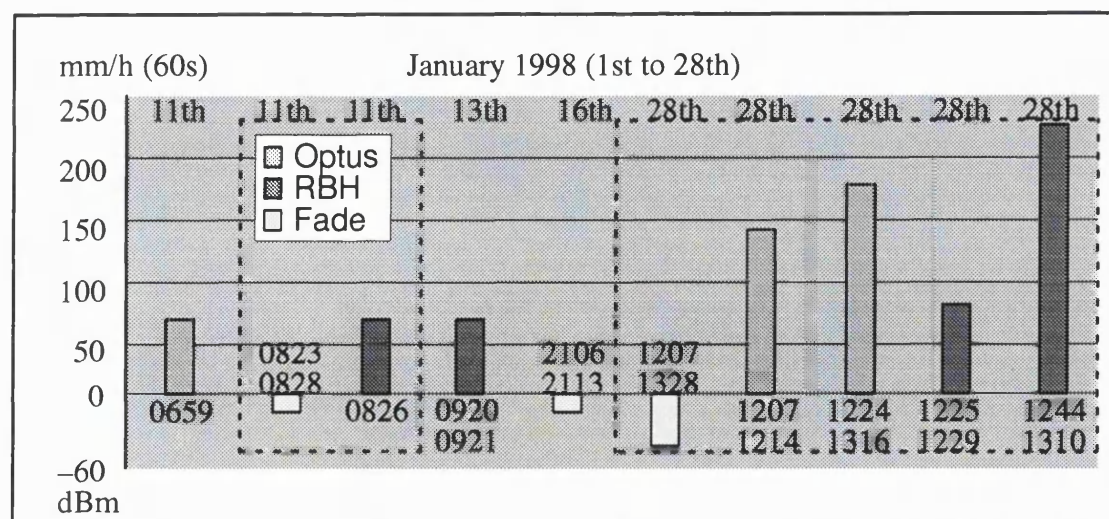
Diagram 1-95   **Fades 15dB or more or rain 60mm/h or more 11–28 January 98**

241
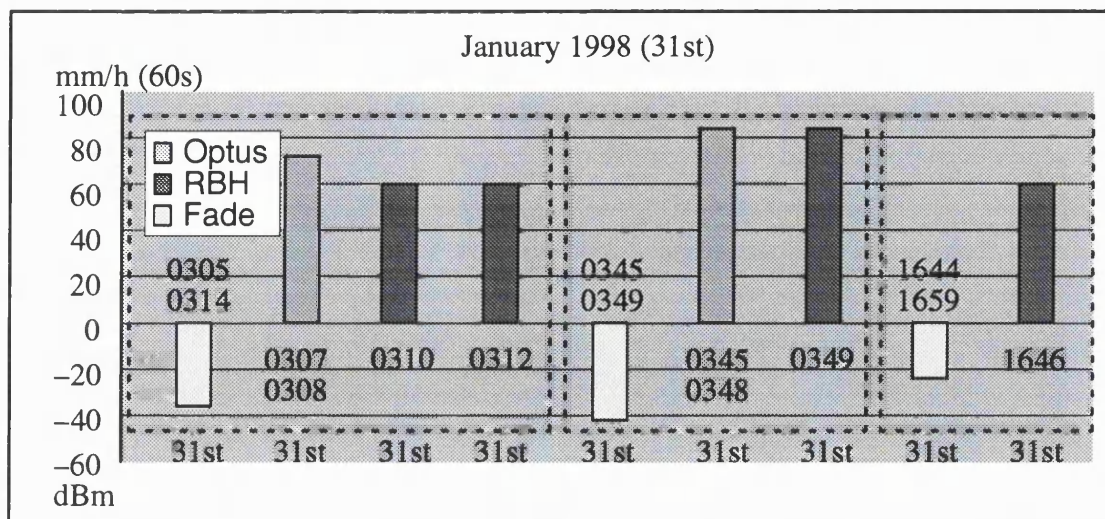
Diagram 1-96   **Fades 15dB or more or rain 60mm/h or more 31 January 98**

Appendix H

14 The influence of El Nino on rainfall

WARM EPISODE RELATIONSHIPS   DECEMBER - FEBRUARY

www.cpc.ncep.noaa.gov/products/

WARM EPISODE RELATIONSHIPS   JUNE - AUGUST

Plot A-36   **The influence of El Nino on rainfall**

Appendix I

15   Average rainfall during fading

The cumulative distribution calculated for fading of 27dB or more was 92.75 minutes

with 34.25 minutes where the minimum fade was greater than 41dB. Therefore the

period that the fading was in the range 27dB to 41dB was 58.5 minutes. This value is

an exact value based on the logged fading data. The table presented here shows that there

were 343 ten second samples recorded for the range 27dB to 41dB, which is 57.16 min-

utes. The difference is due to the ten second samples. The rain event times at the top of

the table represent times that the fade exceeded the 5dB threshold value. The number

of samples at the bottom of the page do not exactly match the storm duration because

on occasions there were long periods where the fade value hovered around 5dB or 6dB

level and since these values were not regarded as significant the measurement period

was truncated.

Min Fade dB	Apr 29 1222 1237	May 1 0111 0114	May 16 1845 1857	May 30 1916 1941	Sep 24 1341 1424	Oct 7 1907 1919 2001 2030	Oct 7 2112 2126 2143 2150	Oct 7 2357 0002	Nov 30 1731 1820	Dec 23 2257 2310	Dec 27 1515 1534	Jan 28 1207 1327	Jan 31 0304 0316	Jan 31 0344 0352	Total Samples (10s)
5	9	30	6	10			12		9.4	12	11.3	9	18	36	43
6	10.2	12	17.3	14.3	13.2	9	14.6		10.6	11.3	10.8	19.5	15	42	92
7	7.5	18	27	12	13	15.8	15		14.9	18	19.2	6	18		64
8	9	18	18	14	13.3	13.8	18		14.8	16	20	18.9	12	36	90
9		18	30	22.5	14	13	16.4	42	16.3	16.8	14	22.5	10.5	12	92
10	6	18	24	18	18	18.6	15.2		14.6	12	36	25.3	15	42	74
11	16.8		24	12	15.7	17.5	20.1		12	27	20	20.4			62
12	18.6		26	23	17.3	18.5	22.5	36	25.7	25.7	27.6	25.7	18	42	138
13	22.8			26	26.3	19.8	23.3		21		20	33.4		36	85
14	24	18		36	22.3	22.9	20.6	33	12	27	33	33.8	6		68
15	19.5		28.7	26.4	23.5	22.5	32	54	18	34	36	37.3	24		92
16	18	18	32.4	31.5	20.7	22	20.4					36	30	39	50
17	30	18		33	24.4	22.8	36		32	12	30	36.3			46
18	12	24	32	37	20.8	22.2	31.5	48	60	35.3	30	38	39	48	89
19	32		42	35.3	23.5	24	26		34.5	38.6	24	45.9	30	32	74
20	18		42	48	33	28.5	48		42	30	30	52.8	36	24	39
21	30		28	43.3	33.8	30.6	22.8	72	63	21	36	39.8			56
22	36	21	30	45	30	18	33					39	34	36	19
23	33.3	24	24	49.2	33	28.8	38.6	12		45	40.7	42.9	18		58
24	30		32	40.5	37.5	31.5	37.5		30	44	48	35			44
25	39		18	36	39		66		42			37.5	45	54	26
27	36	36	36	37.2	30	42	60	84	51		48	42	12		29
28				58	51	36		78	36		42	52	18	36	14
29	27		36	48	51	42	39.4	12	51.9	72	51	36	33		48
30			36	68		32			44	54	49.2	43.2	33		26
31	24		48		46	42	46.6		60			39.6	28		20
32			51.6	63					57			46.8			16
33			57	66			51		84		48	62	33		17
34			66	72	54	46	56		50.4	77.3	48	57	27		38
35				74	54			54	46	81	60	51	36		18
36				72	69			90		78	55.5	52	45	60	18
37				62					72		54	58			10
38					90				60			54			7
39				70.5	77.9				65.6		63	56.3		67.5	47
40				84	56			90	64.3		60				13
41				75	61.5				61.7			62			22

Total number of ten second samples 1744

Table 1-42 **Average rainfall intensity compared with fade levels (only storms with fades greater than 25dB are considered)**

Min Fade dB	Apr 29 1222 1237	May 1 0111 0114	May 16 1845 1857	May 30 1916 1941	Sep 24 1341 1424	Oct 7 1907 1919 2001 2030	Oct 7 2112 2126 2143 2159	Oct 7 2357 0002	Nov 30 1731 1820	Dec 23 2257 2310	Dec 27 1515 1534	Jan 28 1207 1327	Jan 31 0304 0316	Jan 31 0344 0352	(Opt + RBH)/2 mm/t
5	4	2	2	9			2		7	3	9	2	2	1	12
6	10	1	9	8	5	16	7		13	9	5	4	2	3	13.3
7	8	1	2	1	6	8	2		21	4	5	4	2		14.3
8	2	2	2	3	9	10	1		28	3	9	14	4	3	16.3
9		1	1	4	6	18	23	1	21	5	3	4	4	1	16.2
10	1	1	2	1	14	10	19		7	1	1	14	2	1	18.8
11	5		1	1	13	11	17		4	2	3	5			18.1
12	11		3	6	16	26	37	1	17	7	5	7	1	1	21
13	5			3	8	26	8		4		3	27		1	25.8
14	1	1		1	24	17	7	2	2	2	2	8	1		24
15	4		9	5	11	33	6	1	3	3	7	9	1		27
16	5	3	5	4	18	3	5					3	2	2	24.4
17	1	2		4	17	5	2		3	1	1	10			28.3
18	4	2	3	6	17	10	8	2	1	8	2	21	4	1	30.8
19	3		1	8	13	10	3		4	7	2	17	3	3	33.3
20	1		1	2	4	12	1		2	1	2	10	2	1	37.8
21	3		3	9	8	10	5	2	2	2	3	8			36.2
22	3	2	1	2	1	1	2					2	3	2	33.5
23	9	1	2	5	2	5	7	1		2	9	13	2		37.2
24	2		3	4	8	4	4		1	3	3	12			36.8
25	2		1	7	6		1		2			4	2	1	39.5
27	1	2	6	5	2	1	1	1	2		1	6	1		39.3
28				3	2	1		1	1		1	3	1	1	48.4
29	2		2	1	4	3	7	2	14	1	4	6	2		43.5
30			3	3		3			3	2	5	5	2		45.2
31	1		1		3	1	4		2			5	3		42
32			5	2					4			5			52.9
33			2	4			2		1		1	3	4		54.7
34			3	4	2	3	3		5	9	1	6	2		60.3
35				3	2			2	3	4	1	2	1		61
36				3	2			1		1	3	5	2	1	60.7
37				3					2		2	3			61.2
38					3				3			1			72
39				6	17				13		2	6		3	69.2
40				1	3			1	7		1				65.5
41				2	4				7			9			63
Total	88	21	73	133	250	247	184	18	209	80	97	263	55	26	1744

Number of ten second samples (fades greater than 25 dB Min)

Table 1-43 **Average rainfall intensity compared with fade levels (only storms with fades greater than 25dB are considered)**

16 Primary references

[1] Henriksson J.

'Radio wave propagation'

Personal communication, 1998

jukka.henriksson@nokia.com

[2] Martin A.

'Error free microwave'

Martin Communications, 1998

Andrew.Martin@martin.com.au

[3] Crane R.K.

'Propagation phenomena affecting satellite communication systems op

erating in the centimeter and millimeter wavelength band.'

IEEE, Vol. 59, No. 2, Pages 173 to 188, Feb 1971

[4] Knorr J.B.

'Guide EM waves with atmospheric ducts.'

Microwaves and RF, Pages 67 to 70, May 1985

[5] ITU–R P.563–4

'Radiometeorological Data.'

CCIR, Vol. V, Dusseldorf, Pages 105 to 147, 1990

[6] ITU–R P.453–6

'The radio refractive index: its formula and refractivity data'

www.itu.int/publications/, ITU–R P.453–6, Pages 1 to 9, 1997

[7] Doble. J

'Introduction to radio propagation for fixed and mobile communica

tions'

Artech House, ISBN 0–89006–529–2, Pages 1 to 107, 1996

[8] Rogers D.V.

'Propagation considerations for satellite broadcasting at frequencies

above 10 GHz.'

IEEE, Vol. SAC–3. No 1, Pages 100 to 110, Jan 1985

[9] Flavell R.G.

'Refractive index gradients in the lower troposphere – a fresh approach.'

Int A&P Conference, London, Part 2, Pages 182 to 186, Nov 1978

[10] Ruthroff C.L.

'Multiple–path fading on line–of–sight microwave radio systems as a

function of path length and frequency.'

Bell Sys Tech Journ, Vol. 50, No. 7, Pages 2375 to 2398, Sep 1971

[11] ITU–R P.834–2

'Effects of tropospheric refraction on radiowave propagation'

www.itu.int/publications/, ITU–R P.834–2, Pages 1 to 9, 1997

[12] Bye G.D., Howell R.G.

'Average radio refractive index lapse rate or the lower troposphere for

locations in NW Europe.'

Int A&P Conference, Coventry, Part 2, Pages 229 to 233, Apr 1989

[13] Rummler W.D., Liniger M.

'Terrestrial digital microwave communications'

Chapter 4, Pages 123 to 182, Editor Ivanek. F,

Artech House, ISBN 0–89006–302–8, 1989

[14] Green D.C.

'Radio systems technology'

Longman Sc&Tech, ISBN 0–582–02697–0, Pages 163 to 168, 1990

[15] ITU–R P.718–3

'Effects of tropospheric refraction on radiowave propagation'

CCIR, Vol. V, Dusseldorf, Pages 149 to 187, 1990

[16] Kuosmanen M.

'Radio relay link path design and calculations'

Finnish PTT, Chapters 8 & 12, Pages 156 to 174 & 251 to 275, 1978

[17] ITU–R P.530–7

'Propagation data and prediction methods required for the design of ter

restrial line–of–sight systems'

www.itu.int/publications/, ITU–R P.530–7, Pages 1 to 25, 1997

[18] Touhiniemi H.

'Horizontal space diversity'

Personal communication, 1998

heikki.touhiniemi@nokia.com

[19] Shafi M., Rummler W.D.

'Terrestrial digital microwave communications'

Chapter 8, Pages 289 to 341, Editor Ivanek. F,

Artech House, ISBN 0–89006–302–8, 1989

[20] Crane R.K.

'Fundamental limitations caused by RF propagation.'

IEEE, Vol. 69, No. 2, Pages 196 to 209, Feb 1981

[21] Pawlowski W.

'Recent results of radiometeorological studies over the coastal region of

Poland.'

Int A&P Conference, Coventry, Part 2, Pages 224 to 228, Apr 1989

[22] Dutta H.N., Sarkar S.K., Prasad M.V.S.N., Rao D.N.

'EMI potential over the Indian sub–continent: clear air effects.'

Int A&P Conference, Coventry, Part 2, Pages 322 to 326, Apr 1989

[23] Bashir S.O.

'Three years statistics of refractive index gradient and effective earth

radius factor for the state of Bahrain.'

Int A&P Conference, Coventry, Part 2, Pages 220 to 223, Apr 1989

[24] Narayana Rao, Ravi, Kasava Murthy, Sarkar, and Dutta

'Sodar echograms and correlation with microwave propagation char

acteristics in a hilly terrain'

Int A&P Conference, Coventry, Part 2, Pages 234 to 238, Apr 1989

[25] Ko. H

'A practical guide to anomalous propagation.'

Microwaves and RF, Pages 71 to 76, April 1985

[26] Sengupta N.

'Sunrise and sunset effects as observed on microwave propagation over

a line–of–sight path'

IEEE, Vol AP–33, No. 4, Pages 441 to 445, 1985

[27] Craig K.H., Kennedy G.R.

'Studies of microwave propagation on a microwave line–of–sight link.'

European Microwave Conference, Rome, Pages 523 to 528, Sep 1987

[28] Dilworth I.J.

'Preliminary results of anomalous propagation activity at 42 GHz over

a coastal path.'

Int A&P Conference, Eindhoven, Pages 208 to 211, Apr 1995

[29] Narayana Rao, Krishna, Reddy (1995)

'Fading measurements on a 11GHz, 31km terrestrial path at Madras,

India'

Int A&P Conference, Eindhoven, Pages 271 to 274, Apr 1995

[30] Lam W.I., Webster A.R.

'Microwave propagation on two line–of–sight oversea paths.'

IEEE, Vol. AP–33, No. 5, Pages 510 to 516, 1985

[31] Jones T.

'The role of fronts in anomalous microwave propagation.'

Int A&P Conference, York, Pages 185 to 188, Apr 1991

[32] Bundrock A.J., Murphy J.V.

'A broad–band 11 GHz radio propagation experiment.'

IEEE, Vol AP–32, No. 5, Pages 449 to 455, 1984

[33] Di Zenobio D., Russo E.

'Measurement of frequency–dependent variations of amplitude and

group delay in digital links'

Int A&P Conference, York, Pages 669 to 672, Apr 1991

[34] Blanchetiere–Ciarletti V., Sylvain M.

'Physical interpretation or the effects of the antenna heights on multipath

propagation occurence.'

Int A&P Conference, York, Pages 50 to 53, 1991

[35] ITU–R P.338–6

'Propagation data and prediction methods required for terrestrial line–

of–sight systems.'

CCIR, Vol. V, Dusseldorf, Pages 355 to 414, 1990

[36] Sarma A.D., Hill R.J.

'Effect of blowing snow and ground blizzards on millimeter wave scin

tillation spectra'

NOAA/ERL/Wave Prop Lab, Colorado, USA, Pages 1 to 32, 1990

[37] ITU–R P.1008–1

'Reflection from the surface of the earth.'

CCIR, Vol. V, Dusseldorf, Pages 75 to 82, 1990

[38] Hogg D.C., Chu T.

'The role of rain in satellite communications.'

IEEE, Vol. 63, No. 9, Pages 1308 to 1331, Sep 1975

[39] Ishimaru A.

'Introduction to wave propagation and scattering in random media'

IEEE, AP Newsletter, Page 5, Dec 1985

[40] Vilar E., Matthews P.A.

'Summary of scintillation observations in a 36 GHz link across London.'

Int A&P Conference, London, Part 2, Pages 36 to 40, Nov 1978

[41] Ho K.L., Mavrokouloulakis N.D., Cole R.S.

'Propagation studies on a line–of–sight microwave link at 36 GHz and

100 GHz.'

IEE, Microwave O&A Vol. 3, No. 3, Pages 93 to 98, May 1979

[42] Dimitrios. S.

'Scintillations in Australia'

Personal communication, 1997

stephen_dimitrios@yes.optus.com.au

[43] Ali A.A., Alhaider M.A.

'Experimental studies on millemeter wave propagation in arid climate:

scintillations and multipath fading.'

Int A&P Conference, Coventry, Part 2, Pages 428 to 431, Apr 1989

[44] Gibbins C.J., Chadha R.

'Millimetre–wave propagation through hydrocarbon flame.'

IEE, Vol. 134, Pt. H, No. 2, Pages 169 to 173, April 1987

[45] Wilson F.A.

'An introduction to satellite television'

Chapter 8, Pages 39 to 57,

Second ed, Bernard Babani, ISBN 0–85934–169–0, 1990

[46] ITU–R P.341–4

'The concept of transmission loss for radio links'

www.itu.int/publications/, ITU–R P.341–4, Pages 1 to 6, 1995

[47] ITU–R P.452–8

'Prediction procedure for the evaluation of microwave interference

between stations on the surface of the Earth at frequencies above about

0.7GHz'

www.itu.int/publications/, ITU–R P.452–8, Pages 1 to 28, 1997

[48] Olsen R.L., Rogers D.V., Hulays R.A., Kharadly M.M.Z.

'Interference due to hydrometeor scatter on satellite communication

links.'

IEEE, Vol. 81, No. 6, pages 914 to 922, Jun 1993

[49] Dutton E.J., Dougherty H.T.

'Year–to–year variability of rainfall for microwave applications in the

U.S.A..'

IEEE, Vol. COM–27, No. 5, Pages 829 to 832, May 1979

[50] Rice P.L., Holmberg N.H.

'Cumulative time statistics of surface–point rainfall rates.'

IEEE, Vol. Com–21, No. 10, Pages 1131 to 1136, Oct 1973

[51] Ippolito L.J.

'Radio propagation for space communication systems.'

IEEE, Vol. 69, No. 6, Pages 697 to 727, Jun 1981

[52] Fedi F.

'Prediction of attenuation due to rainfall on terrestrial links.'

Radio Science, Vol. 16, No. 5, Pages 731 to 743, Sep – Oct 1981

[53] Crane R.K.

'Prediction of the effects of rain on satellite communications systems.'

IEEE, Vol. 65, No. 3, Pages 456 to 474, Mar 1977

[54] Harris D.J., Milner E.

'The measurement of rainfall in Papua New Guinea, and its effects on

microwave propagation.'

254

Inter Journ of Sat Comms, Vol. 8, Pages 173 to 180, May – Jun 1990

[55] Lin S.H.

'Empirical rain attenuation model for earth–satellite paths.'

IEEE, Vol. Com–27, No. 5, Pages 812 to 817, May 1979

[56] ITU–R PN.837–1

'Characteristics of precipitation for propagation modelling'

www.itu.int/publications/, ITU–R PN.837–1, Pages 1 to 4, 1994

[57] Oguchi T.

'Electromagnetic wave propagation and scattering in rain and other Hy

drometeors.'

IEEE, Vol. 71, No. 9, Pages 1029 to 1078, Sep 1983

[58] Medeiros Filho F.C., Cole R.S., Samara A.D.

'Millimetre–wave rain induced attenuation: theory and experiment.'

IEE, Vol. 133, Pt. H, No. 4, Pages 308 to 314, Aug 1986

[59] Fedi F.

'Attenuation due to rain on a terrestrial path.'

Alta Frequenza, Vol. XLVIII, No. 4, Pages 167 to 184, Apr 1979

[60] Persinger R.R., Stutzman W.L, Castle R.E. Jr., Bostain C.W.

'Millimerer wave attenuation prediction using a piecewise uniform rain

rate model.'

IEEE, Vol. AP–28, No. 2, Pages 149 to 153, Mar 1980

[61] ITU–R Recommendation 838

'Specific attenuation model for rain for use in prediction methods'

www.itu.int/publications/, ITU–R 838, Pages 1 to 2, 1992

[62] Watson P.A., Ahmed H.J., Papaioannou G.

'Long term prediction of attenuation on terrestrial radio links from rain

fall data.'

Int A&P Conference, London, Part 2, Pages 92 to 96, Nov 1978

[63] Harden B.N., Norbury J.R., White W.J.K.

'Use of lognormal distribution of raindrop sizes in millimetric radio at

tenuation studies.'

Int A&P Conference, London, Part 2, Pages 87 to 91, Nov 1978

[64] Sekine M., Chen C.D., Musha T.

'Rain attenuation from log–normal and weibull raindrop–size distribu

tion.'

IEEE, Vol. AP–35, No. 3, Pages 358 to 359, Mar 1987

[65] Ajayi G.O.

'Some aspects of tropical rainfall and their effect on microwave propaga

tion.'

Int Journ of Sat Comms, Vol. 8, Pages 163 to 172, May – Jun 1990

[66] Manabe T., Ihara T., Furuhama Y.

'Inference of drop size distribution from rain attenuation and rain rate

measurements.'

Int A&P Conference, Norwich, Part 2, Pages 29 to 33, Apr 1983

[67] Fang D.J., Chen C.H.

'Propagation of centimeter/Millimeter waves along a slant path through

precipitation.'

Radio Science, Vol. 17, No. 5, Pages 989 to 1005, Sep – Oct 1982

[68] Maciel L.R., Assis M.S.

'Tropical rainfall drop–size distributions.'

Int Journ of Sat Comms, Vol. 8, Pages 181 to 186, May – Jun 1990

[69] Henderson–Sellers A., Robinson P.J.

'Contemporary climatology'

Longman Sc&Tech & John Wiley & Sons

ISBN 0–562–30057–6, Pages 27 to 150, 1986

[70] Allen K.C.

'Observations of the specific attenuation of millimeter waves by rain.'

Int A&P Conference, York, Part 2, Pages 39 to 42, Mar – Apr 1987

[71] Paraboni A., Possenti G., Tirro s.

'Some experimental results about the spreading of ellipsoidal raindrops

orientation during intense rainfall.'

Int A&P Conference, London, Part 2, Pages 82 to 86, Nov 1978

[72] Moupfouma F., Martin L., Spanjaard N., Hughes K.

'Rainfall rate characteristics for microwave systems in tropical and equa

torial areas.'

Int Journ of Sat Comms, Vol. 8, Pages 151 to 161, May – Jun 1990

[73] Misme P., Waldteufel P.

'A model for attenuation by prediction on a microwave earth–space

link.'

Radio Science, Vol. 15, No. 3, Pages 655 to 665, May – Jun 1980

[74] Houze R.A. Jr.

'Structures of atmospheric precipitation systems: A global survey.'

Radio Science, Vol. 16, No. 5, Pages 671 to 689, Sep – Oct 1981

[75] Capsoni C., Fedi F., Paraboni A.

'A comprehensive meteorologically oriented methodology for the pre

diction of wave propagation parameters in telecommunication applica

tions beyond 10 GHz.'

Radio Science, Vol 22, No. 3, Pages 387 to 393, May – Jun 1987

[76] Pan Q.W., Bryant G.H.

'Effective rain cell diameters and rain–column heights in the topics.'

IEE, Electronics Letters, Vol. 30, No. 21, Pages 1800 to 1802, Oct 1994

[77] Silva Mello L.A.R., Costa E., Siqueira G.L., Dhein N.R., Einloft C.M.

'Measurements of rain attenuation in 15 and 18 GHz converging links.'

Int A&P Conference, Eindhoven, Pages 127 to 130 ,Apr 1995

[78] Goldhirsh J.

'Path attenuation statistics influenced by orientation of rain cells.'

IEEE, Vol. AP–24, No. 6, Pages 792 to 799, Nov 1976

[79] Capsoni C., Fedi F., Magistroni C., Paraboni A., Pawlina A.

'Data and theory for a new model of the horizontal structure of rain cells

for propagation applications.'

Radio Science, Vol 22, No. 3, Pages 395 to 404, May – Jun 1987

[80] Cole. R.S.

'Mie Scattering'

Personal Communication, 1997

roy.cole@ucl.ac.uk

[81] Bebbington D.H.O.

'Inference or drop size distribution functions from millimetre wave at tenuation in rain.'

Int A&P Conference, Norwich, Part 2, Pages 19 to 23, Apr 1983

[82] Sakagami S.

'Some experimental results on bistatic scatter from rain.'

IEEE, Vol. AP–28, No. 2, Pages 161 to 165, Mar 1980

[83] Harden B.N., Norbury J.R., White W.J.K.

'Measurements of rainfall for studies of millimetric radio attenuation.'

IEE, Microwave O&A, Vol. 1, No. 6, Pages 197 to 202, Nov 1977

[84] Segal B.

'An analytical examination of mathematical models for the rainfall rate distribution function.'

Ann. Telecommunic, 35, No. 11–12, Pages 434 to 438, 1980

[85] Forknall. N. P.

'Field trials at 38GHz'

Nokia Telecommunications, Page 5, 1998

neil.forknall@nokia.com

[86] Dong Q.S.

'Rainfall characteristics and rain attenuation on millimerer wave.'

Int A&P Conference, Coventry, Pages 189 to 193, Apr 1985

[87] Misme P.

'Experimental results about rain induced attenuation and improvement of calculation methods.'

259

Int A&P Conference, London, Part 2, Pages 102 to 106, Nov 1978

[88] Tattelman P., Grantham D.D.

'A review of models for estimating 1 min rainfall rates for microwave

attenuation calculations.'

IEEE, Vol. COM–33, No. 4, Pages 361 to 372, Apr 1985

[89] Campbell Scientific Ltd.

'Automatic weather station with CM10/2 or CM10/3 tripod'

Cambell Scientific, Pages 1 to 3, Dec 1994

support@campbellsci.co.uk

[90] Moupfouma F.

'More anout rainfall rates and their prediction for radio systems engin

eering'

IEE, Vol. 134, No. 6, Pages 527 to 537, Dec 1987

[91] Auchterlonie L.J., Bryant D.L.

'Experimental study of millimetre–wave scattering from simulated hail

stones in an open resonator.'

IEE, Vol. 128, Pt. H, No. 5, Pages 236 to 242, Oct 1981

[92] Auchterlonie L.J.

'The properties of intense convective precipitation and their infuence on

microwave and millimetre–wave propagation – a review and application

or new and current information.'

Int A&P Conference, Eindhoven, Pages 77 to 80, Apr 1995

[93] ITU–R P.840–2

'Attenuation due to clouds and fog'

www.itu.int/publications/, ITU–R P.840–2, Pages 1 to 7, 1997

[94] Bashir S.O., McEwan N.J.

'Microwave propagation in dust storms: a review.'

IEE, Vol. 133, Pt. H, No. 3, Pages 241 to 247, Jun 1986

[95] Ghobrial S.I., Sharief S.M.

'Microwave attenuation and cross polarisation in dust storms'

IEEE, Vol. COM–35, No. 4, Pages 418 to 425, Apr 1987

[96] Ahmed A.S.

'Role of particle–size distributions on millimetre–wave propagation in

sand/duststorms.'

IEE, Vol. 134, Pt. H, No. 1, Pages 55 to 59, Feb 1987

[97] ITU–R P.719–3

'Attenuation by atmospheric gases.'

CCIR, Vol. V, Dusseldorf, Pages 189 to 203, 1990

[98] Lyback N.

'58GHz research and development'

Personal Communication, 1998

niklas.lyback@nokia.com

[99] Crane R.K.

'Attenuation due to rain – a mini review.'

IEEE, Tutorial papers and reviews, Pages 750 to 752, Sep 1975

[100] Effenberger J.A., Strickland R.R., Joy E.B.

'The effect of rain on a radome's performance'

Microwave Journal, Pages 261 to 272, May 1986

[101] Kajaus T

'Interference measurements at 38GHz'

Personal Communication, 1997

tero.kajaus@nokia.com

[102] ITU–T G.821

'Error performance of an international digital connection forming part

of an integrated services digital network'

www.itu.int/publications/, ITU–T G.821, Pages 1 to 10, 1988,

Reprinted 1993

[103] ITU–T G.826

'Error performance parameters and objectives for international, constant

bit rate digital paths at or above the primary rate'

www.itu.int/publications/, ITU–T G.826, Pages 1 to 14, 1993

[104] ITU–R F.634–4

'Error performance objectives for real digital radio–relay links forming

part of the high–grade portion of international digital connections at a bit

rate below the primary rate within an integrated services digital network'

www.itu.int/publications/, ITU–R F.634–4, Pages 1 to 7, 1997

[105] ITU–R F.594–4

'Error performance objectives of the hypothetical reference digital path

for radio–relay systems providing connections at a bit rate below the pri

mary rate and forming part or all of the high grade portion of an inte

grated services digital network'

www.itu.int/publications/, ITU–R F.594–4, Pages 1 to 3, 1997

[106] ITU–R F.697–2

'Error performance and availability objectives for the local–grade por

tion at each end of an integrated services digital network connections at

a bit rate below the primary rate utilizing digital radio–relay systems'

www.itu.int/publications/, ITU–R F.697–2, Pages 1 to 4, 1997

[107] ITU–R F.696–2.

'Error performance and availability objectives for hypothetical refer

ence digital sections forming part or all of the medium–grade portion of

an integrated services digital network at a bit rate below the primary rate

utilizing digital radio–relay systems'

www.itu.int/publications/, ITU–R F.696–2, Pages 1 to 4, 1997

[108] ITU–R F.557–4

'Availability objectives for radio–relay systems over a hypothetical ref

erence circuit and a hypothetical reference digital path'

www.itu.int/publications/, ITU–R F.557–4, Pages 1 to 4, 1997

[109] ITU–R F.1189–1

'Error performance objectives for constant bit rate digital paths at or

above the primary rate carried by digital radio–relay systems which may

form part or all of the national portion of a 27 500km hypothetical refer

ence path'

www.itu.int/publications/, ITU–R F.1189–1, Pages 1 to 4, 1997

[110] ITU–R F.1092–1

'Error performance objectives for constant bit rate digital paths at or

above the primary rate carried by digital radio–relay systems which may

form part or all of the international portion of a 27 500km hypothetical reference path'

www.itu.int/publications/, ITU–R F.1092–1, Pages 1 to 3, 1997

[111] ITU Recommendation 695

'Availability objectives for real digital radio–relay links forming part of a high–grade circuit within an integrated services digital network'

www.itu.int/publications/, ITU 695, Pages 1 to 2, 1990

[112] ITU Recommendation 556–1

'Hypothetical reference digital path for radio–relay systems which may form part of an integrated services digital network with a capacity above the second hierarchical level'

www.itu.int/publications/, ITU 556–1, Pages 1 to 2, 1986

[113] Lundgren C.W., Rummler W.D.

'Digital radio outage due to selective fading observations versus predic tion from laboratory simulation'

Bell Sys Tech Journ, Vol 58, No 5, Pages 1073 to 1100, May – Jun 1979

[114] Olsen R.L., Rogers D.V., and Hodge D.B.

'The aR(pow)b relation in the calculation of rain attenuation'

IEEE, Vol. AP–26, No. 2, Pages 318 to 328, Mar 1978

[115] Gunn R.G., Kinzer G.D.

'The terminal velocity of fall for water droplets in stagnant air'

Journ Meteorol, Vol 6, No 4, Pages 243 to 248, Aug 1949

[116] Ray P.S.

'Broardband complex refractive indices of ice and water'

Appl Optics, Vol II, No 8, Pages 1836 to 1843, Aug 1972

[117] Sanders J.

'Rain attenuation of millimetre waves at λ = 5.77, 3.3 and 2mm'

IEEE, Vol. AP–23, Pages 213 to 220, Mar 1975

[118] Joss J., Thams J.S., Waldvogel A.

'The variation of raindrop size distribution at Locarno'

Proc Int Conf on Cloud Physics, Pages 369 to 373, 1968

[119] Brussaard G.

'A meteorological model for rain–induced cross polarisation'

IEEE, Vol. AP–24, No. 2, Pages 5 to 11, Jan 1976

[120] Kerr D.E.

'propagation of short radio waves'

Vol 13, MIT Rad Lab series, McGraw–Hill, Page 679, 1951

[121] Ansari A.J., Evans B.G.

'Microwave propagation in sand and dust storms'

IEE, Vol 129, Pt F, No 5, Pages 315 to 322, Oct 1982

[122] Laws J.O., Parsons D.A.

'The relation of raindrop size to intensity'

Trans American Geophys Union, Vol 24, Pages 452 to 460, 1943

[123] Atlas D., Plank V.G.

'Drop size history during a shower'

Journ Meteorol, Vol 10, Pages 291 to 295, Aug 1953

[124] Vigants A.

Microwave radio obstruction fading

Bell Sys Tech Journ, Vol 60, No 6, Pages 785 to 801, Jul – Aug 1981

[125] ITU–R F.1093–1

'Effects of multipath propagation on the design and operation of line–of–

sight digital radio–relay systems'

www.itu.int/publications/, ITU–R F.1093–1, Pages 1 to 12, 1997

[126] Pruppacher H.R., Pitter R.L.

'A semi–empiricol determination of the shape of cloud and raindrops'

Journ Atmos Sci, Vol 28, Pages 86 to 94, Jan 1971

[127] Henriksson J.

'Route planning guide for digital radio links'

Nokia Research Centre, Chapter 3, Page 12, 1988

[128] Black U.D.

'Data networks: concepts, theory and practice'

Prentice Hall, ISBN 0–13–198599–X, Pages 77 to 86, 1989

[129] Held G.

'Data commumications networking devices'

Chapter 2, Pages 117 to 122,

John Wiley and Sons, ISBN 0–471–91869–5, 1989

[130] Shafi S.

'Modulation and countermeasure methods'

Chapter 5, Pages 183 to 205, Editor Ivanek. F,

Artech House, ISBN 0–89006–302–8, 1989

[131] Pruppacher H.R., Beard K.

'A wind tunnel investigation of internal circulation and shape of water

drops falling at terminal velocity in air'

Quart Journ Roy Meteor Soc 96, Pages 247 to 256, 1970

[132] Report TSB10–E

'Interference criteria for microwave systems in the private radio sevices'

EIA / TIA Bulletin, Page 12 to 150, Nov 1990

[133] Chu T.S.(1979)

'Effects of sandstorms on microwave propagation'

Bell Sys Tech Journ, Vol 58, No 2, Pages 549 to 555, Feb 1979

[134] Poiares Baptista, Zhang Z.W., McEwan N.J.

'Stability of rain–rate cumulative distributions.'

IEE, Electronics Letters, Vol. 22, No. 7, Pages 350 to 352, Mar 1986

[135] COST 235 Final Report

'Radiowave propagation effects on next–generation fixed–service ter

restrial telecommunications systems'

European Commission, EUR 16992 EN, Pages 170 to 191, 1996

[136] Jones D.M.A

'The shape of drops'

Journ Meteorol, Vol 16, Pages 504 to 510, Oct 1959

[137] Marshall J.S., McK Palmer W

'The distribution of raindrops with size'

Journ Meteorol, Vol 5, Pages 165 to 166, Aug 1948

17 Secondary references

[S1] Kuhn U., Ogulwicz S.

'Propagation measurements at 500MHz over sea for varying meteoro

logical parameters'

Proc IEE 117, Pages 879–886, 1970

[S2] Suzuki E.

'Secular variations of the rainfall in Japan'

Meteor Geophys (Japan), Vol 19, Pages 363 to 399, 1968

[S3] Mooley D.A., Crutcher H.L.

'An application of the gamma distribution function to Indian rainfall'

US Department of Commerce, Tech Report EDS-5, Aug 1968

[S4] Fedi F., Maggiori D.

'Colcodo dei parametri della relazione tra attenuazione specifica di pre

cipitazione'

FUB Internal Report, 1978

[S5] Oguchi T., Hosoya Y.

'Scattering properties of oblate raindrops and cross polarisation of radio

waves due torain (part II). Calculations at the microwave and millimetre

wave regions'

Journ Meteorol, Vol 21, Pages 191 to 259, 1974

[S6] Harden B.N., Norbury J.R., White W.J.K.

'Estimation of attenuation by rain on terrestrial radio links in the UKat

frequencies from 10 to 100GHz'

IEE, Microwave O&A, Vol 2, No 4, Pages 97 to 104, Jul 1978

[S7] Joss J., Cavalli R., Crane R.K.

'Good agreement between theory and experiment for attenuation data'

Journ Rech Atmos, Vol 8, Pages 89 to 119, 1974

[S8] Ugai S., Kato K., Nishijima M., Kan T., Tazaki K.

'Fine structure of rainfall'

Ann. Telecommunic, Vol 32, Pages 422 to 429, Nov–Dec 1977

[S9] Oguchi T.

'Scattering from hydrometeors: A survey'

Radio Science, Vol 16(5), Pages 691 to 730, 1981

[S10] Pruppacher H.R., Klett J.D.

'Microphysics of clouds and precipitation'

Boston MA, Reidel, 1978

[S11] Magono C., Nakamura T.

'Aerodynamic studies of falling snowflakes'

Journ Meteorol Soc Japan, Vol 43, Pages 139 to 147, Jun 1965

[S12] Nishitsuji A., Matsumoto A.

'The character of falling snow'

Monograph Ser of the Res Inst of Appl Elect, Pages 45 to 61

Hokkaido Univ, Sapporo, Japan 1971

[S13] Oomori T., Aoyagi S.

'A presumptive formula for snowfall attenuation of radio waves'

Trans Inst Electron Commun Eng Japan,

Vol 54–B, Pages 451 to 458, Aug 1971

[S14] Cihlar J., Ulaby F.T.

'Dielectric properties of soil as a function of moisture content'

RSL Technical Report 177–47, CR–141868, University of Kansas, 1974

[S15] Ghobrial S.I., Ali I.A., Hussein H.M.

'Microwave attenuation in sandstorms'

Proc Int Symp Antenna and Propagation,

Sendai, Japan, Pages 447 to 450, 1978

[S16] Goldhirsh J.

'A parameter review and assessment of attenuation and backscatter prop

erties associated with dust storms over dessert regions in the frequency

range of 1 to 10 GHz'

IEEE, Vol. AP–30, Pages 1121 to 1127, 1982

[S17] Best A.C.

'Water in the atmosphere'

Part 1 of The Interim Report of the

Ultra Short Wave Panel Working Committee, Jul 18, 1944